

# BULLETIN OF RUSSIAN STATE MEDICAL UNIVERSITY

BIOMEDICAL JOURNAL OF PIROGOV RUSSIAN NATIONAL  
RESEARCH MEDICAL UNIVERSITY

**EDITOR-IN-CHIEF** Denis Rebrikov, DSc, professor

**DEPUTY EDITOR-IN-CHIEF** Alexander Oettinger, DSc, professor

**EDITORS** Valentina Geidebrekht, PhD; Nadezda Tikhomirova

**TECHNICAL EDITOR** Evgeny Lukyanov

**TRANSLATORS** Nadezda Tikhomirova, Vyacheslav Vityuk

**DESIGN AND LAYOUT** Marina Doronina

## EDITORIAL BOARD

**Averin VI**, DSc, professor (Minsk, Belarus)

**Azizoglu M**, MD PhD (Istanbul, Turkey)

**Alipov NN**, DSc, professor (Moscow, Russia)

**Belousov VV**, DSc, professor (Moscow, Russia)

**Bozhenko VK**, DSc, CSc, professor (Moscow, Russia)

**Bylova NA**, CSc, docent (Moscow, Russia)

**Gainetdinov RR**, CSc (Saint-Petersburg, Russia)

**Gendlin GYe**, DSc, professor (Moscow, Russia)

**Ginter EK**, member of RAS, DSc (Moscow, Russia)

**Gorbacheva LR**, DSc, professor (Moscow, Russia)

**Gordeev IG**, DSc, professor (Moscow, Russia)

**Gudkov AV**, PhD, DSc (Buffalo, USA)

**Gulyaeva NV**, DSc, professor (Moscow, Russia)

**Gusev EI**, member of RAS, DSc, professor (Moscow, Russia)

**Danilenko VN**, DSc, professor (Moscow, Russia)

**Zarubina TV**, DSc, professor (Moscow, Russia)

**Zatevakhin II**, member of RAS, DSc, professor (Moscow, Russia)

**Kagan VE**, professor (Pittsburgh, USA)

**Kzyshkowska YuG**, DSc, professor (Heidelberg, Germany)

**Kobrinikii BA**, DSc, professor (Moscow, Russia)

**Kozlov AV**, MD PhD, (Vienna, Austria)

**Kotelevtsev YuV**, CSc (Moscow, Russia)

**Lebedev MA**, PhD (Darem, USA)

**Manturova NE**, DSc (Moscow, Russia)

**Milushkina OYu**, DSc, professor (Moscow, Russia)

**Mitupov ZB**, DSc, professor (Moscow, Russia)

**Moshkovskii SA**, DSc, professor (Moscow, Russia)

**Munblit DB**, MSc, PhD (London, Great Britain)

**Negrebetsky VV**, DSc, professor (Moscow, Russia)

**Novikov AA**, DSc (Moscow, Russia)

**Pivovarov YuP**, member of RAS, DSc, professor (Moscow, Russia)

**Polunina NV**, corr. member of RAS, DSc, professor (Moscow, Russia)

**Poryadin GV**, corr. member of RAS, DSc, professor (Moscow, Russia)

**Razumovskii AYU**, corr. member of RAS, DSc, professor (Moscow, Russia)

**Rebrova OYu**, DSc (Moscow, Russia)

**Rudoy AS**, DSc, professor (Minsk, Belarus)

**Rylova AK**, DSc, professor (Moscow, Russia)

**Semiglazov VF**, corr. member of RAS, DSc, professor (Saint-Petersburg, Russia)

**Skoblina NA**, DSc, professor (Moscow, Russia)

**Slavyanskaya TA**, DSc, professor (Moscow, Russia)

**Smirnov VM**, DSc, professor (Moscow, Russia)

**Spallone A**, DSc, professor (Rome, Italy)

**Starodubov VI**, member of RAS, DSc, professor (Moscow, Russia)

**Stepanov VA**, corr. member of RAS, DSc, professor (Tomsk, Russia)

**Suchkov SV**, DSc, professor (Moscow, Russia)

**Takhchidi KhP**, member of RAS, DSc, professor (Moscow, Russia)

**Trufanov GE**, DSc, professor (Saint-Petersburg, Russia)

**Tumanova UN**, MD (Moscow, Russia)

**Favorova OO**, DSc, professor (Moscow, Russia)

**Filipenko ML**, CSc, leading researcher (Novosibirsk, Russia)

**Khazipov RN**, DSc (Marsel, France)

**Chundukova MA**, DSc, professor (Moscow, Russia)

**Schegolev AI**, MD, professor (Moscow, Russia)

**Shimanovskii NL**, corr. member of RAS, DSc, professor (Moscow, Russia)

**Shishkina LN**, DSc, senior researcher (Novosibirsk, Russia)

**Yakubovskaya RI**, DSc, professor (Moscow, Russia)

**SUBMISSION** <http://vestnikrgmu.ru/login?lang=en>

**CORRESPONDENCE** [editor@vestnikrgmu.ru](mailto:editor@vestnikrgmu.ru)

**COLLABORATION** [manager@vestnikrgmu.ru](mailto:manager@vestnikrgmu.ru)

**ADDRESS** ul. Ostrovityanova, d. 1, Moscow, Russia, 117997

Indexed in Scopus. CiteScore 2023: 0,8

**Scopus**<sup>®</sup>

SCImago Journal & Country Rank 2020: 0.14

**SJR**

Scimago Journal & Country Rank

Indexed in WoS. JCR 2021: 0.5

**WEB OF SCIENCE**<sup>™</sup>

Listed in HAC 31.01.2020 (№ 507)



**ВЫСШАЯ  
АТТЕСТАЦИОННАЯ  
КОМИССИЯ (ВАК)**

Five-year h-index is 10

**Google**  
scholar

Open access to archive

**CYBERLENINKA**

Issue DOI: 10.24075/brsmu.2025-01

The mass media registration certificate № 012769 issued on July 29, 1994

Founder and publisher is Pirogov Russian National Research Medical University (Moscow, Russia)

The journal is distributed under the terms of Creative Commons Attribution 4.0 International License [www.creativecommons.org](http://www.creativecommons.org)



Approved for print 28.02.2025  
Circulation: 100 copies. Printed by Print.Formula  
[www.print-formula.ru](http://www.print-formula.ru)

# ВЕСТНИК РОССИЙСКОГО ГОСУДАРСТВЕННОГО МЕДИЦИНСКОГО УНИВЕРСИТЕТА

НАУЧНЫЙ МЕДИЦИНСКИЙ ЖУРНАЛ РНИМУ ИМ. Н. И. ПИРОГОВА

**ГЛАВНЫЙ РЕДАКТОР** Денис Ребриков, д. б. н., профессор

**ЗАМЕСТИТЕЛЬ ГЛАВНОГО РЕДАКТОРА** Александр Эттингер, д. м. н., профессор

**РЕДАКТОРЫ** Валентина Гейдебрехт, к. б. н.; Надежда Тихомирова

**ТЕХНИЧЕСКИЙ РЕДАКТОР** Евгений Лукьянов

**ПЕРЕВОДЧИКИ** Надежда Тихомирова, Вячеслав Витюк

**ДИЗАЙН И ВЕРСТКА** Марины Дорониной

## РЕДАКЦИОННАЯ КОЛЛЕГИЯ

**В. И. Аверин**, д. м. н., профессор (Минск, Белоруссия)

**М. Азизоглу**, MD PhD (Стамбул, Турция)

**Н. Н. Алипов**, д. м. н., профессор (Москва, Россия)

**В. В. Белоусов**, д. б. н., профессор (Москва, Россия)

**В. К. Боженко**, д. м. н., к. б. н., профессор (Москва, Россия)

**Н. А. Былова**, к. м. н., доцент (Москва, Россия)

**Р. Р. Гайнетдинов**, к. м. н. (Санкт-Петербург, Россия)

**Г. Е. Гендлин**, д. м. н., профессор (Москва, Россия)

**Е. К. Гинтер**, академик РАН, д. б. н. (Москва, Россия)

**Л. Р. Горбачева**, д. б. н., профессор (Москва, Россия)

**И. Г. Гордеев**, д. м. н., профессор (Москва, Россия)

**А. В. Гудков**, PhD, DSc (Буффало, США)

**Н. В. Гуляева**, д. б. н., профессор (Москва, Россия)

**Е. И. Гусев**, академик РАН, д. м. н., профессор (Москва, Россия)

**В. Н. Даниленко**, д. б. н., профессор (Москва, Россия)

**Т. В. Зарубина**, д. м. н., профессор (Москва, Россия)

**И. И. Затевахин**, академик РАН, д. м. н., профессор (Москва, Россия)

**В. Е. Каган**, профессор (Питтсбург, США)

**Ю. Г. Кжышковска**, д. б. н., профессор (Гейдельберг, Германия)

**Б. А. Кобринский**, д. м. н., профессор (Москва, Россия)

**А. В. Козлов**, MD PhD (Вена, Австрия)

**Ю. В. Котелевцев**, к. х. н. (Москва, Россия)

**М. А. Лебедев**, PhD (Дарем, США)

**Н. Е. Мантурова**, д. м. н. (Москва, Россия)

**О. Ю. Милушкина**, д. м. н., доцент (Москва, Россия)

**З. Б. Митупов**, д. м. н., профессор (Москва, Россия)

**С. А. Мошковский**, д. б. н., профессор (Москва, Россия)

**Д. Б. Мунблит**, MSc, PhD (Лондон, Великобритания)

**В. В. Негребский**, д. х. н., профессор (Москва, Россия)

**А. А. Новиков**, д. б. н. (Москва, Россия)

**Ю. П. Пивоваров**, д. м. н., академик РАН, профессор (Москва, Россия)

**Н. В. Полунина**, член-корр. РАН, д. м. н., профессор (Москва, Россия)

**Г. В. Порядин**, член-корр. РАН, д. м. н., профессор (Москва, Россия)

**А. Ю. Разумовский**, член-корр. РАН, д. м. н., профессор (Москва, Россия)

**О. Ю. Реброва**, д. м. н. (Москва, Россия)

**А. С. Рудой**, д. м. н., профессор (Минск, Белоруссия)

**А. К. Рылова**, д. м. н., профессор (Москва, Россия)

**В. Ф. Семиглазов**, член-корр. РАН, д. м. н., профессор (Санкт-Петербург, Россия)

**Н. А. Скоблина**, д. м. н., профессор (Москва, Россия)

**Т. А. Славянская**, д. м. н., профессор (Москва, Россия)

**В. М. Смирнов**, д. б. н., профессор (Москва, Россия)

**А. Спаллоне**, д. м. н., профессор (Рим, Италия)

**В. И. Стародубов**, академик РАН, д. м. н., профессор (Москва, Россия)

**В. А. Степанов**, член-корр. РАН, д. б. н., профессор (Томск, Россия)

**С. В. Сучков**, д. м. н., профессор (Москва, Россия)

**Х. П. Тахчиди**, академик РАН, д. м. н., профессор (Москва, Россия)

**Г. Е. Труфанов**, д. м. н., профессор (Санкт-Петербург, Россия)

**У. Н. Туманова**, д. м. н. (Москва, Россия)

**О. О. Фаворова**, д. б. н., профессор (Москва, Россия)

**М. Л. Филипенко**, к. б. н. (Новосибирск, Россия)

**Р. Н. Хазипов**, д. м. н. (Марсель, Франция)

**М. А. Чундокова**, д. м. н., профессор (Москва, Россия)

**Н. Л. Шимановский**, член-корр. РАН, д. м. н., профессор (Москва, Россия)

**Л. Н. Шишкина**, д. б. н. (Новосибирск, Россия)

**А. И. Щеголев**, д. м. н., профессор (Москва, Россия)

**Р. И. Якубовская**, д. б. н., профессор (Москва, Россия)

**ПОДАЧА РУКОПИСЕЙ** <http://vestnikrgmu.ru/login>

**ПЕРЕПИСКА С РЕДАКЦИЕЙ** [editor@vestnikrgmu.ru](mailto:editor@vestnikrgmu.ru)

**СОТРУДНИЧЕСТВО** [manager@vestnikrgmu.ru](mailto:manager@vestnikrgmu.ru)

**АДРЕС РЕДАКЦИИ** ул. Островитянова, д. 1, г. Москва, 117997

Журнал включен в Scopus. CiteScore 2023: 0,8

Журнал включен в WoS. JCR 2021: 0,5

Индекс Хирша (h<sup>i</sup>) журнала по оценке Google Scholar: 10

**Scopus**<sup>®</sup>

ScImago Journal & Country Rank 2020: 0,14

**SJR**  
Scimago Journal & Country Rank

**WEB OF SCIENCE**<sup>™</sup>

Журнал включен в Перечень 31.01.2020 (№ 507)



**ВЫСШАЯ  
АТТЕСТАЦИОННАЯ  
КОМИССИЯ (ВАК)**

**Google**  
scholar

Здесь находится открытый архив журнала

**CYBERLENINKA**

DOI выпуска: 10.24075/vrgmu.2025-01

Свидетельство о регистрации средства массовой информации № 012769 от 29 июля 1994 г.

Учредитель и издатель — Российский национальный исследовательский медицинский университет имени Н. И. Пирогова (Москва, Россия)

Журнал распространяется по лицензии Creative Commons Attribution 4.0 International [www.creativecommons.org](http://www.creativecommons.org)



Подписано в печать 28.02.2025  
Тираж 100 экз. Отпечатано в типографии Print.Formula  
[www.print-formula.ru](http://www.print-formula.ru)

<b>REVIEW</b>	<b>4</b>
<b>miRNA biogenesis and functioning: 30 years since their discovery</b> Pisklova MV, Baulina NM, Matveeva NA, Favorova OO <b>Биогенез и функционирование микроРНК: 30 лет после их открытия</b> М. В. Писклова, Н. М. Баулина, Н. А. Матвеева, О. О. Фаворова	<b>11</b>
<b>ORIGINAL RESEARCH</b>	<b>19</b>
<b>Predictive model for mortality in patients with abdominal sepsis</b> Osikov MV, Telesheva LF, Konashov AG, Konashov VA, Gusev AV, Boyko MS <b>Модель прогноза вероятности летального исхода у больных с абдоминальным сепсисом</b> М. В. Осиков, Л. Ф. Телешева, А. Г. Конашов, В. А. Конашов, А. В. Гусев, М. С. Бойко	<b>28</b>
<b>ORIGINAL RESEARCH</b>	<b>35</b>
<b>LIF and sLIFr alterations during reconvalescence (novel coronavirus infection, influenza) in patients with essential hypertension</b> Radaeva OA, Simbirsev AS, Kostina YuA, Iskandaryarova MS, Negodnova EV, Solodovnikova GA, Ereemeev VV, Krasnoglazova KA, Babushkin IO <b>Изменение LIF и sLIFr в период реконвалесценции (новая коронавирусная инфекция, грипп) у пациентов с гипертонической болезнью</b> О. А. Радаева, А. С. Симбирцев, Ю. А. Костина, М. С. Искандарова, Е. В. Негоднова, Г. А. Солодовникова, В. В. Еремеев, К. А. Красноглазова, И. О. Бабушкин	<b>42</b>
<b>ORIGINAL RESEARCH</b>	<b>47</b>
<b>Cognitive reserve of patients with chronic cerebral ischemia</b> Fokin VF, Ponomareva NV, Shabalina AA, Kononov RN, Medvedev RB, Boravova AI, Lagoda OV, Krotenkova MV, Tanashyan MM <b>Когнитивный резерв больных хронической ишемией мозга</b> В. Ф. Фокин, Н. В. Пономарева, А. А. Шабалина, Р. Н. Коновалов, Р. Б. Медведев, А. И. Боровова, О. В. Лагода, М. В. Кротенкова, М. М. Танашян	<b>56</b>
<b>ORIGINAL RESEARCH</b>	<b>62</b>
<b>Features of intrauterine microbiota in patients with endometrial polyps</b> Vanakova AI, Dolgushina NV, Denisov PA, Goncharuk OD, Muravieva VV, Pripitnevich TV <b>Особенности микробиоты полости матки у пациенток с полипами эндометрия</b> А. И. Ванакова, Н. В. Долгушина, П. А. Денисов, О. Д. Гончарук, В. В. Муравьева, Т. В. Припутневич	<b>70</b>
<b>ORIGINAL RESEARCH</b>	<b>77</b>
<b>Assessment of the features of innate lymphoid cells in patients with multiple myeloma</b> Pashkina EA, Boeva OS, Borisevich VI, Abbasova VS, Skachkov IP, Lazarev YaA, Denisova VV <b>Оценка особенностей врожденных лимфоидных клеток у пациентов с множественной миеломой</b> Е. А. Пашкина, О. С. Боева, В. И. Борисевич, В. С. Аббасова, И. П. Скачков, Я. А. Лазарев, В. В. Денисова	<b>85</b>
<b>ORIGINAL RESEARCH</b>	<b>93</b>
<b>Monitoring the spread of COVID-19 across tuberculosis patients in Moscow</b> Kotova EA, Sumarokova EV, Belilovsky EM, Monchakovskaya ES <b>Мониторинг распространения COVID-19 среди больных туберкулезом в Москве</b> Е. А. Котова, Е. В. Сумарокова, Е. М. Белиловский, Е. С. Мончаковская	<b>93</b>
<b>ORIGINAL RESEARCH</b>	<b>93</b>
<b>Genetic polymorphism of the NF-<math>\kappa</math>B1 p105/p50 processing region in pulmonary tuberculosis</b> Meyer AV, Thorenko BA, Imekina DO, Dutchenko AP, Pyanzova TV, Karabchukov KB, Lavryashina MB <b>Генетический полиморфизм области процессинга p105/p50 NF-<math>\kappa</math>B1 при туберкулезе легких</b> А. В. Мейер, Б. А. Тхоренко, Д. О. Иमेкина, А. П. Дутченко, Т. В. Пьянзова, К. Б. Карабчуков, М. Б. Лаврышина	<b>93</b>
<b>ORIGINAL RESEARCH</b>	<b>93</b>
<b>Oxidative protein destruction products as markers of chronic kidney disease progression in diabetes mellitus</b> Osikov MV, Efros LA, Zhuravleva LYu, Fedosov AA <b>Продукты окислительной деструкции белков как маркеры прогрессирования хронической болезни почек при сахарном диабете</b> М. В. Осиков, Л. А. Эфрос, Л. Ю. Журавлева, А. А. Федосов	<b>93</b>
<b>ORIGINAL RESEARCH</b>	<b>93</b>
<b>Feature of bioelectrical impedance analysis and electromyography data in children with cerebral palsy</b> Vlasenko SV, Lyovin GV, Osmanov EA <b>Особенности данных биоимпедансометрии и электромиографии у детей с детским церебральным параличом</b> С. В. Власенко, Г. В. Лёвин, Э. А. Османов	<b>93</b>
<b>ORIGINAL RESEARCH</b>	<b>93</b>
<b>The effect of sterilization methods on the cytotoxicity of ceramic medical implants</b> Bilyalov AR, Piatnitskaia SV, Rafikova GA, Akbashev VN, Bikmeyer AT, Akhatov ISH, Shangina OR, Chugunov SS, Tikhonov AA <b>Влияние методов стерилизации на цитотоксичность керамических медицинских имплантов</b> А. Р. Билялов, С. В. Пятницкая, Г. А. Рафикова, В. Н. Акбашев, А. Т. Бикмеев, И. Ш. Ахатов, О. Р. Шангина, С. С. Чугунов, А. А. Тихонов	<b>93</b>
<b>ORIGINAL RESEARCH</b>	<b>93</b>
<b>Cognitive correlates of deception recognition in the elderly and seniors</b> Petrash EA, Lisichkina AA, Karpenko AS, Nikishina VB, Polonets AI <b>Когнитивные корреляты распознавания обмана в пожилом и старческом возрасте</b> Е. А. Петраш, А. А. Лисичкина, А. С. Карпенко, В. Б. Никишина, А. И. Полонец	<b>93</b>
<b>ERRATUM</b>	<b>93</b>

## miRNA BIOGENESIS AND FUNCTIONING: 30 YEARS SINCE THEIR DISCOVERY

Pisklova MV<sup>1</sup>✉, Baulina NM<sup>1,2</sup>, Matveeva NA<sup>1,2</sup>, Favorova OO<sup>1,2</sup>

<sup>1</sup> Chazov National Medical Research Center of Cardiology, Moscow, Russia

<sup>2</sup> Pirogov Russian National Research Medical University, Moscow, Russia

The role of miRNAs (small non-coding RNAs) in regulation of gene expression is reported. By binding with target mRNAs miRNAs control expression of the genes encoding these mRNAs at post-transcriptional level taking part in physiological and pathological processes, from embryogenesis to neoplastic disorders. Various research teams have been studying the miRNA functions and mechanisms of action since the discovery of these molecules in 1993. The paper reports miRNA biogenesis pathways, modes of interaction between miRNAs and target mRNAs, and the mechanisms underlying suppression of translation and mRNA degradation. The results of numerous studies have shown that miRNAs can be used in medicine as biomarkers for diagnostic and prognostic purposes. Developments in miRNA therapeutics hold promise for the treatment of diseases, in which gene dysregulation plays a key role.

**Keywords:** miRNA, regulation of gene expression, miRNA biogenesis, diagnostics, prognosis of disease progression, therapy

**Funding:** the study was conducted within the framework of the State Assignment of the Chazov National Medical Research Center of Cardiology (No. 12402020013-3).

**Author contribution:** Pisklova MV — literature data acquisition, analysis and systematization, planning and writing the manuscript draft, selecting drawings; Baulina NM, Favorova OO — planning, manuscript structuring, editing; Matveeva NA — literature data analysis and systematization, manuscript writing.

✉ **Correspondence should be addressed:** Maria V. Pisklova  
Akademika Chazova, 15A, Moscow, 121552, Russia; pisklova\_maria@mail.ru

**Received:** 24.11.2024 **Accepted:** 20.12.2024 **Published online:** 28.01.2025

**DOI:** 10.24075/brsmu.2025.001

**Copyright:** © 2025 by the authors. **Licensee:** Pirogov University. This article is an open access article distributed under the terms and conditions of the Creative Commons Attribution (CC BY) license (<https://creativecommons.org/licenses/by/4.0/>).

## БИОГЕНЕЗ И ФУНКЦИОНИРОВАНИЕ микроРНК: 30 ЛЕТ ПОСЛЕ ИХ ОТКРЫТИЯ

М. В. Писклова<sup>1</sup>✉, Н. М. Баулина<sup>1,2</sup>, Н. А. Матвеева<sup>1,2</sup>, О. О. Фаворова<sup>1,2</sup>

<sup>1</sup> Национальный медицинский исследовательский центр кардиологии им. ак. Е. И. Чазова, Москва

<sup>2</sup> Российский национальный исследовательский медицинский университет имени Н. И. Пирогова, Москва

Описана роль микроРНК (малых некодирующих РНК) в регуляции экспрессии генов. Связываясь с мРНК-мишенями, микроРНК контролируют экспрессию кодирующих эти мРНК генов на посттранскрипционном уровне, участвуя в физиологических и патологических процессах от эмбриогенеза до опухолевых заболеваний. С момента открытия этих молекул в 1993 г. различные научные группы исследуют функции и механизмы действия микроРНК. В статье рассмотрены пути биогенеза микроРНК, способы взаимодействия микроРНК с мРНК-мишенями и механизмы подавления трансляции и деградации мРНК. Результаты многочисленных исследований показали, что микроРНК можно использовать в медицине в качестве биомаркеров в диагностических и прогностических целях. Разработки в области терапии с использованием микроРНК открывают перспективы для лечения заболеваний, при которых нарушение регуляции генов играет ключевую роль.

**Ключевые слова:** микроРНК, регуляция экспрессии генов, биогенез микроРНК, диагностика, прогноз течения заболеваний, терапия

**Финансирование:** исследование выполнено в рамках Государственного задания ФГБУ Национальный медицинский исследовательский центр кардиологии им. ак. Е. И. Чазова Минздрава России (№ 12402020013-3).

**Вклад авторов:** М. В. Писклова — сбор, анализ и систематизация литературных данных, планирование и написание первичного текста, подбор рисунков; Н. М. Баулина, О. О. Фаворова — планирование, структурирование текста статьи, редактирование; Н. А. Матвеева — анализ и систематизация литературных данных, написание статьи.

✉ **Для корреспонденции:** Мария Владиславовна Писклова  
ул. Академика Чазова, д. 15А, г. Москва, 121552, Россия; pisklova\_maria@mail.ru

**Статья получена:** 24.11.2024 **Статья принята к печати:** 20.12.2024 **Опубликована онлайн:** 28.01.2025

**DOI:** 10.24075/vrgmu.2025.001

**Авторские права:** © 2025 принадлежат авторам. **Лицензиат:** РНИМУ им. Н.И. Пирогова. Статья размещена в открытом доступе и распространяется на условиях лицензии Creative Commons Attribution (CC BY) (<https://creativecommons.org/licenses/by/4.0/>).

In 1993, research groups of American biologists Victor Ambros and Gary Ruvkun reported a short RNA of the nematode *Caenorhabditis elegans*, which did not encode any protein, but played a key role in regulation of the nematode development via suppression of the LIN-14 protein mRNA translation [1, 2]. This small RNA referred to as lin-4 became the first discovered short RNA having regulatory properties. In 2000, the second short RNA, let-7, having the same mechanism of action, was found in *Caenorhabditis elegans* by Gary Ruvkun and colleagues [3]. From that moment began extensive study of the new type of small non-coding RNAs, 21–24 nucleotides in length, referred to as microRNAs (miRNAs), the discovery of which significantly

influences the established ideas about regulation of gene functioning. While before this discovery the main mechanisms underlying regulation of transcription and RNA splicing implemented by specific proteins in the nucleus were known, currently this knowledge is complemented by the idea about further control of gene expression in the cytoplasm through miRNAs. This mechanism is of fundamental importance for the development and functioning of all cell types, it involves regulation of the target genes expression through the interaction with their mRNAs at post-transcriptional level. The presence of miRNA molecules was reported for various eukaryotic species, including plants and animals, as well as for some viruses [4]. In

2024, V. Ambros and G. Ruvkun were awarded the Nobel Prize in Physiology or Medicine “for the discovery of microRNA and its role in post-transcriptional gene regulation”.

In recent years, it was found that numerous miRNAs are important for regulation of almost all physiological and disease processes: from early stages of embryogenesis to body's ageing and death. Let us consider the current state of knowledge about miRNA biogenesis and functioning.

### miRNA abundance and nomenclature

According to the last version of miRBase, the miRNA sequence and annotation database, by 17.03.2024 a total of 48,860 mature miRNAs have been found in 271 species, of those 2654 have been identified in human body. The number of miRNAs detected continues to grow. The range of miRNAs present in this or that organism depends directly on its structural complexity [5]. The evolutionarily related miRNAs are grouped into various families (there are 267 families in humans), the members of which have highly homologous sequences and some common targets. Highly conservative nature of the nucleotide sequences of some miRNAs (primarily in the target mRNA binding region) in phylogenesis has been demonstrated. In general, miRNA evolution is closely linked to evolution of target genes [5].

miRNAs are numbered consecutively as they are discovered. The experimentally confirmed mature miRNAs are assigned a number, which is attached to the “miR” prefix through a hyphen (for example, miR-499). The “miR” can be preceded by a three-letter abbreviation indicating the species (for example, “hsa” for *Homo sapiens*, “mmu” for *Mus musculus*). miRNAs identical in the sequence but transcribed from different regions of the genome are added a numeric suffix with an ordinal number, for example, hsa-miR-219-1 and hsa-miR-219-2. A letter suffix is added to the names of miRNAs, the sequences of which differ slightly (by 1–2 nucleotides), for example, hsa-miR-130a and hsa-miR-130b; they form miRNA families. miRNAs, the genes of which are located physically close to each other and are often transcribed as a single unit, are grouped in clusters, which are named either based on the lowest miRNA number in the cluster (for example, cluster miR-17), or based on the lowest and highest miRNA numbers written through a hyphen (cluster miR-17-92 consisting of miR-17, miR-91, miR-18, miR-19, miR-19b, miR-20, and miR-92) [6].

### Genes and miRNA biogenesis

Depending on their localization relative to the genome components, miRNA genes can be classified as intergenic, intronic, and exonic. About 50% of genes of miRNAs are located within protein-encoding and non-protein-coding genes (host genes), mainly in introns and less frequently in exons. Genes of miRNAs can be transcribed from both independent promoters and the host gene promoter [7]. New miRNA genes are generated as a result of duplication of the existing miRNA genes (as it happens in the majority of cases) or *de novo* from the hairpin structures located within introns or intergenic regions [8]. *De novo* structures emerge by means of different mechanisms: 1) due to inverted duplication of the gene that will become a miRNA target in the future; 2) from transposons; 3) due to spontaneous evolution from random sequences [8].

The most common miRNA biogenesis pathway is referred to as canonical. In addition, other miRNA biogenesis pathways have been reported, which involve other proteins and in which one or more phases of canonical biogenesis are missing; they are referred to as non-canonical [9].

### Canonical pathway of miRNA biogenesis

In animals, primary miRNA (pri-miRNA) is transcribed from the miRNA gene with the help of RNA polymerase II, and then undergoes 5' capping, 3' polyadenylation, and splicing (Fig. 1).

Then a microprocessor complex consisting of ribonuclease III (Drosha) and the DGCR8 protein (DiGeorge Syndrome Critical Region 8 also referred to as Pasha — Partner of Drosha) cuts primary miRNA to pre-miRNA (precursor miRNA), 70–120 nucleotides in length. Pre-miRNA represents a hairpin consisting of the single-stranded region (terminal loop) and double-stranded stem with two nucleotides protruding at the 3' end. The protruding nucleotides are recognized by the exportin-5 (XPO5) protein, which transports pre-miRNA from the nucleus to the cytoplasm with the participation of the GTP-binding protein Ran. In the cytoplasm (Fig. 1, *on the right*), ribonuclease III Dicer cuts the terminal loop out of pre-miRNA, which results in a duplex consisting of two mature miRNAs, 21–24 nucleotides in length [10]. Depending on the mature miRNA strand position in the pre-miRNA hairpin, their names are followed by suffixes -3p or -5p (for example, the hsa-miR-25-5p strand is located at the 5' end of the hsa-miR-25 pre-miRNA, while the hsa-miR-25-3p strand is located at the 3' end). After cutting out the terminal loop, the miRNA duplex binds to the Argonaute (AGO) family protein being part of the RISC complex (RNA-induced silencing complex): thus the intermediate pre-RISC complex is formed. One of two strands of the RNA duplex dissociates and usually undergoes degradation, while the other remains loaded into the miRISC complex. The strand remaining loaded in this complex is referred to as guide strand, while the dissociated one is referred to as passenger strand [10]. This is followed by binding of the guide strand being part of the miRISC complex to the target mRNA.

In plants, the canonical pathway is slightly different from that of animals. Pri-miRNA is processed in the nucleus directly to the miRNA duplex by the Dicer protein homolog, DICER-LIKE 1 (DCL1), which is responsible for both processing events essential for miRNA maturation [4]. In plants, the stem-loop precursor is longer and more variable. In contrast to bilateral animals, plant miRNAs undergo methylation by the HEN1 protein.

### Non-canonical pathways of miRNA biogenesis

Not all proteins of the canonical pathway are involved in processing in non-canonical (alternative) pathways of miRNA maturation. Drosha- and DGSR8-independent (microprocessor-independent), as well as Dicer-independent miRNA biogenesis pathways are distinguished. In the majority of Drosha-independent pathways, miRNA precursors represent products of processing of other RNAs (for example, small nuclear RNA or transfer RNA) and do not need to be hydrolyzed by the microprocessor complex [11]. In Dicer-independent processing, pri-miRNA is hydrolyzed by the microprocessor complex, but the resulting stem of the hairpin structure is too short for Dicer recognition. Therefore, the miRNA precursor is loaded directly onto the AGO protein, which incises one of the miRNA strands, and then the intermediate product obtained using the poly(A)-specific ribonuclease (PARN) is truncated to produce the mature molecule [10].

### Selection of functionally active miRNA strand

Selection of the guide strand between the -5p and -3p strands is associated with thermodynamic instability of the duplex and miRNA nucleotide composition [12]. The 5' end of miRNA



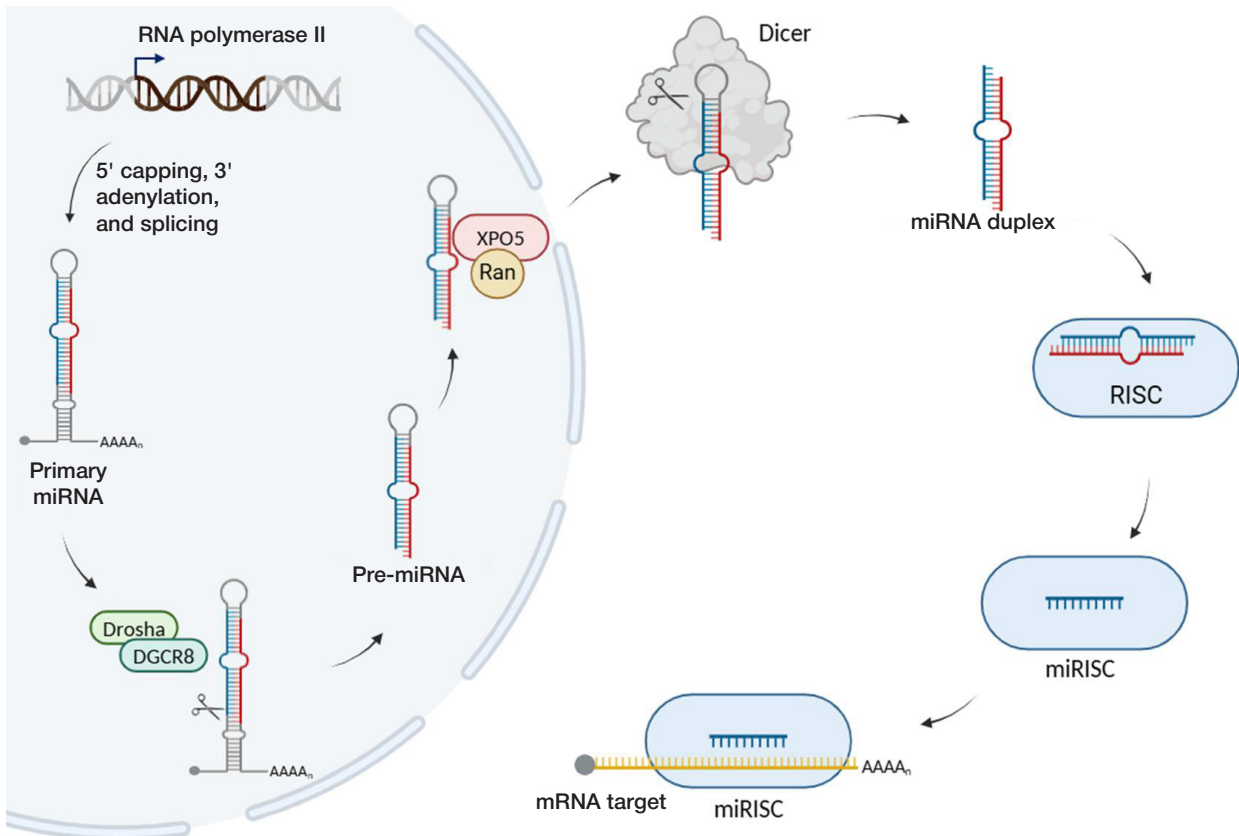


**Fig. 1.** Canonical miRNA biogenesis and generation of the functionally active miRISC complex.  $AAAA_n$  — poly(A) tails at the 3' ends of the mRNA and miRNA molecules; DGCR8 — DiGeorge syndrome critical region 8; Dicer, Drosha — RNase III family endoribonucleases; miRISC — RNA-induced silencing complex bound to the miRNA strand; Ran — Ras-related nuclear protein (GTP-binding nuclear protein); RISC — RNA-induced silencing complex; XPO5 — exportin-5; pre-miRNA — miRNA precursor. The 5' cap is marked with gray circle in the primary miRNA image

duplex is incorporated in specific pocket formed by the MID and PIWI domains of the AGO protein. These domains are sensitive to the nucleotide composition of the duplex and bind uracil twice stronger, than adenine, and 30 times stronger, than cytosine or guanine, i.e. preference is given to the strand that is uracil-rich at the 5' end. AGO is also likely to load the strand showing lower relative thermodynamic stability. It is believed that the first four nucleotides at each end of the duplex are responsible for thermodynamic stability, and the difference in one additional hydrogen bond at one end is enough to affect the choice of the guide and passenger strands. Usually, 5' ends of the degrading passenger strands are pyrimidine-rich, while those of guide strands are purine-rich [12].

### Target mRNA recognition and binding by the miRNA molecule

The miRISC complex bound to the target mRNA interacts with the GW182 protein (182 kDa glycine-tryptophan repeat-containing protein). GW182 functions as a molecular scaffold for linking of the AGO protein being part of the miRISC complex and the downstream effector complexes involved in the miRNA-mediated translational repression of the target mRNA [7].

To facilitate target mRNA recognition and binding, AGO protein ensures spatial positioning of the miRNA guide strand. The miRNA guide strand region between nucleotides 2 and 7 at the 5' end is referred to as seed region; it is responsible for target mRNA binding and is of crucial importance for its recognition [13]. Nucleotides 8 and 13–16 of the miRNA sequence are also involved in recognition [10]. In the mRNA target molecule, the miRISC binding site is usually in the 3'-untranslated region (3'-UTR). Rather rare non-canonical binding sites in the coding

and 5'-UTR regions of mRNA have been reported, during interaction with which miRNAs also suppress mRNA translation. In some cases, miRNAs can interact with promoter regions of genes, thereby ensuring activation of their transcription [14].

### miRNA-mediated gene silencing mechanisms

As stated above, recognition of the target mRNA by the miRNA molecule usually leads to suppression of translation of this mRNA. In the case of complete complementarity observed mainly in plants, the target mRNA is cleaved within miRISC by the AGO protein with RNase H endonuclease activity, in the region complementary to nucleotides 10 and 11 of the miRNA guide strand (endonuclease cleavage of mRNA) [4, 15]. In the majority of animal cells, binding sites within mRNA are not fully complementary to the miRNA seed region. In this case, the miRISC-mediated translation repression and destabilization of mRNA with subsequent degradation are initiated [7].

Despite the fact that the exact mechanisms underlying these processes in mammals remain the matter of debate, it is generally accepted that initially translation repression occurs, followed by destabilization and decay of the target mRNA [16]. Several mechanisms underlying repression of translation have been reported, among which inhibition of the formation of a "closed-loop" structure of the target mRNA (Fig. 2A). The PABPC protein bound to the 3' poly(A) tail of the target mRNA stabilizes interaction between the 5' cap and the eukaryotic translation initiation factor 4F complex consisting of eIF4A, eIF4G and eIF4E through binding to eIF4G. The mRNA ends are brought close together, and the "closed-loop" structure is formed, and thus facilitates translation initiation and ribosome recycling.

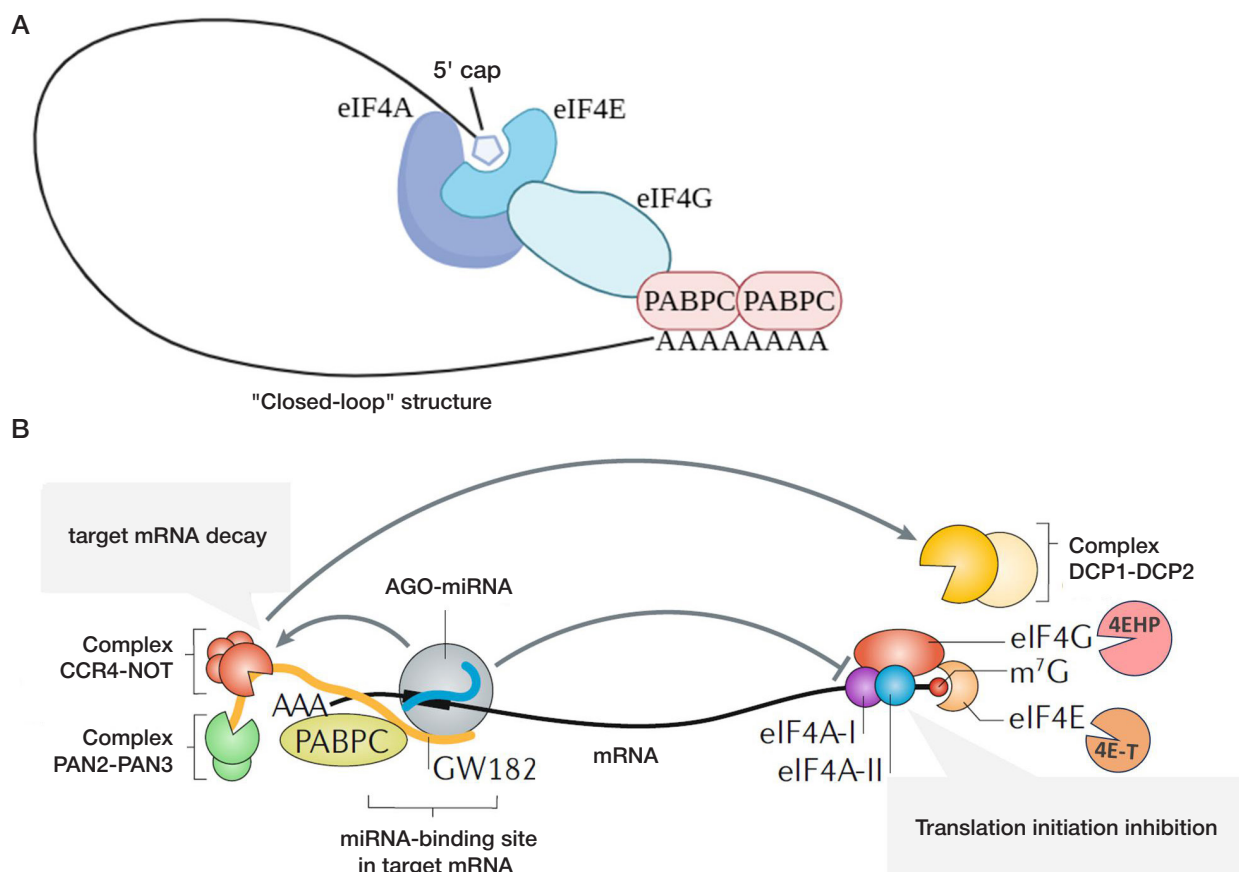


**Fig. 2.** Reported mechanisms underlying miRNA-mediated silencing. **A.** Inhibition of the target mRNA “closed-loop” formation. Under exposure to the RISC complex, PABPC dissociates from the target mRNA poly(A) tail, making it impossible to interact with eIF4G and preventing formation of the “closed-loop” essential for initiation of mRNA translation. **B.** Target mRNA decay (*on the left*) and inhibition of mRNA translation initiation through prevention of the eukaryotic translation initiation factor 4F complex assembly (*on the right*). Target mRNA is marked with *black line*; the GW182 protein representing a scaffold for proteins CCR4-NOT and PAN2-PAN3 is marked with *yellow line*; the guide strand of miRNA being part of the miRISC complex is marked with *light-blue line*. *Gray arrows* point to engagement of the CCR4-NOT complex by the AGO proteins with subsequent recruitment of the DCP1 and DCP2 decapping proteins by the CCR4-NOT complex. Modified from [17]

The AGO protein being part of the miRISC complex causes dissociation of the PABPC protein, which leads to aberrant “closed-loop” formation and inhibition of translation initiation. Other mechanisms include inhibition of mRNA translation via prevention of the eukaryotic translation initiation factor 4F complex assembly. These include attraction of the 4E-T and 4EHP translation inhibitors by the miRISC complex and subsequent dissociation of eIF4E and eIF4G or dissociation of the eIF4A subunit (Fig. 2B, *on the right*). The mechanisms are not mutually exclusive; they can work at different rates at the same time. Predominance of certain mechanism depends on the nature of target mRNA and the cell type [16]. Repression of translation is followed by destabilization of the target mRNA, including deadenylation and decapping with subsequent exonucleolytic degradation of mRNA (miRNA-mediated target mRNA decay) (Fig. 2B, *on the left*). First, proteins of the AGO family recruit the GW182 protein, which interacts with the PABPC poly(A)-binding protein and causes its dissociation from the mRNA poly(A) tail. This increases accessibility of the mRNA poly(A) tail for the CCR4-NOT and PAN2-PAN3 deadenylases, which are also recruited by the GW182 protein. As a result, mRNA deadenylation occurs. Furthermore, the CCR4-NOT complex recruits the DCP1 and DCP2 proteins decapping target mRNA targets, which makes mRNA accessible for degradation by the XRN1 exonuclease [16].

miRNA is characterized by redundancy: expression of one mRNA can be regulated by various miRNAs interacting with its different binding sites. Furthermore, miRNA is pleiotropic: one miRNA can interact with various target mRNAs. In animals, one miRNA has much more targets, than in plants, due to frequently

occurring incomplete complementarity [4]. The combination of such properties results in generation of the complex miRNA-mediated regulatory network.

### miRNA localization in the cell

Previously it was assumed that miRNA performs its function in the cytoplasm only. However, recent studies have shown that the cytoplasmic miRISC complex can be imported to the nucleus [18]. The nuclear miRISC complex is either similar to cytoplasmic one in components, or can exist as a separate AGO-miRNA complex. The nuclear miRISC binds to complementary nuclear transcripts or, if there are none, is exported to the cytoplasm again. Accumulation of miRNA in the cytoplasm or nucleus is partially determined by localization of its target mRNAs. In the nucleus, miRNA can perform several functions: 1) gene expression regulation via binding to their promoter; 2) binding and suppression of function of the long non-coding RNAs; 3) disruption of miRNA biogenesis via binding to pri-miRNA; 4) fine-tuning of target mRNA expression via miRNA retention in the nucleus [19].

It is well known that miRNAs can be released from the cell, to be carried by blood, and to affect other cells of the body, mediating intercellular communication. Outside the cell, miRNAs can be contained in the membrane vesicles (exosomes, microvesicles), as well as in the apoptotic bodies formed when the cells die. In the extracellular environment, the majority of miRNAs (90%) are carried by AGO proteins, the other 10% circulate as complexes with high-density lipoproteins [20].

## miRNA involvement in physiological and pathological processes in the cell

miRNAs regulate almost all processes in the cells: metabolism, cell cycle progression, proliferation, differentiation, and apoptosis, so disruption of their regulatory properties can lead to various diseases [21]. Actually, alterations of miRNA levels in humans are often observed in a broad spectrum of pathologies: tumors, cardiovascular, neurological and autoimmune diseases, inflammation, gastrointestinal tract and skeletal muscle diseases [22]. The role of miRNA has been extensively studied in the context of various disorders since the moment of their discovery, and to date, information has been accumulated about what levels of microRNAs most frequently change in affected tissues in certain conditions, which miRNAs have protective effects and which, on the contrary, contribute to developing pathological phenotype.

miRNAs are examined both directly in the patients' tissue specimens and in *in vivo*, *in vitro* experiments, as well as *in silico*, using the latter approach to construct preliminary hypotheses. Among all patients' biomaterials, biopsy specimens of affected tissues are best suited for investigation of the role of miRNAs in etiopathogenesis, but obtaining them is associated with invasive interventions, so it is usually hardly accessible. In this regard, circulating miRNAs most often become the research object. These are miRNAs that are released into the extracellular space due to tissue damage, apoptosis, necrosis or intense secretion and circulate in the body [7]. Such miRNAs are found in blood serum and plasma, urine, tears, saliva, seminal, peritoneal and cerebrospinal fluids, breast milk and bronchoalveolar lavage [7]. They can regulate the target cell activity, thereby acting as intercellular signaling molecules. For example, endothelium-released miRNAs regulate activity of vascular smooth muscle cells, while oncogenic miRNAs in exosomes increase invasiveness of breast cancer cells [23, 24].

Circulating miRNAs are stable at high pH and temperature and are resistant to degradation, so they seem to be attractive as candidate biomarkers. Actually, there are studies, in which such circulating molecules are used for differential diagnosis, early diagnosis, prediction of the disease course, disease severity assessment, or control over response to therapy [25]. Since miRNAs can regulate translation of several mRNA targets, some authors propose to evaluate diagnostic value of

not only one specific miRNA, but the set of miRNAs (signatures) that would be more specific for the disease [26]. For example, assessment of urinary levels of the set of three miRNAs in individuals with lupus nephritis makes it possible to reveal early renal fibrosis and predict the development of kidney failure [27].

The use of miRNAs for therapeutic purposes is based either on replenishing the levels of essential miRNAs via administration of appropriate synthetic analogues (miRNA mimetics), or on inhibition of target miRNAs via administration of antisense miRNA or sponge RNAs (also referred to as competing endogenous RNAs such as pseudogene transcripts, long non-coding RNAs, circular RNAs and mRNAs, which bind the pool of miRNAs, competing with their targets). Thus, miR-34a suppresses expression of more than 30 oncogenes involved in the tumor cell evasion from the immune system. Since expression of this miRNA is often decreased in various malignant tumors, a synthetic miR-34a mimetic, MRX34, has been developed for treatment of malignant tumors of the skin, lung, kidney, and liver [28]. Currently, a number of biopharmaceutical companies (Santaris Pharma, Roche Pharmaceuticals, Regulus therapeutics, Mirna Therapeutics Inc., miRagen Therapeutics and EnGeneC) have programs focused on using miRNAs for therapy of tumors. Despite the fact that several clinical trials of miRNAs as potential drugs were terminated due to serious side effects and toxicity, studies of the use of miRNAs in therapeutic practice continue and inspire great hope [29].

## CONCLUSION

Thirty years since miRNA discovery is a long time, during which the number of miRNA studies has been increasing steadily. The data accumulated during this period have both expanded our knowledge about the mechanisms underlying gene activity regulation and opened up new horizons in understanding their role in body's physiological and disease processes. In many disorders miRNAs can serve as reliable biomarkers, and in a number of cases miRNA activity modulation is used for treatment of various diseases. However, comprehensive analysis of certain miRNA involvement in cellular processes or pathogenesis of certain diseases is beyond the scope of this review. We have tried to make the reader familiar with the broad range of capabilities of these small RNAs, as well as with the prospects for their further study and use.

## References

- Lee RC, Feinbaum RL, Ambros V. The *C. elegans* heterochronic gene *lin-4* encodes small RNAs with antisense complementarity to *lin-14*. *Cell*. 1993; 75 (5): 843–54. DOI:10.1016/0092-8674(93)90529-Y
- Wightman B, Ha I, Ruvkun G. Posttranscriptional regulation of the heterochronic gene *lin-14* by *lin-4* mediates temporal pattern formation in *C. elegans*. *Cell*. 1993; 75 (5): 855–62. DOI: 10.1016/0092-8674(93)90530-4.
- Reinhart BJ, Slack FJ, Basson M, Pasquinelli AE, Bettinger JC, Rougvie AE, et al. The 21-nucleotide *let-7* RNA regulates developmental timing in *Caenorhabditis elegans*. *Nature*. 2000; 403 (6772): 901–06. DOI: 10.1038/35002607.
- Moran Y, Agron M, Praher D, Technau U. The evolutionary origin of plant and animal microRNAs. *Nat Ecol Evol*. 2017; 1 (3): 27. DOI: 10.1038/s41559-016-0027.
- Dexheimer PJ, Cochella L. MicroRNAs: From Mechanism to Organism. *Front Cell Dev Biol*. 2020; 8: 409. DOI: 10.3389/fcell.2020.00409.
- Bhaskaran M, Mohan M. MicroRNAs: History, Biogenesis, and Their Evolving Role in Animal Development and Disease. *Vet pathol*. 2013; 51 (4): 759. DOI: 10.1177/0300985813502820.
- O'Brien J, Hayder H, Zayed Y, Peng C. Overview of MicroRNA Biogenesis, Mechanisms of Actions, and Circulation. *Front Endocrinol (Lausanne)*. 2018; 9: 402. DOI: 10.3389/fendo.2018.00402.
- Liu N, Okamura K, Tyler DM, Phillips MD, Chung WJ, Lai EC. The evolution and functional diversification of animal microRNA genes. *Cell Res*. 2008; 18 (10): 985. DOI: 10.1038/cr.2008.278.
- Abdelfattah AM, Park C, Choi MY. Update on non-canonical microRNAs. *Biomol Concepts*. 2014; 5 (4): 275. DOI: 10.1515/bmc-2014-0012.
- Treiber T, Treiber N, Meister G. Regulation of microRNA biogenesis and its crosstalk with other cellular pathways. *Nat Rev Mol Cell Biol*. 2019; 20 (1): 5–20. DOI: 10.1038/s41580-018-0059-1.
- Yang JS, Lai EC. Alternative miRNA biogenesis pathways and the interpretation of core miRNA pathway mutants. *Mol Cell*. 2011; 43 (6): 892–903. DOI: 10.1016/j.molcel.2011.07.024.
- Medley JC, Panzade G, Zinovyeva AY. microRNA strand selection: Unwinding the rules. *Wiley Interdiscip Rev RNA*. 2021; 12 (3): e1627. DOI: 10.1002/wrna.1627.



13. Agarwal V, Bell GW, Nam JW, Bartel DP. Predicting effective microRNA target sites in mammalian mRNAs. *Elife*. 2015; 4: e05005. DOI: 10.7554/eLife.05005.
14. Broughton JP, Lovci MT, Huang JL, Yeo GW, Pasquinelli AE. Pairing beyond the Seed Supports MicroRNA Targeting Specificity. *Mol Cell*. 2016; 64 (2): 320–33. DOI: 10.1016/j.molcel.2016.09.004.
15. Pratt AJ, MacRae IJ. The RNA-induced Silencing Complex: A Versatile Gene-silencing Machine. *J Biol Chem*. 2009; 284 (27): 17897. DOI:10.1074/jbc.R900012200.
16. Iwakawa HO, Tomari Y. Life of RISC: Formation, action, and degradation of RNA-induced silencing complex. *Mol Cell*. 2022; 82 (1): 30–43. DOI: 10.1016/j.molcel.2021.11.026.
17. Gebert LFR, MacRae IJ. Regulation of microRNA function in animals. *Nat Rev Mol Cell Biol*. 2019; 20 (1): 21–37. DOI: 10.1038/s41580-018-0045-7.
18. Wong JLL, Ritchie W, Gao D, Lau KA, Gonzalez M, Choudhary A, et al. Identification of nuclear-enriched miRNAs during mouse granulopoiesis. *J Hematol Oncol*. 2014; 7: 42. DOI: 10.1186/1756-8722-7-42.
19. Hu X, Yin G, Zhang Y, Zhu L, Huang H, Lv K. Recent advances in the functional explorations of nuclear microRNAs. *Front Immunol*. 2023; 14: 1097491. DOI: 10.3389/fimmu.2023.1097491.
20. Creemers EE, Tijssen AJ, Pinto YM. Circulating microRNAs: novel biomarkers and extracellular communicators in cardiovascular disease? *Circ Res*. 2012; 110 (3): 483–95. DOI: 10.1161/CIRCRESAHA.111.247452.
21. Ardekani AM, Naeini MM. The Role of MicroRNAs in Human Diseases. *Avicenna J Med Biotechnol*. 2010; 2 (4): 161.
22. Paul P, Chakraborty A, Sarkar D, Langthasa M, Rahman M, Bari M, et al. Interplay between miRNAs and human diseases. *J Cell Physiol*. 2018; 233 (3): 2007–18. DOI: 10.1002/jcp.25854.
23. Zhu JJ, Liu YF, Zhang YP, Zhao CR, Yao WJ, Li YS, et al. VAMP3 and SNAP23 mediate the disturbed flow-induced endothelial microRNA secretion and smooth muscle hyperplasia. *Proc Natl Acad Sci U S A*. 2017; 114 (31): 8271. DOI: 10.1073/pnas.1700561114.
24. Yang M, Chen J, Su F, Yu B, Su F, Lin L, et al. Microvesicles secreted by macrophages shuttle invasion-potentiating microRNAs into breast cancer cells. *Mol Cancer*. 2011; 10: 117. DOI: 10.1186/1476-4598-10-117.
25. Ho PTB, Clark IM, Le LTT. MicroRNA-Based Diagnosis and Therapy. *Int J Mol Sci*. 2022; 23 (13): 7167. DOI: 10.3390/ijms23137167.
26. Backes C, Meese E, Keller A. Specific miRNA Disease Biomarkers in Blood, Serum and Plasma: Challenges and Prospects. *Mol Diagn Ther*. 2016; 20 (6): 509–18. DOI: 10.1007/s40291-016-0221-4.
27. Solé C, Moliné T, Vidal M, Ordi-Ros J, Cortés-Hernández J. An Exosomal Urinary miRNA Signature for Early Diagnosis of Renal Fibrosis in Lupus Nephritis. *Cells*. 2019; 8 (8): 773. DOI: 10.3390/cells8080773.
28. Beg MS, Brenner AJ, Sachdev J, Borad M, Kang YK, Stoudemire J, et al. Phase I study of MRX34, a liposomal miR-34a mimic, administered twice weekly in patients with advanced solid tumors. *Invest new drugs*. 2016; 35 (2): 180. DOI: 10.1007/s10637-016-0407-y.
29. Seyhan AA. Trials and Tribulations of MicroRNA Therapeutics. *Int J Mol Sci*. 2024; 25 (3): 1469. DOI: 10.3390/ijms25031469.

## Литература

1. Lee RC, Feinbaum RL, Ambros V. The *C. elegans* heterochronic gene *lin-4* encodes small RNAs with antisense complementarity to *lin-14*. *Cell*. 1993; 75 (5): 843–54. DOI:10.1016/0092-8674(93)90529-Y
2. Wightman B, Ha I, Ruvkun G. Posttranscriptional regulation of the heterochronic gene *lin-14* by *lin-4* mediates temporal pattern formation in *C. elegans*. *Cell*. 1993; 75 (5): 855–62. DOI: 10.1016/0092-8674(93)90530-4.
3. Reinhart BJ, Slack FJ, Basson M, Pasquinelli AE, Bettinger JC, Rougvie AE, et al. The 21-nucleotide *let-7* RNA regulates developmental timing in *Caenorhabditis elegans*. *Nature*. 2000; 403 (6772): 901–06. DOI: 10.1038/35002607.
4. Moran Y, Agron M, Praher D, Technau U. The evolutionary origin of plant and animal microRNAs. *Nat Ecol Evol*. 2017; 1 (3): 27. DOI: 10.1038/s41559-016-0027.
5. Dexheimer PJ, Cochella L. MicroRNAs: From Mechanism to Organism. *Front Cell Dev Biol*. 2020; 8: 409. DOI: 10.3389/fcell.2020.00409.
6. Bhaskaran M, Mohan M. MicroRNAs: History, Biogenesis, and Their Evolving Role in Animal Development and Disease. *Vet pathol*. 2013; 51 (4): 759. DOI: 10.1177/0300985813502820.
7. O'Brien J, Hayder H, Zayed Y, Peng C. Overview of MicroRNA Biogenesis, Mechanisms of Actions, and Circulation. *Front Endocrinol (Lausanne)*. 2018; 9: 402. DOI: 10.3389/fendo.2018.00402.
8. Liu N, Okamura K, Tyler DM, Phillips MD, Chung WJ, Lai EC. The evolution and functional diversification of animal microRNA genes. *Cell Res*. 2008; 18 (10): 985. DOI: 10.1038/cr.2008.278.
9. Abdelfattah AM, Park C, Choi MY. Update on non-canonical microRNAs. *Biomol Concepts*. 2014; 5 (4): 275. DOI: 10.1515/bmc-2014-0012.
10. Treiber T, Treiber N, Meister G. Regulation of microRNA biogenesis and its crosstalk with other cellular pathways. *Nat Rev Mol Cell Biol*. 2019; 20 (1): 5–20. DOI: 10.1038/s41580-018-0059-1.
11. Yang JS, Lai EC. Alternative miRNA biogenesis pathways and the interpretation of core miRNA pathway mutants. *Mol Cell*. 2011; 43 (6): 892–903. DOI: 10.1016/j.molcel.2011.07.024.
12. Medley JC, Panzade G, Zinovyeva AY. microRNA strand selection: Unwinding the rules. *Wiley Interdiscip Rev RNA*. 2021; 12 (3): e1627. DOI: 10.1002/wrna.1627.
13. Agarwal V, Bell GW, Nam JW, Bartel DP. Predicting effective microRNA target sites in mammalian mRNAs. *Elife*. 2015; 4: e05005. DOI: 10.7554/eLife.05005.
14. Broughton JP, Lovci MT, Huang JL, Yeo GW, Pasquinelli AE. Pairing beyond the Seed Supports MicroRNA Targeting Specificity. *Mol Cell*. 2016; 64 (2): 320–33. DOI: 10.1016/j.molcel.2016.09.004.
15. Pratt AJ, MacRae IJ. The RNA-induced Silencing Complex: A Versatile Gene-silencing Machine. *J Biol Chem*. 2009; 284 (27): 17897. DOI:10.1074/jbc.R900012200.
16. Iwakawa HO, Tomari Y. Life of RISC: Formation, action, and degradation of RNA-induced silencing complex. *Mol Cell*. 2022; 82 (1): 30–43. DOI: 10.1016/j.molcel.2021.11.026.
17. Gebert LFR, MacRae IJ. Regulation of microRNA function in animals. *Nat Rev Mol Cell Biol*. 2019; 20 (1): 21–37. DOI: 10.1038/s41580-018-0045-7.
18. Wong JLL, Ritchie W, Gao D, Lau KA, Gonzalez M, Choudhary A, et al. Identification of nuclear-enriched miRNAs during mouse granulopoiesis. *J Hematol Oncol*. 2014; 7: 42. DOI: 10.1186/1756-8722-7-42.
19. Hu X, Yin G, Zhang Y, Zhu L, Huang H, Lv K. Recent advances in the functional explorations of nuclear microRNAs. *Front Immunol*. 2023; 14: 1097491. DOI: 10.3389/fimmu.2023.1097491.
20. Creemers EE, Tijssen AJ, Pinto YM. Circulating microRNAs: novel biomarkers and extracellular communicators in cardiovascular disease? *Circ Res*. 2012; 110 (3): 483–95. DOI: 10.1161/CIRCRESAHA.111.247452.
21. Ardekani AM, Naeini MM. The Role of MicroRNAs in Human Diseases. *Avicenna J Med Biotechnol*. 2010; 2 (4): 161.
22. Paul P, Chakraborty A, Sarkar D, Langthasa M, Rahman M, Bari M, et al. Interplay between miRNAs and human diseases. *J Cell Physiol*. 2018; 233 (3): 2007–18. DOI: 10.1002/jcp.25854.
23. Zhu JJ, Liu YF, Zhang YP, Zhao CR, Yao WJ, Li YS, et al. VAMP3 and SNAP23 mediate the disturbed flow-induced endothelial microRNA secretion and smooth muscle hyperplasia. *Proc Natl Acad Sci U S A*. 2017; 114 (31): 8271. DOI: 10.1073/pnas.1700561114.
24. Yang M, Chen J, Su F, Yu B, Su F, Lin L, et al. Microvesicles secreted by macrophages shuttle invasion-potentiating microRNAs into breast cancer cells. *Mol Cancer*. 2011; 10: 117. DOI: 10.1186/1476-4598-10-117.
25. Ho PTB, Clark IM, Le LTT. MicroRNA-Based Diagnosis and Therapy. *Int J Mol Sci*. 2022; 23 (13): 7167. DOI: 10.3390/ijms23137167.
26. Backes C, Meese E, Keller A. Specific miRNA Disease Biomarkers in Blood, Serum and Plasma: Challenges and Prospects. *Mol Diagn Ther*. 2016; 20 (6): 509–18. DOI: 10.1007/s40291-016-0221-4.
27. Solé C, Moliné T, Vidal M, Ordi-Ros J, Cortés-Hernández J. An Exosomal Urinary miRNA Signature for Early Diagnosis of

- Renal Fibrosis in Lupus Nephritis. *Cells*. 2019; 8 (8): 773. DOI: 10.3390/cells8080773.
28. Beg MS, Brenner AJ, Sachdev J, Borad M, Kang YK, Stoudemire J, et al. Phase I study of MRX34, a liposomal miR-34a mimic, administered twice weekly in patients with advanced solid tumors. *Invest new drugs*. 2016; 35 (2): 180. DOI: 10.1007/s10637-016-0407-y.
29. Seyhan AA. Trials and Tribulations of MicroRNA Therapeutics. *Int J Mol Sci*. 2024; 25 (3): 1469. DOI: 10.3390/ijms25031469.

## PREDICTIVE MODEL FOR MORTALITY IN PATIENTS WITH ABDOMINAL SEPSIS

Osikov MV<sup>1,3</sup> ✉, Telesheva LF<sup>1</sup>, Konashov AG<sup>1,2</sup>, Konashov VA<sup>1,2</sup>, Gusev AV<sup>1,3</sup>, Boyko MS<sup>1</sup><sup>1</sup> South Ural State Medical University, Chelyabinsk, Russia<sup>2</sup> City Clinical Hospital No. 8, Chelyabinsk, Russia<sup>3</sup> Chelyabinsk Regional Clinical Hospital, Chelyabinsk, Russia

Mortality among patients with various forms of sepsis is 36.2–47.7%. Predicting the likelihood of death associated with sepsis is critically important for clinical decision-making, stratifying patient risk, and improving overall survival. The study aimed to develop a mathematical model for predicting the outcome of sepsis in patients with abdominal surgical pathology. The study involved 64 patients diagnosed with abdominal sepsis (AS). Based on the AS outcomes, group 1 ( $n = 46$ ) with favorable outcomes and group 2 ( $n = 18$ ) with fatal outcomes were allocated. Clinical scales and laboratory testing methods were used to evaluate parameters on days 1, 3, and 7 since the AS diagnosis. On days 3 and 7, SOFA scores of the group with adverse AS outcomes were significantly higher, than that of the group with favorable outcomes. Complete blood counts of patients in group 2 showed the decrease in absolute lymphocyte counts on day 1 compared to group 1. As for blood biochemistry parameters, elevated serum levels of C-reactive protein, urea, creatinine, lactate, procalcitonin, direct bilirubin, as well as aspartate aminotransferase, alanine aminotransferase, and alkaline phosphatase activity were observed. Furthermore, a decrease in respiratory index on days 3 and 7 and venous oxygen saturation on days 1 and 7 was observed. A logistic regression model was constructed, and a software tool "Calculator for Predicting Mortality in AS" was developed. A model to predict the probability of fatal outcome in patients with AS was created. High serum CRP and creatinine levels, as well as the decrease in venous oxygen saturation serve as significant prognostic markers of fatal outcome in patients with AS.

**Keywords:** abdominal sepsis, mortality, prognosis, model**Author contribution:** Osikov MV, Telesheva LF, Konashov AG — study concept and design; Konashov VA, Konashov AG, Gusev AV, Boyko MS — data acquisition and processing; Konashov VA, Konashov AG — manuscript writing; Osikov MV — editing.**Compliance with ethical standards:** the study was approved by the Ethics Committee of the South Ural State Medical University (protocol No. 10 dated 02 November 2023).✉ **Correspondence should be addressed:** Mikhail V. Osikov  
prof.osikov@yandex.ru**Received:** 31.01.2025 **Accepted:** 14.02.2025 **Published online:** 23.02.2025**DOI:** 10.24075/brsmu.2025.008**Copyright:** © 2025 by the authors. **Licensee:** Pirogov University. This article is an open access article distributed under the terms and conditions of the Creative Commons Attribution (CC BY) license (<https://creativecommons.org/licenses/by/4.0/>).

## МОДЕЛЬ ПРОГНОЗА ВЕРОЯТНОСТИ ЛЕТАЛЬНОГО ИСХОДА У БОЛЬНЫХ С АБДОМИНАЛЬНЫМ СЕПСИСОМ

М. В. Осиков<sup>1,3</sup> ✉, Л. Ф. Телешева<sup>1</sup>, А. Г. Конашов<sup>1,2</sup>, В. А. Конашов<sup>1,2</sup>, А. В. Гусев<sup>1,3</sup>, М. С. Бойко<sup>1</sup><sup>1</sup> Южно-Уральский государственный медицинский университет, Челябинск, Россия<sup>2</sup> Городская клиническая больница № 8, Челябинск, Россия<sup>3</sup> Челябинская областная клиническая больница, Челябинск, Россия

Летальность среди пациентов с различными формами сепсиса составляет 36,2–47,7%. Прогнозирование вероятности летального исхода при сепсисе критически важно для принятия клинических решений, стратификации риска пациентов и улучшения общей выживаемости. Целью исследования было разработать математическую модель прогноза исхода сепсиса у пациентов с абдоминальной хирургической патологией. Исследование выполняли на 64 больных с диагностированным абдоминальным сепсисом (АС). В зависимости от исходов АС были выделены группа 1 ( $n = 46$ ) с благоприятным исходом и группа 2 ( $n = 18$ ) с летальным исходом. Использовали клинические шкалы и лабораторные методы исследования с оценкой показателей на 1, 3 и 7 сутки с момента диагностирования АС. На 3 и 7 сутки показатели SOFA в группе с неблагоприятным исходом АС были значимо выше, чем в группе с благоприятным исходом. В общем анализе крови у пациентов в группе 2 наблюдалось уменьшение абсолютного количества лимфоцитов на 1 сутки в сравнении с группой 1. Среди биохимических показателей выявлено увеличение концентрации в сыворотке С-реактивного белка, мочевины, креатинина, лактата, прокальцитонина, прямого билирубина, активности аспартатаминотрансферазы, аланинаминотрансферазы и щелочной фосфатазы. Также в группе 2 выявлено снижение респираторного индекса на 3 и 7 сутки, насыщения венозной крови кислородом — на 1 и 7 сутки. Построена модель логистической регрессии и создана программа для ЭВМ «Калькулятор прогноза летальности при АС». Разработана модель вероятности летального исхода у пациентов с АС. Высокий уровень С-РБ, креатинина в сыворотке крови, а также снижение насыщения венозной крови кислородом служат значимыми прогностическими маркерами летального исхода у пациентов с АС.

**Ключевые слова:** абдоминальный сепсис, летальность, прогноз, модель**Вклад авторов:** М. В. Осиков, Л. Ф. Телешева, А. Г. Конашов — концепция и дизайн исследования; В. А. Конашов, А. Г. Конашов, А. В. Гусев, М. С. Бойко — сбор и обработка материала; В. А. Конашов, А. Г. Конашов — написание текста; М. В. Осиков — редактирование.**Соблюдение этических стандартов:** исследование одобрено этическим комитетом ФГБОУ ВО ЮУГМУ Минздрава России (протокол № 10 от 02 ноября 2023 г.).✉ **Для корреспонденции:** Михаил Владимирович Осиков  
prof.osikov@yandex.ru**Статья получена:** 31.01.2025 **Статья принята к печати:** 14.02.2025 **Опубликована онлайн:** 23.02.2025**DOI:** 10.24075/vrgmu.2025.008**Авторские права:** © 2025 принадлежат авторам. **Лицензиат:** РНИМУ им. Н. И. Пирогова. Статья размещена в открытом доступе и распространяется на условиях лицензии Creative Commons Attribution (CC BY) (<https://creativecommons.org/licenses/by/4.0/>).

Sepsis is a model disorder underpinned by body's response to infection of various genesis (bacterial, viral, fungal) in the form of generalized (systemic) inflammation resulting in acute multiple organ dysfunction [1]. Mortality among patients with various forms of sepsis admitted to intensive care units all over the world is 36.2–47.7% [2]. In sepsis, the most common sources of infection are lungs (64%), abdominal cavity (20%), circulatory system (15%), and urinary tract (14%) [3].

Abdominal sepsis (AS) is a syndrome underpinned by body's systemic inflammatory response to intra-abdominal infection resulting in acute organ dysfunction [4]. Intra-abdominal infections rank second among the causes of sepsis after pulmonary lesions [4]. Complicated intra-abdominal infections lead to the development of local or diffuse peritonitis, thereby causing organ failure and eventually AS [4]. The AS-associated mortality varies between 7.6 and 36% [4].

Many clinical and laboratory markers are not sensitive and specific enough for prediction of sepsis outcomes due to complex pathophysiological mechanisms. Today, the WSES (World Society of Emergency Surgery) sepsis severity score is used to predict the course of AS in patients with complicated intra-abdominal infections, and the PIPAS severity score is used in patients with acute peritonitis to determine treatment efficacy and mortality rate [5, 6]. A multi-marker approach will make it possible to construct a mathematical model of a patient depending on the disease outcome, as well as to characterize a personal forecast. In recent years, the algorithms for predicting AS outcomes involving the use of the Akaike information criterion (AIC) for linear regression models were superior to conventional statistical methods [7]. The mathematical model for predicting the probability of fatal outcome in patients with AS will make it possible to change surgical treatment tactics, ensure timely determination of indications for extracorporeal methods of treatment (selective cytokine hemoadsorption combined with adsorption of lipopolysaccharides, hemodiafiltration, plasma exchange, selective plasma filtration) and intensify therapy.

The study aimed to develop a mathematical model for predicting fatal outcome of sepsis in patients with abdominal surgical pathology.

## METHODS

We conducted a cross-sectional study by the continuous sampling methods as patients with abdominal surgical pathology were admitted to the intensive care unit of the Chelyabinsk City Clinical Hospital No. 8, who earlier underwent surgery involving debridement of primary lesion within the first 24 h of hospital stay. All patients of the sample were diagnosed with sepsis in accordance with the current Sepsis-3 concept. The sample was represented by 64 patients aged 32–82 years. Inclusion criteria: age over 18 years; availability of written informed consent, abdominal surgery within the first 24 h of ongoing hospital stay; verified focus of intra-abdominal infection (bacterial culture test and / or direct monitoring of the site of infection); organ dysfunction (SOFA score > 2 points). Exclusion criteria: developing intra-abdominal infection during the hospital stay; preceding immunotropic, antibacterial therapy, taking anticoagulants within 90 days; malignant neoplasms; history of autoimmune disorder, allergy, immunodeficit; earlier diagnosed hereditary disorders of hemostasis; pregnancy.

Dependence on the disease outcome was chosen as a criterion for patient division: group 1 was formed 1 ( $n = 46$ ) with beneficial AS outcomes and group 2 ( $n = 18$ ) with fatal AS outcomes. In accordance with the Sepsis-3 concept the patient condition severity was assessed using the Sequential Organ

Failure Assessment (SOFA) Score [8, 9]. Thrombohemorrhagic disorders were assessed using the International Society on Thrombosis and Haemostasis ISTH/SSC score, criteria for sepsis-induced coagulopathy (SIC) [10].

Whole peripheral blood, its plasma and serum were used for laboratory testing. Partial pressure of arterial oxygen ( $\text{PaO}_2$ ) for calculation of respiratory index ( $\text{PaO}_2/\text{FiO}_2$ ), acid-base balance of venous blood (blood pH), bicarbonate ion concentration (SB), base excess or deficit (BE), venous oxygen saturation ( $\text{SvO}_2$ ) were tested using the ABL 800 FLEX radiometer (Radiometer Medical ApS, Denmark). Serum biochemistry indicators ( $\alpha$ -amylase, total and direct bilirubin, aspartate aminotransferase (AST), alanine aminotransferase (ALT), urea, creatinine, alkaline phosphatase, blood glucose, lactate) were tested using the Mindray BS — 800 M biochemical analyzer (Mindray, China). Complete blood counts were determined using the Sysmex XT — 1800i / XT – 2000i analyzer (Sysmex, Japan). Prothrombin time (PT), prothrombin index (PI), international normalized ratio (INR), activated partial thromboplastin time (aPTT), plasma fibrinogen concentration were assessed using the Technology Solution coagulometer (Technology Solution, Japan). Serum concentrations of procalcitonin and standard C-reactive protein (CRP) were determined by enzyme immunoassay using the Personal Lab analyzer (Adaltis, Italy).

Statistical processing of the results was performed using the SPSS 17.0 software package (IBM, USA). To describe quantitative traits, the median (Me), lower and upper quartiles (LQ; UQ) were calculated. A distribution was tested for normality using the Kolmogorov–Smirnov test. Based on quantitative traits the groups of patients were compared using the Kruskal–Wallis test and Mann–Whitney  $U$  test. The confidence level was  $p < 0.05$ . The data obtained were used when developing a software tool for predicting sepsis outcomes in patients with abdominal surgical pathology by the logistic regression method.

## RESULTS

Among patients with AS, fatal outcomes were reported in 18 individuals (28.1%) during the follow-up period. The analysis of clinical prognostic scores showed that SOFA scores reported on days 3 and 7 in the group with adverse AS outcomes were significantly higher, than in the group with beneficial outcomes (Table 1).

In the group of patients with adverse AS outcomes, complete blood counts reported on days 1 and 3 showed anemia with the red blood cell counts, hemoglobin concentration, hematocrit decreased relative to the generally accepted reference values, as well as with thrombocytopenia, leukocytosis and neutrophilia, lymphocytopenia. During follow-up absolute basophil and eosinophil counts were elevated on day 7, and monocyte counts were elevated on days 3 and 7 (Table 2). In the group of patients with beneficial outcomes, there was a significant increase in absolute eosinophil counts on day 7 relative to the indicators reported on days 1 and 3. In patients with adverse AS outcomes, a significant decrease in absolute lymphocyte and monocyte counts relative to the group with beneficial AS outcomes was observed on day 1.

In patients with AS of both groups, high CRP, procalcitonin and direct bilirubin levels relative to reference values were reported on days 1, 3, and 7 (Table 3). The group of patients with adverse AS outcomes also showed growth of serum urea, creatinine, lactate and alkaline phosphatase levels. During follow-up of the group of patients with adverse AS outcomes there was a significant decrease in concentrations of  $\alpha$ -amylase, direct and total bilirubin on day 7 relative to the indicators



**Table 1.** Clinical and prognostic scores of patients with beneficial and adverse AS outcomes, Me (LQ; UQ)

Indicators	Group 1 — patients with beneficial AS outcomes (n = 46)			Group 2 — patients with adverse AS outcomes (n = 18)		
	Day 1 (n = 46)	Day 3 (n = 46)	Day 7 (n = 46)	Day 1 (n = 18)	Day 3 (n = 14)	Day 3 (n = 10)
SOFA, points	6.0 [5.0; 9.0]	5.0 [3.0; 8.0]	5.0 [2.5; 10.0]	8.0 [5.0; 14.0]	12.0 [8.0; 14.0]*	10.0 [10.0; 10.0]*
SIC score, points	4.00 [4.00; 5.00]	4.00 [4.00; 5.00]	4.5 [4.00; 5.00]	4.00 [4.00; 5.00]	4.00 [4.00; 5.00]	5.00 [4.00; 5.00]
DIC 1 score, points	4.00 [4.00; 5.00]	4.00 [4.00; 5.00]	4.00 [4.00; 5.50]	4.00 [4.00; 4.00]	5.00 [4.00; 6.00]	5.00 [5.00; 5.00]

**Note:** \* — significant ( $p < 0.05$ ) differences from group 1 on appropriate day.

reported on days 1 and 3. In contrast, ALT activity significantly increased on days 3 and 7, and AST activity increased on day 7 relative to day 1. Serum lactate concentration significantly decreased on days 3 and 7 relative to day 1. Procalcitonin levels significantly increased on day 3 and decreased on day 7 relative to days 1 and 3, respectively. In the group of patients with beneficial AS outcomes there was a significant decrease in serum concentrations of total bilirubin on day 3, as well as of direct bilirubin and procalcitonin levels on days 3 and 7 relative to day 1. In the group of patients with adverse AS outcomes, a significant increase in serum CRP, urea, creatinine, and lactate levels was reported on day 1 relative to the group with beneficial AS outcomes. During follow-up, concentrations of procalcitonin, urea, creatinine, AST, ALT, direct bilirubin and alkaline phosphatase increased on day 3, and concentrations of procalcitonin, creatinine, urea, ALT, alkaline phosphatase and C-reactive protein increased on day 7. In patients with adverse outcomes, GFR was significantly lower on days 3 and 7.

In patients with AS of both groups on all days of follow-up there was growth of D-dimer, fibrinogen and INR relative to reference values. Growth of aPTT and PT was reported for the group with adverse outcomes on day 1 (Table 4). In the group of patients with adverse AS outcomes, there was a significant decrease in PT, INR, and D-dimer levels on day 3 relative to day 1. During follow-up, there was also a significant decrease in

D-dimer levels, aPTT, and PT on day 7 relative to that reported on day 1, along with PI relative to days 1 and 3. A significant decrease in PI on day 7 relative to the values reported on days 1 and 3 was revealed in patients of the group with beneficial outcomes. Patients with adverse AS outcomes showed a significant PI decrease on days 3 and 7, along with the increase in aPTT and PT on day 1 relative to the group with beneficial AS outcomes.

In patients with AS of groups 1 and 2, low respiratory index ( $\text{PaO}_2/\text{FiO}_2$ ), venous oxygen saturation ( $\text{SvO}_2$ ) relative to the generally accepted reference values had been reported throughout all days of follow-up. When interpreting the acid-base balance of patients with adverse AS outcomes, decompensated metabolic acidosis was reported on day 1 of follow-up, and in the group of patients with beneficial AS outcomes there was compensated metabolic acidosis on days 1 and 3 (Table 5). In the group of patients with adverse AS outcomes, there was a significant increase in bicarbonate ion levels (SB) relative to the values reported on day 3, as well as the decrease in  $\text{PaO}_2/\text{FiO}_2$  on day 7 relative to days 1 and 3. In the group of patients with adverse outcomes there was a significant decrease in  $\text{PaO}_2/\text{FiO}_2$  on days 3 and 7 and the decrease in  $\text{SvO}_2$  on days 1 and 7 relative to the group of patients with beneficial AS outcomes. Similar alterations were reported for venous blood pH and SB concentration on day 1.

**Table 2.** Complete blood counts of patients with AS, Me (LQ; UQ)

Indicators/reference values	Group 1 — beneficial AS outcome (n = 46)			Group 2 — adverse AS outcome (n = 18)		
	Day 1 (n = 46)	Day 3 (n = 46)	Day 7 (n = 46)	Day 1 (n = 18)	Day 3 (n = 14)	Day 7 (n = 10)
Red blood cells / $3.5\text{--}6 \times 10^{12}/\text{L}$	4.10 [3.16; 4.87]	3.67 [3.56; 4.05]	3.67 [3.48; 4.16]	3.50 [2.93; 3.85]	3.65 [3.54; 3.84]	4.23 [3.18; 4.45]
Hemoglobin / 120–160 г/л	113.00 [95.00; 135.00]	105.00 [99.00; 117.00]	109.50 [102.00; 118.50]	101.50 [83.00; 130.00]	109.00 [89.00; 125.00]	118.00 [102.00; 128.00]
Hematocrit / 32–52%	32.70 [28.90; 40.10]	31.15 [29.30; 33.90]	32.10 [30.50; 35.15]	29.25 [24.00; 36.40]	31.20 [26.00; 35.70]	35.90 [29.80; 37.00]
Platelets / $150\text{--}400 \times 10^9/\text{L}$	184.00 [135.00; 320.00]	252.00 [156.00; 346.00]	194.50 [142.50; 307.50]	147.00 [92.00; 190.00]	122.00 [36.00; 292.00]	132.00 [116.00; 356.00]
White blood cells / $3.5\text{--}11 \times 10^9/\text{L}$	16.88 [9.39; 24.20]	12.64 [9.62; 15.14]	10.76 [8.37; 13.84]	16.29 [13.86; 18.56]	13.37 [6.46; 20.59]	12.29 [11.41; 17.87]
Neutrophils / $1.5\text{--}7.5 \times 10^9/\text{L}$	15.25 [7.77; 22.77]	10.81 [7.65; 13.32]	9.04 [6.21; 12.41]	15.23 [12.41; 18.93]	10.71 [4.84; 17.93]	10.72 [8.49; 15.98]
Lymphocytes / $1\text{--}4 \times 10^9/\text{L}$	1.59 [0.51; 3.77]	0.84 [0.53; 1.87]	0.76 [0.39; 2.13]	0.71 [0.31; 0.96]*	0.86 [0.18; 2.55]	0.72 [0.49; 1.28]
Basophils / $0\text{--}0.1 \times 10^9/\text{L}$	0.02 [0.01; 0.14]	0.03 [0.02; 0.04]	0.02 [0.01; 0.06]	0.01 [0; 0.01]*	0.01 [0; 0.06]	0.02 [0.01; 0.05]#
Eosinophils / $0\text{--}0.4 \times 10^9/\text{L}$	0.01 [0.01; 0.27]	0.03 [0.01; 0.13]	0.38 [0.11; 0.66]#s	0.01 [0; 0.29]	0.01 [0; 0.16]	0.44 [0.41; 0.64]#s
Monocytes / $0\text{--}0.7 \times 10^9/\text{L}$	0.59 [0.06; 1.4]	0.51 [0.31; 0.94]	0.60 [0.28; 1.27]	0.11 [0.06; 0.18]*	0.70 [0.45; 2.19]#	0.73 [0.46; 1.66]#

**Note:** \* — significant ( $p < 0.05$ ) differences from group 1 on appropriate day; # — differences from indicators reported on day 1 for appropriate group; s — differences from indicators reported on day 3 for appropriate group.

Table 3. Biochemistry indicators of patients with AS, Me (LQ; UQ)

Indicators/reference values	Group 1 — beneficial AS outcomes (n = 46)			Group 2 — adverse AS outcome (n = 18)		
	Day 1 (n = 46)	Day 3 (n = 46)	Day 7 (n = 46)	Day 1 (n = 18)	Day 3 (n = 14)	Day 7 (n = 10)
α-Amylase / 28–100 U/L	27.91 [22.52; 90.67]	36.51 [16.74; 69.18]	47.39 [26.14; 68.51]	57.33 [43.50; 75.61]	52.20 [29.97; 74.42]	25.28 [20.74; 29.59] <sup>§</sup>
Total bilirubin / 0–20.5 μmol/L	23.89 [11.72; 57.93]	9.75 [8.45; 17.89] <sup>#</sup>	14.78 [7.61; 23.14]	17.80 [13.46; 66.86]	15.30 [9.97; 32.96]	10.99 [9.55; 12.96] <sup>§</sup>
Direct bilirubin / 0–5.1 μmol/L	20.38 [8.12; 48.55]	6.53 [4.20; 8.99] <sup>#</sup>	9.81 [4.53; 14.73] <sup>#</sup>	11.80 [10.45; 61.36]	15.30 [9.97; 32.96] <sup>*</sup>	9.25 [5.26; 9.96] <sup>§</sup>
ALT / 0–40 U/L	20.00 [15.00; 29.00]	18.50 [15.00; 23.00]	15.00 [11.50; 21.00]	16.00 [13.00; 22.00]	29.00 [22.00; 196.00] <sup>**</sup>	27.00 [21.00; 39.00] <sup>**</sup>
AST / 0–40 U/L	33.00 [27.00; 49.00]	30.00 [20.00; 37.00]	29.50 [18.50; 41.50]	24.00 [20.00; 44.00]	48.00 [32.00; 1070.00] <sup>*</sup>	33.00 [28.00; 35.00] <sup>#</sup>
C-reactive protein / 0–6 mg/L	152.68 [128.18; 249.62]	171.15 [111.79; 203.17]	115.17 [64.71; 193.28]	326.89 [252.93; 361.27] <sup>*</sup>	224.76 [163.83; 369.78]	274.27 [269.26; 308.39] <sup>*</sup>
Procalcitonin, ng/mL	19.40 [5.10; 22.90]	2.80 [1.10; 4.50] <sup>#</sup>	1.50 [0.80; 4.10] <sup>#</sup>	19.10 [17.00; 28.20]	21.10 [19.80; 22.40] <sup>**</sup>	10.00 [1.20; 12.00] <sup>§*</sup>
Urea / 1,7–8.3 mmol/L	8.70 [7.80; 15.70]	7.90 [4.80; 12.80]	7.30 [4.50; 14.00]	15.90 [13.40; 23.60] <sup>*</sup>	18.30 [11.80; 25.10] <sup>*</sup>	19.80 [11.00; 21.00] <sup>*</sup>
Creatinine / 62–106 μmol/L	102.67 [74.83; 118.85]	70.28 [58.11; 112.52]	66.55 [57.03; 110.43]	170.29 [102.00; 316.08] <sup>*</sup>	263.52 [146.36; 345.00] <sup>*</sup>	215.72 [116.97; 217.10] <sup>*</sup>
GFR / 90–150 mL/min	55.0 [50.0; 60.0]	55.0 [50.0; 60.0]	60.0 [52.5; 65.0]	40.0 [40.0; 55.0]	40.0 [35.0; 50.0] <sup>*</sup>	45.0 [40.0; 50.0] <sup>*</sup>
Alkaline phosphatase / 40–130 U/L	90.88 [67.25; 98.86]	86.56 [69.21; 98.90]	87.30 [68.45; 104.33]	94.90 [84.88; 144.34]	175.50 [102.81; 305.24] <sup>*</sup>	133.70 [103.84; 151.96] <sup>*</sup>
Blood glucose / 3.3–6.1 mmol/L	7.40 [4.80; 8.90]	6.40 [5.80; 9.10]	6.90 [5.60; 9.00]	5.90 [4.50; 19.10]	6.60 [4.70; 16.70]	8.30 [7.70; 9.40]
Venous lactate / 0.5–1.6 mmol/L	1.70 [1.50; 2.00]	1.70 [1.30; 2.10]	1.80 [1.50; 2.50]	4.150 [3.90; 20.00] <sup>*</sup>	1.60 [1.30; 3.20] <sup>#</sup>	2.50 [2.20; 3.00] <sup>#</sup>

Note: \* — significant ( $p < 0.05$ ) differences from group 1 on appropriate day; # — differences from indicators reported on day 1 for appropriate group; § — differences from indicators reported on day 3 for appropriate group.

A logistic regression model was constructed and a software tool “Calculator for Predicting Mortality in Abdominal Sepsis” was developed based on the data obtained to determine the probability of fatal outcomes in patients with AS [11]. Indicators were selected by constructing logistic regression models and step-by-step elimination of traits. The resulting model included three indicators: SvO<sub>2</sub>, SRP concentration, and serum creatinine levels. ROC curve was selected as a metrics for the model for predicting fatal outcomes in AS (see Figure).

Considering the SvO<sub>2</sub>, serum SRP and creatinine level values, the tool estimates the AS-associated mortality forecast expressed as a percentage. The relationship observed is described by the following equation:

$$P = 1 / (1 + \exp(-3.192989 - 0.081246 \times \text{SvO}_2 + 0.016764 \times \text{CRP} + 0.014123 \times \text{creatinine})),$$

where P is the likelihood of fatal outcome (%), SvO<sub>2</sub> is venous oxygen saturation (%), CRP is serum concentration of C-reactive protein (mg/L), creatinine is serum creatinine level (μmol/L).

According to our data and the model constructed, fatal outcomes of AS are more common in patients with high serum concentrations of CRP (above 30 mg/L), creatinine (above 70 μmol/L), as well as with low SvO<sub>2</sub> values (below 65%). Validation of the model involving the data used yielded the following: accuracy — 89.8%, sensitivity — 92.11%, specificity — 81.82%, area under the ROC curve — 96%.

The forecast of the likelihood of fatal outcome in patients with AS can be calculated daily. On the one hand, the result

can be considered as static to determine surgical tactics, establish indications for on-demand relaparotomy. Patients may have indications for repeated debridement relaparotomy in case of growing likelihood of fatal outcome. On the other hand, the results of calculating the probability of fatal outcome can be used as a dynamic indicator to assess efficacy of the ongoing therapy, including surgical treatment and expensive extracorporeal detoxification methods. In this situation, when we see growing likelihood of fatal outcome, it is necessary to change the ongoing therapy and use other extracorporeal detoxification methods.

## DISCUSSION

The analysis of the assessment results using the SOFA clinical score has revealed significant changes in AS patients in two groups, which makes it possible to use the score to assess AS outcomes. This is due to the fact that the SOFA score reflects the function of many organs and systems (respiratory, cardiovascular, nervous, renal, liver, hemostasis systems). Assessment using this score involves quantitative data, which ensures higher objectivity and reproducibility of the results [12]. In patients with adverse AS outcomes, leukocytosis, neutrophilia, anemia with reduced red blood cell counts, hemoglobin concentration, hematocrit, and thrombocytopenia have been reported. Such alterations are associated with activation of innate and adaptive immunity, plasma and platelet components of hemostasis, vascular endothelium with subsequent immunosuppression manifested by lymphopenia, monocytopenia increasing the likelihood of secondary infection

**Table 4.** Hemostasis indicators of patients with AS, Me (LQ; UQ)

Indicators/reference values	Group 1 — beneficial AS outcomes (n = 46)			Group 2 — adverse AS outcomes (n = 18)		
	Day 1 (n = 46)	Day 3 (n = 46)	Day 7 (n = 46)	Day 1 (n = 18)	Day 3 (n = 14)	Day 7 (n = 10)
Prothrombin index, %	56.60 [51.20; 73.30]	67.41 [52.50; 78.90]	42.65 [21.90; 48.50] <sup>#§</sup>	55.20 [48.50; 67.10]	45.90 [25.10; 51.30]*	21.90 [20.90; 21.90] <sup>#§*</sup>
Prothrombin time / 11–17 s	17.00 [15.50; 19.20]	16.50 [15.70; 19.10]	17.95 [16.65; 20.15]	19.95 [17.20; 39.60]*	15.80 [15.40; 18.70] <sup>#</sup>	16.10 [15.50; 16.50] <sup>#</sup>
aPTT / 22–38 s	35.85 [32.65; 36.25]	37.45 [34.80; 43.00]	42.75 [36.25; 48.90]	41.30 [38.60; 69.70]*	32.70 [17.00; 43.00]	33.80 [30.60; 42.00] <sup>#</sup>
Fibrinogen / 2–4 g/L	4.97 [4.33; 6.23]	5.68 [4.97; 6.82]	5.53 [4.59; 6.49]	6.58 [4.30; 8.47]	6.57 [3.65; 8.23]	6.42 [4.68; 8.60]
INR / 0.8–1.2 U	1.31 [1.22; 1.86]	1.28 [1.20; 1.45]	1.37 [1.27; 1.53]	1.53 [1.36; 3.43]	1.22 [1.18; 1.44] <sup>#</sup>	1.24 [1.19; 1.27]
D-dimer / 0–250 ng/mL	2085.00 [965.00; 2595.00]	565.00 [226.00; 2472.00]	1284.50 [631.50; 3382.00]	2488.50 [926.00; 4325.00]	2078.00 [990.00; 3118.00] <sup>#</sup>	2146.00 [1046.00; 3310.00] <sup>#</sup>

**Note:** \* — significant ( $p < 0.05$ ) differences from group 1 on appropriate day; # — differences from indicators reported on day 1 for appropriate group; § — differences from indicators reported on day 3 for appropriate group.

[13, 14]. High serum levels of procalcitonin and CRP in the group with adverse AS outcomes reflect severity of the AS-associated inflammatory response. Growth of these indicators can suggest adverse outcome when predicting the course of AS [15–18]. Among biochemistry indicators of patients with adverse AS outcomes, we should mention growth of serum creatinine, urea, direct bilirubin concentrations, ALT, AST activity, along with the decrease in GFR compared to the group with beneficial AS outcomes. These alterations are associated with organ dysfunction in AS, the development of multiple organ dysfunction syndrome (MODS) due to damage caused by pathogens and endotoxins, activation of innate and adaptive immunity. Mitochondrial dysfunction caused by sepsis is a major cause of the cell metabolism disturbances, insufficient energy supply and oxidative stress, which lead to apoptosis, dysfunction of multiple organs, MODS, thereby increasing patient mortality rate [19–21].

In terms of the hemostasis system, high plasma levels of fibrinogen, D-dimer, increased aPPT, PT, and decreased PI are typical for patients with adverse AS outcomes. These alterations are associated with the hypercoagulable and hypofibrinolytic hemostasis alteration phenotype, activation of extrinsic and intrinsic coagulation pathways, suppression of anticoagulant processes, disturbed fibrinolysis, liver dysfunction with impaired clotting factor synthesis, development of sepsis-induced coagulopathy, DIC syndrome [22–25]. In terms of the acid-base

balance and blood gases, patients with adverse AS outcomes showed more severe metabolic acidosis accompanied by high lactate levels, as well as the decreased PaO<sub>2</sub>/FiO<sub>2</sub> and SvO<sub>2</sub> values, which was due to disturbed central and peripheral hemodynamics, microcirculation, impaired oxygen delivery, consumption and utilization in the tissues, acute kidney damage. Serum lactate levels represent an important biomarker of sepsis that is positively correlated to morbidity and mortality in sepsis or septic shock [26–28].

According to our data and the model constructed, high serum concentrations of CRP and creatinine, as well as low SvO<sub>2</sub> values can serve as valuable clinical tools for prediction of AS outcomes. The laboratory indicators used in the “Calculator for Predicting Mortality in Abdominal Sepsis” are available for all medical institutions providing care to patients with AS, including the non-ICU departments, which makes it possible to timely estimate the likelihood of fatal disease outcome and determine further patient management tactics at any stage.

CONCLUSIONS

The study has shown that the prognostic model based on serum C-reactive protein, creatinine concentrations and venous oxygen saturation is an effective tool for prediction of AS outcomes. The value of these three markers reported emphasizes the key role of renal dysfunction, inflammatory

**Table 5.** Blood acid-base balance and blood gases in patients with AS, Me (LQ; UQ)

Indicators/reference values	Group 1 — beneficial AS outcomes (n = 46)			Group 2 — adverse AS outcomes (n = 18)		
	Day 1 (n = 46)	Day 3 (n = 46)	Day 7 (n = 46)	Day 1 (n = 18)	Day 3 (n = 14)	Day 7 (n = 10)
PaO <sub>2</sub> /FiO <sub>2</sub> / above 300 U	220.00 [210.00; 280.00]	230.00 [210.00; 280.00]	240.00 [200.00; 300.00]	246.70 [200.00; 280.00]	214.00 [190.00; 240.00]*	170.00 [160.00; 180.00] <sup>#§*</sup>
SvO <sub>2</sub> , % / above 70%	73.50 [67.30; 86.40]	69.40 [56.40; 77.50]	71.70 [65.60; 73.60]	70.70 [53.40; 91.10]*	75.00 [65.00; 82.00]	66.60 [64.60; 72.90]*
Venous blood pH / 7.31–7.41	7.38 [7.33; 7.41]	7.38 [7.32; 7.40]	7.34 [7.34; 7.35]	7.27 [7.23; 7.31]*	7.34 [7.24; 7.38]	7.34 [7.34; 7.35]
Venous blood SB / 21–28 mmol/L	20.80 [18.60; 25.80]	22.95 [21.10; 25.20]	20.90 [19.30; 21.60] <sup>§</sup>	15.50 [15.40; 19.10]*	19.30 [17.20; 23.80]	20.90 [19.30; 21.60] <sup>§</sup>
Venous blood BB / 0–2 mmol/L	-3.50 [-6.90; 2.00]	-1.40 [-3.50; 1.40]	-3.70 [-5.80; -2.80]	-8.40 [-10.80; -3.00]	-6.00 [-8.60; -0.40]	-3.70 [-5.80; -2.80]
Venous blood BE / 0–2 mmol/L	-3.50 [-7.20; 1.80]	-1.40 [-3.60; 1.60]	-3.60 [-5.70; -2.70]	-8.30 [-10.90; 22.80]	-6.20 [-8.60; -0.10]	-3.60 [-5.70; -2.70]

**Note:** \* — significant ( $p < 0.05$ ) differences from group 1 on appropriate day; # — differences from indicators reported on day 1 for appropriate group; § — differences from indicators reported on day 3 for appropriate group.

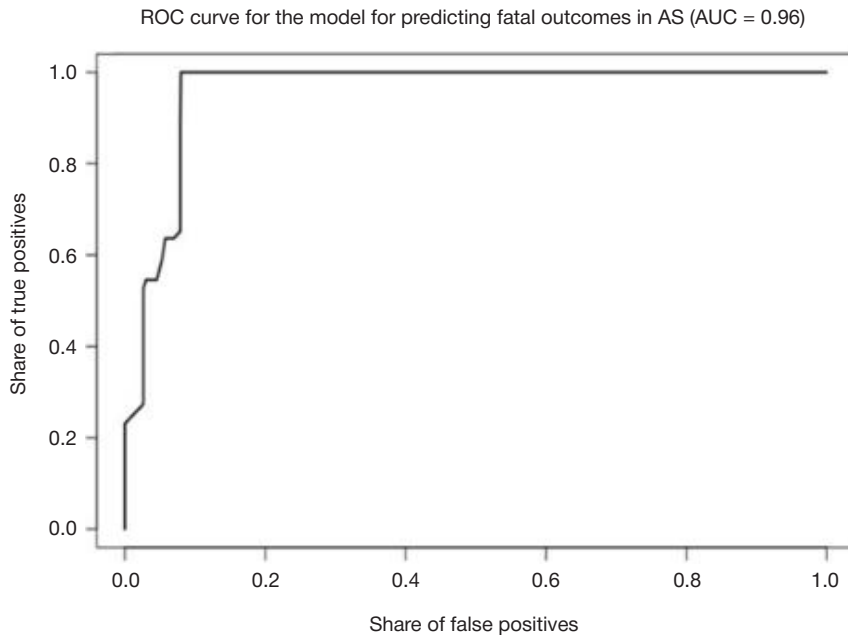


Fig. The metrics used for the model for predicting fatal outcomes in AS

response, and tissue hypoxia in the AS pathogenesis and outcome. The mathematical model for predicting outcome of sepsis in patients with abdominal surgical pathology has been constructed. The software tool “Calculator for Predicting Mortality in Abdominal Sepsis” has been developed. The model constructed represents a valuable tool for clinical practice and further research in the field of pathophysiology of septic conditions. Timely identification of patients with high probability of fatal AS outcome will

make it possible to promptly intensify treatment, including early targeted hemodynamic support, ensure antibacterial therapy adjustment, and repeated surgery in case of the need for repeated lesion debridement. This will allow one to improve treatment outcomes and reduce AS-associated mortality. Improvement of the model for predicting the likelihood of fatal outcome in AS presented through inclusion of other clinical and laboratory markers aimed to increase its prognostic accuracy and feasibility remains promising.

## References

- Singer M, Deutschman CS, Seymour CW, Shankar-Hari M, Annane D, Bauer M, et al. The Third International Consensus definitions for sepsis and septic shock (Sepsis-3): JAMA. 2016; 315 (8): 801–10. DOI: 10.1001/jama.2016.0287.
- Fleischmann-Struzek C, Mellhammar L, Rose N, Cassini A, Rudd KE, Schlattmann P, et al. Incidence and mortality of hospital- and ICU-treated sepsis: results from an updated and expanded systematic review and meta-analysis. Intensive Care Med. 2020; 46 (8): 1552–62. DOI: 10.1007/s00134-020-06151-x.
- Font MD, Thyagarajan B, Khanna AK. Sepsis and Septic Shock — Basics of diagnosis, pathophysiology and clinical decision making. Medical Clinics of North America. 2020; 104 (4): 573–85. DOI: 10.1016/j.mcna.2020.02.011.
- Peksöz R, Ağırman E, Şentürk F, Albayrak Y, Atamanalp SS. A Focus on Intra-Abdominal Sepsis with Biomarkers: A Literature Review. Eurasian J Med. 2022; 54 (Suppl1): 66–70. DOI: 10.5152/eurasianjmed.2022.22296.
- Sartelli M, Abu-Zidan FM, Catena F, et al. Global validation of the WSES Sepsis Severity Score for patients with complicated intra-abdominal infections: a prospective multicentre study (WISS Study). World J Emerg Surg. 2015; 10 (61). DOI: 10.1186/s13017-015-0055-0.
- Sartelli M, Abu-Zidan FM, Labricciosa FM, et al. Physiological parameters for Prognosis in Abdominal Sepsis (PIPAS) Study: a WSES observational study. World J Emerg Surg. 2019; 14 (34). DOI: 10.1186/s13017-019-0253-2.
- Fan Z, Jiang J, Xiao C, Chen Y, Xia Q, Wang J, et al. Construction and validation of prognostic models in critically ill patients with sepsis-associated acute kidney injury: interpretable machine learning approach. J Transl Med. 2023; 21 (1): 406. DOI: 10.1186/s12967-023-04205-4.
- Vincent JL, Moreno R, Takala J, Willatts S, De Mendonça A, Bruining H, et al. The SOFA (Sepsis-related Organ Failure Assessment) score to describe organ dysfunction/failure. On behalf of the Working Group on Sepsis-Related Problems of the European Society of Intensive Care Medicine. Intensive Care Med. 1996; 22 (7): 707–10. DOI: 10.1007/BF01709751. PMID: 8844239.
- Knaus WA, Draper EA, Wagner DP, Zimmerman JE. APACHE II: a severity of disease classification system. Crit Care Med. 1985; 13 (10): 818–29. PMID: 3928249.
- Iba T, Nisio MD, Levy JH, Kitamura N, Thachil J. New criteria for sepsis-induced coagulopathy (SIC) following the revised sepsis definition: a retrospective analysis of a nationwide survey. BMJ Open. 2017; 7 (9): e017046. DOI: 10.1136/bmjopen-2017-017046.
- Kal'kuljator prognoza letal'nosti pri abdominal'nom sepsise: svidetel'stvo o gosudarstvennoj registracii programm dlja JeVM No 2024686256 Rossijskaja Federacija. M. V. Osikov, L. F. Telesheva, A. G. Konashov, A. V. Gusev, V. A. Konashov — No 2024685640; zajavl. 30.10.24; opubl. 06.11.24. Russian
- Dronamraju S, Agrawal S, Kumar S, Acharya S, Gaidhane S, Wanjari A, et al. Comparison of PIRO, APACHE IV, and SOFA Scores in Predicting Outcome in Patients with Sepsis Admitted to Intensive Care Unit: A Two-year Cross-sectional Study at Rural Teaching Hospital. Indian J Crit Care Med. 2022; 26 (10): 1099–105. DOI: 10.5005/jp-journals-10071-24323.
- Wiersinga WJ, van der Poll T. Immunopathophysiology of human sepsis. EBioMedicine. 2022; 86: 104363. DOI: 10.1016/j.ebiom.2022.104363
- Strelcova EI, Peshkova IV, Samatov IJU, Valeeva VA, Vereshhagin EI. Limfopenija kak faktor, opredeljaushhij tjazhest' sepsisa, kak tochnyj kriterij diagnostiki i kak ob#ekt terapii. Journal of Siberian



- Medical Sciences. 2020; (3): 108–25. Russian.
15. Hany A Zaki, Soumaya Bensliman, Khalid Bashir, et al. Accuracy of procalcitonin for diagnosing sepsis in adult patients admitted to the emergency department: a systematic review and meta-analysis. *Syst Rev.* 2024; 13: 37. DOI: 10.1186/s13643-023-02432-w.
  16. Plebani M. Why C-reactive protein is one of the most requested tests in clinical laboratories? *Clin Chem Lab Med.* 2023; 61 (9): 1540–5. DOI: 10.1515/ccm-2023-0086.
  17. El Shabrawy RM, Gawish A, Elgabry R, Nasr FM, Diab M, Gamal D. Presepsin, procalcitonin and C reactive protein as diagnostic biomarkers of sepsis in intensive care unit patients. *Microbes and Infectious Diseases.* 2021; 2. DOI: 10.21608/mid.2021.54196.1100.
  18. Huang N, Chen J, Wei Y, Liu Y, Yuan K, Chen J, et al. Multi-marker approach using C-reactive protein, procalcitonin, neutrophil CD64 index for the prognosis of sepsis in intensive care unit: a retrospective cohort study. *BMC Infect Dis.* 2022; 22 (1): 662. DOI: 10.1186/s12879-022-07650-6.
  19. Balkrishna A, Sinha S, Kumar A, Arya V, Gautam AK, Valis M, Kuca K, Kumar D, Amarowicz R. Sepsis-mediated renal dysfunction: Pathophysiology, biomarkers and role of phytoconstituents in its management. *Biomed Pharmacother.* 2023; 165: 115183. DOI: 10.1016/j.biopha.2023.115183.
  20. Ronco C, Bellomo R, Kellum JA. Acute kidney injury. *Lancet.* 2019; 394: 1949–64. DOI: 10.1016/S0140-6736(19)32563-2.
  21. Peerapornratana S, Manrique-Caballero CL, Gómez H, Kellum JA. Acute kidney injury from sepsis: Current concepts, epidemiology, pathophysiology, prevention and treatment. *Kidney Int.* 2019; 96: 1083–99. DOI: 10.1016/j.kint.2019.05.026.
  22. Marín Oyarzún CP, Glembotsky AC, Goette NP, Lev PR, De Luca G, Baroni Pietto MC, et al. Platelet Toll-Like Receptors Mediate Thromboinflammatory Responses in Patients With Essential Thrombocythemia. *Front Immunol.* 2020; 11: 705. DOI: 10.3389/fimmu.2020.00705.
  23. Pravin Patel, James V. Michael, Ulhas P. Naik, Steven E. McKenzie. Platelet FcγRIIA in immunity and thrombosis: adaptive immunothrombosis. *J Thromb Haemost.* 2021; 19: 1149–60. DOI: 10.1111/jth.15265.
  24. Tsantes AG, Parastatidou S, Tsantes EA, Bonova E, Tsante KA, Mantzios PG, et al. Sepsis-Induced Coagulopathy: An Update on Pathophysiology, Biomarkers, and Current Guidelines. *Life (Basel).* 2023; 13 (2): 350. DOI: 10.3390/life13020350.
  25. Giustozzi M, Ehrlicher H, Bongiovanni D, Borovac JA, Guerreiro RA, Gąsecka A, et al. Coagulopathy and sepsis: Pathophysiology, clinical manifestations and treatment. *Blood Rev.* 2021; 50: 100864. DOI: 10.1016/j.blre.2021.100864.
  26. Sijia Liu, Ting Yang, Qingsong Jiang, et al. Lactate and Lactylation in Sepsis: A Comprehensive Review. *J Inflamm Res.* 2024; 17: 4405–4417. DOI: 10.2147/JIR.S459185.
  27. Rui Yin, Xiaoshan Yang, Yanfen Yao. Risk factors for acute respiratory distress syndrome in sepsis patients: A meta-analysis. *Heliyon.* 2024; 10 (18): e37336. DOI: 10.1016/j.heliyon.2024.e37336.
  28. Sanjana Chetana Shanmukhappa, Srivatsa Lokeshwaran. Affiliations expand. In: *StatPearls. Treasure Island (FL): StatPearls Publishing; 2024. PMID: 33232065 Bookshelf ID: NBK564395.*

## Литература

1. Singer M, Deutschman CS, Seymour CW, Shankar-Hari M, Annane D, Bauer M, et al. The Third International Consensus definitions for sepsis and septic shock (Sepsis-3). *JAMA.* 2016; 315 (8): 801–10. DOI: 10.1001/jama.2016.0287.
2. Fleischmann-Struzek C, Mellhammar L, Rose N, Cassini A, Rudd KE, Schlattmann P, et al. Incidence and mortality of hospital- and ICU-treated sepsis: results from an updated and expanded systematic review and meta-analysis. *Intensive Care Med.* 2020; 46 (8): 1552–62. DOI: 10.1007/s00134-020-06151-x.
3. Font MD, Thyagarajan B, Khanna AK. Sepsis and Septic Shock — Basics of diagnosis, pathophysiology and clinical decision making. *Medical Clinics of North America.* 2020; 104 (4): 573–85. DOI: 10.1016/j.mcna.2020.02.011.
4. Peksöz R, Ağırman E, Şentürk F, Albayrak Y, Atamanalp SS. A Focus on Intra-Abdominal Sepsis with Biomarkers: A Literature Review. *Eurasian J Med.* 2022; 54 (Suppl1): 66–70. DOI: 10.5152/eurasianjmed.2022.22296.
5. Sartelli M, Abu-Zidan FM, Catena F, et al. Global validation of the WSES Sepsis Severity Score for patients with complicated intra-abdominal infections: a prospective multicentre study (WISS Study). *World J Emerg Surg.* 2015; 10 (61). DOI: 10.1186/s13017-015-0055-0.
6. Sartelli M, Abu-Zidan FM, Labricciosa FM, et al. Physiological parameters for Prognosis in Abdominal Sepsis (PIPAS) Study: a WSES observational study. *World J Emerg Surg.* 2019; 14 (34). DOI: 10.1186/s13017-019-0253-2.
7. Fan Z, Jiang J, Xiao C, Chen Y, Xia Q, Wang J, et al. Construction and validation of prognostic models in critically ill patients with sepsis-associated acute kidney injury: interpretable machine learning approach. *J Transl Med.* 2023; 21 (1): 406. DOI: 10.1186/s12967-023-04205-4.
8. Vincent JL, Moreno R, Takala J, Willatts S, De Mendonça A, Bruining H, et al. The SOFA (Sepsis-related Organ Failure Assessment) score to describe organ dysfunction/failure. On behalf of the Working Group on Sepsis-Related Problems of the European Society of Intensive Care Medicine. *Intensive Care Med.* 1996; 22 (7): 707–10. DOI: 10.1007/BF01709751. PMID: 8844239.
9. Knaus WA, Draper EA, Wagner DP, Zimmerman JE. APACHE II: a severity of disease classification system. *Crit Care Med.* 1985; 13 (10): 818–29. PMID: 3928249.
10. Iba T, Nisio MD, Levy JH, Kitamura N, Thachil J. New criteria for sepsis-induced coagulopathy (SIC) following the revised sepsis definition: a retrospective analysis of a nationwide survey. *BMJ Open.* 2017; 7 (9): e017046. DOI: 10.1136/bmjopen-2017-017046.
11. Калькулятор прогноза летальности при абдоминальном сепсисе: свидетельство о государственной регистрации программ для ЭВМ No 2024686256 Российская Федерация. М. В. Осиков, Л. Ф. Телешева, А. Г. Коначов, А. В. Гусев, В. А. Коначов - No 2024685640; заявл. 30.10.24; опубли. 06.11.24.
12. Dronamraju S, Agrawal S, Kumar S, Acharya S, Gaidhane S, Wanjarji A, et al. Comparison of PIR0, APACHE IV, and SOFA Scores in Predicting Outcome in Patients with Sepsis Admitted to Intensive Care Unit: A Two-year Cross-sectional Study at Rural Teaching Hospital. *Indian J Crit Care Med.* 2022; 26 (10): 1099–105. DOI: 10.5005/jp-journals-10071-24323.
13. Wiersinga WJ, van der Poll T. Immunopathophysiology of human sepsis. *EBioMedicine.* 2022; 86: 104363. DOI: 10.1016/j.ebiom.2022.104363
14. Стрельцова Е. И., Пешкова И. В., Саматов И. Ю., Валева В. А., Верещагин Е. И. Лимфопения как фактор, определяющий тяжесть сепсиса, как точный критерий диагностики и как объект терапии. *Journal of Siberian Medical Sciences.* 2020; (3): 108–25.
15. Hany A Zaki, Soumaya Bensliman, Khalid Bashir, et al. Accuracy of procalcitonin for diagnosing sepsis in adult patients admitted to the emergency department: a systematic review and meta-analysis. *Syst Rev.* 2024; 13: 37. DOI: 10.1186/s13643-023-02432-w.
16. Plebani M. Why C-reactive protein is one of the most requested tests in clinical laboratories? *Clin Chem Lab Med.* 2023; 61 (9): 1540–5. DOI: 10.1515/ccm-2023-0086.
17. El Shabrawy RM, Gawish A, Elgabry R, Nasr FM, Diab M, Gamal D. Presepsin, procalcitonin and C reactive protein as diagnostic biomarkers of sepsis in intensive care unit patients. *Microbes and Infectious Diseases.* 2021; 2. DOI: 10.21608/mid.2021.54196.1100.
18. Huang N, Chen J, Wei Y, Liu Y, Yuan K, Chen J, et al. Multi-marker approach using C-reactive protein, procalcitonin, neutrophil CD64 index for the prognosis of sepsis in intensive care unit: a retrospective cohort study. *BMC Infect Dis.* 2022; 22 (1): 662. DOI: 10.1186/s12879-022-07650-6.
19. Balkrishna A, Sinha S, Kumar A, Arya V, Gautam AK, Valis M, Kuca K, Kumar D, Amarowicz R. Sepsis-mediated renal dysfunction: Pathophysiology, biomarkers and role of phytoconstituents in its management. *Biomed Pharmacother.* 2023; 165: 115183. DOI: 10.1016/j.biopha.2023.115183.

20. Ronco C, Bellomo R, Kellum JA. Acute kidney injury. *Lancet*. 2019; 394: 1949–64. DOI: 10.1016/S0140-6736(19)32563-2.
21. Peerapornratana S, Manrique-Caballero CL, Gómez H, Kellum JA. Acute kidney injury from sepsis: Current concepts, epidemiology, pathophysiology, prevention and treatment. *Kidney Int*. 2019; 96: 1083–99. DOI: 10.1016/j.kint.2019.05.026.
22. Marín Oyarzún CP, Glembotsky AC, Goette NP, Lev PR, De Luca G, Baroni Pietto MC, et al. Platelet Toll-Like Receptors Mediate Thromboinflammatory Responses in Patients With Essential Thrombocythemia. *Front Immunol*. 2020; 11: 705. DOI: 10.3389/fimmu.2020.00705.
23. Pravin Patel, James V. Michael, Ulhas P. Naik, Steven E. McKenzie. Platelet FcγRIIA in immunity and thrombosis: adaptive immunothrombosis. *J Thromb Haemost*. 2021; 19: 1149–60. DOI: 10.1111/jth.15265.
24. Tsantes AG, Parastatidou S, Tsantes EA, Bonova E, Tsante KA, Mantzios PG, et al. Sepsis-Induced Coagulopathy: An Update on Pathophysiology, Biomarkers, and Current Guidelines. *Life (Basel)*. 2023; 13 (2): 350. DOI: 10.3390/life13020350.
25. Giustozzi M, Ehrlinder H, Bongiovanni D, Borovac JA, Guerreiro RA, Gaşceca A, et al. Coagulopathy and sepsis: Pathophysiology, clinical manifestations and treatment. *Blood Rev*. 2021; 50: 100864. DOI: 10.1016/j.blre.2021.100864.
26. Sijia Liu, Ting Yang, Qingsong Jiang, et al. Lactate and Lactylation in Sepsis: A Comprehensive Review. *J Inflamm Res*. 2024; 17: 4405–4417. DOI: 10.2147/JIR.S459185.
27. Rui Yin, Xiaoshan Yang, Yanfen Yao. Risk factors for acute respiratory distress syndrome in sepsis patients: A meta-analysis. *Heliyon*. 2024; 10 (18): e37336. DOI: 10.1016/j.heliyon.2024.e37336.
28. Sanjana Chetana Shanmukhappa, Srivatsa Lokeshwaran. Affiliations expand. In: *StatPearls*. Treasure Island (FL): StatPearls Publishing; 2024. PMID: 33232065 Bookshelf ID: NBK564395.

## LIF AND SLIFR ALTERATIONS DURING RECONVALESCENCE (NOVEL CORONAVIRUS INFECTION, INFLUENZA) IN PATIENTS WITH ESSENTIAL HYPERTENSION

Radaeva OA<sup>1</sup> , Simbirtsev AS<sup>2</sup>, Kostina YuA<sup>1</sup>, Iskandryarova MS<sup>1</sup>, Negodnova EV<sup>1</sup>, Solodovnikova GA<sup>1</sup>, Ereemeev VV<sup>1</sup>, Krasnoglazova KA<sup>1</sup>, Babushkin IO<sup>1</sup>

<sup>1</sup> National Research Mordovia State University, Saransk, Russia

<sup>2</sup> State Research Institute of Highly Pure Biopreparations of the Federal Medical Biological Agency, Saint Petersburg, Russia

Today, the analysis of the risk of developing cardiovascular complications in patients with essential hypertension (EH) following recovery from novel coronavirus infection (COVID-19) is relevant. The value of leukemia inhibitory factor (LIF) and its soluble receptor (sLIFr) in EH progression has been shown, along with the relevance of circadian approaches to assessment of the contribution of pro-inflammatory cytokines to the pathogenesis of acute cerebrovascular accidents (CVA). The study aimed to compare alterations of the LIF and sLIFr levels during convalescence after COVID-19 and influenza in patients with stage II EH, to determine the features that are important for the development of acute CVA, and to analyze the associations with circadian rhythms. The study was conducted in four phases ( $n = 180$ ; age 55–60 years): (1) 6–8 months before COVID-19; (2–3) on day 10–14 after primary or recurrent COVID-19; (4) on day 10–14 after influenza. In each phase blood levels of LIF and sLIFr were determined by enzyme immunoassay at 7.00–8.00 h and 19.00–20.00 h, in 12 patients in four phases — at 7.00–8.00 h, 12.00–13.00 h, 19.00–20.00 h, 23.00–1.00 h throughout three days. It has been demonstrated that patients with EH show elevated LIF and sLIFr levels relative to healthy individuals in all time points ( $p < 0.001$ ) and significantly elevated levels at 19.00–20.00 h ( $p < 0.001$ ). The analysis of the relationship between circadian rhythms and blood levels of LIF, sLIFr in patients with stage II EH post COVID-19 and influenza has revealed similar changes in the form of the larger increase in sLIFr levels at 19.00–20.00 h (the ROC analysis data has shown predictive value for developing acute CVA within a year after COVID-19 in cases of the value increase above 7100 pg/L at 19.00–20.00 h). The principles revealed actualize further investigation of the effects of the LIF/sLIFr complex associated with the EH progression after acute infectious diseases.

**Keywords:** essential hypertension, LIF, sLIFr, circadian rhythms, SARS-CoV-2, influenza

**Funding:** the study was supported by the RSF grant “Analysis of changes in circadian rhythms of cytokine synthesis in the blood of patients with essential arterial hypertension as a predictor of the development of cardiovascular complications”, No. 23-25-00147.

**Author contribution:** Radaeva OA — developing the study design, analysis of the results, manuscript formatting; Simbirtsev AS — phrasing of the aim of the study, manuscript editing; Kostina YuA — laboratory testing, manuscript formatting; Iskandryarova MS — literature review, manuscript editing; Negodnova EV — literature review, patient follow-up; Solodovnikova GA — statistical data processing; Ereemeev VV — manuscript editing; Krasnoglazova KA, Babushkin IO — statistical processing of the 6-month follow-up data.

**Compliance with ethical standards:** the study was approved by the Ethics Committee of the Ogarev Mordovia State University (protocol No. 12 dated 14 December 2008, additional protocol No. 85 dated 27 May 2020). The informed consent was submitted by all patients. Biomaterial (blood) was collected for further testing considering provisions of the WMA Declaration of Helsinki (2013) and the protocol of the Convention on Human Rights and Biomedicine developed by the Council of Europe (1999) considering supplementary protocol of the Convention on Human Rights and Biomedicine in the field of biomedical research (2005).


✉ **Correspondence should be addressed:** Olga A. Radaeva  
Ulyanov, 26a, Saransk, 430032, Russia; radaevamed@mail.ru

**Received:** 28.11.2024 **Accepted:** 18.02.2025 **Published online:** 26.02.2025

**DOI:** 10.24075/brsmu.2025.005

**Copyright:** © 2025 by the authors. **Licensee:** Pirogov University. This article is an open access article distributed under the terms and conditions of the Creative Commons Attribution (CC BY) license (<https://creativecommons.org/licenses/by/4.0/>).

## ИЗМЕНЕНИЕ LIF И SLIFR В ПЕРИОД РЕКОНВАЛЕСЦЕНЦИИ (НОВАЯ КОРОНАВИРУСНАЯ ИНФЕКЦИЯ, ГРИПП) У ПАЦИЕНТОВ С ГИПЕРТОНИЧЕСКОЙ БОЛЕЗНЬЮ

О. А. Радаева<sup>1</sup> , А. С. Симбирцев<sup>2</sup>, Ю. А. Костина<sup>1</sup>, М. С. Искандрярова<sup>1</sup>, Е. В. Негоднова<sup>1</sup>, Г. А. Солодовникова<sup>1</sup>, В. В. Еремеев<sup>1</sup>, К. А. Красноглазова<sup>1</sup>, И. О. Бабушкин<sup>1</sup>

<sup>1</sup> Национальный исследовательский Мордовский государственный университет имени Н. П. Огарёва, Саранск, Россия

<sup>2</sup> Государственный научно-исследовательский институт особо чистых биопрепаратов Федерального медико-биологического агентства, Санкт-Петербург, Россия

На сегодняшний день актуален анализ риска развития сердечно-сосудистых осложнений у пациентов с гипертонической болезнью (ГБ) после перенесенной новой коронавирусной инфекции (COVID-19). Показана значимость лейкоemia-ингибирующего фактора (LIF) и его растворимого рецептора (sLIFr) в прогрессировании ГБ и актуальность циркадианных подходов в оценке вклада провоспалительных цитокинов в патогенез острого нарушения мозгового кровообращения (ОНМК). Целью исследования было сопоставить изменения уровня LIF и sLIFr в период реконвалесценции после COVID-19 и гриппа у больных с ГБ II стадии, выделить значимые особенности для формирования ОНМК и проанализировать связи с циркадианными ритмами. Исследование проводили в четыре этапа ( $n = 180$ ; возраст 55–60 лет): (1) за 6–8 месяцев до COVID-19; (2–3) на 10–14-й дни после первичного и повторного COVID-19; (4) на 10–14-й после гриппа. На каждом этапе определяли уровни LIF и sLIFr в крови иммуноферментным методом в 7.00–8.00 ч и 19.00–20.00 ч, 12 пациентам на четырех этапах — в 7.00–8.00 ч, 12.00–13.00 ч, 19.00–20.00 ч, 23.00–1.00 ч в течение трех суток. Показано, что у пациентов с ГБ уровень LIF и sLIFr повышен во всех временных точках по сравнению со здоровыми ( $p < 0,001$ ) и заметно увеличен в 19.00–20.00 ч ( $p < 0,001$ ). При анализе связи циркадианных ритмов и содержания LIF, sLIFr в крови пациентов с ГБ II стадии после COVID-19 и гриппа определены схожие изменения в виде более выраженного увеличения в 19.00–20.00 ч уровня sLIFr (данные ROC-анализа продемонстрировали предикторную ценность в отношении развития ОНМК в течение года после COVID-19 при повышении в 19.00–20.00 ч до значений более 7100 пг/мл). Выявленные принципы актуализируют дальнейшее изучение эффектов комплекса LIF/sLIFr при прогрессировании ГБ после острых инфекционных заболеваний.

**Ключевые слова:** гипертоническая болезнь, LIF, sLIFr, циркадианные ритмы, SARS-COV-2, грипп

**Финансирование:** поддержано грантом РФФ «Анализ изменения циркадианных ритмов синтеза цитокинов в крови пациентов с эссенциальной артериальной гипертензией как предиктор развития сердечно-сосудистых осложнений», № 23-25-00147.

**Вклад авторов:** О. А. Радаева — дизайн исследования, анализ результатов, оформление рукописи; А. С. Симбирцев — формулирование цели исследования, редактирование; Ю. А. Костина — лабораторные исследования, оформление рукописи; М. С. Искандрярова — работа с литературой, редактирование; Е. В. Негоднова — работа с литературой, наблюдение за пациентами; Г. А. Солодовникова — статистическая обработка; В. В. Еремеев — редактирование; К. А. Красноглазова, И. О. Бабушкин — статистическая обработка данных за 6 месяцев наблюдения.

**Соблюдение этических стандартов:** исследование одобрено этическим комитетом МГУ имени Н. П. Огарева (протокол № 12 от 14 декабря 2008 г., дополнительный протокол № 85 от 27 мая 2020). Все пациенты подписали добровольное информированное согласие.

✉ **Для корреспонденции:** Ольга Александровна Радаева  
ул. Ульянова, д. 26а, г. Саранск, 430032, Россия; radaevamed@mail.ru

**Статья получена:** 28.11.2024 **Статья принята к печати:** 18.02.2025 **Опубликована онлайн:** 26.02.2025

**DOI:** 10.24075/vrgmu.2025.005

**Авторские права:** © 2025 принадлежат авторам. **Лицензиат:** РНИМУ им. Н. И. Пирогова. Статья размещена в открытом доступе и распространяется на условиях лицензии Creative Commons Attribution (CC BY) (<https://creativecommons.org/licenses/by/4.0/>).

Leukemia inhibitory factor (LIF) being a member of the interleukin 6 (IL6) family has broad pleiotropic effects due to interaction with both classic IL6 receptor, gp130, and its own membrane receptor found in cardiomyocytes, neurons, endothelial cells, etc. [1]. The role of its soluble receptor, sLIFr, is still a matter of debate, since both agonist and antagonist interactions with LIF are reported. The data are provided on the correlations between the LIF/sLIFr levels and the nitric oxide metabolism products (asymmetric and symmetric dimethylarginine (ADMA, SDMA), etc.), which is significant for pathogenesis of essential hypertension (EH) [2]. A new objective was the search for factors associated with the development of complications in patients with EH in the post-COVID period, which determined introduction of new components to the design of the study focused on the cytokine mechanisms of EH progression. Today, there is limited data on alterations of the associations between the cytokine mechanisms of immune response regulation and human circadian rhythms under exposure to pathogens causing infectious diseases, including viruses [3]. At the same time, as early as in 1995 the relationship between vaccine administration and circadian rhythms of cytokine synthesis considering the significance of individual features of patients with chronic non-communicable diseases was demonstrated [4]. Russian scientific school of chronobiology has a long history of fundamental research [5, 6]. The relevance of the complex problems presented in the paper is also confirmed by the data provided in the review published in 2024, which emphasize the importance of studying the circadian control over immune-vascular interactions in both normal state and cardiovascular disorders [7]. Circadian rhythms affect both immune and vascular components of such interactions, primarily through regulation of chemotactic cytokines, adhesion of their receptors on the immune and endothelial cells, which is especially important in EH. Considering the earlier reported data on the relationship between alterations of LIF and sLIFr blood levels and concentrations of the nitric oxide metabolism products during the post-COVID period in patients with EH [2, 8], the data provided by the colleagues on the importance of circadian approaches to estimation of the contribution of pro-inflammatory cytokines to pathogenesis and outcomes of acute cerebrovascular accidents (CVA) [9], as well as information about topical presentation of membrane LIF receptors on the neurons and endothelial cells [1], we assumed significance of the dependence of the cytokine synthesis circadian rhythm alterations for EH pathogenesis. The study aimed to compare alterations of the LIF and sLIFr levels during reconvalescence after primary COVID-19 or COVID-19 re-infection and influenza in patients with stage II EH, to determine immunopathogenetic features that are important for the development of acute CVA, and to analyze the associations with circadian rhythms.

## METHODS

The study was conducted at the Department of Immunology, Microbiology and Virology with a course of Clinical Immunology and Allergology of the Institute of Medicine, Ogarev Mordovia State University; the clinical phase involving patient enrollment was conducted at the Katkov Republican Clinical Hospital, vascular center of the Republican Clinical Hospital of the Republic of Mordovia No. 4 in 2019–2020 with further follow-up 2020–2024 considering the patient's place of residence.

### Study design

The study included several phases of the group allocation. As a result, 12 patients out of 180 initially included patients

with stage II EH underwent repeated dynamic blood collection for further investigation of the relationship between alteration of blood cytokine (LIF, sLIFr) levels and circadian biorhythms within 24 h (Fig. 1).

### *Phase 1. December 2019 — January–March 2020 (before the pandemic)*

We enrolled 180 patients with stage II EH (80 females and 100 males) to determine morning (7:00–8:00) and evening (19:00–20:00) LIF, sLIFr concentrations, and in 40 patients of this group blood levels of cytokines were determined at four time points (7:00–8:00, 12:00–13:00, 19:00–20:00, 23:00–1:00) throughout three days.

### *Phase 2. May – November 2020 (circulation of the Wuhan-Hu-1 strain)*

In 68 patients (30 females and 38 males) out of 180 included in the study in phase 1, the analysis of morning and evening concentrations of the same set of cytokines was conducted, and in 27 patients (10 females and 17 males) out of 68 blood levels of cytokines were determined at four time points (7:00–8:00, 12:00–13:00, 19:00–20:00, 23:00–1:00) throughout three days on days 10–14 of reconvalescence after primary COVID-19 with recording of the facts of developing cardiovascular complications (acute CVA, TIA, MI). A telephone survey was used to confirm cases of acute CVA, TIA based on medical documents within a subsequent year of follow-up, and statistically independent predictors of developing acute CVA/TIA and MI were identified (11 patients out of 68 had a history of acute CVA and TIA, two patients had a history of MI; furthermore, all 68 patients were characterized by comparable high risk of fatal and non-fatal vascular complications based on the SCORE2-OP scores).

### *Phase 3 — 2022–2023 (circulation of the Omicron strain)*

In 24 patients (out of 27 participants of phase 2 having stage II EH and information about blood levels of cytokines collected throughout three days), blood levels of cytokines were determined at four time points (7:00–8:00, 12:00–13:00, 19:00–20:00, 23:00–1:00) throughout three days on days 10–14 of reconvalescence after COVID-19 re-infection.

### *Phase 4. December 2023 — March 2024 (period of increased influenza incidence)*

In 12 patients out of 24 having stage II EH, who had been assessed in phase 3, blood levels of cytokines were determined at four time points (7:00–8:00, 12:00–13:00, 19:00–20:00, 23:00–1:00) throughout three days on days 10–14 of reconvalescence after influenza (type A).

### Characteristics of patients

The general clinical characteristics of patients during the follow-up period confirm high comparability of the patients included in the study based on systolic blood pressure (SBP), diastolic blood pressure (DBP), average nocturnal systolic (SBPn) and diastolic (DBPn) blood pressure; body mass index (BMI), levels of low-density lipoprotein (LDL), cholesterol, creatinine, urea, glomerular filtration rate (GFR), glucose (see Appendix).

The control group included six healthy individuals matched by gender and age (three females and three males), it was



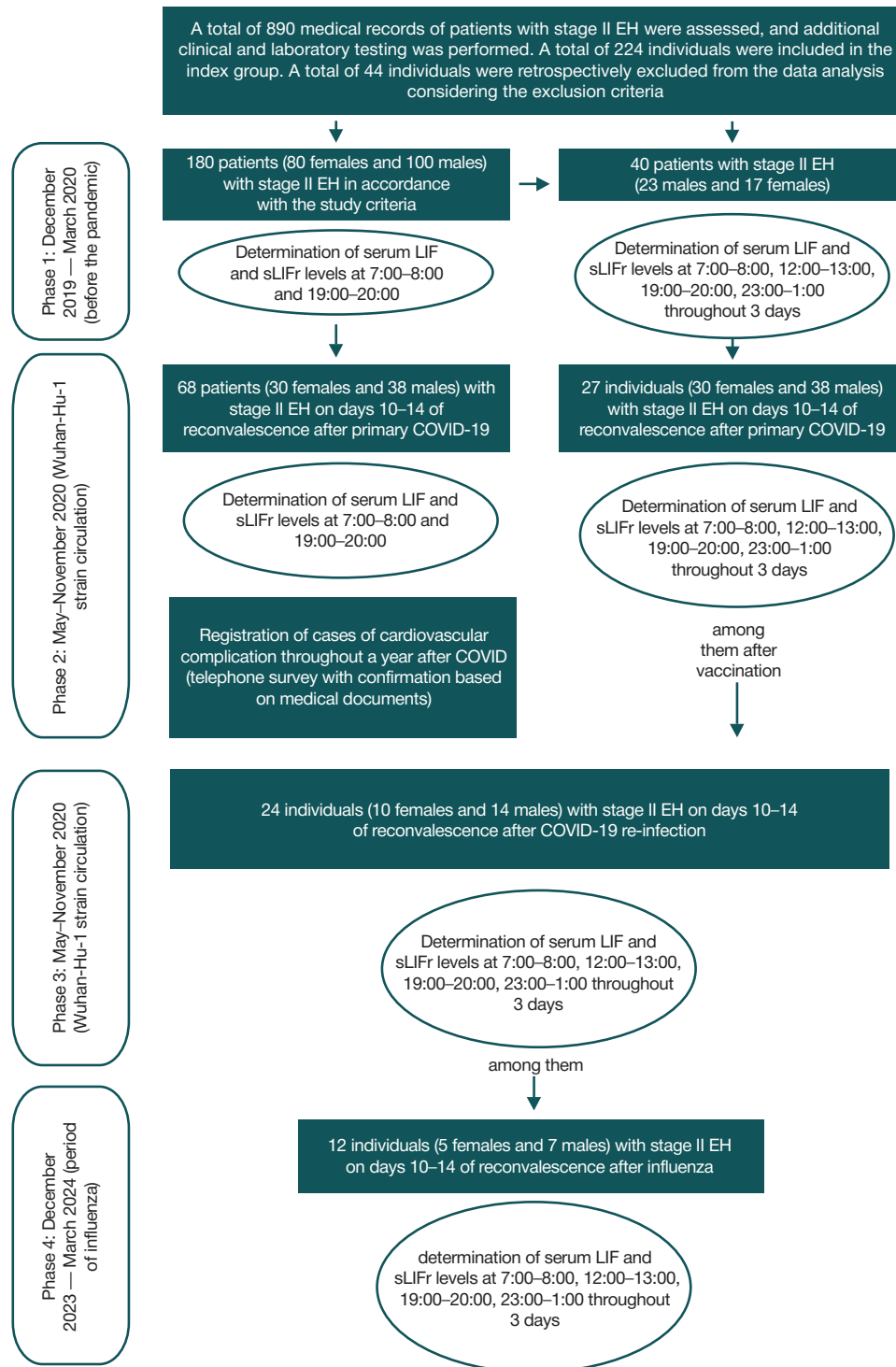


Fig. 1. Study design

formed of 32 healthy individuals included at the same time with the group of patients having EH in phase 1 for further four-phase follow-up.

The diagnosis of COVID-19 was established in accordance with the relevant temporary methodological guidelines on prevention, diagnosis, and treatment of novel coronavirus infection; moderate course of the disease and pneumonia (CT I-II) were reported in patients. The following comparable treatment regimens were used (the researchers had no influence on therapy prescription):

- primary SARS-CoV-2 infection (2020): dexamethasone 16 mg/day with dosage reduction, azithromycin 1500 mg/day, sodium heparin 10,000 IU/day;

- COVID-19 re-infection (2022–2023; moderate course, pneumonia (CT I-II)): molnupiravir 1600 mg/day since day 2–3 after the emergence of clinical manifestations in accordance with the product information, paracetamol to reduce fever up to 1000 mg/day;

- influenza (2023–2024; the diagnosis was established in accordance with the clinical guidelines of treatment of influenza in adults (2022) and confirmed by laboratory testing: immunochromatography express-test for influenza A and B viruses with confirmation by molecular genetic testing): oseltamivir 75 mg twice a day no later than three days since the emergence of initial clinical manifestations in a dose specified

**Table 1.** Blood levels of LIF and sLIFr (pg/mL) in patients with stage II EH on days 10–14 of convalescence after primary COVID-19, COVID-19 re-infection, and influenza

	7.00–8.00	19.00–20.00	
Phase 1. 6–8 months before SARS-CoV-2 infection ( <i>n</i> = 180 individuals)			
LIF	7.18 [4.11–11.3]	12.4 [8.17–14.6]	<i>p</i> < 0.001 7.00–8.00
sLIFr	3820 [2300–4930]	5680 [4200–7100]	<i>p</i> < 0.001 7.00–8.00
Phase 2. Primary SARS-CoV-2 infection, 2020, Wuhan-Hu-1 strain ( <i>n</i> = 68 individuals)			
LIF	7.29 [4.36–9.82]	12.9 [7.92–13.8]	<i>p</i> < 0.001 7.00–8.00
sLIFr	3906 [2470–4660]	7890 [6100–8200]* phase 1	<i>p</i> < 0.001 7.00–8.00
Phase 3. COVID-19 re-infection, 2022–2023, Omicron variant ( <i>n</i> = 27 individuals)			
LIF	7.24 [3.69–10.9]	12.68 [8.78–13.14]*	<i>p</i> < 0.001 7.00–8.00
sLIFr	3970 [2690–5330]	5810 [5140–6900]* phase 2	<i>p</i> < 0.001 7.00–8.00
Phase 4. 2023–2024 ( <i>n</i> = 12 individuals)			
LIF	6.78 [4.24–9.53]	10.9 [8.17–13.7]	<i>p</i> < 0.001 7.00–8.00
sLIFr	4100 [2390–5900]	7600 [5560–9100]* phase 1.3	<i>p</i> < 0.001 7.00–8.00

**Note:** \* — *p* < 0.001 when compared with the specified phases (the Wilcoxon test was used).

in product information; paracetamol to reduce fever up to 1000 mg/day.

#### Inclusion criteria in 2019–2020 (phase 1)

Inclusion criteria: stage II EH; EH age of 10 years; comparable antihypertensive therapy (ACEI + thiazide/thiazide-like diuretic); age 55–60 years; concentration of the lipid metabolism indicators: total cholesterol — no more than 5.0 mmol/L, low-density lipoprotein — no more than 3.0 mmol/L, high-density lipoprotein — more than 1.0 mmol/L, triglycerides — no more than 1.7 mmol/L, thickness of the carotid artery intima media — no more than 0.9 mm, glucose levels — no more than 5.5 mg/dL, BMI — no more than 30 kg/c<sup>2</sup>; comparable characteristics of the daily routine (sleep between 23:00 and 6:00, last meal at 20:00, no sleep disorder or the use of sleeping pills/melatonin-based drugs (these characteristics were assessed by neurologist); informed consent submitted by the patient.

Additional criteria determining inclusion of patients with stage II EH and healthy individuals in the study in 2022–2024 within the framework of allocating the index group with the analysis of circadian dependencies of blood LIF and sLIFr levels: administration of two Gam-COVID-VAC vaccine doses in 2021.

#### Non-inclusion criteria in 2019 and 2020–2024 (common)

Non-inclusion criteria: type 1 or 2 diabetes mellitus, allergy/autoimmune disorder, chronic infectious disease (HIV, hepatitis B and C), mental disorder, symptomatic arterial hypertension, smoking; lack of readiness for prolonged assessment; use of antihypertensive drugs, other than ACE inhibitors and/or thiazide/thiazide-like diuretics (for group with stage II EH only).

#### Exclusion criteria

The exclusion criteria were common: prescription of antihypertensive drugs, other than ACE inhibitors and/or thiazide/thiazide-like diuretics (for group with stage II EH only), developing acute CVA, TIA, MI or other condition determining stage III EH, autoimmune disorder diagnosed during the follow-up period, losing touch with the patient. The exclusion criteria substantiated allocation of the group of 180 patients compliant with the study criteria throughout the follow-up period.

#### Blood collection procedure

Blood was collected at 7:00–8:00, 12:00–13:00, 19:00–20:00, 23:00–1:00. In this study, cytokines LIF and sLIFr were isolated based on the research data on circadian patterns of human cytokine synthesis and own earlier research on the cytokine-mediated mechanisms of EH pathogenesis [6].

Blood was collected using the Vacutainer systems (BD Vacutainer, USA) (the last meal took place at least 4 h before). Blood was centrifuged for 15 min at 1500–2000 rpm. Serum was separated and stored at a temperature –30 °C for no longer than 30 days in the labeled test tubes. An interval between blood collection and freezing of blood was 60 min. The analysis was conducted by a certified specialist using the Personal Lab TM microplate analyzer (Adaltis, Italy). The following test systems were used to record serum levels of LIF and sLIFr: LIF (eBioscience (Bender MedSystems GmbH, Austria)) — the test system sensitivity was 0.66 pg/mL, the detection interval was 0.66–200 pg/mL; sLIFr (eBioscience (Bender MedSystems GmbH, Austria)) — the test system sensitivity was 0.052 ng/mL, the detection interval was 0.052–5 ng/mL.

#### Statistical processing of the results

Given the objectives, two software packages were used for statistical processing of the results: StatTech v. 2.8.8 (StatTech, Russia) and Stat Soft Statistica 10.0 (USA). When there were less than 50 patients (groups with assessment of six circadian points), the distribution was tested for normality using the Shapiro–Wilk test; when the number of patients exceeded 50 (groups with assessment two time points), the Kolmogorov–Smirnov test was used. Then the normally distributed quantitative indicators were described using mean values (M) and standard deviations (SD). When there was no normal distribution, the quantitative data were described using the median (Me), lower and upper quartiles (Q<sub>1</sub>–Q<sub>3</sub>). Given the dispersions were equal, comparison of two unrelated group based on the normally distributed quantitative trait was performed using the Student's *t*-test. Comparison of two unrelated group based on the non-normally distributed quantitative trait was performed using the Mann–Whitney *U* test. The Wilcoxon test was used for related samples (comparison of the dynamic changes in indicators in 12 patients with EH, as well as changes in six healthy individuals). The direction and strength of the correlation between two quantitative traits were assessed using the Spearman's rank

**Table 2.** Blood levels of LIF and sLIFr (pg/mL) in individuals without EH on days 10–14 of convalescence after primary COVID-19, COVID-19 re-infection, and influenza

	7.00–8.00	19.00–20.00	
Phase 1. 6–8 months before SARS-CoV-2 infection ( <i>n</i> = 32 individuals)			
LIF	1.35 [1.09–1.73]	1.29 [1.08–1.83]	<i>p</i> > 0.05 7.00–8.00
sLIFr	3410 [2900–4520]	3640 [3050–4680]	<i>p</i> > 0.05 7.00–8.00
Phase 2. Primary SARS-CoV-2 infection. 2020. Wuhan-Hu-1 strain ( <i>n</i> = 26 individuals)			
LIF	1.44 [1.12–1.83]	1.36 [1.02–1.79]	<i>p</i> > 0.05 7.00–8.00
sLIFr	3490 [2470–4660]	3720 [2200–4170]	<i>p</i> > 0.05 7.00–8.00
Phase 3. COVID-19 re-infection. 2022–2023. Omicron variant ( <i>n</i> = 18 individuals)			
LIF	1.27 [1.14–1.93]	1.31 [1.18–1.42]	<i>p</i> > 0.05 7.00–8.00
sLIFr	3380 [2500–4720]	3460 [2700–3940]	<i>p</i> > 0.05 7.00–8.00
Phase 4. 2023–2024 ( <i>n</i> = 6 individuals)			
LIF	1.42 [1.14–1.68]	1.33 [1.02–1.51]	<i>p</i> > 0.05 7.00–8.00
sLIFr	4070 [3710–4410]	4140 [3680–4630]	<i>p</i> > 0.05 7.00–8.00

correlation coefficient (when the distribution of indicators was non-normal). A predictive model characterizing the dependence of the quantitative variable on the factors was developed using the linear regression method. The ROC curve analysis method was used to assess the diagnostic value of quantitative traits when predicting certain outcomes. The quantitative trait cut-off value was determined based on the highest Youden's index value. The differences were considered significant at *p* < 0.05.

RESULTS

The results of phase 1 of the study including the data of 180 patients with stage II EH and 32 healthy individuals (the indicators obtained at 7:00–8:00 and 19:00–20:00 were analyzed) has shown that patients with stage II EH have higher (*p* < 0.001) levels of LIF and sLIFr at 7:00–8:00 and 19:00–20:00 (Table 1) compared to healthy individuals (Table 2). Furthermore, patients with EH show a significant increase in

blood levels of LIF and sLIFr by 19:00–20:00 relative to the data obtained at 7:00–8:00 (by 65% (95% CI — [43–87]%) and 71.3% (95% CI — [52.8–82.1]%), respectively; *p* < 0.001), Table 1). No fluctuations of LIF and sLIFr levels during the day have been reported (Table 2).

In phase 2 of the study, in 68 patients with stage II EH and 28 patients having no EH from of phase 1 group, repeated analysis of blood LIF and sLIFr levels was performed on days 10–14 of convalescence after primary COVID-19 (Table 1). In patients with EH, no quantitative differences in LIF levels between the period before SARS-CoV-2 infection and early convalescence have been determined (*p* > 0.05). We have revealed higher sLIFr concentrations in blood of patients with stage II EH at 19:00–20:00 with growth by 92% [83–121]% when comparing with the data obtained at 7:00–8:00; the growth percentage in the evening is higher than that reported before the pandemic (*p* < 0.01) (Table 1). In individuals without EH, no differences in quantitative indicators of LIF and sLIFr

**Table 3.** LIF, sLIFr levels depending on the fact of developing acute CVA within a year after COVID-19 in patients with EH (2020–2021, after infection with the Wuhan SARS-CoV-2 variant)

Indicators	Acute CVA development within a year after COVID-19		<i>p</i>
	no	yes	
sLIFr level 7:00–8:00 (pg/mL), Me [IQR]	3469 [3128–3751]	4150.00 [3168.25; 5100.00]	0.051
sLIFr level 19:00–20:00 day 10 post COVID (pg/mL), M (SD)	5974 (853)	7352 (1197)	<i>p</i> < 0.001
LIF level 7:00–8:00 (pg/mL), Me [IQR]	7.17 [3.57–9.24]	7.36 [3.44–9.11]	<i>p</i> > 0.05
LIF level 19:00–20:00 (pg/mL), Me [IQR]	12.4 [7.49–13.9]	12.6 [7.54–14.3]	<i>p</i> > 0.05

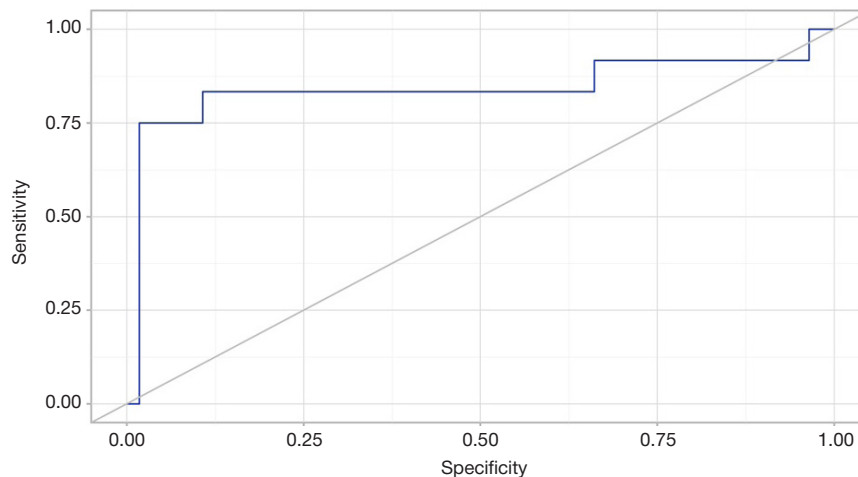


**Fig. 2.** ROC curve characterizing the likelihood of developing acute CVA within a year after COVID-19 as a function of sLIFr levels reported at 19:00–20:00 on days 10–14 of post-COVID period in patients with stage II EH (primary infection)

**Table 4.** Blood levels of LIF and sLIFr (pg/mL) in patients with stage II EH (12 individuals) on days 10–14 of reconvalescence after COVID-19, influenza, and vaccination

		7.00–8.00	12.00–13.00	19.00–20.00	23.00–01.00
1	2	3	4	5	6
6–8 months before SARS-CoV-2 infection					
LIF pg/mL	day 1	7.85 [4.51–11.9]	8.00 [4.6–12.0]	12.3 [8.12–15.2]*3.4	8.80 [4.90–10.7]*5
	day 2	7.68 [4.47–12.9]	7.96 [3.64–11]	13.2 [8.68–15.3]*3.4	9.27 [2.49–11.3]*5
	day 3	7.84 [4.30–12.2]	7.65 [3.82–11.8]	12.23 [8.39–14.3]*1.2	8.5 [3.37–10.1]*5
sLIFr pg/mL	day 1	3690 [2420–5340]	4380 [3340–4510]	5770 [4190–6750]*3.4	3090 [2460–3650]*5
	day 2	4020 [2950–5070]	3720 [3290–4970]	5480 [5070–6930]*3.4	3330 [2680–4490]*5
	day 3	4110 [2830–5610]	3660 [3340–4930]	5960 [5260–7920]*3.4	3990 [2560–4390]*5
Primary SARS-CoV-2 infection (2020, circulation of Wuhan-Hu-1 strain)					
LIF pg/mL	day 1	7.35 [4.20–10.06]	8.03 [4.67–11.56]	12.4 [8.13–14.51]*3.4	10.52 [9.75–12.5]*5
	day 2	7.05 [4.10–10.59]	7.36 [3.81–9.83]	13.8 [7.54–15.5]*3.4	9.52 [8.29–11.6]*5
	day 3	7.23 [4.01–10.12]	7.95 [4.51–10.86]	13.4 [8.96–15.8]*3.4	9.88 [8.66–11.9]*5
sLIFr pg/mL	day 1	4240 [2610–4850]	3650 [2780–4810]	7540 [6400–8220]*3.4. a	3770 [2880–4370]*5
	day 2	3710 [2790–4710]	3690 [2730–4480]	7280 [5840–7550]*3.4.a	3600 [2640–3890]*5
	day 3	4140 [2780–5320]	3840 [2700–4680]	8120 [6340–8840]*3.4. a	3870 [3010–4390]*5
COVID-19 re-infection (2022–2023, circulation of Omicron strain)					
LIF pg/mL	day 1	7.15 [3.98–11.21]	7.89 [4.56–12.05]	12.68 [8.78–13.14]*3.4	7.67 [4.50–11.7]*5
	day 2	7.10 [4.00–12.95]	7.78 [4.08–11.25]	13.05 [8.48–14.98]*3.4	6.28 [4.49–12.9]*5
	day 3	7.19 [4.20–11.5]	7.64 [3.98–12.3]	13.1 [8.40–15.0]*3.4	6.59 [3.60–11.9]*5
sLIFr pg/mL	day 1	4140 [2780–5450]	4390 [3180–5240]	5790 [4830–7800]*3.4.b.d	3110 [2460–4060]*5.d
	day 2	3940 [2890–5080]	3890 [3460–5110]	5520 [4930–6860]*3.4.b	3190 [2410–4080]*5
	day 3	4000 [2550–5350]	3790 [3330–5670]	5900 [5100–7200]*3.4.b	3850 [2500–4300]**5
Influenza (2023–2024)					
LIF pg/mL	day 1	6.93 [4.17–9.86]	7.14 [5.16–9.53]	11.2 [8.29–14.3]*3.4	8.77 [4.48–10.9]*5
	day 2	7.18 [4.43–9.45]	6.97 [5.48–9.11]	11.76 [8.90–14.69]*3.4	8.31 [4.80–10.14]*5.
	day 3	6.56 [3.94–10.55]	7.05 [4.80–9.27]	11.98 [7.71–14.83]*3.4	8.36 [4.17–11.66]*5
sLIFr pg/mL	day 1	3960 [2410–6200]	4160 [2730–4800]	6600 [5400–8300]*3.4.a.c	3520 [2800–4600]*5
	day 2	3890 [2260–6020]	4240 [2890–5120]	7480 [5880–9090]*3.4.a.c	3710 [2910–4830]*5
	day 3	3970 [2430–6310]	4270 [2700–4920]	7640 [5450–10300]*3.4.a.c	3470 [2770–4650]*5

**Note:** \* —  $p < 0.001$  when compared with the specified groups (3 — levels at 7:00–8:00, 4 — 12:00–13:00, 5 — 19:00–20:00, 6 — 23:00–1:00).

from the pre-COVID period were revealed ( $p > 0.05$ ), but deviations from the results of patients with EH reported before SARS-CoV-2 infection were preserved.

In phase 2, we also started monitoring of the development of cardiovascular complications (acute CVA, TIA, and MI) in 68 patients with stage II EH throughout the year after primary COVID-19 and subsequent retrospective comparison with the morning and evening LIF and sLIFr concentrations reported on days 10–14 of reconvalescence after primary COVID-19 (Table 3). When assessing sLIFr levels reported at 7:00–8:00 depending on the acute CVA development within a year after COVID-19, we failed to find significant differences ( $p = 0.051$ ) (Mann–Whitney  $U$  test was used). When assessing sLIFr levels reported at 19:00–20:00 on days 10–14 of early reconvalescence after primary COVID-19 (Wuhan-Hu-1 strain) depending on the acute CVA and TIA development within the next year, considerable differences were revealed ( $p < 0.001$ ) (Student's  $t$ -test was used) (Table 3). The patients' LIF levels reported at 7:00–8:00 and 19:00–20:00 depending on the acute CVA and TIA development within the next year showed no differences ( $p > 0.05$ ). When assessing the correlation between the probability of developing acute CVA or TIA and peripheral blood serum levels of sLIFr reported at 19:00–20:00 on days 10–14 post-COVID using ROC analysis, a curve was plotted (Fig. 2)

(the value of  $0.842 \pm 0.074$  corresponds to the area under the curve with the 95% CI:  $0.697–0.987$ ;  $p < 0.001$ ). Critical elevation of sLIFr levels in blood of patients with stage II EH being through early reconvalescence after COVID-19 reported at 19:00–20:00 was 7100 pg/mL, which was identical to the maximum Youden's index value. Brain damage in patients with stage II EH was predicted, when blood sLIFr levels reported at 19:00–20:00 on days 10–14 post-COVID exceeded this value or were equal to it with sensitivity and specificity of 75% and 98.2%, respectively.

In phase 3 (after COVID-19 re-infection), assessment of morning and evening concentrations of the test cytokines showed that patterns of pre-COVID period were typical for patients with stage II EH (27 individuals) and people without EH (18 individuals), and the differences from healthy individuals were preserved ( $p < 0.001$ ; Table 1, Table 2). No changes in the form of greater degree of sLIFr level increase at 19:00–20:00 in individuals with EH found on days 10–14 of reconvalescence after primary COVID-19 were reported for COVID-19 re-infection.

Phase 4 allowed us to assess changes in blood LIF and sLIFr levels during early reconvalescence after influenza in 12 patients with stage II EH and six individuals without EH followed-up starting from phase 1 of the study. The data obtained demonstrated trends similar to that reported after



**Table 5.** Blood levels of LIF and sLIFr (pg/mL) in healthy people (6 individuals) on days 10–14 of convalescence after COVID-19, influenza, and vaccination

		7.00–8.00	12.00–13.00	19.00–20.00	23.00–01.00
1	2	3	4	5	6
6–8 months before SARS-CoV-2 infection					
LIF pg/mL	day 1	1.32 [1.12–1.71]	1.42 [1.29–1.75]	1.26 [1.21–1.78]	1.32 [1.25–1.68]
	day 2	1.38 [1.10–1.69]	1.49 [1.31–1.80]	1.37 [1.25–1.81]	1.38 [1.26–1.70]
	day 3	1.43 [1.20–1.79]	1.56 [1.39–1.87]	1.42 [1.29–1.85]	1.43 [1.31–1.73]
sLIFr pg/mL	day 1	3890 [3100–4750]	4200 [3390–4580]	4510 [3570–4870]	4210 [3800–4570]
	day 2	4100 [3260–5070]	5250 [3560–5880]	4590 [3760–5000]	4330 [3870–4650]
	day 3	3990 [3240–4880]	5070 [3450–5630]	4470 [3640–4860]	4290 [3910–4540]
Primary SARS-CoV-2 infection (2020, circulation of Wuhan-Hu-1 strain)					
LIF pg/mL	day 1	1.42 [1.14–1.68]	1.50 [1.27–1.75]	1.33 [1.02–1.51]	1.34 [1.18–1.67]
	day 2	1.22 [1.12–1.46]	1.42 [1.18–1.71]	1.37 [0.99–1.48]	1.30 [1.13–1.60]
	day 3	1.29 [1.09–1.58]	1.45 [1.24–1.68]	1.32 [0.95–1.17]	1.34 [1.10–1.53]
sLIFr pg/mL	day 1	4070 [3710–4410]	3920 [3350–4530]	4140 [3680–4630]	4260 [3650–4710]
	day 2	3970 [3460–4270]	3590 [3110–4210]	4150 [3450–4490]	3890 [3360–4440]
	day 3	3980 [3420–4350]	3950 [3180–4330]	4290 [3470–4570]	4210 [3310–4560]
COVID-19 re-infection (2022–2023, circulation of Omicron strain)					
LIF pg/mL	day 1	1.39 [1.12–1.65]	1.47 [1.25–1.72]	1.36 [1.03–1.49]	1.37 [1.16–1.64]
	day 2	1.27 [1.14–1.53]	1.49 [1.20–1.76]	1.31 [0.97–1.52]	1.34 [1.11–1.57]
	day 3	1.49 [1.18–1.85]	1.60 [1.41–1.92]	1.54 [1.27–1.83]	1.38 [1.30–1.75]
sLIFr pg/mL	day 1	3990 [3560–4340]	4040 [3180–4710]	3740 [3650–4550]	4230 [3610–4670]
	day 2	4030 [3510–4350]	3860 [3170–4370]	4010 [3540–4620]	3790 [3290–4340]
	day 3	4070 [3360–4460]	3910 [2870–4170]	4130 [3560–4660]	4140 [3160–4420]
Influenza (2023–2024)					
LIF pg/mL	day 1	1.38 [1.08–1.72]	1.47 [1.31–1.72]	1.36 [0.99–1.54]	1.30 [1.15–1.63]
	day 2	1.29 [1.03–1.56]	1.36 [1.25–1.64]	1.24 [0.94–1.44]	1.20 [1.05–1.52]
	day 3	1.25 [1.06–1.55]	1.49 [1.30–1.67]	1.36 [0.97–1.22]	1.37 [1.12–1.50]
sLIFr pg/mL	day 1	4460 [3420–4600]	3730 [3160–4010]	3880 [3510–4230]	4590 [3480–4330]
	day 2	4030 [3270–4340]	3810 [3020–4270]	3790 [3530–4790]	3640 [3390–4360]
	day 3	4100 [3240–4510]	3910 [3030–4260]	4080 [3660–4700]	4010 [3150–4380]

**Note:** \* —  $p < 0.001$  when compared with the specified groups (3 — levels at 7:00–8:00, 4 — 12:00–13:00, 5 — 19:00–20:00; 6 — 23:00–1:00).

primary COVID-19 in patients with stage II EH (Table 1): more prominent sLIFr growth at 19:00–20:00 (by 91% (95% CI [81–126]%), which was higher ( $p < 0.01$ ), than in pre-COVID period and post COVID-19 re-infection. Earlier, in 2019, we assessed blood levels of sLIFr at 7:00–8:00 and 19:00–20:00 in 60 patients with stage II EH, not included in this part of the study, but taking part in the study of the cytokine mechanisms of EH progression (the study has been going on since 2012 until now). The patients specified are comparable based on all inclusion and exclusion criteria reported in this paper for patients of four phases of follow-up. After having influenza in 2019 patients with stage II EH showed deviation of the 24-h curves from the data of the same patients reported 9–10 months before infection ( $p > 0.05$ ): before influenza at 7:00–8:00 — 3720 [2210–4960] pg/mL, at 19:00–20:00 — 5510 [3700–6240] pg/mL; on days 10–14 of convalescence after influenza at 7:00–8:00 — 4140 [2640–4860] pg/mL, at 19:00–20:00 — 5680 [3380–6420] pg/mL.

Considering different size of the samples used in phases 1–4, groups were formed of 12 patients with stage II EH and six healthy individuals, in whom blood collection at four time points was performed throughout three days in all four phases of the study, in order to confirm the relationships between the patterns revealed and circadian biorhythms and

to ensure higher predictive value of the differences between evening sLIFr quantitative characteristics of patients with EH and healthy individuals. Comparison of blood LIF and sLIFr levels in the specified group after primary COVID-19 in 2020 (phase 2) and COVID-19 re-infection in 2022–2023 (phase 3) caused by different SARS-CoV-2 strains confirmed the data reported for two time points: changes in 24-h dynamics of sLIFr levels in the form of more prominent increase in the evening (19:00–20:00) took place only during early convalescence after primary COVID-19 ( $p < 0.001$ ; Table 4). The analysis of the data of patients with stage II EH infected with influenza A virus in fall-winter 2023–2024 revealed a 3-day trend of the increasing degree of blood sLIFr level elevation at 19:00–20:00 comparable with the reported for the period of primary SARS-CoV-2 infection during circulation of the Wuhan-Hu-1 strain. Changes in patients with EH were correlated to circadian biorhythms.

Healthy individuals showed no changes in blood LIF and sLIFr concentrations within 24 h both before COVID-19 and during convalescence (Table 5); the levels of LIF and sLIFr were significantly lower, than in patients with stage II EH ( $p < 0.001$ ) and did not change during convalescence after influenza. No correlations with circadian rhythms were revealed in the group of healthy individuals.

## DISCUSSION

The pandemic of novel coronavirus infection attracted the researchers' and clinicians' attention to the duration and features of cytokine alterations after the disease; criteria and manifestations of post-COVID syndrome are discussed. It is important to control the increasing risk of cardiovascular complications in patients with EH, and to understand the factors determining the latter. Based on the data of pre-COVID period (phase 1 of the study) our research team determined the features of patients with stage II EH in the form of higher blood concentrations of LIF and sLIFr with the upward trend observed in the evening. In 2017, we showed that growth of the LIF and sLIF levels against the background of EH was reported before prescription of antihypertensive drugs and represented a component of EH pathogenesis; when the target BP was achieved when using antihypertensive drugs, the decrease in sLIF levels was determined, there was no downward trend of LIF levels during treatment in patients with EH [2]. Regarding the fact that information about the LIF expression increase post cerebral ischemia and the neurons as the main source of LIF was published on international scientific platforms [10], the importance was substantiated of studying the relationship between this cytokine and its soluble receptor as predictors of changes in the risk of acute CVA in patients with EH, including after COVID-19, which was confirmed in phase 2 of our study. The main pool of cardiovascular complications in patients with EH reported within a year after primary COVID-19 was constituted by cases of acute CVA and TIA, and the predictor showing high sensitivity and specificity was growth of blood sLIFr levels above 7100 pg/L at 19:00–20:00 on days 10–14 of early convalescence. It has been earlier reported in the literature that there is balance between vasoconstrictor and vasodilator molecules affecting blood supply to the brain and enhancing the electroencephalogram power spectra, which is likely to be regulated by cytokines and related to circadian biorhythms [11]. Perhaps, this is also manifested in the relationship between blood levels of the studied cytokines against the background of hypertension and circadian biorhythms, and it is not reported in individuals with normal blood pressure. However, the question of the mechanism of sLIFr influence on the development of acute CVA and TIA remains open. If we consider sLIFr as a LIF blocking factor, then in the acute period of ischemia its increase may have protective properties, since a number of authors have noted pro-inflammatory role of LIF against the background of acute ischemic damage to neurons [10]. Then, LIF is a neurotrophic factor [10], LIF blockage via sLIFr will be perverse. These data raise new pathogenetic questions for researchers. Can a long-term LIF increase in individuals with hypertension before acute CVA act as a potential protective neurotrophic buffer that increases the resistance of neurons to damaging factors against the background of hypertension, or, conversely, support inflammatory processes, including the increased blood-brain barrier permeability? And what is the role of sLIFr, if it not only shows blocking activity against LIF, but also has its own LIF-independent immunopathogenetic effects in the form of correlation with increasing blood levels of the factors associated with the NO synthesis imbalance progression: SDMA and ADMA [2]. Microglia may be one of the points of the LIF/sLIFr effect application [12–13].

When assessing circadian rhythms of blood LIF, sLIFr levels in patients with stage II EH after COVID-19 and influenza, of greatest interest are the data on the similarity of changes in the form of the more pronounced increase in sLIFr levels at 18:00–19:00 during primary SARS-CoV-2 and after influenza. It should

be noted that according to our data, no such trend following recovery from influenza has been earlier (before the pandemic) reported in patients with EH. Considering the fact that the assessment results reported after primary COVID-19 have shown the relationship between blood sLIFr levels exceeding 7100 pg/mL at 19:00–20:00 and the development of acute CVA, TIA, and that such levels are currently determined in patients with EH and post influenza, it is necessary to attract clinicians' attention to the potential group at increased risk of cardiovascular complications. It is necessary to conduct further studies involving expansion of the group followed-up during the new epidemic period, since the findings emphasize the importance of assessing circadian patterns affecting cytokine regulation of the development of acute CVA associated with EH, and the relevance of those is confirmed by the papers published by other researchers, who study the acute CVA immunopathogenesis [14].

The researchers consider the features and duration of cytokine alterations in the post-COVID period to be related specifically to primary contact of the population members with the virus, which was typical for SARS-CoV-2 in 2020. According to the data we have provided, when patients with EH were re-infected with coronavirus in 2022–2023, no earlier reported more prominent growth of sLIFr levels at 19:00–20:00 has been detected, which can be explained by leveling of the virus immune effect severity against the background of the year-round circulation, decreased virulence, and vaccination effects [15]. According to epidemiological data, the seasonal growth of influenza incidence was less prominent 2020–2022 in the context of SARS-CoV-2 predominance, which can represent the cause of the immune memory effectiveness cancellation. The lack of vaccination in the specified group of patients (submitted refusal of vaccination against influenza) has also determined formation of the “cytokine tail” with the more prominent increase in sLIFr levels post influenza as the “new infection”.

The sLIFr level growth can reduce the percentage of interaction between LIF and its membrane receptor in stem cells, which can affect alteration of their differentiation into neurons, since, according to experimental data, LIF delivery to the murine brain enhances self-renewal of the neuronal stem cells in the subventricular zone and olfactory bulb with the vector of differentiation into neurons [16].

## CONCLUSIONS

The LIF/sLIFr system has a significant pathogenetic component of the acute CVA and TIA development in patients with EH after novel coronavirus infection. The detected similar growth of the evening sLIFr concentrations and post influenza actualized assessment of the contribution of the broader range of viruses (SARS-CoV-2 or influenza variants) to the increase in the risk of developing acute CVA during the subsequent year in patients with EH. Chronobiology of the immune response at the macroorganism-virus interface determines the progression of non-communicable concomitant diseases and should be a part of the personalized approach to calculating the risk of developing complications by comorbid patients in the future. The demonstrated formation of the relationship between sLIFr concentration alterations and circadian biorhythms substantiates scientific and pathogenetic value of studying evening concentrations of this cytokine in patients with hypertension (between 19:00–20:00). The chronobiological patterns of this process identified open up new perspectives for assessment of the LIF/sLIFr complex effects on the EH immunopathogenesis and the development of acute CVA in the specified category of patients considering the history of viral infections (COVID-19, influenza).

## References

1. The Human Protein Atlas project is funded by the Knut & Alice Wallenberg foundation. 2023 [18.10.2024]. Available from: <https://www.proteinatlas.org/>.
2. Radaeva OA, Simbircev AS. Изменения сывороточных уровней фактора, ингибирующего лейкомию (LIF), и растворимого рецептора LIF (sLIFr) при развитии эссенциальной артериальной гипертензии II стадии. Патогенез. 2017; 3 (15): 63–69. Доступно по ссылке: <http://pathogenesis.pro/index.php/pathogenesis/article/view/126> (дата обращения 20.10.2024). Russian.
3. Mok H, Ostendorf E, Ganninger A, Adler AJ, Hazan G, Haspel JA. J Clin Invest. 2024; 134 (3): e175706. Available from: <https://doi.org/10.1172/JCI175706>.
4. Langlois PH, Smolensky MH, Glezen WP, Keitel WA. Diurnal variation in responses to influenza vaccine. Chronobiol Int. 1995; 12 (1): 28–36. Available from: <https://doi.org/10.3109/07420529509064497>.
5. Katinas GS, Chibisov SM, Halabi GM, Dementev MV. Аналитическая хронобиология. М.: Бејрут, 2017; 224 с. Russian.
6. Chibisov SM, Rapoport SI, Blagonravova ML. Хронобиология и хрономедицина. М.: Изд-во РУДН, 2018; 828 с. Russian.
7. Zeng Q, Oliva VM, Moro MÁ, Scheiermann C. Circadian Effects on Vascular Immunopathologies. Circ Res. 2024; 134 (6): 791–809. Available from: <https://doi.org/10.1161/CIRCRESAHA.123.323619>.
8. Radaeva OA, Simbircev AS, Kostina JuA, Iskandjarova MS, Negodnova EV, Mashnina SV, i dr. Изменения циркадианных ритмов уровней цитокинов в крови пациентов с эссенциальной гипертензией в постковидном периоде. Вестник РГМУ. 2023; (6): 14–20. Доступно по ссылке: [https://vestnik.rsmu.press/files/issues/vestnik.rsmu.press/2023/6/2023-6-1385\\_ru.pdf?lang=ru](https://vestnik.rsmu.press/files/issues/vestnik.rsmu.press/2023/6/2023-6-1385_ru.pdf?lang=ru) (дата обращения 20.10.2024). Russian.
9. Mergenthaler P, Balami JS, Neuhaus AA, Mottahedin A, Albers GW, Rothwell PM, et al. Stroke in the Time of Circadian Medicine. Circ Res. 2024; 134 (6): 770–90. Available from: <https://doi.org/10.1161/CIRCRESAHA.124.323508>.
10. Suzuki S, Tanaka K, Suzuki N. Ambivalent Aspects of Interleukin-6 in Cerebral Ischemia: Inflammatory versus Neurotrophic Aspects. Journal of Cerebral Blood Flow & Metabolism. 2009; 29: 464–79. Available from: <https://doi.org/10.1038/jcbfm.2008.141>.
11. Jin RR, Cheung CN, Wong CHY, Lo CCW, Lee CPI, Tsang HW, et al. Sleep quality mediates the relationship between systemic inflammation and neurocognitive performance. Brain Behav Immun Health. 2023; 30: 365–74. Available from: <https://doi.org/10.1016/j.bbih.2023.100634>.
12. Zielinski MR, Gibbons AJ. Neuroinflammation, Sleep, and Circadian Rhythms. Front Cell Infect Microbiol. 2022; 12: 853096. Available from: <https://doi.org/10.3389/fcimb.2022.853096>.
13. Jiao H, Kalsbeek A, Yi CX. Microglia, circadian rhythm and lifestyle factors. Neuropharmacology. 2024; 257: 110029. Available from: <https://doi.org/10.1016/j.neuropharm.2024.110029>.
14. Khan S, Siddique R, Liu Y, Yong VW, Xue M. Towards improving the prognosis of stroke through targeting the circadian clock system. Int J Biol Sci. 2024; 20 (2): 403–13. Available from: <https://doi.org/10.7150/ijbs.88370>.
15. Punj M, Desai A, Hashash JG, Farraye FA, Castillo PR. COVID-19 breakthrough infections and sleep disorders: A population-based propensity matched analysis. Sleep Med X. 2023; 6: 100089. Available from: <https://doi.org/10.1016/j.sleepx.2023.100089>.
16. Bauer S, Patterson PH. Leukemia inhibitory factor promotes neural stem cell self-renewal in the adult brain. The Journal of neuroscience: the official journal of the Society for Neuroscience. 2006; 26:12089–99. Available from: <https://doi.org/10.1523/JNEUROSCI.3047-06.2006>.

## Литература

1. The Human Protein Atlas project is funded by the Knut & Alice Wallenberg foundation. 2023 [18.10.2024]. Available from: <https://www.proteinatlas.org/>.
2. Радаева О. А., Симбирцев А. С. Изменения сывороточных уровней фактора, ингибирующего лейкомию (LIF), и растворимого рецептора LIF (sLIFr) при развитии эссенциальной артериальной гипертензии II стадии. Патогенез. 2017; 3 (15): 63–69. Доступно по ссылке: <http://pathogenesis.pro/index.php/pathogenesis/article/view/126> (дата обращения 20.10.2024).
3. Mok H, Ostendorf E, Ganninger A, Adler AJ, Hazan G, Haspel JA. J Clin Invest. 2024; 134 (3): e175706. Available from: <https://doi.org/10.1172/JCI175706>.
4. Langlois PH, Smolensky MH, Glezen WP, Keitel WA. Diurnal variation in responses to influenza vaccine. Chronobiol Int. 1995; 12 (1): 28–36. Available from: <https://doi.org/10.3109/07420529509064497>.
5. Катинас Г. С., Чибисов С. М., Халаби Г. М., Деметьев М. В. Аналитическая хронобиология. М.: Бейрут, 2017; 224 с.
6. Чибисов С. М., Рапопорт С. И., Благонравова М. Л. Хронобиология и хрономедицина. М.: Изд-во РУДН, 2018; 828 с.
7. Zeng Q, Oliva VM, Moro MÁ, Scheiermann C. Circadian Effects on Vascular Immunopathologies. Circ Res. 2024; 134 (6): 791–809. Available from: <https://doi.org/10.1161/CIRCRESAHA.123.323619>.
8. Радаева О. А., Симбирцев А. С., Костина Ю. А., Исканджарова М. С., Негоднова Е. В., Машнина С. В. и др. Изменения циркадианных ритмов уровней цитокинов в крови пациентов с эссенциальной гипертензией в постковидном периоде. Вестник РГМУ. 2023; (6): 14–20. Доступно по ссылке: [https://vestnik.rsmu.press/files/issues/vestnik.rsmu.press/2023/6/2023-6-1385\\_ru.pdf?lang=ru](https://vestnik.rsmu.press/files/issues/vestnik.rsmu.press/2023/6/2023-6-1385_ru.pdf?lang=ru) (дата обращения 20.10.2024).
9. Mergenthaler P, Balami JS, Neuhaus AA, Mottahedin A, Albers GW, Rothwell PM, et al. Stroke in the Time of Circadian Medicine. Circ Res. 2024; 134 (6): 770–90. Available from: <https://doi.org/10.1161/CIRCRESAHA.124.323508>.
10. Suzuki S, Tanaka K, Suzuki N. Ambivalent Aspects of Interleukin-6 in Cerebral Ischemia: Inflammatory versus Neurotrophic Aspects. Journal of Cerebral Blood Flow & Metabolism. 2009; 29: 464–79. Available from: <https://doi.org/10.1038/jcbfm.2008.141>.
11. Jin RR, Cheung CN, Wong CHY, Lo CCW, Lee CPI, Tsang HW, et al. Sleep quality mediates the relationship between systemic inflammation and neurocognitive performance. Brain Behav Immun Health. 2023; 30: 365–74. Available from: <https://doi.org/10.1016/j.bbih.2023.100634>.
12. Zielinski MR, Gibbons AJ. Neuroinflammation, Sleep, and Circadian Rhythms. Front Cell Infect Microbiol. 2022; 12: 853096. Available from: <https://doi.org/10.3389/fcimb.2022.853096>.
13. Jiao H, Kalsbeek A, Yi CX. Microglia, circadian rhythm and lifestyle factors. Neuropharmacology. 2024; 257: 110029. Available from: <https://doi.org/10.1016/j.neuropharm.2024.110029>.
14. Khan S, Siddique R, Liu Y, Yong VW, Xue M. Towards improving the prognosis of stroke through targeting the circadian clock system. Int J Biol Sci. 2024; 20 (2): 403–13. Available from: <https://doi.org/10.7150/ijbs.88370>.
15. Punj M, Desai A, Hashash JG, Farraye FA, Castillo PR. COVID-19 breakthrough infections and sleep disorders: A population-based propensity matched analysis. Sleep Med X. 2023; 6: 100089. Available from: <https://doi.org/10.1016/j.sleepx.2023.100089>.
16. Bauer S, Patterson PH. Leukemia inhibitory factor promotes neural stem cell self-renewal in the adult brain. The Journal of neuroscience: the official journal of the Society for Neuroscience. 2006; 26:12089–99. Available from: <https://doi.org/10.1523/JNEUROSCI.3047-06.2006>.

## COGNITIVE RESERVE OF PATIENTS WITH CHRONIC CEREBRAL ISCHEMIA

Fokin VF , Ponomareva NV, Shabalina AA, Konovalov RN, Medvedev RB, Boravova AI, Lagoda OV, Krotenkova MV, Tanashyan MM

Research Center of Neurology, Moscow, Russia

Cognitive reserve (CR) is characterized by the ability to engage neural networks for adaptive reorganization of brain functions in response to damage or stress. This study aimed to identify the structural and functional organization of neural networks in patients with chronic cerebral ischemia (CCI) having different CR. The study involved 137 women aged 50–85 years suffering from CCI without diabetes. The average duration of CCI was  $10.1 \pm 0.7$  years. CCI patients were divided into two groups: with secondary (SE) and higher (HE) education. Salivary cortisol levels were measured before and after cognitive load, along with the differences in brain connectivity organization based on fMRI data in two patient groups. Connectivity patterns were primarily found in the auditory areas, different in two groups after applying multiple comparison correction (FDR) and were responsive to cortisol levels. Patients with greater CR developed CCI later, showed significantly more positive connectivity values, had lower baseline cortisol levels, and displayed larger shifts in cortisol levels during cognitive load.

**Keywords:** cognitive reserve, chronic cerebral ischemia, higher and secondary education, resting fMRI, connectivity, cortisol, cognitive load

**Author contribution:** Fokin VF — manuscript writing; Ponomareva NV — study design; Shabalina AA — biochemical testing, determining salivary cortisol levels; Konovalov RN — design of neuroimaging tests; Medvedev RB — Doppler tests; Boravova AI — psychophysiological tests; Lagoda OV — clinical tests; Krotenkova MV — neuroimaging test management; Tanashyan MM — clinical test management, general study design.

**Compliance with ethical standards:** the study was approved by the Ethics Committee of the Research Center of Neurology (protocol No. 5-6/22 dated 1 June 2022). The informed consent was submitted by all study participants.


✉ **Correspondence should be addressed:** Vitaly F. Fokin  
Volokolamskoye shosse, 80, Moscow, 125367, Russia; fvf@mail.ru

**Received:** 28.11.2024 **Accepted:** 08.01.2025 **Published online:** 31.01.2025

**DOI:** 10.24075/brsmu.2025.002

**Copyright:** © 2025 by the authors. **Licensee:** Pirogov University. This article is an open access article distributed under the terms and conditions of the Creative Commons Attribution (CC BY) license (<https://creativecommons.org/licenses/by/4.0/>).

## КОГНИТИВНЫЙ РЕЗЕРВ БОЛЬНЫХ ХРОНИЧЕСКОЙ ИШЕМИЕЙ МОЗГА

В. Ф. Фокин , Н. В. Пономарева, А. А. Шабалина, Р. Н. Коновалов, Р. Б. Медведев, А. И. Боровова, О. В. Лагода, М. В. Кротенкова, М. М. Танашян

Научный центр неврологии, Москва, Россия

Когнитивный резерв (КР) характеризуется способностью активировать нейронные сети для адаптивной реорганизации функций мозга в ответ на повреждение или стресс. Целью работы было выявление структурно-функциональной организации нейросетей у больных хронической ишемией мозга (ХИМ) с различным КР. В исследовании участвовали 137 женщин в возрасте 50–85 лет больных ХИМ без диабета. Средняя давность заболевания ХИМ —  $10,1 \pm 0,7$  года. Больные ХИМ были разделены на две группы: со средним (СО) и с высшим (ВО) образованием. Определяли содержание кортизола в слюне до и после когнитивной нагрузки, а также различие коннективной организации мозга по данным фМРТ в двух группах больных. Найдены коннективности преимущественно в слуховых областях, различные в двух группах, с учетом поправки на множественность сравнений (FDR), и чувствительные к уровню кортизола. Больные с более высоким КР позже заболели ХИМ, имели достоверно более положительные значения коннективностей, более низкий уровень фонового кортизола и более высокий сдвиг кортизола при когнитивной нагрузке.

**Ключевые слова:** когнитивный резерв, хроническая ишемия мозга, высшее образование, среднее образование, фМРТ покоя, коннективность, кортизол, когнитивная нагрузка

**Вклад авторов:** В. Ф. Фокин — написание статьи; Н. В. Пономарева — дизайн исследования; А. А. Шабалина — биохимические исследования, определение кортизола в слюне; Р. Н. Коновалов — дизайн нейровизуализационных исследований; Р. Б. Медведев — доплерографические исследования; А. И. Боровова — психофизиологические исследования; О. В. Лагода — клинические исследования; М. В. Кротенкова — руководство нейровизуализационными исследованиями; М. М. Танашян — руководство клиническими исследованиями, общий дизайн работы.

**Соблюдение этических стандартов:** исследование одобрено локальным этическим комитетом Научного центра неврологии (протокол № 5-6/22 от 1 июня 2022 г.). Все участники обследований подписали добровольное информированное согласие.

✉ **Для корреспонденции:** Виталий Федорович Фокин  
Волоколамское шоссе, д. 80, г. Москва, 125367, Россия; fvf@mail.ru

**Статья получена:** 28.11.2024 **Статья принята к печати:** 08.01.2025 **Опубликована онлайн:** 31.01.2025

**DOI:** 10.24075/vrgmu.2025.002

**Авторские права:** © 2025 принадлежат авторам. **Лицензиат:** РНИМУ им. Н. И. Пирогова. Статья размещена в открытом доступе и распространяется на условиях лицензии Creative Commons Attribution (CC BY) (<https://creativecommons.org/licenses/by/4.0/>).

Cognitive reserve (CR) is a concept describing the brain's ability to adapt to damage or aging. CR is characterized by the capability of engaging neural networks and ensuring adaptive reorganization of brain functions in response to damage or stress [1]. The concept of CR is widely used when describing aging, as well as neurodegenerative and vascular disorders of the brain.

There are two oppositely directed factors playing a key role in the CR organization: education and the effects of stress, which are often replaced by a more measurable trait, stress

hormone cortisol levels. Let us consider carefully these three characteristics.

The studies describing the effects of person's education on his/her body are divided into two large groups: the effects of social benefits associated with pursuing higher education (HE) and alterations of brain's structural and functional organization occurring under the influence of education. The period of cognitive training associated with pursuing HE can be considered as longer, than that associated with pursuing



secondary education (SE). HE is often finished at a relatively young age characterized by high brain plasticity, so there is an opportunity to optimally shape brain networks. The larger accumulated CR also manifesting itself in attitude to stress caused by cognitive stress represents one of the major benefits for individuals with HE.

The course of stress is different in men and women, so it is feasible to consider it separately. This paper is focused on the responses associated with cognitive stress in women with HE and SE suffering from chronic cerebral ischemia (CCI). Women with HE have potentially improved stress regulation mechanisms. This can be due to the dynamic changes in cortisol levels [2]. In women with HE, there is possibility of more intense activation of the prefrontal cortex (PFC) playing an important role in executive functions and emotional regulation [3]. HE is likely to result in stronger PFC cortex activation during stress, thereby contributing to better cognitive control and emotional regulation. This is especially true for interconnections between PFC and cingulate gyrus. Furthermore, HE is associated with enlargement of the hippocampus playing a role in regulation of memory and responses to stress, possibly ensuring a protective effect of education on hippocampal integrity [4].

One can see various patterns of activation of the amygdala involved in developing responses to fear and threat. HE can result in the less prominent and better controlled activation of the amygdala during stress [5].

Women with lower socioeconomic status that is often associated with little education have elevated basal cortisol levels, even when there seem to be no severe stressors [6]. Reduced hippocampal volume under conditions of chronic stress can negatively affect its functioning, which results in deterioration of memory and impaired stress regulation [7], as well as to reduction of CR.

In individuals with inadequate education, the increased amygdala reactivity and chronic stress can sensitize the amygdala, thereby contributing to enhanced fear response. Furthermore, PFC is not always able to regulate responses of the amygdala, which results in the less effective emotional regulation [8].

Studies of the neuronal correlates of cognitive load in women with different levels of education are still fairly limited, and the results of different studies are not always consistent. Higher cognitive load require larger cerebral energy resources, which results in the increased neuronal activity. This is suggested by the functional magnetic resonance imaging (fMRI) studies, where the increase in BOLD signal (Blood Oxygen Level Dependent) is associated with activation in parietal lobes and PFC. The increased activation in parietal lobes is associated with spatial processing, attention, and working memory, and their activity increases with increasing cognitive problems [9].

## METHODS

The study involved 137 women aged 50–85 years suffering from CCI without diabetes. The average duration of CCI was  $10.1 \pm 0.7$  years. CCI patients were divided into two groups: with SE and HE. The main etiological causes of CCI are as follows: atherosclerosis, hypertension (including hypertensive heart disease), venous insufficiency, diabetic angiopathy, vasculitis of various etiology, etc. Inclusion criteria: initial manifestations and subcompensated CCI; no need for permanent care from others in patients' daily life [10]. Non-inclusion criteria: dementia severity score 1 or more (Clinical Dementia Rating) [11]; history of acute cerebrovascular accident, traumatic brain injury, severe heart or renal failure, uncompensated thyroid dysfunction. The diagnosis of CCI was further verified

by duplex scan and follow-up MRI. All the patients were right-handed. The patients' body height and body weight were measured to determine body mass index (BMI).  $BMI = \text{body weight/body height}^2$ . Two age characteristics were taken into account: patient's age at the time of recording and age at first referral to a medical institution due to CCI symptoms. The first referral was usually associated with memory and concentration problems accompanying arterial hypertension, as well as with cerebrovascular accidents. The second trait was age at the time of experimental assessment. It was assumed that patients with different levels of education reached this stage at different age. Both groups of women were mainly knowledge workers, while women with SE were mainly accountants or nursing staff.

## Resting state fMRI

The subjects (25 CCI patients) underwent T2\* weighted resting state fMRI of the brain in order to record BOLD signal in the Magnetom Verio magnetic resonance imaging scanner (Siemens, Germany) with the magnetic field strength of 3.0 Tesla. The subjects were offered to follow the instructions: to relax as much as possible, lay still with the eyes closed (to avoid stimulation of visual sensory system), not to think about anything in particular. MRI data were processed using the SPM12 software in the MATLAB computing environment. The CONN-18b application on the SPM-12 platform was used to assess connectivity. Connectivity was assessed in various neural networks of the brain. We compared connectivity in two groups of CCI patients with different levels of education. Significance of differences in these groups was assessed based on the standardized regression coefficient adjusted for multiple comparisons (FDR, False Discovery Rate) in CONN-18b.

The MAGNETOM Verio magnetic resonance imaging unit (Siemens, Germany) had the magnetic field strength of 3.0 Tesla. Functional scans were acquired in the resting state using the T2\* weighted EPI sequence: TR = 1500 ms, TE = 30 ms, flip angle 70°, slice thickness 2 mm, FOV = 190 mm, FoV phase 100.0%.

## Cognitive tests

Patients were assessed using the previously reported correction test, verbal fluency test, Luria's verbal working memory test, MoCA test [12]. Furthermore, we recorded blood pressure, calculated pulse pressure (difference between systolic and diastolic blood pressure) and heart rate.

## Biochemical tests

The patients' salivary cortisol levels were determined using the Abbott i2000 ARCHITECT immunochemiluminescence analyzer (Abbott Laboratories, Illinois, USA) using the reagent kit of the same brand.

Saliva samples were collected in accordance with the previously reported protocol [13]. The patients did not drink alcohol for a week, tea or coffee for 1 h before saliva collection, rinsed their mouth with water 10 min before this. Saliva collection was accomplished through spitting into a test tube with the volume of at least 1.5 mL. Saliva samples contaminated with blood were excluded from the study. For that the enzyme immunoassay kit was used to determine contamination of saliva with blood [13].

## Statistical processing

Analysis of the data obtained was performed using the Statistica-12 software package (Dell, USA). The Kolmogorov–Smirnov test

**Table 1.** Demographic data of women with SE and HE suffering from CCI and significance of differences between the values of these groups

	CCI Women	BMI	Average age at the time of assessment	Initial presentation
SE	$n = 72$	$28.3 \pm 0.7$	$65.0 \pm 0.9$	$51.3 \pm 1.8$
HE	$n = 65$	$27.7 \pm 0.6$	$70.2 \pm 0.8$	$58.2 \pm 1.8$
$p$	0.48	0.55	0.00003	0.0077

**Note:** SE — secondary education, HE — higher education,  $p$  — significance of differences; the first value is the mean, the second value is the standard error. BMI — body mass index; Average age at the time of assessment — average age of patients at the time of experimental data recording; Initial presentation — average age of the patient's first referral to the medical institution due to the objectively confirmed CCI symptoms.

was used to test the distribution for normality. We calculated mean values, standard errors, conducted one-way analysis of variance and correlation analysis. To analyze neural networks, Student's t-test was calculated, and adjustment for multiple comparisons was applied — FDR (False Discovery Rate).

### Assessment procedure

Saliva was first collected at least 2 h after the meal; initially, we performed background recording of slow electrical activity (for no more than 5 min), then, with the 1–2 min break, the patients performed three cognitive tests: Kirchner' correction test (3 min), verbal fluency test (phonemic variant) (4–5 min), Luria's verbal working memory test (5–7 min). Saliva was collected again immediately after performing tests, within 1–2 min. The MoCa test was performed after the end of the experiments and saliva collection.

## RESULTS

In CCI patients, contingency between the level of education and age characteristics is significantly manifested in women. Table 1 provides demographic data showing the role of education in the dynamics of abnormal vascular aging (CCI).

There is a clearly visible effect of HE on the women's age characteristics: women with HE seek medical care for CCI later (Table 1). Initial presentation to the medical institution of individuals with SE took place about 7 years earlier compared to patients with HE. Since there are literature data on the impact of continued education on stress, let us consider the effects of education on the stress mechanisms, specifically on cortisol, the stress hormone (Table 2).

In women with HE, baseline cortisol levels were about 14 nmol/L lower, and responsiveness to cognitive load was about 3.5–5 times higher (Table 2). There are no significant differences in cortisol values after cognitive load in two groups. This largely explains different cortisol shift values reported for both groups. It seems that there is some maximum possible cortisol level associated with cognitive load, and the difference

in cortisol shift values is explained by different baseline cortisol levels reported for both groups. We have revealed a significant correlation between baseline cortisol levels and relative cortisol reactivity:  $r = 0.41$ ;  $n = 88$ ;  $p = 0.00008$ .

The cortisol level shift associated with cognitive load is related to the age of first referral to the medical institution due to the emergence of CCI symptoms in patients with HE (Fig. 1).

The greater the cortisol reactivity, the later the patient seeks medical help due to the emergence of CCI symptoms. It should be noted that patients with almost the same disease severity were selected in the hospital for assessment. Individuals with HE had lower baseline cortisol levels, than women with SE (Table 1), while the patients' age had no significant effect on cortisol levels ( $p = 0.14$ ). Under cognitive load, cortisol levels of individuals with HE and SE were almost the same: on average  $63.0 \pm 3.4$  nmol/L ( $n = 83$ ).

What are the differences in organization of neural networks based on fMRI data in patients with different levels of education? Let us consider the differences in indicators of connectivities connecting brain regions in individuals with HE and SE (Fig. 2).

Predominance of positive connectivity differences showing that contingency of some brain structures in patients with HE is higher, than in patients with SE, can be seen (Fig. 2). These differences relate mainly to the temporal regions of both hemispheres and hippocampus, as well as to some regions of the cerebellum and cerebellar vermis.

Let us consider statistical characteristics of the difference in connectivities significant taking into account multiple comparisons and different in both groups of patients (Table 3). The analysis of these connectivities shows, which connections predominate in patients with HE and SE.

It should be noted that positive connections predominate in individuals with HE (Table 3). The only negative connectivity linking the Heschl's gyrus with the cerebellar vermis is non-significant considering multiple comparisons ( $p$ -FDR > 0.5). This connectivity is provided in Table 3, since the  $p$ -FDR value exceeds significant by less than 0.008.

Connectivities between the above regions can be digitized and presented as vectors, where a regression coefficient would

**Table 2.** Effects of education on cortisol levels in women suffering from CCI with higher and secondary education

	$n$	F	$p$	SE	HE
Baseline cortisol, nmol/L	93	6.256	0.014	$62.2 \pm 3.4$ (52)	$48.0 \pm 4.7$ (41)
Cortisol after cognitive load, nmol/L	83	0.206	0.651	$64.4 \pm 4.4$ (47)	$61.3 \pm 5.3$ (36)
Cortisol shift after cognitive load, nmol/L	83	8.597	0.004	$3.4 \pm 2.6$ (47)	$14.0 \pm 2.2$ (36)
Relative cortisol shift relative to baseline cortisol	83	19.666	0.00002	$0.08 \pm 0.04$ (47)	$0.4 \pm 0.07$ (36)

**Note:**  $n$  — number of surveyed individuals, F — Fisher's exact test,  $p$  — significance of differences between the values of two groups; in brackets the number of individuals surveyed; other abbreviations are the same, as in Table 1.

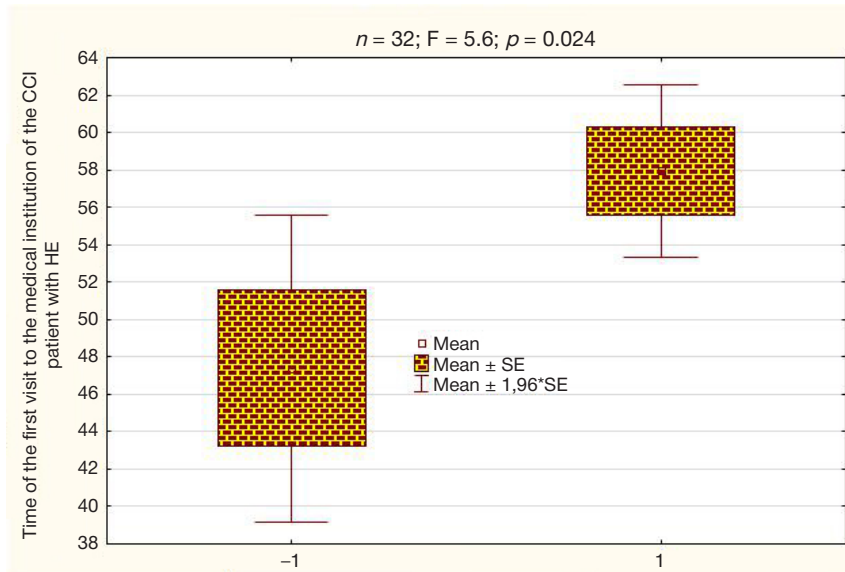


**Fig. 1.** Value of the cortisol shift associated with cognitive load is related to the time of initial presentation to the medical institution in patients with HE. -1 — average cortisol shift is close to zero ( $0.02 \pm 2.4$  nmol/L); 1 — average cortisol shift is  $20.09 \pm 2.1$  nmol/L. On the top there are statistical characteristics of differences in the age of first visit to the medical institution vs. cortisol shift

be correlated to each connectivity of each patient. These connectivities show significant differences in both groups based on the F-test varying between 17.5 and 27.4 with the significance levels between 0.00035 and 0.00003.

Some connectivities are related to cortisol regulation (Table 4).

Connectivities that are positive by sign are negatively correlated to baseline cortisol levels and positively correlated with relative cortisol reactivity; negative connectivity (HGr-Ver10) is negatively correlated to relative cortisol reactivity.

Thus, certain connectivities are significantly different in individuals with different levels of education and are associated with regulation of cortisol levels. The contribution of the PPr-

pSTGI, CO<sub>r</sub>-PTI, and HGr-Ver10 connectivities to ensuring cognitive reserve is likely to be associated with their connections with the auditory-speech system.

#### DISCUSSION

Our studies have revealed a later incidence of CCI in women with HE. It is likely that direct impact of education has a significant effect on CR. CR of women with HE combined with such factors, as social status and a more healthy lifestyle, contribute to stress reduction and, therefore, to the later CCI onset. This is also confirmed by lower baseline cortisol levels

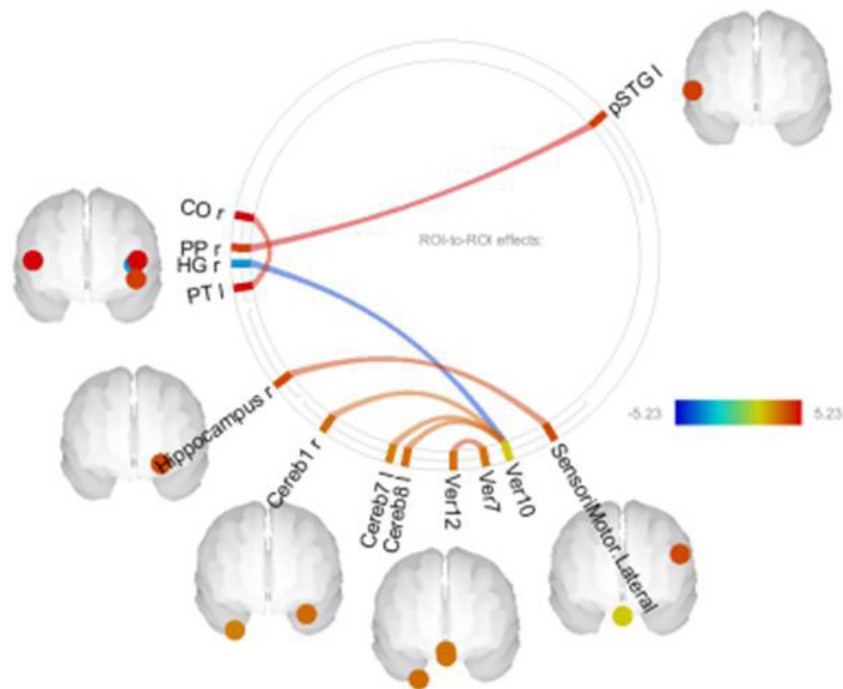


**Fig. 2.** Connectivity showing significant differences in patients with HE and SE. Red lines are positive, these correspond to higher connectivity values in patients with HE. Blue lines are negative, these correspond to higher connectivity values in patients with SE. Significance was calculated considering multiple comparisons ( $p\text{-FDR} < 0.05$ ). On the right there is a color chart of differences based on the t-test. CO — central operculum cortex, PP — planum polare (part of superior temporal gyrus), HG — Heschl's gyrus, PT — planum temporale, Hippocampus — hippocampus, SensorMotor.Lateral — sensorimotor lateral neural network, STG — superior temporal gyrus, Cereb — cerebellum, Ver — cerebellar vermis, numbers after Cereb and Ver are areas of the cerebellum and vermis, *p* — posterior, *r* — right hemisphere, *l* — left hemisphere

**Table 3.** Connectivities that are significantly different in the groups of patients with HE and SE and their statistical characteristics

Коннективности	<i>beta</i>	T (25)	<i>p-unc</i>	<i>p-FDR</i>
PP r-pSTG l	0.29	5.23	0.000026	0.004331
Hippocampus-SensoriMotor.Lateral	0.28	4.36	0.000229	0.037552
HG r-Ver 10	-0.19	-4.19	0.000353	0.057909
COr-PTI	0.36	4.69	0.000101	0.016558
Ver7-Ver12	0.23	4.56	0.000138	0.022645

**Note:** *beta* — average regression coefficient, T — T-test, *p-unc* — uncorrected significance level, *p-FDR* — significance level considering multiple comparisons. Number of patients — 25 individuals.

in patients with HE and increased cortisol responsiveness to cognitive load. High cortisol reactivity in such individuals supports a more effective energy supply of cognitive functions and their successful realization, especially when the mental load is relatively brief. The fact of higher brain connectivity in women with HE and the relationship between these connectivities and cognitive functions seems to be important.

According to our data, women with HE develop chronic cerebral ischemia (CCI) later, which is suggested by their later referral to medical institutions (on average by 7 years) and the older age of the beginning of assessment, given they have the same disease stage corresponding to stage 1 or 2 dyscirculatory encephalopathy. The fact that CCI patients with HE age slower is confirmed by higher connectivity of the brain neural networks, which is generally considered to be the sign of the better functioning and younger brain [14].

Modern literature describes differences in aging of women with HE and SE. These differences relate to biological age and external manifestations of age-related changes. Undoubtedly, several factors, including the level of education, contribute to slowing down the aging processes [15]. HE is often correlated to higher socioeconomic status, which results in better access to the resources affecting health and aging. This includes access to high-quality healthcare, proper diet and healthy habits. Well-educated women can be more prone to maintaining healthy lifestyle, including regular physical exercise, smoking cessation, and body weight control. All of them also know more about the health risks and preventive measures.

HE is associated with the larger CR, i.e. the brain's ability to cope with damage and maintain normal functioning [1]. This can result in the later onset or slower progression of the age-related cognitive decline. Women with HE develop CCI at older age and show slower disease progression, which is also true for Alzheimer's disease and the development of other dementia types [16].

The relationship between education and cortisol levels suggesting lower baseline cortisol levels in individuals with HE is also worth attention. The issue of connectivities that are

different in individuals with different levels of education and sensitive to cortisol levels suggests that there is a principal relationship between two major CR factors.

Functional connectivity between certain brain regions, such as posterior parietal region (PPr), posterior superior temporal gyrus (pSTG), corticomotor output region (COr), parietal cortex (PTI), and the cerebellar vermis (HGr-Ver10), play an important role in auditory processing, speech and cognitive functions in general. Neuroimaging studies have shown that the characteristics of these connectivities are often different in patients with various disorders of auditory processing, such as verbal and auditory load. These connectivities are also correlated to cortisol levels, especially in response to cognitive load [17–18].

Based on the structural and physiological organization of these brain regions, it can be assumed that the PPr-pSTG connectivity being part of the auditory association system contributes to integration of auditory information and understanding of language [19]. The COr-PTI connection is considered to be involved in synthesis of speech and sensorimotor integration essential for speech functions [20]. The HGr-Ver10 connectivity connecting primary auditory cortex with the cerebellar vermis is considered to be basic for auditory-motor regulation, which contributes to implementation of the tasks requiring coordination of auditory stimuli and motor responses under normal and abnormal conditions [21]. Thus, the role of these connections in construction and organization of CR becomes more evident.

## CONCLUSION

HE of women is highly likely to ensure a number of extra benefits. This is often associated with the higher material wealth, awareness of healthy lifestyle, lower adherence to harmful habits, and other factors. All the above, along with lower cortisol levels in individuals with HE, contribute to higher CR and longer health preservation. This is also confirmed by higher connectivity values associated with lower cortisol levels in individuals with HE.

**Table 4.** Correlation coefficients (*r*) and significance levels (*p*) for connectivities and cortisol characteristics

<i>n</i> = 25	PPr-pSTGl	COr-PTI	HGr-Ver10
Cortisol, baseline, <i>r</i>	-0.437	-0.418	0.2981
<i>p</i>	0.029	0.038	0.148
Relative cortisol shift, <i>r</i>	0.517	0.485	-0.498
<i>p</i>	0.008	0.014	0.011

**Note:** *n* — number of patients. PP — right planum polare, pSTGl — posterior part of the left superior temporal gyrus; COr — right central operculum cortex, PTI — left planum temporale; HGr — right Heschl's gyrus, Ver10 — Vermis 10.



## References

1. Stern Y. What is cognitive reserve? Theory and findings. *Journal of the International Neuropsychological Society*. 2002; 8 (3): 450–58. Available from: <https://doi.org/10.1017/S1355617702814268>.
2. Schuurmans IK, Hoepel SJW, Cecil CAM, Hillegers MHJ, Ikram MA, Luik AI. The Association of Life Stress with Subsequent Brain and Cognitive Reserve in Middle-Aged Women. *J Alzheimers Dis*. 2023; 93 (1): 97–106. DOI: 10.3233/JAD-220923. PMID: 36938734; PMCID: PMC10200172.
3. Ochsner KN, Gross JJ. The cognitive control of emotion. *Trends in Cognitive Sciences*. 2005; 9 (5): 242–9. Available from: <https://doi.org/10.1016/j.tics.2005.03.005>.
4. Tang X, Varma VR, Miller MI, Carlson MC. Education is associated with sub-regions of the hippocampus and the amygdala vulnerable to neuropathologies of Alzheimer's disease. *Brain Struct Funct*. 2017; 222 (3): 1469–79. DOI: 10.1007/s00429-016-1287-9. Epub 2016 Aug 17. PMID: 27535407; PMCID: PMC5850930.
5. Phelps EA. Emotion and cognition: insights from studies of the human amygdala. *Annu Rev Psychol*. 2006; 57: 27–53. DOI: 10.1146/annurev.psych.56.091103.070234. PMID: 16318588.
6. Dowd JB, Simanek AM, Aiello AE. Socio-economic status, cortisol and allostatic load: a review of the literature. *Int J Epidemiol*. 2009; 38 (5): 1297–309. DOI: 10.1093/ije/dyp277. Epub 2009 Aug 31. PMID: 19720725; PMCID: PMC2755130.
7. Wingenfeld K, Wolf OT. Stress, memory, and the hippocampus. *Front Neurol Neurosci*. 2014; 34: 109–20. DOI: 10.1159/000356423. Epub 2014 Apr 16. PMID: 24777135.
8. Davidson RJ, Jackson DC, Kalin NH. Emotion, plasticity, context, and regulation: perspectives from affective neuroscience. *Psychol Bull*. 2000; 126 (6): 890–909. DOI: 10.1037/0033-2909.126.6.890. PMID: 11107881.
9. Culham JC, Kanwisher NG. Neuroimaging of cognitive functions in human parietal cortex. *Curr Opin Neurobiol*. 2001; 11 (2): 157–63. DOI: 10.1016/S0959-4388(00)00191-4. PMID: 11301234.
10. Tanashyan MM, Maksimova MYu, Domashenko MA. Discirkuljatornaja jencefalopatija. *Putevoditel' vrachebnyh naznachenij*. 2015; 2: 1–25.
11. Morris JC. Clinical dementia rating: a reliable and valid diagnostic and staging measure for dementia of the Alzheimer type. *Int Psychogeriatric*. 1997; (9 Suppl 1): 173–76.
12. Fokin VF, Ponomareva NV, Kononov RN, Krotchenkova MV, Medvedev RB, Lagoda OV, Tanashyan MM. Vlijanie urovnja obrazovanija na funkcional'nuju organizaciju mozga bol'nyh hronicheskoj cerebral'noj ishemijsk. *Annaly klinicheskoj i jeksperimental'noj nevrologii*. 2021; 15 (2): 35–41. DOI: 10.25692/ACEN.2021.2.5.
13. Fokin VF, Shabalina AA, Ponomareva NV, Medvedev RB, Lagoda OV, Tanashyan MM. Kortizol, citokiny i vegetativnye izmenenija pri kognitivnoj nagruzke u bol'nyh hronicheskoj ishemijsk mozga. *Patologicheskaja fiziologija i jeksperimental'naja terapija*. 2023; 67 (3): 51–57. DOI: 10.25557/0031-2991.2023.03.51-57.
14. Cansino S. Brain connectivity changes associated with episodic recollection decline in aging: A review of fMRI studies. *Front Aging Neurosci*. 2022; 14: 1012870. DOI: 10.3389/fnagi.2022.1012870. PMID: 36389073; PMCID: PMC9640923.
15. Seblova D, Berggren R, Lövdén M. Education and age-related decline in cognitive performance: Systematic review and meta-analysis of longitudinal cohort studies. *Ageing Res Rev*. 2020; 58: 101005. DOI: 10.1016/j.arr.2019.101005. Epub 2019 Dec 24. PMID: 31881366.
16. Zahodne LB, Stern Y, Manly JJ. Differing effects of education on cognitive decline in diverse elders with low versus high educational attainment. *Neuropsychology*. 2015; 29 (4): 649–57. DOI: 10.1037/neu0000141. Epub 2014 Sep 15. PMID: 25222199; PMCID: PMC4362867.
17. Rivera-Bonet CN, Birn RM, Ladd CO, Meyerand ME, Abercrombie HC. Cortisol effects on brain functional connectivity during emotion processing in women with depression. *J Affect Disord*. 2021; 287: 247–54. DOI: 10.1016/j.jad.2021.03.034. Epub 2021 Mar 17. PMID: 33799044; PMCID: PMC8128282.
18. Jentsch VL, Merz CJ, Wolf OT. Restoring emotional stability: Cortisol effects on the neural network of cognitive emotion regulation. *Behav Brain Res*. 2019; 18 (374): 111880. DOI: 10.1016/j.bbr.2019.03.049. Epub 2019 Apr 1. PMID: 30946860.
19. Hickok G, Poeppel D. The cortical organization of speech processing. *Nature Reviews Neuroscience*. 2007; 8 (5): 393–402. Available from: <https://doi.org/10.1038/nrn2113>.
20. Heald SL, Nusbaum HC. Speech perception as an active cognitive process. *Front Syst Neurosci*. 2014; 8: 35. DOI: 10.3389/fnsys.2014.00035. PMID: 24672438; PMCID: PMC3956139.
21. Wang Z, Wang Y, Sweeney JA, Gong Q, Lui S, Mosconi MW. Resting-State Brain Network Dysfunctions Associated With Visuomotor Impairments in Autism Spectrum Disorder. *Front Integr Neurosci*. 2019; 13: 17. DOI: 10.3389/fnint.2019.00017. PMID: 31213995; PMCID: PMC6554427.

## Литература

1. Stern Y. What is cognitive reserve? Theory and findings. *Journal of the International Neuropsychological Society*. 2002; 8 (3): 450–58. Available from: <https://doi.org/10.1017/S1355617702814268>.
2. Schuurmans IK, Hoepel SJW, Cecil CAM, Hillegers MHJ, Ikram MA, Luik AI. The Association of Life Stress with Subsequent Brain and Cognitive Reserve in Middle-Aged Women. *J Alzheimers Dis*. 2023; 93 (1): 97–106. DOI: 10.3233/JAD-220923. PMID: 36938734; PMCID: PMC10200172.
3. Ochsner KN, Gross JJ. The cognitive control of emotion. *Trends in Cognitive Sciences*. 2005; 9 (5): 242–9. Available from: <https://doi.org/10.1016/j.tics.2005.03.005>.
4. Tang X, Varma VR, Miller MI, Carlson MC. Education is associated with sub-regions of the hippocampus and the amygdala vulnerable to neuropathologies of Alzheimer's disease. *Brain Struct Funct*. 2017; 222 (3): 1469–79. DOI: 10.1007/s00429-016-1287-9. Epub 2016 Aug 17. PMID: 27535407; PMCID: PMC5850930.
5. Phelps EA. Emotion and cognition: insights from studies of the human amygdala. *Annu Rev Psychol*. 2006; 57: 27–53. DOI: 10.1146/annurev.psych.56.091103.070234. PMID: 16318588.
6. Dowd JB, Simanek AM, Aiello AE. Socio-economic status, cortisol and allostatic load: a review of the literature. *Int J Epidemiol*. 2009; 38 (5): 1297–309. DOI: 10.1093/ije/dyp277. Epub 2009 Aug 31. PMID: 19720725; PMCID: PMC2755130.
7. Wingenfeld K, Wolf OT. Stress, memory, and the hippocampus. *Front Neurol Neurosci*. 2014; 34: 109–20. DOI: 10.1159/000356423. Epub 2014 Apr 16. PMID: 24777135.
8. Davidson RJ, Jackson DC, Kalin NH. Emotion, plasticity, context, and regulation: perspectives from affective neuroscience. *Psychol Bull*. 2000; 126 (6): 890–909. DOI: 10.1037/0033-2909.126.6.890. PMID: 11107881.
9. Culham JC, Kanwisher NG. Neuroimaging of cognitive functions in human parietal cortex. *Curr Opin Neurobiol*. 2001; 11 (2): 157–63. DOI: 10.1016/S0959-4388(00)00191-4. PMID: 11301234.
10. Танашян М. М., Максимова М. Ю., Домашенко М. А. Дисциркуляторная энцефалопатия. *Путеводитель врачебных назначений*. 2015; 2: 1–25.
11. Morris JC. Clinical dementia rating: a reliable and valid diagnostic and staging measure for dementia of the Alzheimer type. *Int Psychogeriatric*. 1997; (9 Suppl 1): 173–76.
12. Фокин В. Ф., Пономарева Н. В., Коновалов Р. Н., Кротенкова М. В., Медведев Р. Б., Лагода О. В., Танашян М. М. Влияние уровня образования на функциональную организацию мозга больных хронической церебральной ишемией. *Анналы клинической и экспериментальной неврологии*. 2021; 15 (2): 35–41. DOI: 10.25692/ACEN.2021.2.5
13. Фокин В. Ф., Шабалина А. А., Пономарева Н. В., Медведев Р. Б., Лагода О. В., Танашян М. М. Кортизол, цитокины и вегетативные изменения при когнитивной нагрузке у больных хронической ишемией мозга. *Патологическая физиология и*

- экспериментальная терапия. 2023; 67 (3): 51–57. DOI: 10.25557/0031-2991.2023.03.51-57.
14. Cansino S. Brain connectivity changes associated with episodic recollection decline in aging: A review of fMRI studies. *Front Aging Neurosci.* 2022; 14: 1012870. DOI: 10.3389/fnagi.2022.1012870. PMID: 36389073; PMCID: PMC9640923.
  15. Seblova D, Berggren R, Lövdén M. Education and age-related decline in cognitive performance: Systematic review and meta-analysis of longitudinal cohort studies. *Ageing Res Rev.* 2020; 58: 101005. DOI: 10.1016/j.arr.2019.101005. Epub 2019 Dec 24. PMID: 31881366.
  16. Zahodne LB, Stern Y, Manly JJ. Differing effects of education on cognitive decline in diverse elders with low versus high educational attainment. *Neuropsychology.* 2015; 29 (4): 649–57. DOI: 10.1037/neu0000141. Epub 2014 Sep 15. PMID: 25222199; PMCID: PMC4362867.
  17. Rivera-Bonet CN, Birn RM, Ladd CO, Meyerand ME, Abercrombie HC. Cortisol effects on brain functional connectivity during emotion processing in women with depression. *J Affect Disord.* 2021; 287: 247–54. DOI: 10.1016/j.jad.2021.03.034. Epub 2021 Mar 17. PMID: 33799044; PMCID: PMC8128282.
  18. Jentsch VL, Merz CJ, Wolf OT. Restoring emotional stability: Cortisol effects on the neural network of cognitive emotion regulation. *Behav Brain Res.* 2019; 18 (374): 111880. DOI: 10.1016/j.bbr.2019.03.049. Epub 2019 Apr 1. PMID: 30946860.
  19. Hickok G, Poeppel D. The cortical organization of speech processing. *Nature Reviews Neuroscience.* 2007; 8 (5): 393–402. Available from: <https://doi.org/10.1038/nrn2113>.
  20. Heald SL, Nusbaum HC. Speech perception as an active cognitive process. *Front Syst Neurosci.* 2014; 8: 35. DOI: 10.3389/fnsys.2014.00035. PMID: 24672438; PMCID: PMC3956139.
  21. Wang Z, Wang Y, Sweeney JA, Gong Q, Lui S, Mosconi MW. Resting-State Brain Network Dysfunctions Associated With Visuomotor Impairments in Autism Spectrum Disorder. *Front Integr Neurosci.* 2019; 13: 17. DOI: 10.3389/fnint.2019.00017. PMID: 31213995; PMCID: PMC6554427.

## FEATURES OF INTRAUTERINE MICROBIOTA IN PATIENTS WITH ENDOMETRIAL POLYPS

Vanakova AI<sup>1,2</sup> ✉, Dolgushina NV<sup>1,2</sup>, Denisov PA<sup>1</sup>, Goncharuk OD<sup>1</sup>, Muravieva VV<sup>1</sup>, Priputnevich TV<sup>1</sup><sup>1</sup> Kulakov National Medical Research Center for Obstetrics, Gynecology and Perinatology, Moscow, Russia<sup>2</sup> Sechenov First Moscow State Medical University (Sechenov University), Moscow, Russia

Endometrial polyps (EPs) represent the most common form of benign intrauterine disorder. Microbial factor is one of the possible etiological factors of EPs. Investigation of endometrial microbiota can provide new opportunities for improvement of the EP diagnosis and treatment. The study is aimed to assess intrauterine microbiota composition in patients with endometrial polyps. A total of 84 patients with endometrial polyps based on histology assessment data were enrolled. The comparison group included 44 patients having no endometrial abnormality. Endometrial microbiota composition was assessed by the culturomics method using the extended set of selective and nonselective growth media. The endometrium sample was obtained before performing hysteroscopy. In patients with EP, growth of bacterial microflora in the uterine cavity was observed 2.4 times more often compared to patients having no endometrial abnormality (OR — 2.4, 95% CI — 1.1; 5.5). In cases of EP, intrauterine microbiota composition was characterized by larger species and taxonomic diversity. Microorganisms of the genera *Staphylococcus* and *Lactobacillus* prevailed. Further research focused on endometrial microecology can provide new opportunities for further improvement of the EP diagnosis and treatment strategies.

**Keywords:** intrauterine microbiota, cervical canal microbiota, endometrial polyps**Author contribution:** Dolgushina NV — study concept, design; Vanakova AI — data acquisition, manuscript writing; Goncharuk OD, Muravieva VV — laboratory testing; Denisov PA — statistical analysis, visualization; Muravieva VV, Priputnevich TV — data editing.✉ **Correspondence should be addressed:** Angelina I. Vanakova  
Trubetskaya, 8/2, Moscow, 119991, Russia; angelinavanakova@gmail.com**Received:** 21.01.2025 **Accepted:** 10.02.2025 **Published online:** 24.02.2025**DOI:** 10.24075/brsmu.2025.007**Copyright:** © 2025 by the authors. **Licensee:** Pirogov University. This article is an open access article distributed under the terms and conditions of the Creative Commons Attribution (CC BY) license (<https://creativecommons.org/licenses/by/4.0/>).

## ОСОБЕННОСТИ МИКРОБИОТЫ ПОЛОСТИ МАТКИ У ПАЦИЕНТОК С ПОЛИПАМИ ЭНДОМЕТРИЯ

А. И. Ванакова<sup>1,2</sup> ✉, Н. В. Долгушина<sup>1,2</sup>, П. А. Денисов<sup>1</sup>, О. Д. Гончарук<sup>1</sup>, В. В. Муравьева<sup>1</sup>, Т. В. Припутневич<sup>1</sup><sup>1</sup> Национальный медицинский исследовательский центр акушерства, гинекологии и перинатологии имени В. И. Кулакова, Москва, Россия<sup>2</sup> Первый Московский государственный медицинский университет имени И. М. Сеченова (Сеченовский университет), Москва, Россия

Полипы эндометрия (ПЭ) — наиболее распространенная форма доброкачественной внутриматочной патологии. Одним из возможных этиологических факторов ПЭ является микробный фактор. Изучение микробиоты эндометрия может предоставить новые возможности для совершенствования диагностики и лечения ПЭ. Целью исследования было изучить состав микробиоты полости матки у пациенток с полипами эндометрия. В исследование включены 84 пациентки с полипами эндометрия по данным гистологического исследования. В группу сравнения вошли 44 пациентки без патологии эндометрия. Состав микробиоты эндометрия исследовали методом культуromики с использованием расширенного набора селективных и неселективных питательных сред. Эндометрий получали перед проведением гистерорезектоскопии. У пациенток с ПЭ рост бактериальной микрофлоры в полости матки наблюдался в 2,4 раза чаще по сравнению с пациентками без патологии эндометрия (ОШ — 2,4, 95%-й ДИ — 1,1; 5,5). Состав микробиоты полости матки при наличии ПЭ отличался большим видовым и таксономическим разнообразием, преобладали микроорганизмы родов *Staphylococcus* и *Lactobacillus*. Дальнейшее изучение микроэкологии эндометрия может предоставить новые возможности для дальнейшего совершенствования диагностики и стратегий лечения ПЭ.

**Ключевые слова:** микробиота полости матки, микробиота цервикального канала, полипы эндометрия**Вклад авторов:** Н. В. Долгушина — концепция, дизайн исследования; А. И. Ванакова — сбор материала, написание текста; О. Д. Гончарук, В. В. Муравьева — лабораторная часть исследования; П. А. Денисов — статистический анализ данных, визуализация; В. В. Муравьева, Т. В. Припутневич — редактирование данных.✉ **Для корреспонденции:** Ангелина Игоревна Ванакова  
ул. Трубецкая, д. 8/2, г. Москва, 119991, Россия; angelinavanakova@gmail.com**Статья получена:** 21.01.2025 **Статья принята к печати:** 10.02.2025 **Опубликована онлайн:** 24.02.2025**DOI:** 10.24075/vrgmu.2025.007**Авторские права:** © 2025 принадлежат авторам. **Лицензиат:** РНИМУ им. Н. И. Пирогова. Статья размещена в открытом доступе и распространяется на условиях лицензии Creative Commons Attribution (CC BY) (<https://creativecommons.org/licenses/by/4.0/>).

Endometrial polyps (EPs) represent the most common form of benign intrauterine disorder [1]. According to hysteroscopy data, the prevalence of EP is 6–27%, depending on the fact of having complaints [2]. The rate of EP recurrence after surgical treatment varies between 13% and 43% [3–5]. The EP emergence can be associated with many factors, such as imbalance in expression of sex hormone receptors, long-term sustained stimulation with high estrogen levels, abnormal apoptosis and cell proliferation, gene mutation, inflammation, endometrial cell oxidative stress, etc. [6].

One possible etiological factor of EPs is microbial factor, both associated [7] and not associated [8] with chronic endometritis (CE). The research conclusions about the composition of uterine cavity microbiota associated with EP are different, which is largely associated with the complexity of sample collection without contamination from the lower reproductive tract. It has been found that alteration of intrauterine microbiota composition relative to healthy women results mainly from the increase in the rate of detecting vaginal bacteria (such as *Lactobacillus*, *Bifidobacterium*) [9, 10]. This can contribute to migration

and proliferation of cells, thereby causing local endometrial hyperplasia and the emergence of EPs [11].

Endometrial polyps play an important role in disturbance of female reproductive function [12] and deterioration of women's quality of life [13]. High risk of EP recurrence leads to repeated surgical interventions increasing the risk of intrauterine adhesions and infertility [14]. In this regard, the studies focused on identification of the causes of EP development and recurrence, as well as on the efficacy of the associated etiologically targeted therapy and EP prevention are of high relevance. For this purpose, the study to assess microbiota of the uterine cavity in patients with endometrial polyps was conducted.

## METHODS

A prospective study conducted in 2022–2024 at the Kulakov National Medical Research Center for Obstetrics, Gynecology and Perinatology involved 84 patients with the histologically confirmed endometrial polyps and 44 patients of the comparison group having no endometrial abnormality. Inclusion criteria: age from 18 years to the onset of menopause; informed consent to enrollment; presence of the histologically confirmed endometrial polyp for inclusion in the index group and no endometrial abnormality for inclusion in the comparison group. Exclusion criteria: cancer; stage 3–4 endometriosis/adenomyosis; submucosal uterine fibroid or intramural fibroid showing centripetal growth; acute or chronic inflammatory disorder; infectious disease; antibacterial or hormone drug intake within 3 months before inclusion in the study. The comparison group included patients with suspected endometrial abnormalities based on the pelvic ultrasound data, but having no endometrial pathology following the histology assessment data (proliferation stage according to histology report).

All the patients were assessed in accordance with the Endometrial Polyps clinical guidelines before admission to the hospital. Since there is a correlation between the menstrual cycle phase and microbial composition of the endometrium [15–18], biomaterial was collected in phase 1 of menstrual cycle.

To assess microbiota of the cervical canal before hysteroscopy, we collected the cervical canal content with a sterile Dacron swab to the test tube with the Amies transport medium (Copan, Italy). To reduce contamination of the uterine cavity contents with microflora of lower genitalia, various loci were sequentially treated with antiseptic: first, a sterile swab was used to remove mucus from the cervix, and the cervix was cleansed with a topical antiseptic containing octenidine 0.1% and phenoxyethanol 2%; after collecting the cervical discharge for further testing, the cervical canal was twice inundated using a bacteriological swab soaked with antiseptic with an interval of 5 min. The hysteroscope operating sheath was inserted transcervically through the internal orifice into the uterine cavity without prior cervical canal dilation. Surgical forceps were inserted into the vagina/cervix, biomaterial was collected at the first attempt. Then biospecimens were taken out of forceps, put in a sterile disposable container, and delivered to the laboratory.

To isolate facultative anaerobic microorganisms, a set of universal and selective media was used: Columbia agar, chocolate agar, mannitol salt agar (Conda, Spain), Endo's medium and Sabouraud agar (State Research Center for Applied Microbiology and Biotechnology; Obolensk, Russia). Lactobacilli were cultured in the Lactobacagar growth medium (State Research Center for Applied Microbiology and Biotechnology; Obolensk, Russia), obligate anaerobes in the pre-reduced Schaedler agar (Conda, Spain) with essential

supplementation and the Anaerob Basal Agar (Oxoid, UK). Obligate anaerobes were grown in the anaerobic box (Whitley DG 250 Anaerobic Workstation, UK) in the atmosphere representing a 3-component gas mixture (80% N<sub>2</sub>; 10% CO<sub>2</sub>; 10% H<sub>2</sub>) for 48 h. Species were identified by time-of-flight mass spectrometry (MALDI-TOF MS) in the MicroFlex mass spectrometer with the MALDI BioTyper v. 5.0 software (Bruker Daltonics, Germany).

The Originlab Pro 2021 (version 9.8.0.200, OriginLab Corporation, USA) and Statistica 10 (USA) software packages were used for statistical analysis of the data obtained and for visualization. We also used the Kolmogorov–Smirnov test to assess the normality of distribution. The normally distributed data were presented as mean ± standard deviation (SD), and comparison was performed using the Student's *t*-test. In other cases, the median with interquartile range (Me (Q25–Q75)) and the Mann–Whitney *U* test were used. Proportions (%) were calculated when assessing qualitative data. The  $\chi^2$  test helped us to compare categorical data and estimate significance of differences. Spearman's rank correlation coefficient was calculated to estimate correlations between the variables. OR with the 95% confidence interval (95% CI) was determined to compare binary data. The Margalef and Menhinick indices were applied to calculate species richness, and taxonomic diversity was calculated using the Simpson and Shannon indices (Table 1). The differences between statistical values were considered significant at  $p < 0.05$ .

## RESULTS

The median age of patients in two groups was 37 years, i.e. half of patients were of late fertile age. The average body mass index (BMI) was 21.7 kg/m<sup>2</sup>, 19% of patients were overweight or obese. The analysis of clinical and medical history data showed that there were no significant differences in basic clinical and medical history data between patients of two groups (Table 2). Patients with EPs three times more often used intrauterine contraceptive devices (IUCD) ( $p = 0.25$ ). A total of 39% of patients with EPs already had the history of polypectomy against the lack of such surgical history in the comparison group ( $p < 0.001$ ).

Patients with EPs were more commonly presented with meno-/merorrhagia and infertility than the patients in the comparison group (Table 3). The fact of having menorrhagia was directly related to the polyp size ( $r = 0.22$ ;  $p = 0.04$ ). Other complaints were not correlated to the polyp size, number or location inside the uterine cavity. Infertility was correlated to the history of polypectomy: among 42 infertile patients polypectomy was performed in 17 individuals (40.5%), while among patients having no infertility only 16 (18.6%) underwent polypectomy ( $p = 0.007$ ).

Investigation of the cervical canal microbiota revealed microflora growth in all the patients included in the study. A total of 49 species of microorganisms were identified: 41 species in the EP group, 28 species in the group without EPs. There were no significant differences in the species and taxonomic diversity in two groups, but it was higher in the EP group: the median Margalef index with interquartile range was 0.39 (0.19–0.39) in the EP group, 0.22 (0.22–0.45) in the group without EP, while that of Menhinick index were 0.31 (0.15–0.79) and 0.19 (0.19–0.21), of Simpson index 0.56 (0.5–0.66) and 0.5 (0.48–0.66), of Shannon index 0.95 (0.69–1.58) and 0.69 (0.66–1.39), respectively. Microorganisms of the genus *Lactobacillus* were most often identified (in 82.8% of patients), microorganisms of the genera *Streptococcus* (in 18.7% of patients) and



**Table 1.** Formulae for the species richness and diversity indices

Richness or diversity index	Formula
Margalef index	$d = (s - 1) / \ln N$
Menhinick index	$d_M = (s - 1) / (N)^{1/2}$
Simpson index	$\frac{S}{\sum_{i=1}^S p_i^2}$
Shannon index	$-\sum_{i=1}^S p_i \times \ln p_i$

**Note:**  $S$  — species richness (number of species);  $N$  — sample size (community size);  $n_i$  — number of species  $i$  bacteria;  $c$  — number of species common for two communities;  $a$  — number of species in the first community;  $b$  — number of species in the second community.

*Gardnerella* (in 14.8% of patients) ranked second (Fig. 1). When comparing colonization of individual microorganisms, no significant intergroup differences were revealed ( $p > 0.05$ ). Each vertical line represents microbiota of one woman, each cell represents bacterial content of the cervical canal in lg CFU/mL.

When assessing composition of intrauterine microbiota, microflora growth was reported in 52 patients out of 128: in 40 patients of the group with EPs (47.6%) and 12 patients of the comparison group (27.3%) ( $p = 0.026$ ). OR of detecting uterine microbial colonization in cases of EP relative to women without endometrial abnormality was 2.4 (95% CI — 1.1; 5.5). A total of 23 microbial species were isolated, which suggests more scarce species diversity of intrauterine microbiota compared to that of the cervical canal: 20 species of 9 genera in the group with EPs, 10 species of 8 genera in the group without EPs.

When comparing microbial colonization of the cervical canal and the uterine cavity, significant weak correlations ( $r = 0.2$ – $0.4$ ) were revealed for 10 microorganisms out of 53 (18.8%) in

24 patients. In more than a half of observations, no match between microbiota of the cervical canal and the uterine cavity was revealed.

The species and taxonomic diversity of intrauterine microbiota showed no significant differences in two groups, despite the fact that it was higher in the EP group: the median Shannon index with interquartile range was 1.98 (1.98–1.98) and 0.69 (0.67–0.69) in the groups, respectively (Fig. 2).

In the EP group, the genus *Staphylococcus* were the most frequently observed microorganisms (in 50% of patients), with the genus *Lactobacillus* in the second place (in 37.5% of patients). In the group without EPs, in contrast, microorganisms of the genus *Lactobacillus* prevailed (in 41.7% of patients), microorganisms of the genus *Staphylococcus* ranked second (in 25% of patients) (Fig. 3).

Comparison of the uterine cavity colonization with distinct microorganisms revealed differences in the form of more prominent colonization with *Lactobacillus crispatus* and

**Table 2.** Clinical and medical history characteristics of patients

Parameter	Group 1, $n = 84$	Group 2, $n = 44$	$P$ -value
Age, years *	38.5 (32–42)	35.5 (31.5–40.5)	0.43
BMI, kg/m <sup>2</sup> *	21.7 (19.5–24.2)	21.8 (19.8–23.7)	0.98
BMI $\geq 25$ kg/m <sup>2</sup> **	18 (21.4%)	6 (13.6%)	0.28
Smoking **	14 (16.7%)	10 (22.7%)	0.28
Menstrual cycle length, days *	28 (28–30)	28 (27–29)	0.23
Menstruation duration, days *	5 (5–7)	5 (5–6)	0.13
Gravidity ***	1 (0–6)	1 (0–6)	0.21
Parity ***	0 (0–3)	1 (0–3)	0.89
History of taking COCs **	26 (31%)	11 (25%)	0.48
History of using IUCD **	6 (7.1%)	1 (2.3%)	0.25
Endometriosis **	15 (17.8%)	9 (20.4%)	0.72
Adenomyosis **	15 (17.8%)	5 (11.4%)	0.33
Fibroid**	28 (33.3%)	14 (31.8%)	0.86
History of polypectomia **	33 (39.3%)	0	< 0.001

**Note:** \* — Me (Q25–Q75); \*\*\* — Me (min–max), Mann–Whitney  $U$  test; \*\* — abs (%),  $\chi^2$  test; COCs — combined oral contraceptives; GIT — gastrointestinal tract.

**Table 3.** Patient complaints

Parameter	Group 1, $n = 84$	Group 2, $n = 44$	$P$ -value
Menorrhagia	23 (27.4%)	6 (13.6%)	0.07
Metrorrhagia	37 (44%)	8 (18.2%)	0.003
Intermenstrual bleeding	8 (9.5%)	1 (2.3%)	0.12
Algomenorrhea	2 (2.4%)	6 (13.6%)	0.01
Chronic pelvic pain	16 (19%)	8 (18.2%)	0.9
Infertility	31 (36.9%)	11 (25%)	0.17
Miscarriage	17 (20.2%)	6 (13.6%)	0.35

**Note:** abs (%),  $\chi^2$  test.

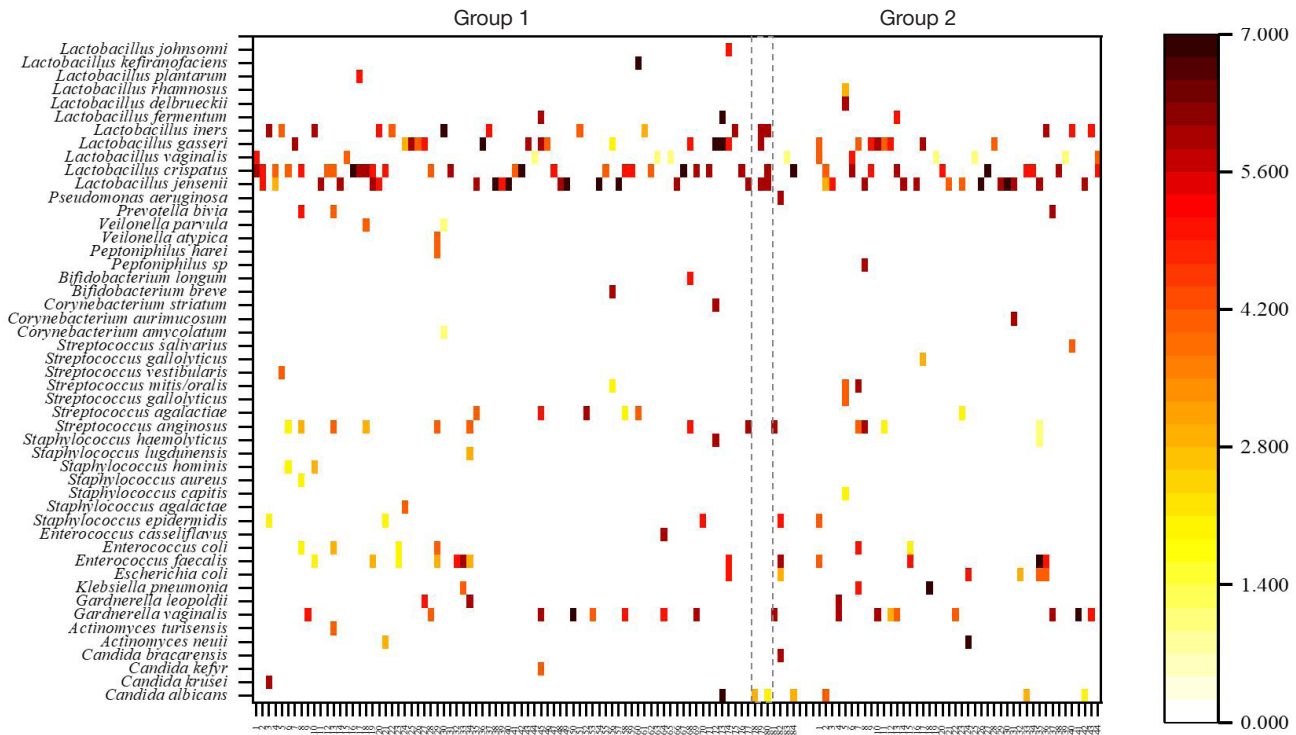


Fig. 1. Cervical canal microbiota in patients with endometrial polyps (group 1) and the comparison group (group 2) (each cell represents bacterial content of the cervical canal in lg CFU/mL)

*Staphylococcus hominis*, as well as with all *Staphylococcus spp.* in total in the group with EPs ( $p < 0.05$ ).

DISCUSSION

Meno-/metrorrhagia and infertility were the main clinical manifestations in patients with EPs included in the study, which is in line with the available data on the complaints that are most common in this cohort of patients. According to the literature data, abnormal menstrual bleeding is reported in more than a half of patients with EPs [13]. The second most common complaint was infertility, with endometrial polyps represented in 1/3 of cases. Polypectomy increases the probability of getting pregnant [12]. Furthermore, large proportion of patients with recurrent EPs is also notable (39.3% in the studied group).

When studying microbial composition in the uterine cavity, colonization of the uterine cavity with microorganisms was revealed in 40.6% of patients. The literature has already accumulated a sufficient amount of data confirming non-sterility of the uterine cavity both in pathology and in the norm [15, 19–26]. The earlier studies have also shown that the number of bacteria in the endometrial microbiota is reduced 2–4-fold relative to vaginal and cervical microbiota, while

bacterial diversity is increased [9, 27–29]. According to our data, the number of bacteria was actually less in the uterine cavity, but its species and taxonomic diversity was also reduced. The analysis of the association of intrauterine and cervical canal microbiota revealed no correlation in more than a half of cases. Thus, it has been confirmed again that endometrial microbiota is not identical to vaginal and cervical microbiota and has its own unique microbial composition. When comparing predominance of *Lactobacillus* in the uterine cavity and cervical canal, the 3 times lower relative abundance of *Lactobacillus* in the endometrium with regard to the cervix was reported, which is in line with the literature data [30, 31].

In our study, comparative analysis of intrauterine microbiota in patients with EPs and no endometrial abnormality was of major scientific interest. A number of studies have shown the importance of uterine microbiota for the development of disorders of female reproductive system, specifically endometrial hyperplasia and adenomyosis [23, 32]. There are sporadic studies of EP. Thus, compared to healthy women, the changes in intrauterine microbiota composition in women with EPs result largely from the increase in the detection rate of vaginal bacteria, such as *Lactobacillus* [9, 10]. In terms of pathogenesis, *Lactobacillus* and *Bifidobacterium* can contribute

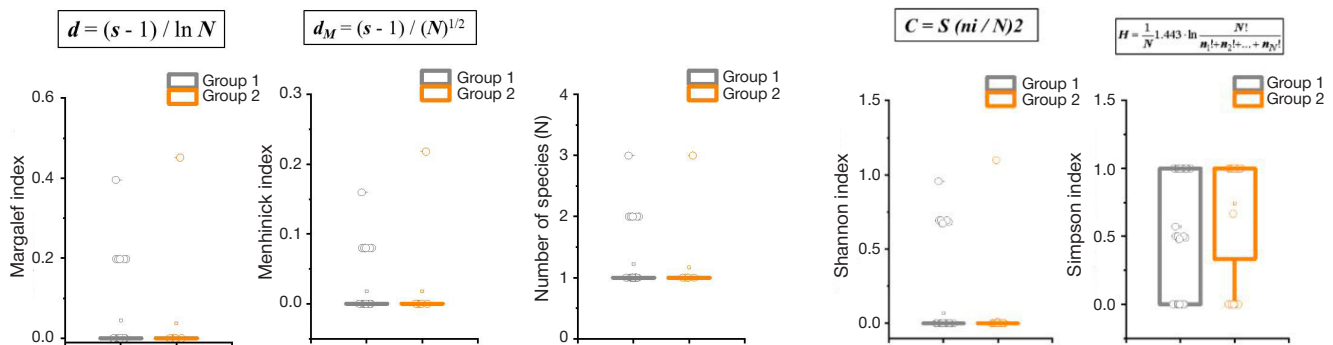


Fig. 2. Species richness and taxonomic diversity indices of intrauterine microbiota in patients of the studied groups

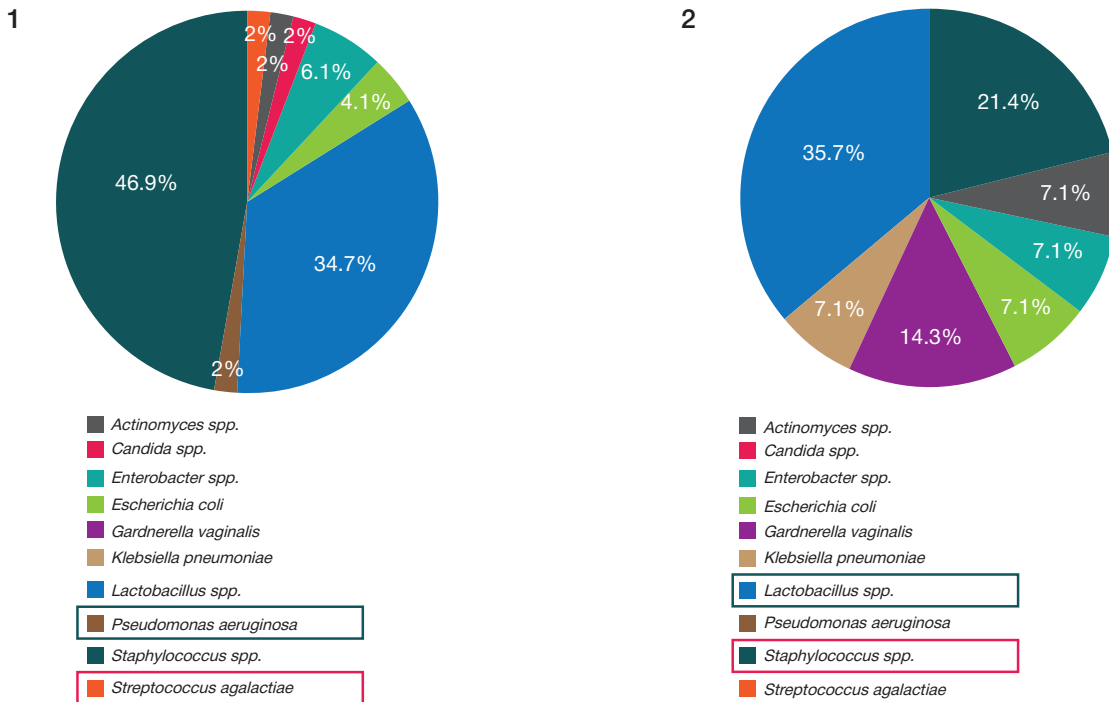


Fig. 3. Species diversity of intrauterine microbiota in patients of the studied groups: 1 — group with EPs, 2 — group without EPs

to cell migration and proliferation, which lead to local endometrial hyperplasia and the emergence of EPs [11]. We have found that microbial growth in the uterine cavity was reported 2.4 times more often in cases of having EPs compared to normal (OR — 2.4; 95% CI — 1.1; 5.5). Species diversity was higher in patients with EPs relative to the comparison group in both cervical canal (24 and 14 species, respectively) and the uterine cavity (10 and 4 species, respectively). In cases of EPs, genus *Staphylococcus* (50%) were found to be predominant species in the uterine cavity, while microorganisms of the genus *Lactobacillus* ranked second (37.5%). In contrast, in the group without EPs, microorganisms of the genus *Lactobacillus* prevailed (41.7%), and microorganisms of the genus *Staphylococcus* were found in the second place (25%).

## CONCLUSIONS

In patients with EPs, growth of bacterial microflora in the uterine cavity was observed 2.4 times more often, than in patients without endometrial abnormality. The species spectrum of the uterine cavity in cases of EPs was characterized by higher taxonomic diversity, microorganisms of the genera *Staphylococcus* and *Lactobacillus* prevailed. Since chronic endometritis is one of the causes of the EP development and recurrence, prescription of antibiotic therapy when performing polypectomy in routine clinical practice can reduce the rate of EP recurrence. Thus, further investigation of endometrial microecology can provide new opportunities for improvement of the EP diagnosis and treatment strategies.

## References

- Nijkang NP, et al. Endometrial polyps: Pathogenesis, sequelae and treatment. SAGE Open Medicine. SAGE Publications Ltd. 2019; 7.
- Fatemi HM, et al. Prevalence of unsuspected uterine cavity abnormalities diagnosed by office hysteroscopy prior to in vitro fertilization. Hum Reprod. 2010; 25 (8): 1959–65.
- Paradisi R, et al. Recurrence of Endometrial Polyps. Gynecol Obstet Invest. 2014; 78 (1): 26–32.
- Al-Hilli MM, et al. Long-Term Outcomes After Intrauterine Morcellation vs Hysteroscopic Resection of Endometrial Polyps. J Minim Invasive Gynecol. 2013; 20 (2): 215–21.
- Yang J-H, et al. Factors Influencing the Recurrence Potential of Benign Endometrial Polyps after Hysteroscopic Polypectomy. PLoS One. 2015; 10 (12): e0144857.
- Indraccolo U, et al. The pathogenesis of endometrial polyps: a systematic semi-quantitative review. Eur J Gynaecol Oncol. 2013; 34 (1): 5–22.
- Tapilskaja NI, Budilovskaja OV, Krysanova AA, Tolibova GH, Kopylova AA, Cypurdeeva ND, i dr. Mikrobiota jendometrija zhenshin s hronicheskim jendometritom i idiopatcheskim besplodiem. Akusherstvo i ginekologija. 2020; 4: 72–81. Russian.
- Cicinelli E, et al. Chronic Endometritis, a Common Disease Hidden Behind Endometrial Polyps in Premenopausal Women: First Evidence From a Case-Control Study. J Minim Invasive Gynecol. 2019; 26 (7): 1346–50.
- Cicinelli E, et al. Poor Reliability of Vaginal and Endocervical Cultures for Evaluating Microbiology of Endometrial Cavity in Women with Chronic Endometritis. Gynecol Obstet Invest. 2009; 68 (2): 108–15.
- Fang R-L, et al. Barcoded sequencing reveals diverse intrauterine microbiomes in patients suffering with endometrial polyps. Am J Transl Res. 2016; 8 (3): 1581–92.
- Teame T, et al. Paraprobiotics and Postbiotics of Probiotic Lactobacilli, Their Positive Effects on the Host and Action Mechanisms: A Review. Frontiers in Nutrition. Frontiers Media S.A. 2020; 7.
- Di Spiezo Sardo A, et al. Efficacy of hysteroscopy in improving reproductive outcomes of infertile couples: a systematic review and meta-analysis. Hum Reprod Update. 2016; 22 (4): 479–96.
- Clark TJ, Stevenson H. Endometrial Polyps and Abnormal Uterine Bleeding (AUB-P): What is the relationship, how are they diagnosed and how are they treated? Best Pract Res Clin Obstet Gynaecol. 2017; 40: 89–104.
- Tchente NC, Brichant G, Nisolle M. Asherman's syndrome : management after curettage following a postnatal placental

- retention and literature review. *Rev Med Liege*. 2018; 73 (10): 508–12.
15. Zhu N, et al. "Iron triangle" of regulating the uterine microecology: Endometrial microbiota, immunity and endometrium. *Frontiers in Immunology*. Frontiers Media S.A. 2022; 13.
  16. Critchley HOD, et al. Menstruation: science and society. *American Journal of Obstetrics and Gynecology*. Mosby Inc. 2020; 223 (5): 624–64.
  17. Lopes dos Santos Santiago G. et al. Longitudinal qPCR Study of the Dynamics of *L. crispatus*, *L. iners*, *A. vaginae*, (Sialidase Positive) *G. vaginalis*, and *P. bivia* in the Vagina. *PLoS One*. 2012; 7 (9).
  18. Pelzer ES, et al. A role for the endometrial microbiome in dysfunctional menstrual bleeding. *Antonie van Leeuwenhoek. Int J Gen Mol Microbiol*. 2018; 111 (6): 933–43.
  19. Ansbacher R, Boyson WA, Morris JA. Sterility of the uterine cavity. *Am J Obstet Gynecol*. 1967; 99 (3): 394–96.
  20. Mitchell CM, et al. Colonization of the upper genital tract by vaginal bacterial species in nonpregnant women. *Am J Obstet Gynecol Mosby Inc*. 2015; 212 (5): 611.e1-611.e9.
  21. Verstraelen H, et al. Characterisation of the human uterine microbiome in non-pregnant women through deep sequencing of the V1-2 region of the 16S rRNA gene. *PeerJ PeerJ Inc*. 2016; 2016: 1.
  22. Giudice LC. Challenging dogma: the endometrium has a microbiome with functional consequences! *Am J Obstet Gynecol*. 2016; 215 (6): 682–3.
  23. Chen C, et al. The microbiota continuum along the female reproductive tract and its relation to uterine-related diseases. *Nat Commun Nature Publishing Group*. 2017; 8 (1).
  24. Miles SM, Hardy BL, Merrell DS. Investigation of the microbiota of the reproductive tract in women undergoing a total hysterectomy and bilateral salpingo-oophorectomy. *Fertil Steril Elsevier Inc*. 2017; 107 (3): 813-20.e1.
  25. Koedooder R, et al. Identification and evaluation of the microbiome in the female and male reproductive tracts. *Hum Reprod Update*. 2019; 25 (3): 298–325.
  26. Keburija LK, Smolnikova VYu, Priputnevich TV. M.V.V. Mikrobiota polosti matki i ee vliyanie na reproduktivnye ishody. *Akusherstvo i ginekologija*. 2019; 2: 22–7. Russian.
  27. Peterson J, et al. The NIH Human Microbiome Project. *Genome Res*. 2009; 19 (12): 2317–23.
  28. Kitaya K, et al. Chronic Endometritis: Potential Cause of Infertility and Obstetric and Neonatal Complications. *Am J Reprod Immunol*. 2016; 75 (1): 13–22.
  29. Liang J, et al. Analysis of the microbiota composition in the genital tract of infertile patients with chronic endometritis or endometrial polyps. *Front Cell Infect Microbiol*. 2023; 13.
  30. Moreno I, et al. Evidence that the endometrial microbiota has an effect on implantation success or failure. *American Journal of Obstetrics and Gynecology*. Mosby Inc. 2016; 215 (6): 684–703.
  31. Fransiak JM, et al. Endometrial microbiome at the time of embryo transfer: next-generation sequencing of the 16S ribosomal subunit. *J Assist Reprod Genet*. 2016; 33 (1): 129–36.
  32. Margulies SL, et al. Chronic endometritis: A prevalent yet poorly understood entity. *Int J Gynecol Obstet*. 2022; 158 (1): 194–200.

#### Литература

1. Nijkang NP, et al. Endometrial polyps: Pathogenesis, sequelae and treatment. SAGE Open Medicine. SAGE Publications Ltd. 2019; 7.
2. Fatemi HM, et al. Prevalence of unsuspected uterine cavity abnormalities diagnosed by office hysteroscopy prior to in vitro fertilization. *Hum Reprod*. 2010; 25 (8): 1959–65.
3. Paradisi R, et al. Recurrence of Endometrial Polyps. *Gynecol Obstet Invest*. 2014; 78 (1): 26–32.
4. AlHilli MM, et al. Long-Term Outcomes After Intrauterine Morcellation vs Hysteroscopic Resection of Endometrial Polyps. *J Minim Invasive Gynecol*. 2013; 20 (2): 215–21.
5. Yang J-H, et al. Factors Influencing the Recurrence Potential of Benign Endometrial Polyps after Hysteroscopic Polypectomy. *PLoS One*. 2015; 10 (12): e0144857.
6. Indraccolo U, et al. The pathogenesis of endometrial polyps: a systematic semi-quantitative review. *Eur J Gynaecol Oncol*. 2013; 34 (1): 5–22.
7. Тапиловская Н. И., Будиловская О. В., Крысанова А. А., Толибова Г. Х., Копылова А. А., Цыгурдеева Н. Д., и др. Микробиота эндометрия женщин с хроническим эндометритом и идиопатическим бесплодием. *Акушерство и гинекология*. 2020; 4: 72–81.
8. Cicinelli E, et al. Chronic Endometritis, a Common Disease Hidden Behind Endometrial Polyps in Premenopausal Women: First Evidence From a Case-Control Study. *J Minim Invasive Gynecol*. 2019; 26 (7): 1346–50.
9. Cicinelli E, et al. Poor Reliability of Vaginal and Endocervical Cultures for Evaluating Microbiology of Endometrial Cavity in Women with Chronic Endometritis. *Gynecol Obstet Invest*. 2009; 68 (2): 108–15.
10. Fang R-L, et al. Barcoded sequencing reveals diverse intrauterine microbiomes in patients suffering with endometrial polyps. *Am J Transl Res*. 2016; 8 (3): 1581–92.
11. Teame T, et al. Paraprobiotics and Postbiotics of Probiotic Lactobacilli, Their Positive Effects on the Host and Action Mechanisms: A Review. *Frontiers in Nutrition*. Frontiers Media S.A. 2020; 7.
12. Di Spiezio Sardo A, et al. Efficacy of hysteroscopy in improving reproductive outcomes of infertile couples: a systematic review and meta-analysis. *Hum Reprod Update*. 2016; 22 (4): 479–96.
13. Clark TJ, Stevenson H. Endometrial Polyps and Abnormal Uterine Bleeding (AUB-P): What is the relationship, how are they diagnosed and how are they treated? *Best Pract Res Clin Obstet Gynaecol*. 2017; 40: 89–104.
14. Tchente NC, Brichant G, Nisolle M. Asherman's syndrome : management after curettage following a postnatal placental retention and literature review. *Rev Med Liege*. 2018; 73 (10): 508–12.
15. Zhu N, et al. "Iron triangle" of regulating the uterine microecology: Endometrial microbiota, immunity and endometrium. *Frontiers in Immunology*. Frontiers Media S.A. 2022; 13.
16. Critchley HOD, et al. Menstruation: science and society. *American Journal of Obstetrics and Gynecology*. Mosby Inc. 2020; 223 (5): 624–64.
17. Lopes dos Santos Santiago G. et al. Longitudinal qPCR Study of the Dynamics of *L. crispatus*, *L. iners*, *A. vaginae*, (Sialidase Positive) *G. vaginalis*, and *P. bivia* in the Vagina. *PLoS One*. 2012; 7 (9).
18. Pelzer ES, et al. A role for the endometrial microbiome in dysfunctional menstrual bleeding. *Antonie van Leeuwenhoek. Int J Gen Mol Microbiol*. 2018; 111 (6): 933–43.
19. Ansbacher R, Boyson WA, Morris JA. Sterility of the uterine cavity. *Am J Obstet Gynecol*. 1967; 99 (3): 394–96.
20. Mitchell CM, et al. Colonization of the upper genital tract by vaginal bacterial species in nonpregnant women. *Am J Obstet Gynecol Mosby Inc*. 2015; 212 (5): 611.e1-611.e9.
21. Verstraelen H, et al. Characterisation of the human uterine microbiome in non-pregnant women through deep sequencing of the V1-2 region of the 16S rRNA gene. *PeerJ PeerJ Inc*. 2016; 2016: 1.
22. Giudice LC. Challenging dogma: the endometrium has a microbiome with functional consequences! *Am J Obstet Gynecol*. 2016; 215 (6): 682–3.
23. Chen C, et al. The microbiota continuum along the female reproductive tract and its relation to uterine-related diseases. *Nat Commun Nature Publishing Group*. 2017; 8 (1).
24. Miles SM, Hardy BL, Merrell DS. Investigation of the microbiota of the reproductive tract in women undergoing a total hysterectomy and bilateral salpingo-oophorectomy. *Fertil Steril Elsevier Inc*. 2017; 107 (3): 813-20.e1.
25. Koedooder R, et al. Identification and evaluation of the microbiome in the female and male reproductive tracts. *Hum Reprod Update*. 2019; 25 (3): 298–325.
26. Кебурия Л. К., Смольникова В. Ю., Припутневич Т. В. М.В.В.



- Микробиота полости матки и ее влияние на репродуктивные исходы. *Акушерство и гинекология*. 2019; 2: 22–7.
27. Peterson J, et al. The NIH Human Microbiome Project. *Genome Res*. 2009; 19 (12): 2317–23.
  28. Kitaya K, et al. Chronic Endometritis: Potential Cause of Infertility and Obstetric and Neonatal Complications. *Am J Reprod Immunol*. 2016; 75 (1): 13–22.
  29. Liang J, et al. Analysis of the microbiota composition in the genital tract of infertile patients with chronic endometritis or endometrial polyps. *Front Cell Infect Microbiol*. 2023; 13.
  30. Moreno I, et al. Evidence that the endometrial microbiota has an effect on implantation success or failure. *American Journal of Obstetrics and Gynecology*. Mosby Inc. 2016; 215 (6): 684–703.
  31. Franasiak JM, et al. Endometrial microbiome at the time of embryo transfer: next-generation sequencing of the 16S ribosomal subunit. *J Assist Reprod Genet*. 2016; 33 (1): 129–36.
  32. Margulies SL, et al. Chronic endometritis: A prevalent yet poorly understood entity. *Int J Gynecol Obstet*. 2022; 158 (1): 194–200.

## ASSESSMENT OF THE FEATURES OF INNATE LYMPHOID CELLS IN PATIENTS WITH MULTIPLE MYELOMA

Pashkina EA<sup>1,2</sup>✉, Boeva OS<sup>1</sup>, Borisevich VI<sup>1,2</sup>, Abbasova VS<sup>1,2</sup>, Skachkov IP<sup>1,2</sup>, Lazarev YaA<sup>1</sup>, Denisova VV<sup>1</sup><sup>1</sup> Research Institute of Fundamental and Clinical Immunology, Novosibirsk, Russia<sup>2</sup> Faculty of Medicine, Novosibirsk State Medical University, Novosibirsk, Russia

Multiple myeloma (MM) is a B-cell malignant tumor, the morphological substrate of which are plasma cells that produce monoclonal immunoglobulin. This is one of the most common tumors of lymphoid origin. It is known that during oncogenesis, the immune balance shifts towards suppression of the antitumor immune response. Innate lymphoid cells (ILC) are one of the key factors influencing the said balance. This study aimed to assess the features of ILC in MM patients. The peripheral blood levels of ILC1, ILC2, and ILC3, as well as the expression of HLA-DR on ILC2, were measured with the help of flow cytometry. We found that MM patients ( $n = 14$ ; 7 male and 7 female, mean age  $59.2 \pm 2.08$ ) had significantly more ILC2 in the peripheral blood, with the content thereof amounting to  $63.1 \pm 4.51\%$  among "helper" ILC, while in donors the proportion of ILC2 was  $43.2 \pm 6.17\%$  ( $p = 0.03$ ). MM patients were also found to have a decreased amount of ILC2 that express HLA-DR: the proportion of such cells was only  $2.2 \pm 1.53\%$ , compared to  $15.6 \pm 5.29\%$  in donors ( $p = 0.003$ ). The results of this study point to the shift in the immune balance and polarization of the immune response towards type 2 (T<sub>2</sub>), which may contribute to the suppression of the antitumor immune response.

**Keywords:** innate lymphoid cells, antigen presentation, immune balance, multiple myeloma**Funding:** financial support from the Government of the Novosibirsk Region, Agreement #ML-1 of October 26, 2023.**Author contribution:** Pashkina EA, Denisova VV — study planning and design, Denisova VV — selection of participants, collection of clinical data; Borisevich VI, Abbasova VS, Skachkov IP, Lazarev YaA — data collection and study execution; Pashkina EA, Boeva OS — data analysis and interpretation, manuscript drafting; Pashkina EA — text editing.**Compliance with ethical standards:** the study was approved by the Ethics Committee of the Research Institute of Fundamental and Clinical Immunology (Minutes #145 of April 19, 2024). All participants signed the voluntary informed consent form.✉ **Correspondence should be addressed:** Ekaterina A. Pashkina  
Yadrintsevskaya, 14, Novosibirsk, 630099, Russia; pashkina.e.a@yandex.ru**Received:** 02.12.2024 **Accepted:** 14.02.2025 **Published online:** 25.02.2025**DOI:** 10.24075/brsmu.2025.006**Copyright:** © 2025 by the authors. **Licensee:** Pirogov University. This article is an open access article distributed under the terms and conditions of the Creative Commons Attribution (CC BY) license (<https://creativecommons.org/licenses/by/4.0/>).

## ОЦЕНКА ОСОБЕННОСТЕЙ ВРОЖДЕННЫХ ЛИМФОИДНЫХ КЛЕТОК У ПАЦИЕНТОВ С МНОЖЕСТВЕННОЙ МИЕЛОМОЙ

Е. А. Пашкина<sup>1,2</sup>✉, О. С. Боева<sup>1</sup>, В. И. Борисевич<sup>1,2</sup>, В. С. Аббасова<sup>1,2</sup>, И. П. Скачков<sup>1,2</sup>, Я. А. Лазарев<sup>1</sup>, В. В. Денисова<sup>1</sup><sup>1</sup> Научно-исследовательский институт фундаментальной и клинической иммунологии, Новосибирск, Россия<sup>2</sup> Новосибирский государственный медицинский университет, Новосибирск, Россия

Множественная миелома (ММ) — В-клеточная злокачественная опухоль, морфологическим субстратом которой являются плазматические клетки, продуцирующие моноклональный иммуноглобулин. Это одна из часто встречающихся опухолей лимфоидного происхождения. Известно, что в процессе онкогенеза происходит изменение иммунного баланса в сторону супрессии противоопухолевого иммунного ответа. Одними из ключевых факторов, влияющих на баланс параметров иммунной системы, являются врожденные лимфоидные клетки (innate lymphoid cells, ILC). Целью исследования было провести оценку особенностей врожденных лимфоидных клеток у пациентов с ММ. Оценка содержания в периферической крови ILC1, ILC2 и ILC3, а также экспрессии HLA-DR на ILC2 проводили методом проточной цитометрии. Обнаружено, что в периферической крови у пациентов ( $n = 14$ ; 7 мужчин и 7 женщин, средний возраст  $59,2 \pm 2,08$ ) с ММ доля ILC2 существенно выше и составляет  $63,1 \pm 4,51\%$  среди «хелперных» ILC, тогда как у доноров доля ILC2  $43,2 \pm 6,17\%$  ( $p = 0,03$ ). Выявлено, что у пациентов с ММ снижено относительное количество ILC2, экспрессирующих HLA-DR: доля этих клеток составила всего  $2,2 \pm 1,53\%$  по сравнению с  $15,6 \pm 5,29\%$  у доноров ( $p = 0,003$ ). Полученные результаты свидетельствуют об изменении иммунного баланса и поляризации иммунного ответа в сторону иммунного ответа 2-го типа (T<sub>2</sub>), что может способствовать супрессии противоопухолевого иммунного ответа.

**Ключевые слова:** врожденные лимфоидные клетки, презентация антигена, иммунный баланс, множественная миелома**Финансирование:** выполнено при финансовой поддержке от Правительства Новосибирской области, соглашение № МЛ-1 от 26 октября 2023 г.**Вклад авторов:** Е. А. Пашкина, В. В. Денисова — планирование и дизайн исследования, В. В. Денисова — подбор группы пациентов для проведения исследования и сбор клинических данных; В. И. Борисевич, В. С. Аббасова, И. П. Скачков и Я. А. Лазарев — сбор данных и проведение исследования; Е. А. Пашкина, О. С. Боева — анализ и интерпретация данных, подготовка рукописи; Е. А. Пашкина — редактирование текста.**Соблюдение этических стандартов:** исследование одобрено этическим комитетом НИИФКИ (протокол № 145 от 19 апреля 2024 г.). Все участники исследования подписали добровольное информированное согласие.✉ **Для корреспонденции:** Екатерина Александровна Пашкина  
ул. Ядринцевская, д. 14, г. Новосибирск, 630099, Россия; pashkina.e.a@yandex.ru**Статья получена:** 02.12.2024 **Статья принята к печати:** 14.02.2025 **Опубликована онлайн:** 25.02.2025**DOI:** 10.24075/vrgmu.2025.006**Авторские права:** © 2025 принадлежат авторам. **Лицензиат:** РНИМУ им. Н. И. Пирогова. Статья размещена в открытом доступе и распространяется на условиях лицензии Creative Commons Attribution (CC BY) (<https://creativecommons.org/licenses/by/4.0/>).

It is known that there are three main types of immune response [1]: T1, T2, and T17, which are regulated by T helper (Th) populations Th1, Th2, and Th17, respectively. The immune system is balanced between possible types of immune response [2]. Under the influence of a number of external and internal factors, this state, the immune equilibrium, changes over the person's lifetime in terms of the proportions of various types of immune responses [3-5]. In addition to the Th, innate lymphoid cells (ILC) are capable of influencing the immune balance. They can synthesize cytokines characteristic of Th much faster and in greater quantities, and thus either enhance or suppress the immune response at the earliest stages of its development [6].

By the ability to produce cytokines characteristic of the T1, T2, and T17 immune responses, ILC 1, ILC 2, and ILC3, respectively, are distinguished. However, it is currently believed that, in addition to acting similarly to T helper cells, ILCs form a link between the environment monitoring sensory cells (track all changes, not necessarily pathogenic) and effector cells, which translates into the support of body's homeostasis and immune balance [7]. Several mice studies demonstrated the MHC-dependent (major histocompatibility complex) cross-interaction of ILC-T cells [8–12], but the antigen-presenting properties of human ILC are still poorly understood. It has been shown that human intestinal tumor tissues contain ILCs that actively express HLA-DR, and most ILCs lack additional signaling molecules T cells stimulation. Together with T cells, HLA-DR<sup>+</sup>CD127<sup>+</sup> phenotype ILC cells localize in the unaffected colon tissue and by the edge of the tumor, which indicates the possibility of physical interaction between these two types of cells. Earlier, ILCs were shown to suppress T cell response to intestinal commensal bacteria in mesenteric lymph nodes in mice [10, 11]. Therefore, presentation of ILC antigen in a complex with MHC class II without costimulatory signals may play a role in the development of immunosuppression while protecting the tumor from destruction by cells of the immune system. However, in the case of ILC2, the antigen presentation process may be significantly different. It has been shown that in addition to the production of T2 cytokines, ILC2 express MHCII in combination with costimulating molecules CD80, CD86, and the OX40L ligand. Thus, ILC2 can act as antigen-presenting cells (APC), processing and presenting antigens to T cells, thereby inducing the antigen-specific response of CD4<sup>+</sup>T cells [13, 14].

In an oncopathology, an immune imbalance is one of the key factors triggering its development: T1 cytokines are associated with the increased antitumor immune response, whereas T2 cytokines can promote tumor growth and metastasis [15, 16]. In case of solid tumors of non-hematopoietic origins, cytokines are primarily a means of achieving immunosuppression of the antitumor response, but in hemoblastosis cases they can act as growth factors for tumor cells. In patients with chronic lymphocytic leukemia, characterized by the production of atypical mature B lymphocytes, a shift towards Th2 was noted, which is corrected by ibrutinib (Bcr-1 tyrosine kinase inhibitors) [17].

In the case of multiple myeloma (MM), the number of CD4<sup>+</sup>-Th1 and CD4<sup>+</sup>-Th17 in patients was higher than in donors [18]. However, despite the greater numbers in this cell population, the concentration of T2 cytokine IL4 (interleukin-4) was significantly increased in the blood serum. Therefore, the high production of this cytokine may be primarily associated with its secretion by the ILC2 cells.

The purpose of this study is to evaluate the features of innate lymphoid cells in patients with MM.

## METHODS

The study included 14 MM patients and 13 conditionally healthy donors. Both study groups were comparable in terms of gender and age characteristics. The study was conducted from May to November 2024. Test group inclusion criteria: MM diagnosis, any sex, age 18–65 years; II and III clinical stages (Durie-Salmon Staging System); complete remission (CR) or very good partial remission (VGPR) at the moment of inclusion; written informed consent. Control group inclusion criteria: good health, any sex, age 18–65 years; no autoimmune, oncological and chronic recurrent viral infections.

Exclusion criteria (both groups): non-compliance with the inclusion criteria; severe decompensated cardiovascular, respiratory, and liver failure; acute infectious diseases; pregnancy; mental disorders; refusal of the patient or donor to participate in the study.

Peripheral blood mononuclear cells (PBMC) were the studied material; it was isolated in the volume of 30–50 ml from the samples taken in both groups by standard Ficoll-Urografin density gradient centrifugation.

To determine the immunophenotype of the ILC, the isolated PBMC were stained with monoclonal antibodies conjugated with fluorochromes: anti-Lineage (CD2/3/14/16/19/20/56/235a), anti-CD11c and anti-FcεR1 alpha-FITC, anti-CD294-PE, anti-CD127-PerCP/Cy5.5, anti-CD117-APC, HLA-DR-PE/Cy7. The total number of ILC was established as Lin<sup>–</sup>CD127<sup>+</sup>, since these cells do not carry linear markers, but have an alpha chain of the IL7 receptor on their surface. To assess the ratio of different ILC subpopulations, we counted CD294<sup>+</sup>ILC (ILC2); CD117<sup>–</sup>CD294<sup>–</sup>ILC was taken as ILC1, and CD117<sup>+</sup>CD294<sup>–</sup>ILC as ILC3. The cell phenotype was established using a LongCyte flow cytometer (Challenger, China).

Statistical processing of the results was performed using GraphPadPrizm 9.0.0 (GraphPad Software, Inc., USA). The Mann–Whitney test was used to compare the values registered in the groups. The results are presented as a median (Me) with interquartile range [25<sup>th</sup>; 75<sup>th</sup> percentile]. The results were considered significant at  $p < 0.05$ .

## RESULTS

We have established that MM patients have a lower relative amount of peripheral blood "helper" ILC compared to the conditionally healthy individuals: 0.05% [0.03; 0.16] versus 0.24% [0.06; 0.48] (Fig. 1). It should be noted that the smaller total number of ILC is the result of erosion of the subpopulation composition of these cells. The relative amount of ILC2 in PBMC was 0.06% [0.02; 0.17] and 0.04% [0.02; 0.09], healthy donors and MM patients, respectively, the difference being insignificant (Fig. 2). In healthy donors, the predominant type was ILC1, the proportion of which in the peripheral blood was 0.07% [0.02; 0.19], while that of ILC3 amounted to 0.008% [0.003; 0.018]; in MM patients, the relative amounts of ILC1 (Fig. 3) and ILC3 (Fig. 4) were 0.02% [0.01; 0.04] and 0.001% [0; 0.004], respectively, which is significantly lower than in the control group.

Naturally, such changes altered the balance of different ILC populations. Assessing the proportion of ILC2 in MM patients, we noticed that it was greater than in the control group (Fig. 5).

We have also investigated the expression of HLA-DR (one of the MHC class II antigens needed for antigen presentation) on the surface of ILC2, and found that MM patients had significantly fewer ILC2 expressing the HLA-DR antigen on their membrane than healthy donors (Fig. 6). Consequently,

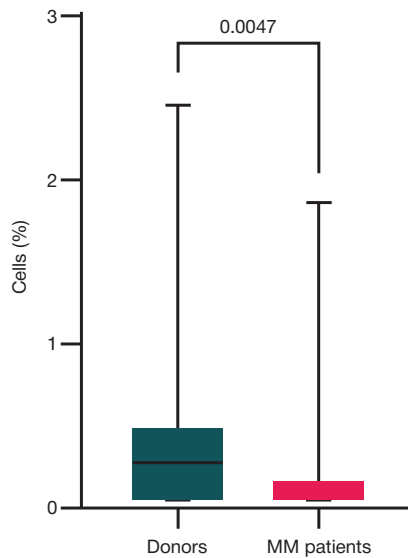


**Fig. 1.** The relative amount of ILC in the total PB MNC, MM patients and conditionally healthy individuals

despite the increased relative amount of ILC2 in MM patients, the ability of cells to present the antigen in this disease is hampered, which can weaken the antitumor immune response and decrease activation of T-lymphocytes.

## DISCUSSION

According to the literature, there may be several specific features of functioning of ILC in hematologic cancers, which were demonstrated for acute myeloid leukemia and chronic lymphocytic leukemia [19]. Firstly, in such cases, the amount of ILC is smaller, and their functional activity weaker, which translates into a lower concentration of cytokines in the tumor microenvironment, and, as a result, suppression of the immune response. Secondly, activation of ILC 2 and polarization of the immune response towards T2 can boost the activity of suppressor cells. Thirdly, outside the tumor, in normal tissues, ILC maintain homeostasis and participate in tissue repair, including in the context of a graft-versus-host reaction, which is a common complication after allogeneic stem cell transplantation.

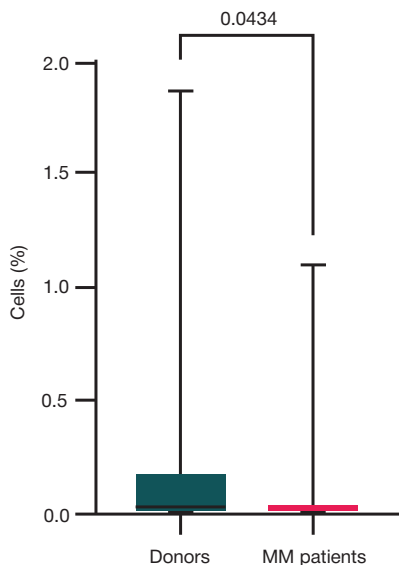


**Fig. 3.** The relative amount of ILC1 in the total PB MNC, MM patients and conditionally healthy individuals

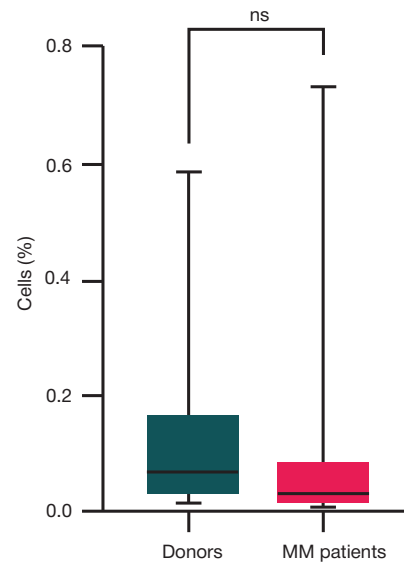


**Fig. 2.** The relative amount of ILC2 in the total PB MNC, MM patients and conditionally healthy individuals

In this study, we found that in MM patients, despite the decreased relative content of "helper" ILC in PBMC, the ILC2 subpopulation count remained similar to that registered in healthy individuals. Consequently, such changes could have broken the ILC subpopulations balance, triggered growth of the proportion of ILC2 and direct the immune response towards T2, as well as cause the drop in the number of ILC1 that support the T1 type of immune response, which is most effective against tumor cells. It is known that polarization of the immune response towards T2 and weakening of the T1 immune response promote inactivation of anti-tumor immunity and thus boost tumor growth, a situation often observed in malignant neoplasm cases.

It should also be noted that our results are consistent with the reported growth of the level of T2 cytokines in MM patients [18]. In addition, with monoclonal gammopathy of undetermined significance (MGUS) in the background, which precedes MM, the peripheral blood level of ILC2 is increased [20]. Bone marrow level of ILC1 is known to grow MGUS cases, but the functional activity of ILC1 and ILC2 determined by the intracellular cytokine content goes down. In our study, MM also

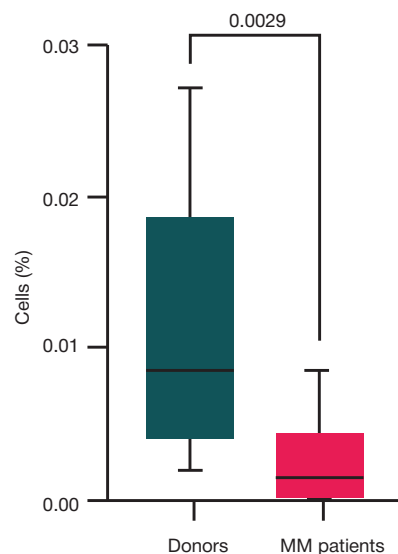


**Fig. 4.** The relative amount of ILC3 in the total PB MNC, MM patients and conditionally healthy individuals



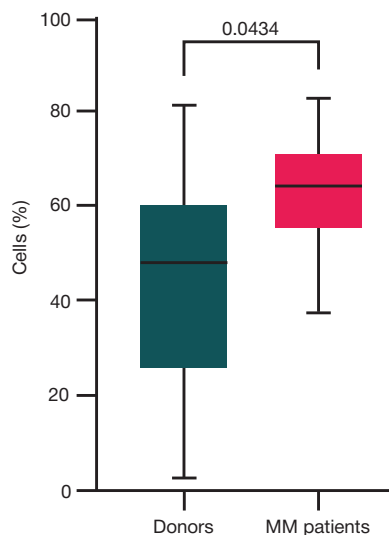


**Fig. 5.** The relative amount of ILC2 in the total number of ILC, MM patients and conditionally healthy individuals

triggered a drop of the share of ILC2 cells capable of presenting the antigen. Other authors have demonstrated a decrease in the proportion of ILC2 among peripheral blood Lin-CD127<sup>+</sup> cells [21], which may be due to differences between patient groups, since this study included patients with a fresh diagnosis before start of the therapy. At the same time, functional properties of peripheral blood ILC2 in patients with MGUS and MM were different from those in conditionally healthy individuals: the former had these cells developing cytotoxic activity against tumor cells. It is possible that such changes are associated with the differentiation of ILC2 into ILC1-like cells in MM patients [23], and the antitumor activity of such cells, on the one hand, may increase due to the polarization of the immune response towards T1 and the development of cytotoxic activity, and on the other hand, may be impaired in hematologic cancers, acute myeloblastic leukemia in particular [24].

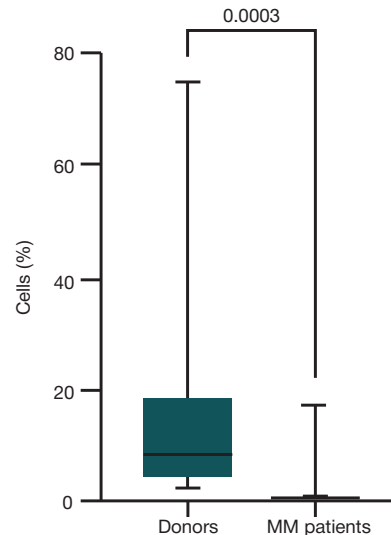


**Fig. 6.** The relative amount of HLA-DR+ILC2 in the total number of ILC2, MM patients and conditionally healthy individuals

## CONCLUSIONS

Thus, MM patients exhibit changing ILC subpopulations composition, with ILC2 share growing and promoting polarization towards T2-type immune response. We have also shown that HLA-DR expression on the surface of the ILC2 cell membrane decreases, which lowers the ability to activate the immune response. Therefore, it is interesting to further study the mechanisms and features of polarization of the immune response, with one of such studies designed to comprehensively evaluate of production of T1/T2/T17 cytokines by various populations of regulatory cells in the cases of MM and other hematologic cancers. In addition, the search for potential targets for targeted therapy in MM patients remains relevant.

## References

- Annunziato F, Romagnani C, Romagnani S. The 3 major types of innate and adaptive cell-mediated effector immunity. *J Allergy Clin Immunol.* 2015; 135 (3): 626–35. DOI: 10.1016/j.jaci.2014.11.001.
- Eberl G. Immunity by equilibrium. *Nat Rev Immunol.* 2016; 16 (8): 524–32. DOI: 10.1038/nri.2016.75.
- Uciechowski P, Kahmann L, Plümäkers B, Malavolta M, Mocchegiani E, Dedoussis G, et al. TH1 and TH2 cell polarization increases with aging and is modulated by zinc supplementation. *Exp Gerontol.* 2008; 43 (5): 493–8. DOI: 10.1016/j.exger.2007.11.006.
- Zhou Y, Yu K. Th1, Th2, and Th17 cells and their corresponding cytokines are associated with anxiety, depression, and cognitive impairment in elderly gastric cancer patients. *Front Surg.* 2022; 9: 996680. DOI: 10.3389/fsurg.2022.996680.
- Alanazi H, Zhang Y, Fatunbi J, Lu T, Kwak-Kim J. The impact of reproductive hormones on T cell immunity; normal and assisted reproductive cycles. *Journal of Reproductive Immunology.* 2024; 165: 104295. DOI: 10.1016/j.jri.2024.104295.
- Fol M, Karpik W, Zablotni A, Kulesza J, Kulesza E, Godkovicz M, Druszczynska M. Innate Lymphoid Cells and Their Role in the Immune Response to Infections. *Cells.* 2024; 13 (4): 335. <https://doi.org/10.3390/cells13040335>.
- Xiong L, Nutt SL, Seillet C. Innate lymphoid cells: More than just immune cells. *Front Immunol.* 2022; 13: 1033904. DOI: 10.3389/fimmu.2022.1033904.
- Oliphant CJ, Hwang YY, Walker JA, Salimi M, Wong SH, Brewer JM, et al. MHCII-mediated dialog between group 2 innate lymphoid cells and CD4(+) T cells potentiates type 2 immunity and promotes parasitic helminth expulsion. *Immunity.* 2014; 41: 283–95. DOI: 10.1016/j.immuni.2014.06.016.
- von Burg N, Chappaz S, Baerenwaldt A, Horvath E, Bose Dasgupta S, Ashok D, et al. Activated group 3 innate lymphoid cells promote T-cell-mediated immune responses. *Proc Natl Acad Sci USA.* 2014; 111: 12835–40. DOI: 10.1073/pnas.1406908111.
- Hepworth MR, Fung TC, Masur SH, Kelsen JR, McConnell FM, Dubrot J, et al. Immune tolerance. Group 3 innate lymphoid cells mediate intestinal selection of commensal bacteria-specific CD4(+) T cells. *Science.* 2015; 348: 1031–5. DOI: 10.1126/science.aaa4812.
- Hepworth MR, Monticelli LA, Fung TC, Ziegler OG, Grunberg S, Sinha R, et al. Innate lymphoid cells regulate CD4+ T-cell responses to intestinal commensal bacteria. *Nature.* 2013; 498: 113–7. DOI: 10.1038/nature12240.
- Lehmann FM, von Burg N, Ivanek R, Teufel C, Horvath E, Peter A, Turchinovich G, Staehli D, Eichlisberger T, Gomez de Agüero M, Coto-Llerena M, Prchal-Murphy M, Sexl V, Bentires-Alj M, Mueller C, Finke D. Microbiota-induced tissue signals regulate ILC3-mediated antigen presentation. *Nat Commun.* 2020; 11 (1): 1794. DOI: 10.1038/s41467-020-15612-2.
- Halim TYF, Rana BMJ, Walker JA, Kerscher B, Knolle MD, Jolin HE, et al. Tissue-restricted adaptive type 2 immunity is orchestrated by expression of the costimulatory molecule OX40L on group 2 innate lymphoid cells. *Immunity.* 2018; 48: 1195–1207.e6 DOI: 10.1016/j.immuni.2018.05.003

14. Frech M, Omata Y, Schmalzl A, Wirtz S, Taher L, Schett G, et al. Bln2a2 Regulates ILC2-T Cell Cross Talk in Type 2 Immune Responses. *Front Immunol.* 2022; 13: 757436. DOI: 10.3389/fimmu.2022.757436.
15. Lee HL, Jang JW, Lee SW, Yoo SH, Kwon JH, Nam SW, et al. Inflammatory cytokines and change of Th1/Th2 balance as prognostic indicators for hepatocellular carcinoma in patients treated with transarterial chemoembolization. *Sci Rep.* 2019; 9 (1): 3260. DOI: 10.1038/s41598-019-40078-8.
16. Chraa D, Naim A, Olive D, Badou A. T lymphocyte subsets in cancer immunity: Friends or foes. *J Leukoc Biol.* 2019; 105 (2): 243–55. DOI: 10.1002/JLB.MR0318-097R.
17. Puzzolo MC, Del Giudice I, Peragine N, Mariglia P, De Propriis MS, Cappelli LV, et al. TH2/TH1 Shift Under Ibrutinib Treatment in Chronic Lymphocytic Leukemia. *Front Oncol.* 2021; 11: 637186. DOI: 10.3389/fonc.2021.637186.
18. Musolino C, Allegra A, Innao V, Allegra AG, Pioggia G, Gangemi S. Inflammatory and Anti-Inflammatory Equilibrium, Proliferative and Antiproliferative Balance: The Role of Cytokines in Multiple Myeloma. *Mediators Inflamm.* 2017; 1852517. DOI: 10.1155/2017/1852517.
19. Blom B, van Hoeven V, Hazenberg MD. ILCs in hematologic malignancies: Tumor cell killers and tissue healers. *Semin Immunol.* 2019; 41: 101279. DOI: 10.1016/j.smim.2019.06.002.
20. Kini Bailur J, Mehta S, Zhang L, Neparidze N, Parker T, Bar N, et al. Changes in bone marrow innate lymphoid cell subsets in monoclonal gammopathy: target for IMiD therapy. *Blood Adv.* 2017; 1 (25): 2343–7. DOI: 10.1182/bloodadvances.
21. Drommi F, Calabrà A, Pezzino G, Vento G, Freni J, Costa G, et al. Multiple Myeloma Cells Shift the Fate of Cytolytic ILC2s Towards TIGIT-Mediated Cell Death. *Cancers.* 2025; 17 (2): 263. Available from: <https://doi.org/10.3390/cancers17020263>.
22. Corral D, Charton A, Krauss MZ, Blanquart E, Levlain F, Lefrançois E, et al. ILC precursors differentiate into metabolically distinct ILC1-like cells during Mycobacterium tuberculosis infection. *Cell Rep.* 2022; 39 (3): 110715. DOI: 10.1016/j.celrep.2022.110715.
23. Salomé B, Gomez-Cadena A, Loyon R, Suffiotti M, Salvestrini V, Wyss T, et al. CD56 as a marker of an ILC1-like population with NK cell properties that is functionally impaired in AML. *Blood Adv.* 2019; 3 (22): 3674–87. DOI: 10.1182/bloodadvances.2018030478.

## Литература

1. Annunziato F, Romagnani C, Romagnani S. The 3 major types of innate and adaptive cell-mediated effector immunity. *J Allergy Clin Immunol.* 2015; 135 (3): 626–35. DOI: 10.1016/j.jaci.2014.11.001.
2. Eberl G. Immunity by equilibrium. *Nat Rev Immunol.* 2016; 16 (8): 524–32. DOI: 10.1038/nri.2016.75.
3. Uciechowski P, Kahmann L, Plümäkers B, Malavolta M, Mocchegiani E, Dedoussis G, et al. TH1 and TH2 cell polarization increases with aging and is modulated by zinc supplementation. *Exp Gerontol.* 2008; 43 (5): 493–8. DOI: 10.1016/j.exger.2007.11.006.
4. Zhou Y, Yu K. Th1, Th2, and Th17 cells and their corresponding cytokines are associated with anxiety, depression, and cognitive impairment in elderly gastric cancer patients. *Front Surg.* 2022; 9: 996680. DOI: 10.3389/fsurg.2022.996680.
5. Alanazi H, Zhang Y, Fatunbi J, Lu T, Kwak-Kim J. The impact of reproductive hormones on T cell immunity; normal and assisted reproductive cycles. *Journal of Reproductive Immunology.* 2024; 165: 104295. DOI: 10.1016/j.jri.2024.104295.
6. Fol M, Karpik W, Zablotni A, Kulesza J, Kulesza E, Godkowitz M, Druszczynska M. Innate Lymphoid Cells and Their Role in the Immune Response to Infections. *Cells.* 2024; 13 (4): 335. <https://doi.org/10.3390/cells13040335>.
7. Xiong L, Nutt SL, Seillet C. Innate lymphoid cells: More than just immune cells. *Front Immunol.* 2022; 13: 1033904. DOI: 10.3389/fimmu.2022.1033904.
8. Oliphant CJ, Hwang YY, Walker JA, Salimi M, Wong SH, Brewer JM, et al. MHCII-mediated dialog between group 2 innate lymphoid cells and CD4(+) T cells potentiates type 2 immunity and promotes parasitic helminth expulsion. *Immunity.* 2014; 41: 283–95. DOI: 10.1016/j.immuni.2014.06.016.
9. von Burg N, Chappaz S, Baerenwaldt A, Horvath E, Bose Dasgupta S, Ashok D, et al. Activated group 3 innate lymphoid cells promote T-cell-mediated immune responses. *Proc Natl Acad Sci USA.* 2014; 111: 12835–40. DOI: 10.1073/pnas.1406908111.
10. Hepworth MR, Fung TC, Masur SH, Kelsen JR, McConnell FM, Dubrot J, et al. Immune tolerance. Group 3 innate lymphoid cells mediate intestinal selection of commensal bacteria-specific CD4(+) T cells. *Science.* 2015; 348: 1031–5. DOI: 10.1126/science.aaa4812.
11. Hepworth MR, Monticelli LA, Fung TC, Ziegler CG, Grunberg S, Sinha R, et al. Innate lymphoid cells regulate CD4+ T-cell responses to intestinal commensal bacteria. *Nature.* 2013; 498: 113–7. DOI: 10.1038/nature12240.
12. Lehmann FM, von Burg N, Ivanek R, Teufel C, Horvath E, Peter A, Turchinovich G, Staehli D, Eichlisberger T, Gomez de Agüero M, Coto-Llerena M, Prchal-Murphy M, Sexl V, Bentires-Alj M, Mueller C, Finke D. Microbiota-induced tissue signals regulate ILC3-mediated antigen presentation. *Nat Commun.* 2020; 11 (1): 1794. DOI: 10.1038/s41467-020-15612-2.
13. Halim TYF, Rana BMJ, Walker JA, Kerscher B, Knolle MD, Jolin HE, et al. Tissue-restricted adaptive type 2 immunity is orchestrated by expression of the costimulatory molecule OX40L on group 2 innate lymphoid cells. *Immunity.* 2018; 48: 1195–1207.e6 DOI: 10.1016/j.immuni.2018.05.003
14. Frech M, Omata Y, Schmalzl A, Wirtz S, Taher L, Schett G, et al. Bln2a2 Regulates ILC2-T Cell Cross Talk in Type 2 Immune Responses. *Front Immunol.* 2022; 13: 757436. DOI: 10.3389/fimmu.2022.757436.
15. Lee HL, Jang JW, Lee SW, Yoo SH, Kwon JH, Nam SW, et al. Inflammatory cytokines and change of Th1/Th2 balance as prognostic indicators for hepatocellular carcinoma in patients treated with transarterial chemoembolization. *Sci Rep.* 2019; 9 (1): 3260. DOI: 10.1038/s41598-019-40078-8.
16. Chraa D, Naim A, Olive D, Badou A. T lymphocyte subsets in cancer immunity: Friends or foes. *J Leukoc Biol.* 2019; 105 (2): 243–55. DOI: 10.1002/JLB.MR0318-097R.
17. Puzzolo MC, Del Giudice I, Peragine N, Mariglia P, De Propriis MS, Cappelli LV, et al. TH2/TH1 Shift Under Ibrutinib Treatment in Chronic Lymphocytic Leukemia. *Front Oncol.* 2021; 11: 637186. DOI: 10.3389/fonc.2021.637186.
18. Musolino C, Allegra A, Innao V, Allegra AG, Pioggia G, Gangemi S. Inflammatory and Anti-Inflammatory Equilibrium, Proliferative and Antiproliferative Balance: The Role of Cytokines in Multiple Myeloma. *Mediators Inflamm.* 2017; 1852517. DOI: 10.1155/2017/1852517.
19. Blom B, van Hoeven V, Hazenberg MD. ILCs in hematologic malignancies: Tumor cell killers and tissue healers. *Semin Immunol.* 2019; 41: 101279. DOI: 10.1016/j.smim.2019.06.002.
20. Kini Bailur J, Mehta S, Zhang L, Neparidze N, Parker T, Bar N, et al. Changes in bone marrow innate lymphoid cell subsets in monoclonal gammopathy: target for IMiD therapy. *Blood Adv.* 2017; 1 (25): 2343–7. DOI: 10.1182/bloodadvances.
21. Drommi F, Calabrà A, Pezzino G, Vento G, Freni J, Costa G, et al. Multiple Myeloma Cells Shift the Fate of Cytolytic ILC2s Towards TIGIT-Mediated Cell Death. *Cancers.* 2025; 17 (2): 263. Available from: <https://doi.org/10.3390/cancers17020263>.
22. Corral D, Charton A, Krauss MZ, Blanquart E, Levlain F, Lefrançois E, et al. ILC precursors differentiate into metabolically distinct ILC1-like cells during Mycobacterium tuberculosis infection. *Cell Rep.* 2022; 39 (3): 110715. DOI: 10.1016/j.celrep.2022.110715.
23. Salomé B, Gomez-Cadena A, Loyon R, Suffiotti M, Salvestrini V, Wyss T, et al. CD56 as a marker of an ILC1-like population with NK cell properties that is functionally impaired in AML. *Blood Adv.* 2019; 3 (22): 3674–87. DOI: 10.1182/bloodadvances.2018030478.

## MONITORING THE SPREAD OF COVID-19 ACROSS TUBERCULOSIS PATIENTS IN MOSCOW

Kotova EA, Sumarokova EV , Belilovsky EM, Monchakovskaya ES


Moscow Research and Clinical Center for Tuberculosis Control of the Moscow Government Department of Health, Moscow, Russia

The COVID-19 pandemic necessitated making timely managerial decisions when providing medical care to patients with tuberculosis (TB). The study aimed to develop a system for monitoring of TB combined with COVID-19 and estimate the prevalence of COVID-19 among TB patients, along with the efficacy of the measures applied. A registry of TB/COVID-19 patients was developed based on the Barclay-SV Medical Database Management System. It was used to perform comparative analysis of the information about 1837 patients with active TB forms and confirmed COVID-19 for two periods of the pandemic, 2020–2021 and 2022–2023, and against the data on all new TB cases and TB relapses registered in Moscow in 2020–2023: 7812 and 1243 individuals respectively, from the TB surveillance registries, excluding those identified posthumously. The socio-demographic structure of patients with TB/COVID-19 co-infection identified in 2020–2023 did not change and corresponded to that of TB patients. In the second period analyzed, mild COVID-19 cases were registered more often (60.9% vs. 41.6%;  $p < 0.01$ ), the share of moderate COVID-19 cases decreased from 48.2% to 20.6% ( $p < 0.01$ ), and the share of severe cases decreased from 6.4% to 4.9% ( $p = 0.19$ ). In 2022–2023, the share of individuals with COVID lung damage decreased from 45.1% to 17.6%, while the number of cases of COVID upper respiratory tract lesion increased from 47.1% to 64.5% ( $p < 0.05$ ). The fact of having HIV infection, CAD and hypertension, kidney and genitourinary diseases increased the chance of developing COVID-19 by TB patients 1.5–2-fold, and disseminated pulmonary tuberculosis, caseous pneumonia, lung tissue destruction and bacterial excretion increased it 1.4–1.6-fold. The registry made it possible to control routing of TB/COVID-19 patients, as well as treatment outcomes: the total share of individuals cured reached 90.1%.

**Keywords:** monitoring, novel coronavirus infection, SARS-CoV-2, tuberculosis, tuberculosis/COVID-19 co-infection, tuberculosis epidemiological monitoring system

**Author contribution:** Kotova EA, Belilovsky EM — developing the method, literature review, manuscript writing, editing; Sumarokova EV — data acquisition and analysis, developing the method, literature review, manuscript writing, editing; Monchakovskaya ES — statistical data processing.

**Compliance with ethical standards:** retrospective processing of the registry data did not involve personal information

 **Correspondence should be addressed:** Elena V. Sumarokova  
Stromynka, 10, Moscow, 107014, Russia; sumarokovaEV1@zdrav.mos.ru

**Received:** 11.12.2024 **Accepted:** 15.01.2025 **Published online:** 11.02.2025

**DOI:** 10.24075/brsmu.2025.003

**Copyright:** © 2025 by the authors. **Licensee:** Pirogov University. This article is an open access article distributed under the terms and conditions of the Creative Commons Attribution (CC BY) license (<https://creativecommons.org/licenses/by/4.0/>).

## МОНИТОРИНГ РАСПРОСТРАНЕНИЯ COVID-19 СРЕДИ БОЛЬНЫХ ТУБЕРКУЛЕЗОМ В МОСКВЕ

Е. А. Котова, Е. В. Сумарокова , Е. М. Белиловский, Е. С. Мончаковская

Московский городской научно-практический центр борьбы с туберкулезом Департамента здравоохранения города Москвы, Москва, Россия

Пандемия COVID-19 вызвала необходимость принятия своевременных управленческих решений при оказании медицинской помощи больным туберкулезом (ТБ). Целью работы было создание системы мониторинга ТБ, сочетанного с COVID-19, и проведение оценки распространения COVID-19 среди больных ТБ и эффективности проводимых мероприятий. Разработан регистр больных ТБ, сочетанным с COVID-19, на основе Системы управления базами медицинских данных «Барклай-СВ». С его помощью проводили сравнительный анализ информации о 1837 больных активными формами ТБ с подтвержденной COVID-19 по двум периодам пандемии: 2020–2021 гг. и 2022–2023 гг. и в сравнении с данными обо всех впервые выявленных больных и рецидивах ТБ, зарегистрированных в г. Москве в 2020–2023 гг.: 7812 и 1243 человека соответственно из регистров систем эпидемиологического мониторинга ТБ, исключая выявленных посмертно. Социально-демографическая структура больных сочетанной инфекцией ТБ/COVID-19, выявленных в 2020–2023 гг., не менялась, соответствовала этому параметру у больных ТБ. Во втором анализируемом периоде случаи легкого течения COVID-19 регистрировали чаще (60,9% против 41,6%;  $p < 0,01$ ), доля случаев среднетяжелого течения COVID-19 снизилась с 48,2% до 20,6% ( $p < 0,01$ ), тяжелого течения — с 6,4% до 4,9% ( $p = 0,19$ ). Доля лиц с ковидным поражением легких без дыхательной недостаточности в 2022–2023 гг. уменьшилась с 45,1% до 17,6%, при росте случаев ковидного поражения верхних дыхательных путей с 47,1% до 64,5% ( $p < 0,05$ ). Наличие ВИЧ-инфекции, ИБС и гипертонической болезни, болезней почек и мочеполовой системы в 1,5–2 раза увеличивало шанс проявления COVID-19 у больных ТБ, а диссеминированный ТБ легких, казеозная пневмония, наличие деструкции легочной ткани и бактериовыделения — в 1,4–1,6 раза. Регистр позволил осуществлять контроль маршрутизации пациентов ТБ/COVID-19, а также результаты лечения: доля излеченных в совокупности достигла 90,1%.

**Ключевые слова:** мониторинг, новая коронавирусная инфекция, SARS-CoV-2, туберкулез, сочетанная инфекция туберкулез/COVID-19, система эпидемиологического мониторинга туберкулеза

**Вклад авторов:** Е. А. Котова, Е. М. Белиловский — разработка метода, обзор литературы, написание статьи, редактирование; Е. В. Сумарокова — сбор и обработка материала, разработка метода, обзор литературы, написание статьи, редактирование; Е. С. Мончаковская — статистическая обработка материала.

**Соблюдение этических стандартов:** ретроспективную обработку данных регистра вели без использования персональной информации

 **Для корреспонденции:** Елена Викторовна Сумарокова  
ул. Стромынка, д. 10, г. Москва, 107014, Россия; sumarokovaEV1@zdrav.mos.ru

**Статья получена:** 11.12.2024 **Статья принята к печати:** 15.01.2025 **Опубликована онлайн:** 11.02.2025

**DOI:** 10.24075/vrgmu.2025.003

**Авторские права:** © 2025 принадлежат авторам. **Лицензиат:** РНИМУ им. Н. И. Пирогова. Статья размещена в открытом доступе и распространяется на условиях лицензии Creative Commons Attribution (CC BY) (<https://creativecommons.org/licenses/by/4.0/>).

The pandemic of novel coronavirus infection (COVID-19) has become an example of the rise of a serious challenge for public health system having a rather limited exposure time. On March 11, 2020, the World Health Organization declared the beginning of the pandemic of the disease assigned the name COVID-19, and on May 5, 2023 declared the end of the pandemic [1–3]. The sheer scale of the influence of novel infection on public health system, arrangement of medical care, and economy requires not only timely response through temporary rearrangement of methods to deal with population and patients, but also arrangement of the temporary system for control and monitoring of the efficacy of the measures applied with continuous assessment of the epidemic process manifestations aimed at using the data for development of temporary methodological guidelines on prevention, diagnosis, and treatment of the disease, timely amendment of the latter, and prediction of the epidemiological situation development.

Moscow was among the first cities of the Russian Federation to face COVID-19. On March 2, 2020, the first disease case was reported in the capital, and red alert was declared as early as on March 5 [4, 5]. The main objective was to prevent the blast load on Moscow's healthcare system and avoid the scenario when the hospitals are overwhelmed and healthcare professionals do not have time to provide care to patients.

In April 2020, the Clinical Committee that included senior external experts of the Moscow Government Department of Health and chief physicians of municipal hospitals repurposed for treatment of patients with COVID-19 was established. The following goal was set for specialists: to promptly develop a clinical protocol for diagnosis of novel coronavirus infection (COVID-19) in patients undergoing inpatient treatment in medical institutions of Moscow [6]. A Protocol for treatment of patients with tuberculosis combined with novel coronavirus infection was developed at the Moscow Research and Clinical Center for Tuberculosis Control of the Moscow Government Department of Health (hereinafter, MRCCTC or Center).

In MRCCTC including two multidisciplinary clinics (Clinic No. 1, Clinic No. 2) and 9 branches in administrative districts of Moscow, beds were repurposed for COVID-19 patients. Beds in the Clinic No. 2 were used for inpatient treatment of patients with the combined infection (tuberculosis and COVID-19). Beds in two branches of the Center (in the South-Eastern and North-Western districts of Moscow) were used for treatment of patients with tuberculosis and mild novel coronavirus infection, as well as for observation of patients, who had contacted COVID-19 patients, and novel coronavirus infection convalescents in different time periods [7–9].

Under conditions of the developing pandemic of novel coronavirus infection, it became necessary to promptly develop and implement the system for monitoring of measures to detect and treat COVID-19 in patients with tuberculosis, which could ensure timely analysis of the epidemiological situation with the combined TB/COVID-19 infection and control of patient routing [10].

Today, one of the country's most well-developed tuberculosis surveillance systems (TBSS) functions in the city, which is used to acquire, process, and analyze the case-based data on detection, treatment and follow-up of TB patients for almost 25 years based on the scientifically grounded information structures that remain versatile and stable enough over a long time [11].

In Moscow, TBSS is based on the flexible Barclay-SV Medical Database Management System (MDBMS) allowing one to promptly develop and modify (if necessary) the information structure of the registries with arrangement of data entry, processing, and analysis.

During the pandemic the question arose about the need to create a temporary registry for monitoring of combined tuberculosis/COVID-19 infection and control over the effectiveness of the measures applied with the timely retrospective analysis of data on the patients having tuberculosis combined with COVID-19. The study aimed to promptly develop a system for monitoring of tuberculosis combined with COVID-19, analyze the spread of novel coronavirus infection among tuberculosis patients, and assess the effectiveness of the anti-epidemic measures applied.

## METHODS

The temporary registry of patients with tuberculosis combined with novel coronavirus infection (TB/COVID-19) was developed based on the flexible Barclay-SV MDBMS (developed by MRCCTC together with Elecard-Med LLC, certificate of state registration of software No. 2019661941 dated 12.09.2019, Russian software registry entry No. 21931 dated 20.03.2024) [11]. The Barclay-SV MDBMS, in which the Moscow tuberculosis surveillance system registries are implemented, has a built-in designer of configurations (tasks or information structures) with the automated construction of input data entry forms and a report designer.

In the registry created, which was modified a limited number of times during the pandemic, as the regulatory documents and the COVID-19 patient management algorithm changed, in 2020–2023 the data were acquired on 2171 patients (2473 records), which included both information about the patients with active tuberculosis forms and the confirmed diagnosis of COVID-19 and the records of patients, in whom the diagnosis of tuberculosis was not confirmed based on the assessment results, and patients clinically cured of tuberculosis and transferred to the dispensary supervision group III [12, 13].

The analysis included information about 1837 patients with active forms of tuberculosis and the confirmed diagnosis of COVID-19 (2102 records), who were admitted to Moscow COVID hospitals for the first time, including cases when tuberculosis/COVID-19 was identified posthumously, or underwent outpatient treatment due to novel coronavirus infection (64 cases).

To compare patients having active tuberculosis forms and concomitant COVID-19 and those, in whom no novel coronavirus infection was detected, information was taken about all new cases and tuberculosis relapses reported in Moscow in 2020–2023: 7812 and 1243 individuals, respectively, from the city's TBSS registries, excluding those identified posthumously.

In accordance with the Temporary Guidelines on Prevention, Diagnosis, and Treatment of Novel Coronavirus Infection (COVID-19), approved by the Ministry of Health of the Russian Federation [1], Clinical Protocols for diagnosis of novel coronavirus infection (COVID-19) in patients undergoing inpatient treatment in medical institutions of the state public health system of Moscow [6], in 2020–2023 in Moscow, novel coronavirus infection (COVID-19) was diagnosed at the MRCCTC using the direct etiological laboratory diagnosis methods (SARS-CoV-2 RNA detection by polymerase chain reaction (PCR), as well as SARS-CoV-2 antigen detection by immunochromatographic assay (ICA) performed when assessing nasopharyngeal and oropharyngeal smears, regardless of clinical manifestations), indirect etiological diagnosis methods (detection of patients' serum immunoglobulins M, G (IgM and IgG) by immunochemistry methods), instrumental diagnosis method — computed tomography (CT) of lungs.

Immunological testing of the patients' serum was performed at the laboratory of the Center using the reagent



kits for identification of IgM and IgG antibodies against the SARS-CoV-2 strain by immunochromoluminescence assay in clinical samples using the CL analyzers for in vitro diagnosis (Shenzhen Mindray Bio-Medical Electronics Co., Ltd.; China, Mindray Medical Rus LLC). The coefficient used to recalculate the data obtained in BAU/mL was 1.32.

The registry data were analyzed using the chi-squared test and parametric statistical methods. Information about tuberculosis patients having and not having COVID-19 was compared using multiple logistic regression analysis.

## RESULTS

During the COVID-19 pandemic, since March 2020, the Barclay-SV MDBMS was used in Moscow to implement monitoring of COVID-19 incidence among tuberculosis patients; the following was controlled when performing monitoring:

- information about the disease detection and diagnosis (dates, detection methods);
- patient routing;
- dynamic changes in assessment results (complete blood counts, D-dimer, anti-HIV, HBs Ag, anti-HCV, RW, PCR and ICA tests for COVID-19, serum IgM and IgG, chest radiography);
- ongoing COVID-19 treatment;
- COVID-19 treatment outcomes.

Information structure of the registry included the following:

- heading part with the main identification data on the patient;
- basic information about the patient: job/educational institution, position, actual residence address, permanent residence address, population category, nationality, social and professional background, information about COVID-19 vaccination;
- information about COVID-19 registration: dates of suspicion and confirmation of the diagnosis; confirmation methods; date of the emergence of clinical symptoms and description of the symptoms; data of seeking medical care due to symptoms of novel coronavirus infection; name of the medical institution the patient had contacted; information about the COVID-19 clinical variants and manifestations, disease severity; concomitant disorders; fact of contacting a COVID-19 patient; initial assessment results; treatment prescribed; measures in the outbreak of infection;
  - complete blood counts, D-dimer levels; results of tests for COVID-19 (up to 15) with the automated comparison with normal IgM and IgG levels;
  - information about routing specifying the names of medical institutions, where the patient was treated (up to six), specifying the admission ways and final COVID bed-days;
  - COVID-19 treatment outcomes with saved information about the data of the last COVID-19-positive smear, achieving smear negativity, and overall COVID-19 treatment outcome;
  - basic information about tuberculosis, including the patient's group based on medical history, data on detection, and the diagnosis results.

The Certificate of state registration No. 2022623380 dated 02.12.2022 was obtained for the registry structure and the database "Registry of Patients with Tuberculosis Combined with COVID-19 Registered in Moscow".

Due to temporary nature of the task, the database was developed as a pilot project, separately from the tuberculosis patient registry functioning in Moscow within the framework of TBSS.

The use of the Barclay-SV MDBMS as a basis made it possible to modify the registry data structure during

operation, to promptly update the questionnaire and reports with the emergence of new diagnosis, treatment, and prevention methods, to clarify COVID-19 clinical variants and manifestations, and to classify the disease based on severity.

The analysis of the data of patients with tuberculosis combined with COVID-19 registered over four years of the pandemic (2020–2023) by MRCCTC was performed based on the information entered in the registry.

Here are the results of processing the data on 1837 patients, among them 699, 449, 542, and 147 patients, respectively, got COVID-19 in 2020–2023. Hospital readmissions due to COVID-19 were reported for 222 patients (265 hospital readmissions: 51, 77, 112, and 25, respectively in the specified period), which in a number of cases resulted from re-detection of SARS-CoV-2 after achieving negative nasopharyngeal and oropharyngeal smears within the course of the same case of novel coronavirus infection.

One of the data processing goals was to conduct the analysis of changes in the course of novel coronavirus infection under conditions of COVID-19 epidemiological situation changing throughout 4 years based on the registry data. The specified time period was conditionally divided into two 2-year periods: the period of the pandemic development — 2020–2021 and the period of its decline — 2022–2023.

Table 1 provides information about the methods for COVID-19 detection and diagnosis in patients with tuberculosis and confirmed coronavirus infection, who were admitted to the city's COVID beds at least once. The data are provided on the number of patients, in whom novel coronavirus infection was detected primarily by laboratory testing (while CT could also be performed), on the number of patients, in whom the diagnosis of COVID-19 was confirmed based on chest CT (while laboratory testing was also performed), and, finally, on the number of patients, in whom the diagnosis was established based on both CT and laboratory testing results.

The results show significant ( $p < 0.01$ ) changes in predominant methods for detection of novel coronavirus infection over the last two years of monitoring (2022–2023) compared to the first two years of the COVID-19 pandemic (2020–2021): the role of laboratory methods in detection of novel coronavirus infection became overwhelming.

The registry data were used to implement control over routing and the ways of admission of the patients with tuberculosis combined with novel coronavirus infection to the COVID beds deployed at the MRCCTC. Admission to the hospital via ambulance took place in 43.8% of cases, scheduled admission — in 38.8% of cases, transfer from other medical institutions involving the use of sanitary transport — in 13.8% of cases, while in 3.6% of cases the admission ways were different.

Almost one fifth of TB/COVID-19 patients (20.7% or 377 patients) were admitted to the MRCCTC via non-tuberculosis medical institutions, including non-tuberculosis hospitals (149 individuals), municipal outpatient clinics (93 individuals), infection disease hospitals (121 individuals), research and clinical centers and federal institutions (14 individuals).

According to their medical history, about one third of TB/COVID-19 patients identified during this period had a confirmed contact with the patients suffering from COVID-19 — 29.4%.

The socio-demographic structure of the patients having combined TB/COVID-19 infection, who were identified in 2020–2023, was rather stable.

Distribution of patients with tuberculosis combined with novel coronavirus infection across the population categories is

**Table 1.** Methods to detect and diagnose COVID-19 in tuberculosis patients with confirmed coronavirus infection admitted for treatment for the first time (Moscow, 2020–2023)\*

Year	2020	2021	2020–2021	2022	2023	2022–2023	Total
Total number of admissions	699	449	942	497	130	689	1837
Laboratory method, including combined with CT, abs.	578	364	942	497	130	627	1569
%	82.7	81.1	82.1	91.7	88.4	91	85.4
Computed tomography, including combined with laboratory methods, abs.	219	214	433	103	31	134	567
%	31.3	47.7	37.7	19	21.1	19.4	30.9
By two methods, abs.	119	137	256	61	17	78	334
%	17	30.5	23.3	11.3	11.6	11.3	18.2
Unspecified detection method	21	8	29	3	3	6	35
%	3	1.8	2.5	0.6	2	0.8	1.9

Note: \* — No information was available for 35 patients.

similar to that of tuberculosis patients: slightly less than half or 45.6% were permanent residents (41.7%, 50.7%, 46.2%, and 47.3% in 2020–2023, respectively), almost a quarter or 23.8% were residents of other Russian regions (23.3%, 24.2%, 25.3%, and 19.9%, respectively), every seventh person was homeless (16.7%), and every eighth was a foreign citizen (13.9%).

More than a half of TB/COVID-19 patients or 53.1% were jobless and unemployed (56.3%, 50.7%, 51.8%, and 51.4% in 2020–2023, respectively), 16.8% were employed (14.7%, 20.8%, 15.7%, and 17.9% in 2020–2023 respectively), and 14.8% were disabled (13.9%, 14.8%, 15.3%, and 17.1% in 2020–2023, respectively). Others were retirees (11.4%), students (3.1%), and preschool children (0.8%).

More than a half of affected individuals or 54% were incident tuberculosis patients (50.9%, 60.1%, 54.8%, and 63.9% in 2020–2023, respectively), 13.4% had tuberculosis relapses, 9.3% were arriving tuberculosis patients, 21.9% were registered for follow-up as tuberculosis patients before the COVID-19 diagnosis.

We compared all new cases and tuberculosis relapses registered in 2020–2023 (excluding those identified posthumously), in which COVID-19 was detected (group 1) or not detected (group 2): 762 and 8293 individuals, respectively.

There were no gender differences in the groups: males accounted for 66.4% and 68.0%, respectively ( $p > 0.05$ ). Patients with TB/COVID-19 were on average older (Fig. 1): the average age in group 1 (with TB/COVID-19) was 44.7 years

(95% CI: 43.6–45.8), while in group 2 it was 40.5 years (95% CI: 40.2–40.9),  $p < 0.05$ .

Table 2 and Fig. 2A and 2B provide the multivariate analysis and multiple logistic regression results for assessment of factors that are statistically related to the presence of COVID-19 in tuberculosis patients, i.e. the probability of the relationship of those with the fact of having novel coronavirus infection exceeds 95% ( $p < 0.05$ ).

The presence of COVID-19 in the tuberculosis patients is associated with a rather large number of individual factors (univariate analysis), such as age over 30 years, fact of having HIV infection, some forms of pulmonary tuberculosis (disseminated, caseous pneumonia), lung tissue destruction and bacterial excretion, as well as the number of concomitant disorders determined by population groups. At the same time, if we take into account the relationship between these factors and apply multivariate analysis, then the following concomitant diseases remain the leading factors most strongly associated with the presence of COVID-19 in tuberculosis patients in terms of statistics: HIV infection, CAD and hypertension, kidney and genitourinary diseases, as well as severe and advanced pulmonary tuberculosis forms.

Thus, among the studied factors associated with tuberculosis, the facts of having disseminated disease forms, caseous pneumonia, bacterial excretion or destruction cavity in the lung show a significant correlation with getting COVID-19. Limited forms of tuberculosis, such as tuberculoma, represent the so-called “protective factors” against COVID-19.

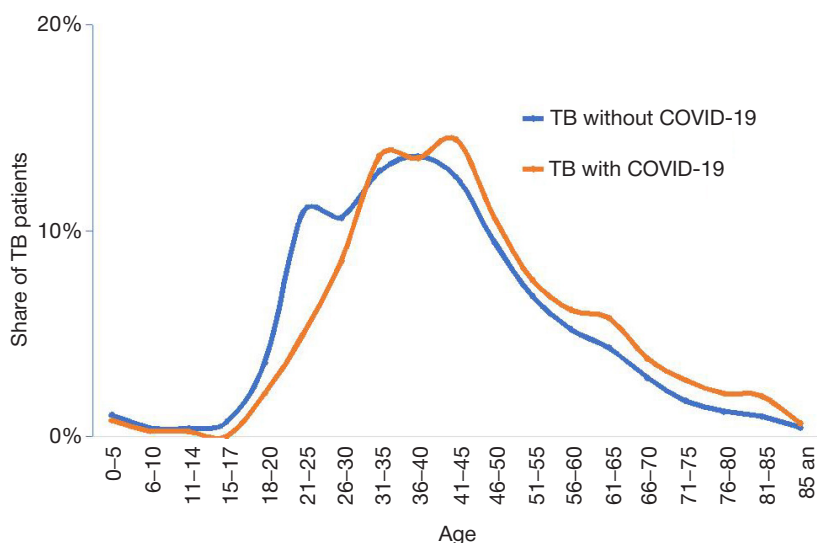


Fig. 1. Age dependence of new tuberculosis cases and tuberculosis relapses depending on the fact of COVID-19 detection (Moscow, 2020–2023)

**Table 2.** Factors associated with the fact of having COVID-19 in new tuberculosis cases and relapses of tuberculosis (Moscow, 2020–2023). Univariate and multivariate analysis

Factor	Univariate analysis					Multiple logistic regression
	Number in group 1	Share in group 1, %	Number in group 2	Share in group 2, %	OR (95% CI)	OR (95% CI)
Age under 30 years	127	16.7	2291	27.6	0.52 (0.43–0.64)	$p > 0.05$
HIV infection	225	29.5	1213	14.6	2.45 (2.07–2.89)	1.86 (1.55–2.25)
Disseminated PTB	249	32.7	1479	17.8	2.24 (1.9–2.63)	1.56 (1.3–1.86)
Tuberculoma	11	1.4	459	5.5	0.25 (0.14–0.46)	0.33 (0.18–0.61)
Caseous pneumonia	41	5.4	196	2.4	2.35 (1.66–3.32)	1.72 (1.19–2.47)
Lung tissue destruction	377	49.5	2946	35.5	1.78 (1.53–2.06)	1.41 (1.19–1.67)
Bacterial excretion	401	52.6	2670	32.2	2.34 (2.01–2.72)	1.62 (1.36–1.91)
Diabetes mellitus	51	6.7	370	4.5	1.53 (1.13–2.08)	$p > 0.05$
COPD	92	12.1	646	7.8	1.63 (1.29–2.05)	$p > 0.05$
CAD and hypertension	90	11.8	538	6.5	1.93 (1.52–2.45)	1.84 (1.44–2.37)
Alcohol abuse	33	4.3	232	2.8	1.57 (1.08–2.28)	$p > 0.05$
Drug addiction	22	2.9	102	1.2	2.39 (1.5–3.81)	$p > 0.05$
Diseases of the kidneys and genitourinary system	25	3.3	122	1.5	2.27 (1.47–3.52)	1.78 (1.14–2.79)
Liver and gallbladder diseases	44	5.8	301	3.6	1.63 (1.18–2.25)	$p > 0.05$
Employee	60	7.9	852	10.3	0.75 (0.57–0.98)	$p > 0.05$
Retired person	93	12.2	679	8.2	1.56 (1.24–1.96)	$p > 0.05$
Permanent resident	409	53.7	3422	41.3	1.65 (1.42–1.91)	1.19 (1–1.42)
Homeless person	94	12.3	685	8.3	1.56 (1.24–1.97)	$p > 0.05$
Feign citizen	113	14.8	2711	32.7	0.36 (0.29–0.44)	0.59 (0.46–0.75)

**Note:** group 1 — TB/COVID-19 patients, group 2 — newly diagnosed patients with tuberculosis and relapses of tuberculosis that have not been added to the TB/COVID-19 registry. PTB — pulmonary tuberculosis, CAD — coronary artery disease, COPD — chronic non-specific lung diseases.

The analysis of information about patients with tuberculosis combined with COVID-19, who were entered in the registry, has shown significant differences in clinical manifestations and immune status of these patients in the initial and final 2-year periods of the pandemic.

Table 3 provides the results of testing for immunoglobulins M (IgM) and G (IgG) obtained when the TB/COVID-19 patients sought medical care in 2020–2023. These data can show the phase of the infectious process course at the time when the patient sought medical care, time since SARS-CoV-2 infection.

Considering provisions of the regulatory documents [1, 6], detection of IgM and IgG levels below normal (1 and 10, respectively) can indicate that less than 7 days have passed since the patient was infected with coronavirus [1, 6, 13–15]; when this IgM level is exceeded and IgG remain within normal (IgM > 1, IgG within normal range) — that there is acute infection, and the patient got infected 1–3 weeks ago [6, 14]; when the levels of immunoglobulins of both classes are elevated — that the infectious process history is 3–10 weeks [15]; when IgM are within normal range and IgG are above normal (IgG  $\geq$  10, IgM within normal range) — that the patient was exposed to the virus more than 10–12 weeks ago [15].

Comparison of the 2-year periods (2020–2021 and 2022–2023) has shown a significantly reduced share of cases with the IgG and IgM below normal in the second period: 55.4% and 29.3%, respectively ( $p < 0.05$ ), the decrease in the number of cases with the combination, when only IgM are above normal (7.4% and 4.3%, respectively;  $p = 0.095$ ), and a significantly increased share of patients with only IgG above normal: 18.6% and 43.0%, respectively ( $p < 0.05$ ). Furthermore, the results obtained for 616 patients with concomitant HIV infection were similar.

In Moscow, mass vaccination against novel coronavirus infection (COVID-19) was started in December 2020. That

is why patients assigned to the last group (IgG  $\geq$  10, IgM within normal range) also could have elevated IgG levels due to vaccination since 2021. Furthermore, elevated IgG levels can persist for a long time past novel coronavirus infection (about 6 months or more according to different reports) [14, 16, 17].

The findings reflect the pandemic subsides in 2022–2023 and, to some extent, immunization of the population (and therefore tuberculosis patients) due to past contacts with COVID-19 patients and mass vaccination.

The COVID-19 pandemic transformation into routine seasonal infection in 2022–2023 is also evident from the description of clinical symptoms and severity of the course of novel coronavirus infection at the time of case registration.

This registry have been used to monitor the symptoms, course, clinical variants, and manifestations of novel coronavirus infection, disease severity in the registered TB/COVID-19 cases for 4 years (Fig. 3).

While in the first two years of the pandemic dry cough, feeling of tightness in the chest, and decreased sense of smell and taste (significance of the decrease in the share of each symptom;  $p < 0.05$ ), as well as dyspnea ( $p = 0.2$ ) prevailed among the disease symptoms, sore throat and runny nose were more commonly reported during the next two years ( $p < 0.05$ ), i.e. the symptoms of ordinary acute viral infection (Fig. 3A).

Mild COVID-19 cases were significantly more often registered in the last two years (Fig. 3B). The share of those increased from 41.6% to 60.9% ( $p < 0.01$ ), while the share decreased of both moderate (from 48.2% to 20.6% ( $p < 0.01$ )) and severe (from 6.4% to 4.9% ( $p = 0.19$ )) COVID-19.

It should be noted that the COVID-19 classification based on severity changed in accordance with the regulatory documents [1]. Initially, there were three degrees: mild, moderate, and severe forms. After Version 5 (08.04.2020) of the

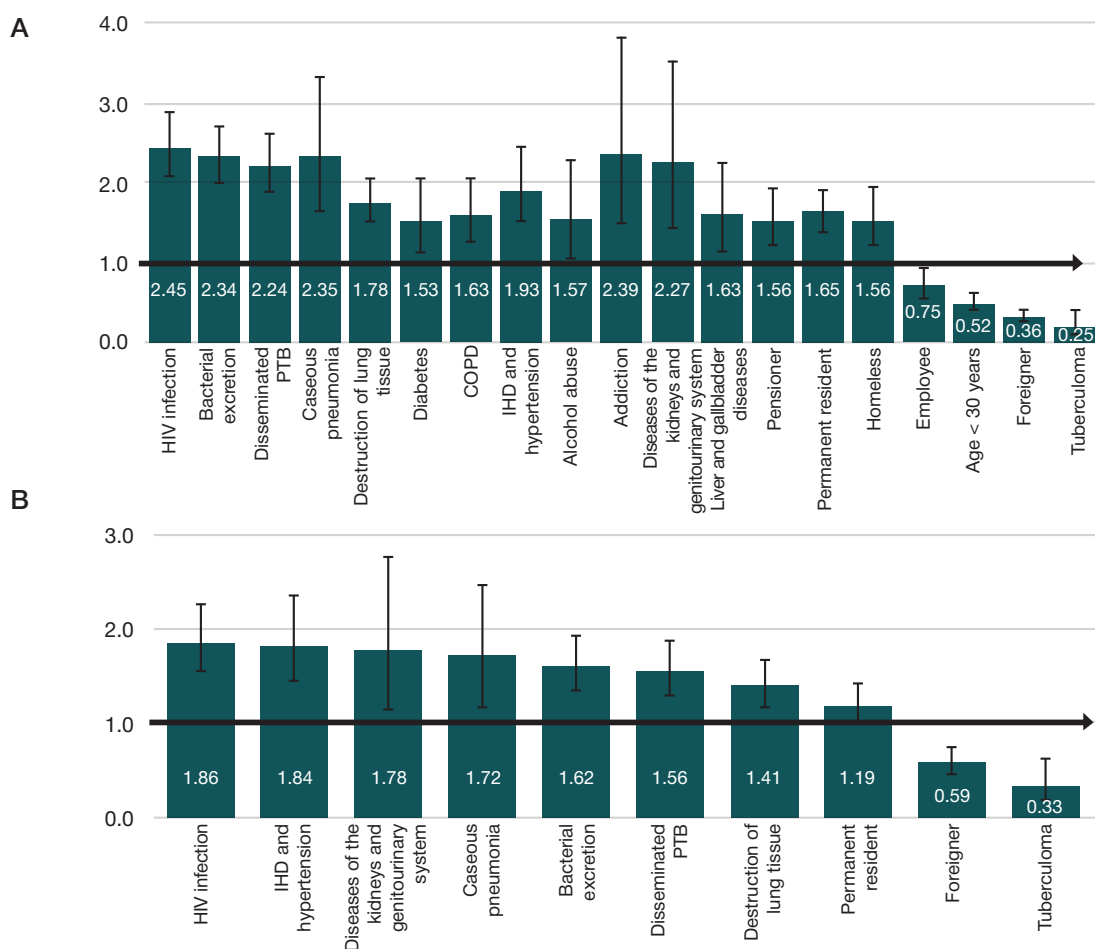


**Fig. 2.** Factors associated with the presence of COVID-19 in tuberculosis patients, univariate (A) and multivariate (B) analysis. Odds ratio (OR) of detecting COVID-19 co-infection in the presence of this symptom in a tuberculosis patient or the relationship between this symptom and the fact of having COVID-19 (Moscow, 2020–2023)

Temporary methodological guidelines “Prevention, Diagnosis, and Treatment of Novel Coronavirus Infection (COVID-19)” was issued, the classification became as follows: mild course, moderate course, severe course, extremely severe course.

Furthermore, the decrease in the share of individuals having the COVID lung damage without respiratory failure from 45.1% to 17.6% is reported, along with the growth of the number of cases of COVID upper respiratory tract (URT) lesion: from 47.1% to 64.5% in both cases,  $p < 0.05$  (Fig. 3C).

It should be noted that 222 patients, who were readmitted to hospital due to COVID-19 in 2020–2023 had the structure of the clinical variants and severity of novel coronavirus infection similar to that reported for primary hospital admissions during the period of the pandemic subside (2022–2023). The COVID upper respiratory tract lesions at readmission were reported in 62.2% of cases, COVID lung damage without acute respiratory

failure (ARF) — in 29.2% of cases, and mild-to-moderate disease course — in 69.8% and 25.0% of cases, respectively. The share of COVID upper respiratory tract lesions and mild disease course was higher at readmission ( $p < 0.05$ ) relative to the data reported for those, who sought medical care for the first time, in whom these indicators were 53.3% and 48.8%, respectively.

The average COVID bed-days of a patient with TB/COVID-19 decreased every year (from 15.5 days in 2020 to 14.4, 12.8, and 10.6 days, respectively, in 2021–2023), which was due not only to the fact that the course of novel coronavirus infection (COVID-19) became milder, but also to the fact that the terms of the COVID-19 convalescent discharge from the COVID bed for isolation changed.

We conducted analysis of the novel coronavirus infection treatment outcomes in the tuberculosis patients undergoing

**Table 3.** Results of immunoglobulin IgM and IgG tests obtained when detecting COVID-19 in patients with tuberculosis (Moscow, 2020–2023)

Year	Total (examination results are available upon admission)	IgM $\geq 1$		IgG $\geq 10$		Both are below normal*		IgM >1, IgG normal (<10)**		Both are above normal.***		IgG $\geq 10$ IgM normal (<1)****	
		Abs.	%	Abs.	%	Abs.	%	Abs.	%	Abs.	%	Abs.	%
2020	218	51	23.4	65	29.8	134	61.5	19	8.7	32	14.7	33	15.1
2021	337	95	28	143	42.5	172	50.7	22	6.5	73	21.5	70	20.6
2022	249	70	28	164	65.6	74	29.6	11	4.4	59	23.6	105	42
2023	7	1	12.5	6	75	1	12.5	0	0	1	12.5	5	62.5
Всего	811	217	26.6	378	46.5	381	46.7	52	6.4	165	20.2	213	26.1

**Note:** \* — no more than 7 days have passed since the infection; \*\* — acute infection, infection history 1–3 weeks. \*\*\* — infection history 3–10 weeks; \*\*\*\* — body's exposure to the virus took place more than 10–12 weeks ago.



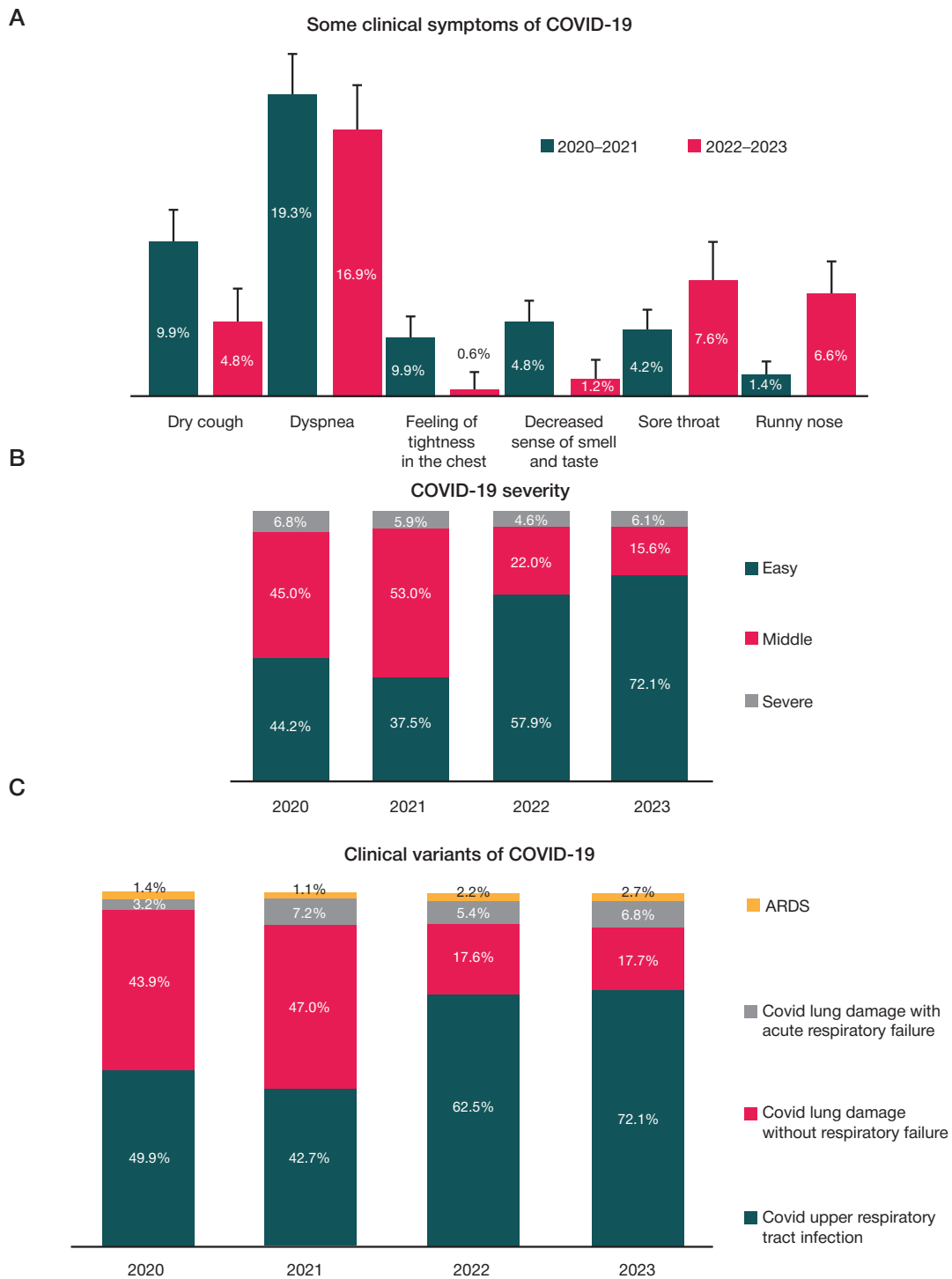


**Fig. 3.** Results of monitoring the course of COVID-19 in 1837 patients with TB combined with COVID-19, who were admitted for treatment for the first time in 2020–2023 in Moscow. Severe cases also include extremely severe COVID-19 (ARDS or pneumonia with ARF and the need for mechanical ventilation)

treatment in Moscow, primarily occupying COVID beds in hospitals: the share of those cured in 2020–2023 was 84.9% (95% CI: 83.2–86.4%), 5.2% were referred to continue treatment of COVID-19 in outpatient settings, and 9.9% (95% CI: 8.6–11.4%) died. Given the fact that the patients, who had mild coronavirus infection or showed regression of the infection due to treatment, were referred to continue treatment in outpatient settings after discharge from hospital, it can be considered that the total share of the patients with TB/COVID-19 cured is 90.1%.

Three quarters (77.7%) of fatalities were caused by COVID-19, 8.5% (95% CI: 4.9–13.5%) — by HIV infection, and

7.4% (95% CI: 4.9–13.5%) — by tuberculosis. Other causes of death accounted for 6.4%.

DISCUSSION

During the pandemic of novel coronavirus infection the temporary registry of patients having tuberculosis combined with COVID-19 was realized, which ensured the necessary control of information about registration, management and treatment outcomes of the patients.

Successful prompt realization of the TB/COVID-19 temporary registry through efforts of the head anti-tuberculosis

medical institution of the region became possible due to the use of flexible software shell of Barclay-SV MDBMS [11]. The development of this registry represents an example of prompt modification and development of the regional tuberculosis surveillance system in cases of challenges in the form of significant spread of novel hazardous infections. A state certificate was obtained for the registry.

The registry realized made it possible to perform ongoing and retrospective assessment of the structure of affected individuals, determine the factors most strongly statistically associated with the fact of getting novel coronavirus infection in tuberculosis patients, such as concomitant disorders, including HIV infection and pulmonary tuberculosis forms, population groups. Facts of having HIV infection, CAD and hypertension, kidney and genitourinary diseases increased the chance of developing novel coronavirus infection by tuberculosis patients almost 1.5–2-fold (OR = 1.9, 1.8, and 1.8, respectively), and disseminated pulmonary tuberculosis, caseous pneumonia, lung tissue destruction and bacterial excretion increased it 1.4–1.6-fold (OR = 1.6, 1.7, 1.4, and 1.6, respectively).

The registry operation enabled continuous control over the routing of patients, among whom one fifth were transferred to the MRCCTC COVID beds from non-tuberculosis medical institutions, and the treatment outcomes in tuberculosis/

COVID-19 patients were as follows: the total share of those cured reached 90.1%.

The information obtained made it possible to assume termination of significant effects of the pandemic on public health system in 2022–2023, which could affect distribution of appropriate resources. The leading clinical symptoms of the infection changed in the last two years of the pandemic, COVID-19 more often progressed to the COVID upper respiratory tract lesion, and the share of cases of COVID lung damage and severe course of novel coronavirus infection was significantly reduced. Immunological testing performed in patients also confirmed the fact of getting out of the pandemic since 2022 and gradual formation of population immunity.

## CONCLUSIONS

Prompt arrangement of temporary monitoring of the effects of the novel coronavirus infection pandemic on epidemiology of tuberculosis has demonstrated the necessary flexibility of the regional TBSS. Realization of the registry of patients having the combined tuberculosis/COVID-19 infection in Moscow has enabled prompt and retrospective analysis of data of the patients, control over their routing, treatment outcomes, spread of COVID-19 across tuberculosis patients, and effectiveness of the applied anti-epidemic measures in general.

## References

1. Профилактика, диагностика и лечение новой коронавирусной инфекции (COVID-19). Временные методические рекомендации Минздрава России. Версия 1 (29.01.2020) — Версия 18 (26.10.2023). Доступно по ссылке: [https://minzdrav.gov.ru/ministry/med\\_covid19](https://minzdrav.gov.ru/ministry/med_covid19). Russian.
2. Bogorodskaja EM, редактор. Protivotuberkuleznaja rabota v gorode Moskve v period pandemii COVID-19 (2020 g.). M.: Izd-vo «Sputnik +», 2021; 277 s. Russian.
3. Vasileva IA, Testov VV, Sterlikov SA. Jepidemičeskaja situacija po tuberkulezu v gody pandemii COVID-19 — 2020–2021 gg. Tuberkulez i bolezni legkih. 2022; 100 (3): 6–12. DOI: 10.21292/2075-1230-2022-100-3-6-12. Russian.
4. O vvedenii rezhima povyšhennoj gotovnosti. Ukaz Mjera Moskvy ot 5 marta 2020 g. № 12-UM. Доступно по ссылке: <https://www.mos.ru/authority/documents/doc/43503220/?ysclid=m42ryxni7570692807>. Russian.
5. Bogorodskaja EM, Bellilovskij EM. Jepidemiologija tuberkuleza v Moskve v period pandemii novoj koronavirusnoj infekcii COVID-19. Pedagogika professional'nogo medicinskogo obrazovanija. 2022; 1. Доступно по ссылке: <https://www.profmedobr.ru/articles/jepidemiologija-tuberkuleza-v-moskve-v-period-pandemii-novoj-koronavirusnoj-infekcii-covid-19>. Russian.
6. Ageev FA, Ambrosi OE, Anciferov MB, i dr. Kliničeskij protokol diagnostiki novoj koronavirusnoj infekcii (COVID-19) u bol'nyh, nahodjashhhsja na stacionarnom lečenii v medicinskih organizacijah gosudarstvennoj sistemy zdravooхранenija goroda Moskvy. Hripun A. I., редактор. M.: GBU «NII OZMM DZM», 2021; 32 s. Russian.
7. Bogorodskaja EM. Vlijanie pandemii COVID-19 na organizaciju protivotuberkuleznoj pomoshhi v gorode Moskve. Tuberkulez i social'no znachimye zaboлевanija. 2020; 4: 3–9. Russian.
8. Bogorodskaja EM, Kotova EA. Organizacija protivotuberkuleznoj raboty v g. Moskve v period pandemii novoj koronavirusnoj infekcii COVID-19. Protivotuberkuleznaja rabota v gorode Moskve v period pandemii COVID-19 (2020 g.). M.: Izd-vo «Sputnik +»; 2021: 16–30. Russian.
9. Bogorodskaja EM, Kotova EA. Organizacija protivotuberkuleznoj raboty v gorode Moskve v period prodolzhaushhegosja rasprostraneniya COVID-19. Protivotuberkuleznaja rabota v gorode Moskve vo vtoroj god pandemii COVID-19 (2021 g.). M.: MRCCTC Belgorod: KONSTANTA, 2023; s. 17–30. Russian.
10. Kotova EA, Sumarokova EV, Bellilovskij EM. Sochetannaja infekcija COVID-19 sredi bol'nyh tuberkulezom v gorode Moskve. Tuberkulez i social'no znachimye zaboлевanija. 2023; 11 (1): 12–15. DOI: 10.54921/2413-0346-2023-11-1-12-15. Russian.
11. Bellilovskij EM, Borisov SE. Osnovy organizacii sistemy jepidemiologičeskogo monitoringa tuberkuleza. Sovremennye problemy zdravooхранenija i medicinskoj statistiki. 2021; 1: 1–26. Russian.
12. Tadolini M, Codecasa LR, García-García J-M, Blanc F-X, Borisov S, Alffenaar J-W, et al. Active tuberculosis, sequelae and COVID-19 co-infection: first cohort of 49 cases. European Respiratory Journal. 2020; 56 (1): 2001398. Доступно по ссылке: <https://www.scopus.com/record/display.uri?eid=2-s2.0-85085193210&origin=inward&txGid=60b5e75024a82cf39cd7d4888ee584a6>.
13. Bogorodskaja E, Borisov S, Bellilovskij E, Sumarokova E, Chizhova O. Characteristics of tuberculosis patients co-infected with COVID-19. European Respiratory Journal. 2021; 58 (65): PA1031. DOI: <https://doi.org/10.1183/13993003.CONGRESS-2021.PA1031>.
14. Pashhenkov MV, Haitov MR. Immunnyj otvet protiv jepidemičeskikh koronavirusov. Immunologija. 2020; 41 (1): 5–18. DOI: 10.33029/0206-4952-2020-41-1-5-18. Russian.
15. Fedorov VS, Ivanova ON, Karpenko IL, Ivanov AV. Immunnyj otvet na novuju koronavirusnuju infekciju. Kliničeskaja praktika. 2021; 12 (1): 33–40. DOI: <https://doi.org/10.17816/clinpract64677>. Russian.
16. Novikova LI, Bochkareva SS, Aleshkin AV, Kombarova SYu, Karpov OYe, Pulih AA, i dr. Dinamika antitel k različnym antigenam koronavirusa SARS-CoV-2 u bol'nyh s podtverzhennoj infekciej Covid-19. V sbornike: Molekuljarnaja diagnostika i biobezopasnost' — 2020. Vserossijskaja nauchno-praktičeskaja konferencija s mezhdunarodnym učastiem (6–8 oktjabrja 2020 goda): sbornik materialov. M.: FBUN CNII Jepidemiologii Rospotrebnadzora, 2020; s. 159–165. Russian.
17. Tovanova AA. Sozdanie kollektivnogo immuniteta kak osnovnaja profilaktičeskaja mera pri rasprostraneni novoj koronavirusnoj infekcii (COVID-19). Vestnik Sankt-Peterburgskogo universiteta. Medicina. 2022; 17 (3): 212–20. DOI: <https://doi.org/10.21638/spbu11.2022.306>. Russian.

## Литература

1. Профилактика, диагностика и лечение новой коронавирусной инфекции (COVID-19). Временные методические рекомендации Минздрава России. Версия 1 (29.01.2020) — Версия 18 (26.10.2023). Доступно по ссылке: [https://minzdrav.gov.ru/ministry/med\\_covid19](https://minzdrav.gov.ru/ministry/med_covid19).
2. Богородская Е. М., редактор. Противотуберкулезная работа в городе Москве в период пандемии COVID-19 (2020 г.). М.: Изд-во «Спутник +», 2021; 277 с.
3. Васильева И. А., Тестов В. В., Стерликов С. А. Эпидемическая ситуация по туберкулезу в годы пандемии COVID-19 — 2020–2021 гг. Туберкулез и болезни легких. 2022; 100 (3): 6–12. DOI: 10.21292/2075-1230-2022-100-3-6-12
4. О введении режима повышенной готовности. Указ Мэра Москвы от 5 марта 2020 г. № 12-УМ. Доступно по ссылке: <https://www.mos.ru/authority/documents/doc/43503220/?ysclid=m42ryxni7570692807>.
5. Богородская Е. М., Белиловский Е. М. Эпидемиология туберкулеза в Москве в период пандемии новой коронавирусной инфекции COVID-19. Педагогика профессионального медицинского образования. 2022; 1. Доступно по ссылке: <https://www.profmedobr.ru/articles/jepidemiologija-tuberkuleza-v-moskve-v-period-pandemii-novoj-koronavirusnoj-infekcii-covid-19>.
6. Агеев Ф. А., Амброси О. Е., Анциферов М. Б. и др. Клинический протокол диагностики новой коронавирусной инфекции (COVID-19) у больных, находящихся на стационарном лечении в медицинских организациях государственной системы здравоохранения города Москвы. Хрипун А. И., редактор. М.: ГБУ «НИИОЗММ ДЗМ», 2021; 32 с.
7. Богородская Е. М. Влияние пандемии COVID-19 на организацию противотуберкулезной помощи в городе Москве. Туберкулез и социально-значимые заболевания. 2020; 4: 3–9.
8. Богородская Е. М., Котова Е. А. Организация противотуберкулезной работы в г. Москве в период пандемии новой коронавирусной инфекции COVID-19. Противотуберкулезная работа в городе Москве в период пандемии COVID-19 (2020 г.). М.: Изд-во «Спутник +»; 2021: 16–30.
9. Богородская Е. М., Котова Е. А. Организация противотуберкулезной работы в городе Москве в период продолжающегося распространения COVID-19. Противотуберкулезная работа в городе Москве во второй год пандемии COVID-19 (2021 г.). М.: МНПЦБТ Белгород; КОНСТАНТА, 2023; с. 17–30.
10. Котова Е. А., Сумарокова Е. В., Белиловский Е. М. Сочетанная инфекция COVID-19 среди больных туберкулезом в городе Москве. Туберкулез и социально значимые заболевания. 2023; 11 (1): 12–15. DOI: 10.54921/2413-0346-2023-11-1-12-15.
11. Белиловский Е. М., Борисов С. Е. Основы организации системы эпидемиологического мониторинга туберкулеза. Современные проблемы здравоохранения и медицинской статистики. 2021; 1: 1–26.
12. Tadolini M, Codecasa LR, García-García J-M, Blanc F-X, Borisov S, Alffenaar J-W, et al. Active tuberculosis, sequelae and COVID-19 co-infection: first cohort of 49 cases. *European Respiratory Journal*. 2020; 56 (1): 2001398. Доступно по ссылке: <https://www.scopus.com/record/display.uri?eid=2-s2.0-85085193210&origin=inward&txGid=60b5e75024a82cf39dc7d4888ee584a6>.
13. Bogorodskaya E, Borisov S, Belilovsky E, Sumarokova E, Chizhova O, Characteristics of tuberculosis patients co-infected with COVID-19. *European Respiratory Journal*. 2021; 58 (65): PA1031. DOI: <https://doi.org/10.1183/13993003.CONGRESS-2021.PA1031>.
14. Пашенков М. В., Хаитов М. Р. Иммуный ответ против эпидемических коронавирусов. *Иммунология*. 2020; 41 (1): 5–18. DOI: 10.33029/0206-4952-2020-41-1-5-18.
15. Федоров В. С., Иванова О. Н., Карпенко И. Л., Иванов А. В. Иммуный ответ на новую коронавирусную инфекцию. *Клиническая практика*. 2021; 12 (1): 33–40. DOI: <https://doi.org/10.17816/clinpract64677>.
16. Новикова Л. И., Бочарева С. С., Алешкин А. В., Комбарова С. Ю., Карпов О. Э., Пулин А. А. и др. Динамика антител к различным антигенам коронавируса SARS-CoV-2 у больных с подтвержденной инфекцией Covid-19. В сборнике: Молекулярная диагностика и биобезопасность — 2020. Всероссийская научно-практическая конференция с международным участием (6–8 октября 2020 года): сборник материалов. М.: ФБУН ЦНИИ Эпидемиологии Роспотребнадзора, 2020; с. 159–165.
17. Тованова А. А. Создание коллективного иммунитета как основная профилактическая мера при распространении новой коронавирусной инфекции (COVID-19). *Вестник Санкт-Петербургского университета. Медицина*. 2022; 17 (3): 212–20. DOI: <https://doi.org/10.21638/spbu11.2022.306>.

## GENETIC POLYMORPHISM OF THE NF-KB1 P105/P50 PROCESSING REGION IN PULMONARY TUBERCULOSIS

Meyer AV <sup>✉</sup>, Thorenko BA, Imekina DO, Dutchenko AP, Pyanzova TV, Karabchukov KB, Lavryashina MB

Kemerovo State Medical University, Kemerovo, Russia

Pulmonary tuberculosis (TB) is a socially significant disease and a global challenge faced by public health. The NF-κB signaling pathway is involved in differential expression of the genes involved in immune responses and regulation of inflammation in response to infection. The study aimed to assess associations of the *NFKB1* allelic variants with TB based on the panel of SNPs (rs4648050, rs4648051, rs4648055, rs4648058, rs4648068, rs1609993) located within the NF-κB1 p105→p50 processing region. Total DNA was extracted from blood samples (phenol-chloroform extraction) of patients with TB ( $n = 93$ ) and the population control group ( $n = 96$ ) consisting of residents of the Kemerovo Region. Genotyping was performed by real-time PCR, and the results were processed using the resources of the Statistica, SNPStats, Arlequin software packages. Ethnic features ( $p < 0.05$ ) of the Russian population of Siberia (population control group) were demonstrated based on the rs4648050 and rs4648051 allele frequencies. Differences ( $p < 0.05$ ) of the genetic profile of the sample of patients with pulmonary tuberculosis throughout the entire SNP complex, except for rs1609993, were noted. We showed differences ( $p < 0.05$ ) in the rs4648068 allelic frequencies between the population control sample and patients with pulmonary tuberculosis. The association with susceptibility to pulmonary tuberculosis was determined for genotypes AA\*rs4648055 (OR = 2.51;  $p = 0.05$ ) and GG\*rs4648068 (OR = 2.16;  $p = 0.03$ ). The findings are indirect evidence of modifying effects of the SNP located within the processing zone in the gene *NFKB1* and its possible contribution to the NF-κB1 p105/p50 protein balance and immune response to mycobacterial infection.

**Keywords:** *NFKB1*, genetic polymorphism, pulmonary tuberculosis, transcription factors, inflammation

**Funding:** the study was conducted within the framework of the basic budgetary funding source for project of the State Assignment of the Ministry of Health of the Russian Federation (agreement No. 056-03-2023-050 dated 17.01.2023).

**Author contribution:** Meyer AV, Lavryashina MB — developing the study concept and design, manuscript writing and final approval; Thorenko BA — genotyping, statistical analysis, working with the database; Imekina DO — genotyping, statistical analysis, technical editing; Dutchenko AP — search for literature, manuscript writing; Pyanzova TV — research management, clinical and biological material collection, final approval of the manuscript; Karabchukov KB — clinical history taking.

**Compliance with ethical standards:** the study was approved by the Ethics Committee of the Kemerovo State Medical University (protocol No. 301 dated 08 February 2023) and conducted in accordance with the ethical principles stated in the WMA Declaration of Helsinki; the written informed consent to participation in the study was obtained from all patients.

✉ **Correspondence should be addressed:** Alina V. Meyer  
Voroshilov, 22a, Kemerovo, 650056, Russia; shapo-alina@yandex.ru

**Received:** 23.12.2024 **Accepted:** 06.02.2025 **Published online:** 19.02.2025

**DOI:** 10.24075/brsmu.2025.004

**Copyright:** © 2025 by the authors. **Licensee:** Pirogov University. This article is an open access article distributed under the terms and conditions of the Creative Commons Attribution (CC BY) license (<https://creativecommons.org/licenses/by/4.0/>).

## ГЕНЕТИЧЕСКИЙ ПОЛИМОРФИЗМ ОБЛАСТИ ПРОЦЕССИНГА P105/P50 NF-KB1 ПРИ ТУБЕРКУЛЕЗЕ ЛЕГКИХ

А. В. Мейер <sup>✉</sup>, Б. А. Тхоренко, Д. О. Имекина, А. П. Дутченко, Т. В. Пьянзова, К. Б. Карабчуков, М. Б. Лавряшина

Кемеровский государственный медицинский университет, Кемерово, Россия

Туберкулез легких (ТБ) — социально значимое заболевание, общемировая проблема здравоохранения. NF-κB-сигнальный путь вовлечен в дифференциальную экспрессию генов, задействованных в иммунных реакциях и регулирующих воспаление в ответ на инфицирование. Целью исследования было изучить ассоциации с ТБ аллельных вариантов гена *NFKB1* по панели SNP (rs4648050, rs4648051, rs4648055, rs4648058, rs4648068, rs1609993), локализованных в зоне процессинга NF-κB1 p105→p50. Тотальную ДНК выделяли из образцов крови (метод фенол-хлороформной экстракции) пациентов, больных ТБ ( $n = 93$ ), и группы популяционного контроля ( $n = 96$ ) жителей Кемеровской области. Генотипирование проводили методом ПЦР в режиме реального времени, обработку результатов — с использованием ресурсов программ Statistica, SNPStats, Arlequin. Продемонстрированы этнические особенности ( $p < 0,05$ ) русского населения Сибири (группа популяционного контроля) по частотам аллелей rs4648050 и rs4648051. Отмечено отличие ( $p < 0,05$ ) генетического профиля выборки пациентов с туберкулезом легких от общемировой и европейской популяций по всему комплексу SNP, за исключением rs1609993. Показано различие ( $p < 0,05$ ) аллельных частот rs4648068 между выборкой популяционного контроля и пациентов с туберкулезом легких. Установлена ассоциация с подверженностью туберкулезу легких для генотипов AA\*rs4648055 (OR = 2,51;  $p = 0,05$ ) и GG\*rs4648068 (OR = 2,16;  $p = 0,03$ ). Полученные результаты косвенно свидетельствуют о модифицирующем влиянии SNP, локализованных в зоне процессинга, в гене *NFKB1* и его возможном вкладе в баланс белков NF-κB1 p105/p50 и иммунный ответ на микобактериальную инфекцию.

**Ключевые слова:** *NFKB1*, генетический полиморфизм, туберкулез легких, транскрипционные факторы, воспаление

**Финансирование:** работа выполнена в рамках базового бюджетного источника финансирования работ государственного задания Минздрава РФ (Соглашение № 056-03-2023-050 от 17.01.2023).

**Вклад авторов:** А. В. Мейер, М. Б. Лавряшина — разработка концепции и дизайна исследования, подготовка и окончательное утверждение рукописи; Б. А. Тхоренко — генотипирование, статистический анализ, работа с базой данных; Д. О. Имекина — генотипирование, статистический анализ, техническое редактирование; А. П. Дутченко — поиск литературы, подготовка рукописи; Т. В. Пьянзова — организация исследования, сбор клинического и биологического материала, окончательное утверждение рукописи; К. Б. Карабчуков — сбор клинического анамнеза.

**Соблюдение этических стандартов:** исследование одобрено этическим комитетом ФГБОУ ВО КемГМУ Минздрава России (протокол № 301 от 08 февраля 2023 г.), проведено согласно этическим принципам, изложенным в Хельсинкской декларации ВМА; от всех пациентов получено добровольное письменное согласие на участие.

✉ **Для корреспонденции:** Алина Викторовна Мейер  
ул. Ворошилова 22а, г. Кемерово, 650056, Россия; shapo-alina@yandex.ru

**Статья получена:** 23.12.2024 **Статья принята к печати:** 06.02.2025 **Опубликована онлайн:** 19.02.2025

**DOI:** 10.24075/vrgmu.2025.004

**Авторские права:** © 2025 принадлежат авторам. **Лицензиат:** РНИМУ им. Н. И. Пирогова. Статья размещена в открытом доступе и распространяется на условиях лицензии Creative Commons Attribution (CC BY) (<https://creativecommons.org/licenses/by/4.0/>).



Pulmonary tuberculosis (TB) is a pressing global issue of theoretical medicine and practical healthcare [1]. High incidence and mortality rates persist in a number of countries, which are caused by drug resistance of the pathogen, high prevalence of HIV infection among tuberculosis patients, low patient adherence to treatment, and the genetically determined features of the response to infection and treatment [2–5].

Diverse studies, including the analysis of genomes of *Mycobacterium tuberculosis* (*M. tuberculosis*) and the host, are conducted in order to investigate the genetic component value. One avenue in this field is the search for associations between the fact of carrying certain genotypic and allelic variants of genes and the specifics of human body's response to *M. tuberculosis* infection and anti-tuberculosis therapy. Despite a significant amount of data accumulated [6–9], there is still ambiguity and even some inconsistency of the results obtained, which determines the need for further research in this field.

Considering current ideas about the key immune mechanisms ensuring recognition of *M. tuberculosis* and subsequent destruction of the pathogen [10, 11], intracellular signaling pathways and molecular cascades involved in differential expression of the genes engaged in immune responses and ensuring regulation of inflammation as the body's systemic protective response are of great interest for scientific community [12–14]. These include the NF- $\kappa$ B signaling pathway, activation of which results in stimulation of inflammation via enhanced biosynthesis of TNF $\alpha$ , IFN $\gamma$ , IL6, IL8 pro-inflammatory factors and other cytokines [15].

The NF- $\kappa$ B1 transcription factor (nuclear factor kappa-light-chain-enhancer of activated B cells) is represented in the cell by the full-length precursor protein (p105) and its processed form (p50). NF- $\kappa$ B1/p50 as part of the complex with p65 (RelA) is a transcription activator, while NF- $\kappa$ B1/p105 in the form of homodimers (or together with I $\kappa$ B, the NF- $\kappa$ B inhibitor) functions as a suppressor of this process. Therefore, the p105→p50 processing modification can affect the NF- $\kappa$ B pathway direction and effectiveness, while intracellular p105/p50 balance can determine adequacy of the cellular response to activation signals, thereby contributing to the tuberculosis pathogenesis.

The Ub-independent p105→p50 posttranslational processing involving the 20S proteasome is currently considered as the main mechanism underlying generation of NF- $\kappa$ B1/p50 [16]. The endoproteolysis region is long enough and includes amino acid bases (AA) 430–530. At the gene level this region covers the exon region (E) E13 (403–433 AA) — E15 (499–546 AA) with the overall length of 2771 bp. The study aimed to assess associations with tuberculosis of the light *NFKB1* gene allelic variants localized within the NF- $\kappa$ B1 p105→p50 processing zone based on the SNP panel.

## METHODS

The study involved total DNA extracted from blood samples of the patients of the Kopylova Kuzbass Clinical Phthisiopulmonology Medical Center (Kemerovo) with pulmonary tuberculosis (TB group,  $n = 93$ ) and the population control group (PC group,  $n = 96$ ) represented by the sample of residents of the city of Kemerovo and Kemerovo Region. The group of patients with pulmonary tuberculosis included 74 males and 19 females aged 26–88 years diagnosed for the first time ( $n = 78$ ) and having relapses ( $n = 15$ ). Clinical forms were represented by infiltrative ( $n = 49$ ), disseminated ( $n = 23$ ), focal ( $n = 6$ ), fibrous-cavernous ( $n = 5$ ) pulmonary tuberculosis, tuberculoma ( $n = 7$ ), pleurisy ( $n = 3$ ). Both groups were formed considering ethnicity (based on self-determination), demographic and medical history data.

Inclusion criteria for the TB group: established diagnosis of incident tuberculosis or tuberculosis relapse; age over 18 years. Exclusion criteria: HIV infection; fact of detecting antibodies against hepatitis C virus (HCVAg) and hepatitis B virus (HBsAg) in blood serum; refusal of participation in the study. All the patients were assessed in accordance with the standard regulated by current clinical guidelines. A complex of clinical, laboratory, and instrumental testing data was used to verify the diagnosis. The diagnosis of tuberculosis was established by the central medical board of the Kopylova Kuzbass Clinical Phthisiopulmonology Medical Center. DNA was extracted from biological samples by the phenol-chloroform extraction method. Genotyping based on rs4648050, rs4648051, rs4648055, rs4648058, rs4648068, rs1609993 was performed by real-time PCR in the Applied Biosystems QuantStudio 5 Real-Time PCR System (Thermo Fisher Scientific, USA) using the commercially available kits (DNA-Synthesis, Russia). According to the manufacturer's instruction, the amplification programs had the following settings: initial denaturation for 3 min at a temperature of 95 °C; 40 cycles of primer annealing at a temperature specific for each polymorphism (54–59 °C); chain elongation at a temperature of 72 °C, and denaturation at a temperature of 95 °C. The amplification reagent mixture composition was as follows: DNA of the studied sample — 1  $\mu$ L, Taq DNA polymerase — 0.5  $\mu$ L, 10 $\times$  buffer for Taq DNA polymerase — 2.5  $\mu$ L, primer mixture (forward F, reverse R) — 2.5  $\mu$ L, solution of four dNTP — 1  $\mu$ L, fluorescent labeling probes TaqMan (FAM, VIC) — 1  $\mu$ L each, deionized water — to the total mixture volume of 25  $\mu$ L. Primary results were subjected to standard analysis using the resources of the Statistica, SNPStats, Arlequin software packages. Genotypic and allelic frequencies were calculated. The Hardy–Weinberg equilibrium was assessed using the Pearson's chi-squared ( $\chi^2$ ) test ( $\chi^2_{x-w}$ ). The analysis of associations of the candidate genes' polymorphic variants was conducted based on the odds ratio (OR) considering the confidence interval (CI) for the odds ratio (95% CI). The null hypothesis was rejected when  $p$ -value was below 0.05.

## RESULTS

The *NFKB1* gene (HGNC:7794) located in 4q24 with the length of 115,973 kbp (GRCh38: CM000666.2 – 4: 102,501,330–102,617,302) contains 27 exons (E). The SNP (Single Nucleotide Polymorphism) panel for the study was generated considering the following: 1) SNP location within the processing zone — the region of exons E13–E15 was used as a target, together with the adjacent introns (I) — I12, I15; 2) minor allele frequency (MAF) in the population of at least 0.1. Information was taken from the Ensembl genome browser (<http://www.ensembl.org>), and the NCBI data were used (<https://www.ncbi.nlm.nih.gov/>).

The total number of SNPs in the *NFKB1* gene is 41,781. The number of SNPs in the populations with the minor allele frequency (MAF) exceeding 0.1 was 152. After selecting polymorphic variants in the target region I12–E13–I13–E14–I14–E15–I15 with the length of 7325 bp (102,593,569–102,600,894 bp) a total of five variants located in introns were identified, along with one exonic variant. The characteristics of the SPN panel generated are provided in Table 1.

The data characterizing frequencies of the alternative allele based on the panel of six SNPs (rs4648050, rs4648051, rs4648055, rs4648058, rs4648068, rs1609993) in the gene *NFKB1* in patients with TB and in the PC group, along with the indicators of the genotypic frequency equilibrium ( $\chi^2_{x-w}$ ), as well as the data on the alternative allele frequencies in the

**Table 1.** Characteristics of the studied *NFKB1* SNP complex (according to Ensembl, <http://www.ensembl.org>)

RefSec	Localization	Type of variant	Position of variant (GRCh38)	Ancestral allele	Alternative variants
rs4648050	I 12	SNV	102593584	T	A, C*, G
rs4648051	I 12	SNV	102593836	A	G*
rs4648055	I 12	SNV	102594156	G	A*, C
rs4648058	I 12	SNV	102594434	G	C*
rs4648068	I 14	SNV	102597148	A	G*
rs1609993	E 12	SNV	102593501	T	A, C*, G

**Note:** I — intron, E — exon, \* — alternative variants analyzed in the study.

global (Global) and European (EUR) populations are provided in Table 2.

Determination of the state of genotype frequency equilibrium in the studied samples has shown the following. Values of the  $\chi^2_{x-w}$  parameter in the PC group suggest that there was no significant deviation from the Hardy–Weinberg equilibrium throughout the entire studied SNP panel in the gene *NFKB1*. In the sample of TB patients, genotypic frequency deviation ( $p < 0.05$ ) was reported based on two SNPs (rs4648068 and rs1609993):  $\chi^2_{x-w}$  was 5.06 and 9.15, respectively.

To analyze specifics of the gene pool of Russians of Siberia, we performed pairwise comparison of the rs4648050, rs4648051, rs4648055, rs4648058, rs4648068, rs1609993 allele frequencies in the gene *NFKB1* in the studied sample of Russians of the Kemerovo Region (Kuzbass; PC group) with the available data on the global and European populations. The results obtain reflect the features of the genetic profile of the Russian population of Siberia compared to global frequencies and the frequencies typical for populations of Europe based on rs4648050 ( $p < 0.05$ ), as well as in terms of matching with the global population based on rs4648051 ( $p < 0.05$ ). As for other studied SNPs, there were no significant differences in allelic frequencies in the PC group.

Comparison of the nature of allelic frequency distribution in the TB sample and PC group revealed a significant difference ( $p < 0.05$ ) based on rs4648068, for which the  $\chi^2$  value was 3.86. The fact attracts attention that comparison of allelic frequencies in the sample of TB patients with the frequencies in the global and European populations demonstrates specifics throughout

the entire SNP complex, except for rs1609993. This suggests that the increase in sample size will make it possible to reveal a broader range of associations between the studied SNPs and TB in the future.

Frequencies of the rs4648050, rs4648051, rs4648055, rs4648058, rs4648068, rs1609993 genotypes in the gene *NFKB1* and the results of assessing the association of the generated SNP panel with TB are provided in Table 3.

Comparison of genotypic frequencies revealed significant differences for two SNPs: rs4648068 ( $p = 0.03$ ) and rs4648055 ( $p = 0.05$ ). As for rs4648068, as mentioned above, we have shown significant differences based on the data of comparing the allelic frequencies as well. The study demonstrates the increased frequency of the homozygous GG variant comprising the alternative allele. As for rs4648055, in this case the sample of TB patients also shows higher frequency of the homozygous genotype comprising the alternative allele, AA. Both genotypes, GG\*rs4648068 and AA\*rs4648055, are considered as the etiological fraction genotypes, i.e. the genotype carrier state is associated with the increased susceptibility to developing TB in case of mycobacterial infection. The study has determined a significant correlation with TB of the genotypic variants AA\*rs4648055 (OR = 2.51;  $p = 0.05$ ) and GG\*rs4648068 (OR = 2.16;  $p = 0.03$ ).

## DISCUSSION

The results of matching the alternative allele frequencies to the cumulative data by projects (ALFA dataset, <https://ncbiinsights>).

**Table 2.** Frequencies of the rs4648050, rs4648051, rs4648055, rs4648058, rs4648068, rs1609993 alternative alleles in the gene *NFKB1* in the studied sample, global and European populations

SNP	Samples	$\chi^2_{x-w}$	Alt	$\chi^2_{TB}$	MAF «ALFA»		$\chi^2_{GLOBAL}$	$\chi^2_{EUR}$
					Global	EUR		
rs4648050	PC	1.41	0.531	0.001	0.278	0.293	<b>28.26</b>	<b>24.21</b>
	TB	1.43	0.528				<b>27.59</b>	<b>23.61</b>
rs4648051	PC	0.47	0.389	1.24	0.274	0.309	<b>6.27</b>	2.96
	TB	0.01	0.471				<b>16.86</b>	<b>10.61</b>
rs4648055	PC	0.83	0.338	2.96	0.291	0.304	1.02	0.52
	TB	0.07	0.461				<b>12.82</b>	<b>10.64</b>
rs4648058	PC	2.49	0.411	1.14	0.324	0.331	3.29	2.75
	TB	0.27	0.489				<b>11.24</b>	<b>10.17</b>
rs4648068	PC	2.85	0.395	<b>3.86</b>	0.339	0.321	1.34	2.4
	TB	<b>5.06</b>	0.538				<b>16.22</b>	<b>19.8</b>
rs1609993	PC	0.35	0.942	0.58	0.924	0.916	0.44	0.84
	TB	9.15	0.913				0.15	0.01

**Note:**  $\chi^2_{x-w}$  — criterion for estimation of the Hardy–Weinberg equilibrium;  $\chi^2$  — criterion for pairwise comparison of frequencies; Alt — alternative allele frequency; MAF — minor allele frequency in the global population (Global) and European population (EUR), the  $\chi^2$  indices represent variants of pairwise comparison: TB — of population control with the group of TB patients; GLOBAL — of both studied samples with frequencies in the global population; EUR — with frequencies in the European population. Statistically significant values are highlighted in bold.

**Table 3.** Distribution of the rs4648050, rs4648051, rs4648055, rs4648058, rs4648068, rs1609993 genotypes in the gene *NFKB1* and indicators of association with TB

SNP	Genotype	Frequency %		X <sup>2</sup> test value with the Yates's correction (significance level <i>p</i> )	Odds ratio OR (95% confidence interval)
		PC (n = 96)	TB (n = 93)		
rs4648050	TT	25	19.1	0.62 ( <i>p</i> = 0.43)	0.70 (0.35–1.42)
	TC	43.75	56.18	2.37 ( <i>p</i> = 0.12)	1.64 (0.92–2.94)
	CC	31.25	24.72	0.67 ( <i>p</i> = 0.41)	0.72 (0.37–1.37)
rs4648051	AA	38.94	27.58	2.14 ( <i>p</i> = 0.10)	0.59 (0.32–1.11)
	AG	44.22	50.58	0.50 ( <i>p</i> = 0.47)	1.26 (0.70–2.25)
	GG	16.84	21.84	0.44 ( <i>p</i> = 0.50)	1.38 (0.65–2.89)
rs4648055	GG	41.66	28.27	3.14 ( <i>p</i> = 0.07)	0.552 (0.30–1.01)
	GA	48.96	51.08	0.02 ( <i>p</i> = 0.88)	1.08 (0.61–1.92)
	AA	9.38	20.65	<b>3.86 (<i>p</i> = 0.05)</b>	<b>2.51 (1.07–5.89)</b>
rs4648058	GG	38.54	27.47	2.10 ( <i>p</i> = 0.14)	0.60 (0.32–1.12)
	GC	40.62	47.25	0.58 ( <i>p</i> = 0.44)	1.30 (0.73–2.33)
	CC	20.84	25.28	0.30 ( <i>p</i> = 0.58)	1.28 (0.64–2.54)
rs4648068	AA	40.62	27.17	3.21 ( <i>p</i> = 0.07)	0.54 (0.29–1.00)
	AG	39.58	38.05	0.004 ( <i>p</i> = 0.94)	0.93 (0.52–1.68)
	GG	19.8	34.78	<b>4.60 (<i>p</i> = 0.03)</b>	<b>2.16 (1.11–4.18)</b>
rs1609993	TT	0	3.27	1.44 ( <i>p</i> = 0.23)	0
	TC	11.46	10.87	0.01 ( <i>p</i> = 0.91)	0.942 (0.38–2.33)
	CC	88.54	85.86	0.10 ( <i>p</i> = 0.74)	0.786 (0.33–1.85)

ncbi.nlm.nih.gov/2020/03/26/alfa/) (Table 2) indicate the differences between the values obtained in this study for the population groups of the Siberian region relative to both global values (Global) and Caucasoid populations (EUR) throughout the range of studied SNPs, except for rs1609993. This suggests the features of the “genetic portrait” of the Russian population of Siberia related to the studied complex, which should be considered when conducting meta-analysis, arranging association studies, and determining the range of informative TB biomarkers.

In this study, significant associations with the risk of developing TB were reported for intronic variants rs4648055, rs4648068 (Table 3). In case of variant rs4648055, the alternative allele A in homozygous state increases the risk of disease 2.5-fold, while the 2-fold increased disease risk reported for rs4648068 results from the presence of alternative variant of allele G in homozygous state in the genotype. The trend towards statistical significance for protective effects of the major genotypes GG\*rs4648055 (OR = 0.55; *p* = 0.07) and AA\*rs4648068 (OR = 0.54; *p* = 0.07) can also be noted.

It should be noted that to date the literature data on the rs4648055 and rs4648068 contribution to the development of disorders are scarce, and the results are ambiguous. A number of papers report that there are no significant associations of rs4648055 and rs4648068 with the development of such disorders, as lung cancer [17] and coronary artery disease [18]. At the same time, when studying head and neck cancer in residents of Pakistan infected with HPV, the role of allele G in heterozygous and homozygous states in the increased risk of developing cancer was reported for rs4648068 [19]. When studying the risk factors of developing gastric cancer in the population of Han Chinese, significant results were reported for allele G of rs4648068 (OR = 1.43; *p* = 0.0001) [20]. Frequencies of genotype distribution in the control group were as follows: AA — 27.71%, AG — 53.58%, GG — 18.71%; in the group of patients — 22.94%, 45.64%, 31.42%. The alternative allele G frequency in the comparison group was 0.455, and in the cancer

group it was 0.542, which is similar to the data obtained in our study for the TB group (0.538). Similar results were reported when studying the rs4648055 and rs4648068 contribution to ovarian cancer development in the Chinese population, and significant associations were also reported only for allele G of rs4648068 (OR = 1.38; *p* = 0.001), frequency of which in the group of patients was 0.532, and in the comparison group it was 0.454 [21].

## CONCLUSIONS

The following aspects can be considered as the main findings of the study. First, new research data on the frequencies of rs4648050, rs4648051, rs4648055, rs4648058, rs4648068, rs1609993 in the gene *NFKB1* in Russians of Siberia were obtained. These data make it possible to draw a conclusion about the specifics of genetic structure of the Russian population that should be considered when conducting association studies. Second, the statistically significant differences of the rs4648050, rs4648051, rs4648055, rs4648058, rs4648068 allelic frequencies in the sample of tuberculosis patients from the global frequencies and frequencies typical for populations of Europe suggest potential informational value of the generated SNP panel, which requires further research. Third, the detection of associations between susceptibility to TB and homozygous genotypes based on the alternative allele for rs4648055 and rs4648068 is indirect evidence in favor of modifying effects of genetic polymorphism, SNPs located within the processing zone in the gene *NFKB1*, and its possible contribution to the p105→p50 processing effectiveness, balance of the NF-κB1 gene products (p105/p50), and regulation of target gene expression. This assumption requires further research based on the analysis of the p105 and p50 levels with parallel assessment of transcription activity of the target genes of this transcription factor. Identification and analysis of the features of molecular mechanisms at the population and individual

levels not only provide detailed understanding of molecular mechanisms underlying the TB pathogenesis, but also contribute to improvement of diagnostic procedures, including

those involving prediction of disease progression, as well as to improvement of therapeutic strategies and the search for the ways to develop new drugs.

## References

1. Global Tuberculosis Report 2023. Available from: <https://www.who.int/teams/global-tuberculosis-programme/tb-reports/global-tuberculosis-report-2023> (30.11.2024).
2. Khan PY, Yates TA, Osman M, Warren RM, van der Heijden Y, Padayatchi N, et al. Transmission of drug-resistant tuberculosis in HIV-endemic settings. *Lancet Infect Dis.* 2019; 19 (3): e77–e88. DOI: 10.1016/S1473-3099(18)30537-1.
3. Liebenberg D, Gordhan BG, Kana BD. Drug resistant tuberculosis: Implications for transmission, diagnosis, and disease management. *Front Cell Infect Microbiol.* 2022; 12: 943545. DOI: 10.3389/fcimb.2022.943545.
4. Dohal M, Porvaznik I, Solovič I, Mokry J. Advancing tuberculosis management: the role of predictive, preventive, and personalized medicine. *Front Microbiol.* 2023; 14: 1225438. DOI: 10.3389/fmicb.2023.1225438.
5. Shabani S, Farnia P, Ghanavi J, Velayati AA, Farnia P. Pharmacogenetic Study of Drugs Affecting Mycobacterium tuberculosis. *Int J Mycobacteriol.* 2024; 13 (2): 206–12. DOI: 10.4103/ijmy.ijmy\_106\_24.
6. Aravindan PP. Host genetics and tuberculosis: Theory of genetic polymorphism and tuberculosis. *Lung India.* 2019; 36 (3): 244–52. DOI: 10.4103/lungindia.lungindia\_146\_15.
7. Abhimanyu Bose M, Giri A, Varma-Basil M. Comparative Genetic Association Analysis of Human Genetic Susceptibility to Pulmonary and Lymph Node Tuberculosis. *Genes (Basel).* 2023; 14 (1): 207. DOI: 10.3390/genes14010207.
8. Murugesan H, Sampath P, A VK, R S, Veerasamy A, Ranganathan U, et al. Association of CYP27B1 gene polymorphisms with pulmonary tuberculosis and vitamin D levels. *Gene.* 2024; 927: 148679. DOI: 10.1016/j.gene.2024.148679.
9. Samimi R, Hosseinpanahi A, Zaboli R, Peymani A, Rouhi S, Ahmadi Gooraji S, et al. Prevalence of Vitamin D Receptor Genes Polymorphisms in People with Pulmonary Tuberculosis: A Systematic Review and Meta-Analysis. *Med J Islam Repub Iran.* 2024; 38: 32. DOI: 10.47176/mjiri.38.32.
10. Ferluga J, Yasmin H, Al-Ahdal MN, Bhakta S, Kishore U. Natural and trained innate immunity against Mycobacterium tuberculosis. *Immunobiology.* 2020; 225 (3): 151951. DOI: 10.1016/j.imbio.2020.151951.
11. Wang Y, Shi Q, Chen Q, Zhou X, Yuan H, Jia X, et al. Emerging advances in identifying signal transmission molecules involved in the interaction between Mycobacterium tuberculosis and the host. *Front Cell Infect Microbiol.* 2022; 12: 956311. DOI: 10.3389/fcimb.2022.956311.
12. Stutz MD, Clark MP, Doerflinger M, Pellegrini M. Mycobacterium tuberculosis: Rewiring host cell signaling to promote infection. *J Leukoc Biol.* 2018; 103 (2): 259–68. DOI: 10.1002/JLB.4MR0717-277R.
13. Gallant J, Heunis T, Beltran C, Schildermans K, Bruijns S, Mertens I, et al. PPE38-Secretion-Dependent Proteins of M. tuberculosis Alter NF- $\kappa$ B Signalling and Inflammatory Responses in Macrophages. *Front Immunol.* 2021; 12: 702359. DOI: 10.3389/fimmu.2021.702359.
14. Bullen CK, Singh AK, Krug S, Lun S, Thakur P, Srikrishna G, et al. MDA5 RNA-sensing pathway activation by Mycobacterium tuberculosis promotes innate immune subversion and pathogen survival. *JCI Insight.* 2023; 8 (20): e166242. DOI: 10.1172/jci.insight.166242.
15. Mitchell S, Vargas J, Hoffmann A. Signaling via the NF $\kappa$ B system. *Wiley Interdiscip Rev Syst Biol Med.* 2016; 8 (3): 227–41. DOI: 10.1002/wsbm.1331.
16. Moorthy AK, Savinova OV, Ho JQ, Wang VYa-F, Vu D, Ghosh G. The 20S proteasome processes NF-kappaB1 p105 into p50 in a translation-independent manner. *EMBO J.* 2006; 25 (9): 1945–56. DOI: 10.1038/sj.emboj.7601081.
17. Liu CW, Wu LS, Lin CJ, Wu HC, Liu KC, Lee SW. Association of tuberculosis risk with genetic polymorphisms of the immune checkpoint genes PDCD1, CTLA-4, and TIM3. *PLoS One.* 2024; 19 (5): e0303431. DOI: 10.1371/journal.pone.0303431.
18. Guo XL, Liu XC, Su GB, Zhou CY, Cui QT. Association of NF- $\kappa$ B1 gene polymorphisms with coronary artery disease in a Han Chinese population. *Genet Mol Res.* 2016; 15 (3). DOI: 10.4238/gmr.15038072.
19. Sarwar S, Tareen MU, Sabir M, Sultan A, Malik SA. NF- $\kappa$ B1 Intronic Region Polymorphisms as Risk Factor for Head and Neck Cancer in HPV-Infected Population from Pakistan. *Curr Mol Med.* 2022; 22 (1): 74–82. DOI: 10.2174/1566524021666210302144344.
20. Hua T, Qinsheng W, Xuxia W, Shuguang Z, Ming Q, Zhenxiang L, et al. Nuclear factor-kappa B1 is associated with gastric cancer in a Chinese population. *Medicine (Baltimore).* 2014; 93 (28): e279. DOI: 10.1097/MD.0000000000000279.
21. Chen LP, Cai PS, Liang HB. Association of the genetic polymorphisms of NFKB1 with susceptibility to ovarian cancer. *Genet Mol Res.* 2015; 14 (3): 8273–82. DOI: 10.4238/2015.July.27.15.

## Литература

1. Global Tuberculosis Report 2023. Available from: <https://www.who.int/teams/global-tuberculosis-programme/tb-reports/global-tuberculosis-report-2023> (30.11.2024).
2. Khan PY, Yates TA, Osman M, Warren RM, van der Heijden Y, Padayatchi N, et al. Transmission of drug-resistant tuberculosis in HIV-endemic settings. *Lancet Infect Dis.* 2019; 19 (3): e77–e88. DOI: 10.1016/S1473-3099(18)30537-1.
3. Liebenberg D, Gordhan BG, Kana BD. Drug resistant tuberculosis: Implications for transmission, diagnosis, and disease management. *Front Cell Infect Microbiol.* 2022; 12: 943545. DOI: 10.3389/fcimb.2022.943545.
4. Dohal M, Porvaznik I, Solovič I, Mokry J. Advancing tuberculosis management: the role of predictive, preventive, and personalized medicine. *Front Microbiol.* 2023; 14: 1225438. DOI: 10.3389/fmicb.2023.1225438.
5. Shabani S, Farnia P, Ghanavi J, Velayati AA, Farnia P. Pharmacogenetic Study of Drugs Affecting Mycobacterium tuberculosis. *Int J Mycobacteriol.* 2024; 13 (2): 206–12. DOI: 10.4103/ijmy.ijmy\_106\_24.
6. Aravindan PP. Host genetics and tuberculosis: Theory of genetic polymorphism and tuberculosis. *Lung India.* 2019; 36 (3): 244–52. DOI: 10.4103/lungindia.lungindia\_146\_15.
7. Abhimanyu Bose M, Giri A, Varma-Basil M. Comparative Genetic Association Analysis of Human Genetic Susceptibility to Pulmonary and Lymph Node Tuberculosis. *Genes (Basel).* 2023; 14 (1): 207. DOI: 10.3390/genes14010207.
8. Murugesan H, Sampath P, A VK, R S, Veerasamy A, Ranganathan U, et al. Association of CYP27B1 gene polymorphisms with pulmonary tuberculosis and vitamin D levels. *Gene.* 2024; 927: 148679. DOI: 10.1016/j.gene.2024.148679.
9. Samimi R, Hosseinpanahi A, Zaboli R, Peymani A, Rouhi S, Ahmadi Gooraji S, et al. Prevalence of Vitamin D Receptor Genes Polymorphisms in People with Pulmonary Tuberculosis: A Systematic Review and Meta-Analysis. *Med J Islam Repub Iran.* 2024; 38: 32. DOI: 10.47176/mjiri.38.32.
10. Ferluga J, Yasmin H, Al-Ahdal MN, Bhakta S, Kishore U. Natural and trained innate immunity against Mycobacterium tuberculosis. *Immunobiology.* 2020; 225 (3): 151951. DOI: 10.1016/j.imbio.2020.151951.



11. Wang Y, Shi Q, Chen Q, Zhou X, Yuan H, Jia X, et al. Emerging advances in identifying signal transmission molecules involved in the interaction between *Mycobacterium tuberculosis* and the host. *Front Cell Infect Microbiol.* 2022; 12: 956311. DOI: 10.3389/fcimb.2022.956311.
12. Stutz MD, Clark MP, Doerflinger M, Pellegrini M. *Mycobacterium tuberculosis*: Rewiring host cell signaling to promote infection. *J Leukoc Biol.* 2018; 103 (2): 259–68. DOI: 10.1002/JLB.4MR0717-277R.
13. Gallant J, Heunis T, Beltran C, Schildemans K, Bruijns S, Mertens I, et al. PPE38-Secretion-Dependent Proteins of *M. tuberculosis* Alter NF- $\kappa$ B Signaling and Inflammatory Responses in Macrophages. *Front Immunol.* 2021; 12: 702359. DOI: 10.3389/fimmu.2021.702359.
14. Bullen CK, Singh AK, Krug S, Lun S, Thakur P, Srikrishna G, et al. MDA5 RNA-sensing pathway activation by *Mycobacterium tuberculosis* promotes innate immune subversion and pathogen survival. *JCI Insight.* 2023; 8 (20): e166242. DOI: 10.1172/jci.insight.166242.
15. Mitchell S, Vargas J, Hoffmann A. Signaling via the NF $\kappa$ B system. *Wiley Interdiscip Rev Syst Biol Med.* 2016; 8 (3): 227–41. DOI: 10.1002/wsbm.1331.
16. Moorthy AK, Savinova OV, Ho JQ, Wang VYa-F, Vu D, Ghosh G. The 20S proteasome processes NF-kappaB1 p105 into p50 in a translation-independent manner. *EMBO J.* 2006; 25 (9): 1945–56. DOI: 10.1038/sj.emboj.7601081.
17. Liu CW, Wu LS, Lin CJ, Wu HC, Liu KC, Lee SW. Association of tuberculosis risk with genetic polymorphisms of the immune checkpoint genes PDCD1, CTLA-4, and TIM3. *PLoS One.* 2024; 19 (5): e0303431. DOI: 10.1371/journal.pone.0303431.
18. Guo XL, Liu XC, Su GB, Zhou CY, Cui QT. Association of NF- $\kappa$ B1 gene polymorphisms with coronary artery disease in a Han Chinese population. *Genet Mol Res.* 2016; 15 (3). DOI: 10.4238/gmr.15038072.
19. Sarwar S, Tareen MU, Sabir M, Sultan A, Malik SA. NF- $\kappa$ B1 Intronic Region Polymorphisms as Risk Factor for Head and Neck Cancer in HPV-Infected Population from Pakistan. *Curr Mol Med.* 2022; 22 (1): 74–82. DOI: 10.2174/1566524021666210302144344.
20. Hua T, Qinsheng W, Xuxia W, Shuguang Z, Ming Q, Zhenxiong L, et al. Nuclear factor-kappa B1 is associated with gastric cancer in a Chinese population. *Medicine (Baltimore).* 2014; 93 (28): e279. DOI: 10.1097/MD.0000000000000279.
21. Chen LP, Cai PS, Liang HB. Association of the genetic polymorphisms of NFKB1 with susceptibility to ovarian cancer. *Genet Mol Res.* 2015; 14 (3): 8273–82. DOI: 10.4238/2015.July.27.15.

## OXIDATIVE PROTEIN DESTRUCTION PRODUCTS AS MARKERS OF CHRONIC KIDNEY DISEASE PROGRESSION IN DIABETES MELLITUS

Osikov MV<sup>1,2</sup>, Efros LA<sup>1,2</sup>, Zhuravleva LY<sup>1,2</sup>✉, Fedosov AA<sup>3</sup>

<sup>1</sup> South Ural State Medical University, Chelyabinsk, Russia

<sup>2</sup> Chelyabinsk Regional Clinical Hospital, Chelyabinsk, Russia

<sup>3</sup> Patrice Lumumba Peoples' Friendship University of Russia, Moscow, Russia

Chronic kidney disease (CKD) represents one of the most common complications of type 1 diabetes mellitus (T1D). Oxidative stress (OS) can be considered as a key link of pathogenesis of CKD associated with T1D, therefore, identification of the redox status markers is important for prevention of the development and progression of this disorder. The study aimed to assess the substances generated during oxidative destruction of proteins and their correlation with glomerular filtration rate (GFR) in patients with T1D and stage 1–3 CKD. The study involved healthy individuals ( $n = 14$ ), patients with T1D showing no signs of CKD ( $n = 30$ ), as well as patients with T1D and stage 1 CKD ( $n = 60$ ), stage 2 CKD ( $n = 38$ ), and stage 3 CKD ( $n = 31$ ). Healthy participants were matched to the index group by age and gender: 42.9% were males, 57.1% were females, the average age was  $30.6 \pm 4.2$  years; body mass index, systolic and diastolic blood pressure, lipid profile were within normal. It has been found that patients with T1D and stage 1–3 CKD demonstrate plasma accumulation of early and delayed neutral and base products of oxidative protein modification (OPM): spontaneous 157% based on median, metal-induced 143% based on median relative to healthy individuals. We have revealed a decrease in overall antioxidant status (OAS) of plasma in 51% of patients with T1D and stage 3 CKD compared to patients with T1D without CKD. Estimated GFR, the integral indicator of renal function, decreases with increasing plasma levels of OPM products, decreasing OAS. The data obtained allow us to consider plasma levels of OPM products, OAS as affordable and informative methods to assess progression of early stage CKD in patients with T1D.

**Keywords:** type 1 diabetes mellitus, stage 1–3 chronic kidney disease progression, oxidative protein destruction

**Author contribution:** Osikov MV, Efros LA — study planning, developing the study concept and design, literature review, data interpretation, manuscript draft writing; Zhuravleva LY — data acquisition, statistical processing, data interpretation, manuscript draft writing; Fedosov AA — literature review, data interpretation, manuscript draft writing.

**Compliance with ethical standards:** the study was approved by the Ethics Committee of the South Ural State Medical University (protocol No. 5 dated 10 June 2024).

✉ **Correspondence should be addressed:** Lyudmila Yu. Zhuravleva  
Vorovsky, 70 (Medgorodok), str. 8, 454048, Chelyabinsk, Russia; milana\_1610@mail.ru

**Received:** 27.01.2025 **Accepted:** 15.02.2025 **Published online:** 26.02.2025

**DOI:** 10.24075/brsmu.2025.011

**Copyright:** © 2025 by the authors. **Licensee:** Pirogov University. This article is an open access article distributed under the terms and conditions of the Creative Commons Attribution (CC BY) license (<https://creativecommons.org/licenses/by/4.0/>).

## ПРОДУКТЫ ОКИСЛИТЕЛЬНОЙ ДЕСТРУКЦИИ БЕЛКОВ КАК МАРКЕРЫ ПРОГРЕССИРОВАНИЯ ХРОНИЧЕСКОЙ БОЛЕЗНИ ПОЧЕК ПРИ САХАРНОМ ДИАБЕТЕ

М. В. Осиков<sup>1,2</sup>, Л. А. Эфрос<sup>1,2</sup>, Л. Ю. Журавлева<sup>1,2</sup>✉, А. А. Федосов<sup>3</sup>

<sup>1</sup> Южно-Уральский государственный медицинский университет, Челябинск, Россия

<sup>2</sup> Челябинская областная клиническая больница, Челябинск, Россия

<sup>3</sup> Российский университет дружбы народов имени Патриса Лумумбы, Москва, Россия

Одно из наиболее частых осложнений сахарного диабета 1-го типа (СД1) — это хроническая болезнь почек (ХБП). Окислительный стресс (ОС) можно рассматривать как ключевое звено в патогенезе ХБП при СД1, в связи с чем востребовано выявление маркеров редокс-статуса для предотвращения развития и прогрессирования этого заболевания. Целью исследования было провести анализ веществ, образующихся при окислительном повреждении белков, и их связь со скоростью клубочковой фильтрации (СКФ) у пациентов с СД1 при ХБП 1–3 стадий. В исследовании участвовали здоровые люди ( $n = 14$ ), больные СД1 без признаков ХБП ( $n = 30$ ), а также больные СД1 с 1-й стадией ХБП ( $n = 60$ ), 2-й стадией ХБП ( $n = 38$ ) и 3-й стадией ХБП ( $n = 31$ ). Здоровые участники сопоставимы по возрасту и полу с основной группой: мужчин 42,9%, женщин 57,1%, средний возраст  $30,6 \pm 4,2$  лет, показатели индекса массы тела, систолического и диастолического артериального давления, липидограммы в пределах нормальных значений. Выявлено, что у больных с СД1 и ХБП 1–3-й стадий в плазме накапливаются ранние и поздние нейтрального и основного характера продукты окислительной модификации белков (ОМБ) в спонтанном режиме по медиане 157%, в металл-индуцированном режиме по медиане 143% в сравнении со здоровыми. Отмечено снижение общего антиоксидантного статуса (ОАС) плазмы на 51% у пациентов с СД1 и ХБП 3-й стадии в сравнении с пациентами СД1 без ХБП. Интегральный показатель функции почек — расчетная СКФ — снижается по мере увеличения продуктов ОМБ в плазме, снижения ОАС. Полученные данные позволяют рассматривать содержание в плазме продуктов ОМБ, ОАС как доступные и информативные методы оценки прогрессирования начальных стадий ХБП у больных с СД1.

**Ключевые слова:** сахарный диабет 1-го типа, прогрессирование хронической болезни почек 1–3-й стадий, окислительная деструкция белков

**Вклад авторов:** М. В. Осиков, Л. А. Эфрос — планирование исследования, разработка концепции и дизайна исследования, анализ литературы, интерпретация данных, подготовка черновика рукописи; Л. Ю. Журавлева — сбор данных, статистическая обработка, интерпретация данных, подготовка черновика рукописи; А. А. Федосов — анализ литературы, интерпретация данных, подготовка черновика рукописи.

**Соблюдение этических стандартов:** одобрено этическим комитетом ФГБОУ ВО ЮУГМУ Минздрава России (протокол № 5 от 10 июня 2024 г.).

✉ **Для корреспонденции:** Людмила Юрьевна Журавлева  
ул. Воровского, 70 (Медгородок), корпус 8, 454048, г. Челябинск, Россия; milana\_1610@mail.ru

**Статья получена:** 27.01.2025 **Статья принята к печати:** 15.02.2025 **Опубликована онлайн:** 26.02.2025

**DOI:** 10.24075/vrgmu.2025.011

**Авторские права:** © 2025 принадлежат авторам. **Лицензиат:** РНИМУ им. Н. И. Пирогова. Статья размещена в открытом доступе и распространяется на условиях лицензии Creative Commons Attribution (CC BY) (<https://creativecommons.org/licenses/by/4.0/>).

Diabetes mellitus (DM) and chronic kidney disease (CKD) are significant medical and social challenges faced by the global community. According to the International Diabetes Federation, in 2021, there were 537 million people with DM registered in the world, which is 6% of the global population [1]. As of January 1, 2023, the number of DM patients in Russia was 4.9 million (3.31% of the population), and 277.1 thousand of them (5.58%) suffered from type 1 DM (T1DM). The trend for T1DM prevalence is upward: in 2010, there were 146 cases registered per 100 thousand population, and in 2022, the figure was 191, which gives an annual growth of 2–3% [2]. Diabetic nephropathy is the most common complication: 40% of T1DM patients have it, and the probability of diagnosing this condition after 8–10 years with T1DM is 50%, growing to 75% after 15–20 years [3]. The risks of developing CKD in T1DM increase significantly as the target parameters of carbohydrate metabolism grow (HbA1c above 7%) [4, 5]. The prevalence of CKD among T1DM patients reaches 25–75%; the disease remains the main microvascular complication [7, 8]. Globally, the prevalence of CKD is 10–18%, and in Russia it is about 11% [9]. It is assumed that by 2040, CKD will become one of the main reasons for the shortening of life expectancy [10]. In high-income states, dialysis and kidney transplantation consume 2–3% of the overall healthcare budget, and the share of patients receiving such treatment is less than 0.03% of the country's population [11].

In 2022, one of the topics discussed at the KDIGO conference was the importance of establishing the risk factors associated with CKD development and progression, since the impact of the disease on the health of the population is growing, and there are obvious gaps in this subject matter [12]. Early diagnosing of CKD and the introduction of modern treatment methods can significantly reduce the need for renal replacement therapy in the late stages of the disease. The progression of CKD in T1DM patients causes death in over 70% of patients within five years; in addition, CKD affects the cost of diabetes treatment [13]. Deliberate interferences at the early stages of CKD in T1DM patients help prevent deterioration of kidney function and improve treatment outcomes, which necessitates regular screenings for CKD [14]. Understanding the molecular and cellular mechanisms contributing to the progression of CKD in DM patients is a key factor for the development of effective diagnostic and therapeutic strategies [8, 15]. An important aspect thereof is the spectrophotometric assessment of the plasma total antioxidant capacity (TAC) that enables oxidative stress (OS) monitoring.

The purpose of the study was to analyze substances resulting from the oxidative degradation of proteins, and to determine their connection to the glomerular filtration rate (GFR) in T1DM patients with stage 1–3 CKD.

## METHODS

The study was conducted at the Chelyabinsk Regional Clinical Hospital under the South Ural State Medical University of the Ministry of Health of the Russian Federation. Criteria for inclusion in the study: informed consent, T1DM diagnosed over 3 months as per the clinical recommendations of the Russian National Medical Research Center for Endocrinology [16]. Exclusion criteria: the age of men- over 60 years old, postmenopausal age for women; estimated glomerular filtration rate (eGFR)  $\leq 29$  ml/min/1.73 m<sup>2</sup>; diagnosed T2DM, pheochromocytoma, primary hyperparathyriosis, Itsenko–Cushing's disease, acromegaly, hypothyroidism, thyrotoxicosis; diagnosed hypertension before the onset of T1DM; severe concomitant diseases of the liver, lungs, tuberculosis, rheumatological,

autoimmune and oncological diseases; inflammatory kidney diseases, congenital kidney abnormalities; active inflammatory processes; intake of glucocorticoids and cytostatics, vitamin D preparations, phosphatebinders; pregnancy; non-standard body size; paraplegia and quadriplegia; acute renal injury; transplanted kidney.

Group 1 included healthy people comparable in age and gender to the treatment group ( $n = 14$ ), group 2 consisted of T1DM patients without CKD ( $n = 30$ ), group 3 was comprised of T1DM patients with CKD ( $n = 129$ ), subdivided by stages [17] (stage 1, subgroup 3.1,  $n = 60$ ; stage 2, subgroup 3.2,  $n = 38$ ; stage 3, subgroup 3.3,  $n = 31$ ). eGFR was assessed using the CKD-EPI equation that reveals serum creatinine according to standard methods, the equipment was Cobas Integra 400 analyzers (Roche, Switzerland), using kinetic colorimetric method. The protein oxidative modification (POM) was analyzed by spectrophotometry [18], the reaction with 2,4-dinitrophenylhydrazine [19]. TAC was measured using the B-7501 Total Antioxidant Capacity test system (Vector-Best, Russia). The result was expressed in mmol/L. In the heptane and isopropanol phases of the lipid extract, we measured the optical density at wavelengths of 220 nm (shows content of isolated double bonds), 232 nm (shows content of diene conjugates, DC), 278 nm (shows content of ketodienes and conjugated trienes, KCT), 400 nm (shows content of Schiff bases, SB). The relative content of lipid peroxidation products (LPP) was expressed in units of oxidation indices (UOI): E232/E220 (DC), E278/E220 (KCT) and E400/E220 (SB). Blood plasma POM products were determined by the reaction of carbonyl derivatives of proteins with 2,4-dinitrophenylhydrazine in spontaneous and metal-dependent Fenton reaction (metal-catalyzed oxidation, MCO), with spectrophotometric registration of aldehyde 2,4-dinitrophenylhydrazine (ADNPH) and ceton 2,4-dinitrophenylhydrazine (CDNPH) in the ultraviolet (uv) and visible light (vs) parts of the spectrum with the calculation of the reserve and adaptive potential. The result was expressed in units of optical density per 1 mg of protein (cu/mg). For statistical processing of the data, we used Microsoft Office Excel (Microsoft Corporation, USA) and IBM SPSS Statistics v. 23 (SPSS: IBM Company, USA). Quantitative data were presented as a median (Me) with interquartile intervals ( $Q_1$ ;  $Q_3$ ), the values of the lower (25) and upper (75) quartiles, respectively. Nonparametric Kruskal–Wallis and Mann–Whitney tests were used for intergroup comparison of quantitative data. Spearman's rank correlation coefficient allowed determining the interrelationships of the indicators, and the Chaddock scale was used to assess the strength of the connection (weak — from 0.1 to 0.3, moderate — from 0.3 to 0.5, noticeable — from 0.5 to 0.7, high — from 0.7 to 0.9, very high — from 0.9 to 1.0). The differences were considered statistically significant at  $p < 0.05$ .

## RESULTS

Initially, we established eGFR in the groups (Table 1). This assessment revealed the indicator to be 17% higher in group 1 than in group 2 (be median), which is a significant difference; in subgroup 3.1, the value was 10% lower, in subgroup 3.2 — 28% lower, and in subgroup 3.3 — 62% lower. In addition, eGFR was significantly lower in subgroups 3.1, 3.2, 3.3 compared to group 2. eGFR values in patients of subgroup 3.2 significantly differed from those registered in subgroup 3.1, and in patients of subgroup 3.3 they were significantly differed from the values in subgroups 3.1 and 3.2. In T1DM patients, including those with CKD, the changes of the content of blood plasma POM

**Table 1.** Estimated glomerular filtration rate in T1DM patients with CKD, ml/min/1.73 m<sup>2</sup> (Iu [Q<sub>1</sub>; Q<sub>3</sub>])

Group 1 (n = 14)	Group 2 (n = 30)	Group 3 (DM+CKD)			p-value, with p < 0,05
		Subgroup 3.1 (n = 60)	Subgroup 3.2 (n = 38)	Subgroup 3.3 (n = 31)	
105.000 [91.000; 118.000]	123.000 [120.000; 134.000]	94.000 [92.000; 126.000]	76.000 [67.000; 78.000]	40.000 [31.000; 58.000]	$p_{1-2} < 0.001$ $p_{1-3.1} < 0.001$ $p_{1-3.2} < 0.001$ $p_{1-3.3} < 0.001$ $p_{2-3.1} = 0.016$ $p_{2-3.2} < 0.001$ $p_{2-3.3} < 0.001$ $p_{3.1-3.2} < 0.001$ $p_{3.1-3.3} < 0.001$ $p_{3.2-3.3} < 0.001$

products were the following; specifically, in group 2, the total concentration of such products was elevated, contributed to by both early- and late-stage neutral and basic products. A proportional increase in the content of POM products in spontaneous and metal-induced modes did not lead to significant changes in the reserve and adaptive potential. Accordingly, blood plasma TAC in group 2 was decreasing (Table 2).

The most pronounced changes were recorded in group 2. In subgroups 3.1, 3.2, 3.3, the total concentration of blood plasma POM products increased with early- and late-stage products, neutral and basic types, both in the spontaneous and metal-induced modes. The most significant growth of concentration of the products was observed in subgroup 3.3, both in spontaneous mode (median 157% compared with group 1) and in metal-induced mode (median 143% compared with group 1). In subgroup 3.3, the total number of POM products, both early- and late-stage, significantly differed from the values registered in group 2 and subgroup 3.1. Group 3.1 was also found to have a diminished reserve and adaptive potential in plasma. In addition, TAC in blood plasma in group 3 also decreased: by 19% in subgroup 3.1, by 39% in subgroup 3.2, and by 51% in subgroup 3.3.

To assess the relationship between the changes in OS parameters and renal function — eGFR in group 3 patients — we conducted a correlation analysis (Table 3).

In group 2, we registered a significant direct correlation with the overall antioxidant level. A strong inverted correlation was observed with the total amount of blood plasma POM products, late-stage POM products in the spontaneous mode, the total volume of POM products, as well as neutral POM products in the metal-induced test; a very strong inverted correlation was established for the content of neutral and basic POM products in the spontaneous test, as well as basic POM products in the metal-induced test. In subgroup 3.1, we found inverted correlation with the content of late-stage POM products, and a direct correlation with the reserve adaptive potential and TAC. In subgroup 3.2, the correlation with TAC was also direct, but it turned out to be inverted for the plasma levels of late-stage POM products. In subgroup 3.3, we established an inverted correlation with various POM products, both early- and late-stage, as well as with neutral products. In subgroup 3.3, a strong inverted correlation was observed with the amount of early and late-stage POM products. Ultimately, the number of correlations between eGFR and the plasma redox status increases from group 2 to subgroup 3.3, which confirms the growing importance of these correlations, group 2 (8 in total, including 1 notable, 4 strong, and 3 very strong) to subgroup 3.1 (10 in total, including 4 notable, 1 strong, 5 very strong), to subgroup 3.2 (10 in total, including 1 notable, 3 strong, 6 very strong), and, maximizing, to subgroup 3.3 (11 in total, including 4 notable, 5 strong, 2 very strong).

## DISCUSSION

Analysis of the level of eGFR showed that it increased in group 2. From 10 to 67% of the respective patients had higher eGFR and hyperfiltration, with the maximum values up to 162 ml/min/1.73 m<sup>2</sup>. Various pathogenetic factors can cause this situation, including compensatory hypertrophy and hyperfunction of the kidneys against the background of chronic hyperglycemia, and the impact of inflammatory cytokines, growth factors, local angiotensin II, imbalanced vasoactive substances regulating blood flow at the levels of pre- and postglomerular arterioles.

Altered reabsorption of sodium, glucose, and hydrogen ions in the proximal tubules of nephrons are important factors, too [20–22]. Currently, intracubular hyperfiltration is considered one of the key mechanisms triggering the onset and progression of diabetic nephropathy [23, 24].

Elevated levels of POM products and deteriorating TAC in T1DM patients, including those stages 1–3 CKD, point to the impact of OS in this group. Oxidative stress is one of the main pathogenetic forces influencing the development of CKD in DM patients. It appears with excessive amounts of active oxygen forms and nitrogen derivatives in the background, and weakening antioxidant protection [25]. The key processes contributing to the formation of active forms include activation of various NADPH oxidase isoforms (NOX1-NOX5, DUOX1 and DUOX2) in the immune system cells, as well as various forms of NO synthase (NOS) and other enzymes. In DM patients, blood sugar levels are rising constantly, and the immune cells and the related processes are activated, which translates into formation of excessive amounts of glycated compounds that trigger intracellular signaling pathways such as phosphoinositide-3-kinase and nuclear factor kappa B, which, in turn, aggravate the inflammatory processes. As a result, vascular walls and metabolic shunts are damaged, and the DM becomes exacerbated, since chronic inflammation is an important factor contributing to complications, such as diabetic nephropathy.

The growing level of glycated compounds in the blood contributes to the accumulation of toxic metabolites, which also exacerbates OS and damages cells and tissues. Moreover, activation of the nuclear factor kappa B boosts production of pro-inflammatory cytokines such as TNF $\alpha$  and IL6. These molecules play a key role in the development of DM complications, intensifying pain, impairing organ functions, and causing other systemic disorders.

To minimize the risks, it is important to control blood glucose level, since it affects the metabolic state and also suffocates the inflammatory processes, which eventually translates into slower development of DM complications [26].

It was previously noted that DM boosts the activity of NADPH oxidase isoenzymes, especially NOX4 and NOX5, while the activity of antioxidant enzymes slows down; these effects are associated with hyperglycemia. Activating NADPH



**Table 2.** Blood plasma POM and TAC indicators, T1DM patients with CKD (Me [Q<sub>1</sub>; Q<sub>3</sub>])

Indicators	Group 1	Group 2 (n = 30)	Group 3			p-value, with p < 0,05
			Subgroup 3.1 (n = 60)	Subgroup 3.2 (n = 38)	Subgroup 3.3 (n = 31)	
S POM cu/mg of protein	5.956 [5.286; 7.744]	8.443 [7.330; 14.752]	8.561 [5.762; 14.639]	9.500 [8.307; 16.915]	15.319 [13.323; 33.675]	$p_{1-2} = 0.002$ $p_{1-3.1} = 0.044$ $p_{1-3.2} < 0.001$ $p_{1-3.3} < 0.001$ $p_{2-3.3} = 0.009$ $p_{3.1-3.3} = 0.001$ $p_{3.2-3.3} = 0.012$
S ADNPH, cu/mg protein	5.735 [5.088; 7.361]	8.069 [7.016; 14.003]	8.205 [5.483; 14.078]	9.124 [7.967; 16.124]	13.755 [12.626; 31.956]	$p_{1-2} = 0.002$ $p_{1-3.1} = 0.044$ $p_{1-3.2} < 0.001$ $p_{1-3.3} < 0.001$ $p_{2-3.3} = 0.012$ $p_{3.1-3.3} = 0.002$ $p_{3.2-3.3} = 0.016$
S KDNPH, cu/mg protein	0.220 [0.198; 0.296]	0.374 [0.314; 0.749]	0.431 [0.297; 0.561]	0.465 [0.372; 0.741]	1.031 [0.564; 1.649]	$p_{1-2} = 0.001$ $p_{1-3.1} < 0.001$ $p_{1-3.2} < 0.001$ $p_{1-3.3} < 0.001$ $p_{2-3.3} = 0.003$ $p_{3.1-3.3} = 0.001$ $p_{3.2-3.3} = 0.002$
S uv, cu/mg protein	5.862 [5.199; 7.574]	8.291 [7.187; 14.423]	8.396 [5.656; 14.393]	9.346 [8.162; 16.537]	15.064 [12.994; 32.893]	$p_{1-2} = 0.002$ $p_{1-3.1} = 0.044$ $p_{1-3.2} < 0.001$ $p_{1-3.3} < 0.001$ $p_{2-3.3} = 0.008$ $p_{3.1-3.3} = 0.001$ $p_{3.2-3.3} = 0.012$
S vl, cu/mg protein	0.087 [0.082; 0.122]	0.152 [0.143; 0.329]	0.167 [0.106; 0.246]	0.243 [0.146; 0.378]	0.388 [0.298; 0.782]	$p_{1-2} < 0.001$ $p_{1-3.1} = 0.009$ $p_{1-3.2} < 0.001$ $p_{1-3.3} < 0.001$ $p_{2-3.3} = 0.002$ $p_{3.1-3.3} = 0.001$ $p_{3.2-3.3} = 0.009$
S POM, metal-induced mode, cu/mg protein	9.660 [9.240; 12.865]	14.303 [11.269; 24.749]	14.225 [12.550; 21.752]	15.155 [13.222; 28.696]	23.498 [18.848; 57.269]	$p_{1-2} < 0.001$ $p_{1-3.1} = 0.002$ $p_{1-3.2} < 0.001$ $p_{1-3.3} < 0.001$ $p_{2-3.3} = 0.002$ $p_{3.1-3.3} = 0.050$ $p_{3.2-3.3} = 0.009$
S ADNPH, metal- induced mode cu/mg of protein	8.481 [8.235; 11.308]	12.435 [10.002; 21.855]	12.503 [11.029; 19.443]	13.087 [11.243; 24.884]	20.323 [16.572; 49.375]	$p_{1-2} = 0.001$ $p_{1-3.1} = 0.002$ $p_{1-3.2} = 0.001$ $p_{1-3.3} < 0.000$ $p_{2-3.3} = 0.002$ $p_{3.1-3.3} = 0.007$ $p_{3.2-3.3} = 0.009$
S KDNPH, metal- induced mode, cu/mg protein	1.034 [0.974; 1.556]	1.868 [1.267; 3.414]	1.722 [1.507; 2.309]	2.090 [1.592; 3.812]	3.175 [2.049; 7.895]	$p_{1-2} = 0.001$ $p_{1-3.1} = 0.001$ $p_{1-3.2} < 0.001$ $p_{1-3.3} < 0.001$ $p_{2-3.3} = 0.002$ $p_{3.1-3.3} = 0.044$
S uv, metal-induced mode, cu/mg protein	8.740 [8.441; 11.618]	12.803 [10.252; 22.393]	12.788 [11.328; 19.872]	13.556 [11.708; 25.301]	21.012 [16.878; 51.153]	$p_{1-2} = 0.001$ $p_{1-3.1} = 0.002$ $p_{1-3.2} < 0.001$ $p_{1-3.3} < 0.001$ $p_{2-3.3} = 0.002$ $p_{3.1-3.3} = 0.040$ $p_{3.2-3.3} = 0.044$
S vl, metal-induced mode, cu/mg protein	0.803 [0.788; 1.247]	1.500 [1.017; 2.668]	1.440 [1.222; 1.883]	1.599 [1.154; 3.395]	2.486 [1.687; 6.116]	$p_{1-2} < 0.001$ $p_{1-3.1} = 0.002$ $p_{1-3.2} < 0.001$ $p_{1-3.3} < 0.001$ $p_{2-3.3} = 0.002$ $p_{3.1-3.3} = 0.044$
RAP, %	39.715 [36.706; 44.284]	37.413 [34.960; 42.280]	36.030 [35.385; 37.722]	37.454 [33.686; 41.064]	41.199 [35.385; 44.320]	$p_{1-3.1} = 0.021$
TAC, mmol/L	1.800 [1.610; 1.960]	1.610 [1.470; 1.680]	1.145 [0.980; 1.670]	1.100 [0.780; 1.410]	0.890 [0.800; 1.100]	$p_{1-2} = 0.021$ $p_{1-3.1} = 0.004$ $p_{1-3.2} < 0.001$ $p_{1-3.3} < 0.001$ $p_{2-3.3} = 0.004$ $p_{3.1-3.3} = 0.002$ $p_{3.2-3.3} = 0.019$

**Note:** the table gives total (S) POM products content values, spontaneous and metal-induced modes; ADNPH — aldehyde-dinitrophenylhydrozone; KDNPH — ketone-dinitrophenylhydrozone; S uv — the level of carbonyl derivatives measured in the UV spectrum; S vl — the level of carbonyl derivatives measured in the visible light spectrum; RAP — reserve adaptive potential.

**Table 3.** Correlation between eGFR (ml/min/1.73 m<sup>2</sup>) and POM, LPP, and TAC, T1DM patients with CKD

Indicators	Group 2 (n = 30)	Group 3		
		Subgroup 3.1 (n = 60)	Subgroup 3.2 (n = 38)	Subgroup 3.3 (n = 31)
S POM, cu/mg protein	<i>R</i> = -0.75 <i>p</i> = 0.002	<i>R</i> = -0.99 <i>p</i> < 0.001	<i>R</i> = -0.99 <i>p</i> < 0.001	<i>R</i> = -0.67 <i>p</i> = 0.008
S ADNPH, cu/mg protein	<i>R</i> = -0.52 <i>p</i> = 0.057	<i>R</i> = -0.98 <i>p</i> < 0.001	<i>R</i> = -0.99 <i>p</i> < 0.001	<i>R</i> = -0.67 <i>p</i> = 0.008
S KDNPH, cu/mg protein	<i>R</i> = -0.83 <i>p</i> < 0.001	<i>R</i> = -0.62 <i>p</i> = 0.018	<i>R</i> = -0.74 <i>p</i> = 0.002	<i>R</i> = -0.63 <i>p</i> = 0.016
S uv, cu/mg protein	<i>R</i> = -0.91 <i>p</i> < 0.001	<i>R</i> = -0.98 <i>p</i> < 0.001	<i>R</i> = -0.99 <i>p</i> < 0.001	<i>R</i> = -0.60 <i>p</i> = 0.023
S vl, cu/mg protein	<i>R</i> = -0.91 <i>p</i> < 0.001	<i>R</i> = -0.97 <i>p</i> < 0.001	<i>R</i> = -0.68 <i>p</i> = 0.007	<i>R</i> = -0.91 <i>p</i> < 0.001
S POM, metal-induced mode, cu/mg protein	<i>R</i> = -0.83 <i>p</i> < 0.001	<i>R</i> = -0.62 <i>p</i> = 0.018	<i>R</i> = -0.97 <i>p</i> < 0.001	<i>R</i> = -0.77 <i>p</i> < 0.001
S ADNPH, metal-induced mode, cu/mg protein	<i>R</i> = -0.46 <i>p</i> = 0.102	<i>R</i> = -0.62 <i>p</i> = 0.018	<i>R</i> = -0.97 <i>p</i> < 0.001	<i>R</i> = -0.76 <i>p</i> < 0.001
S KDNPH, metal-induced mode, cu/mg protein	<i>R</i> = -0.53 <i>p</i> = 0.050	<i>R</i> = -0.58 <i>p</i> = 0.028	<i>R</i> = -0.84 <i>p</i> < 0.001	<i>R</i> = -0.72 <i>p</i> = 0.004
S uv, metal-induced mode, cu/mg protein	<i>R</i> = -0.89 <i>p</i> < 0.001	<i>R</i> = -0.62 <i>p</i> = 0.018	<i>R</i> = -0.97 <i>p</i> < 0.001	<i>R</i> = -0.76 <i>p</i> < 0.001
S vl, metal-induced mode, cu/mg protein	<i>R</i> = -0.92 <i>p</i> < 0.001	<i>R</i> = -0.52 <i>p</i> = 0.055	<i>R</i> = -0.89 <i>p</i> < 0.001	<i>R</i> = -0.76 <i>p</i> < 0.001
RAP, %	<i>R</i> = -0.04 <i>p</i> = 0.903	<i>R</i> = 0.75 <i>p</i> = 0.002	<i>R</i> = -0.21 <i>p</i> = 0.462	<i>R</i> = -0.22 <i>p</i> = 0.458
TAC, mmol/L	<i>R</i> = 0.68 <i>p</i> = 0.007	<i>R</i> = 0.93 <i>p</i> < 0.000	<i>R</i> = 0.58 <i>p</i> = 0.030	<i>R</i> = 0.98 <i>p</i> < 0.000

**Note:** the table gives the Spearman's rank correlation coefficient (*R*) values; the statistically significant connections are highlighted in bold (*p* < 0.05).

oxidase, angiotensin II plays a key role in the development of OS associated with diabetic nephropathy. Mitochondrial dysfunction with increased activity of complex-I and increased production of reactive oxygen species (ROS) also contribute to the onset and aggravation of diabetic nephropathy, but not as significantly as NADPH oxidase [15, 27, 28].

Oxidative stress and mitochondrial dysfunction mutually reinforce each other in the pathogenesis of the disease. Against the background of hyperglycemia, the activity of cytochrome P450, especially CYP4A, grows, which boosts the synthesis of the NADPH oxidase activator, 20-hydroxyeicosatetraenoic acid. In preclinical studies, it was established that a drip in the expression of Nrf2 has a significant impact on the overall level of antioxidant activity in patients with T1DM and signs of CKD [15]. The positive effect of various antioxidants confirms the weight of OS in the pathogenesis of renal pathology [26, 30]. High levels of ROS and nitrogen damage cellular structures and DNA, causing endothelial dysfunction, inflammation, and fibrosis [24, 31]. The need to assess the progression of CKD and the associated risks substantiates the search for specific biomarkers enabling diabetic nephropathy diagnosing and monitoring.

Given that OS is a significant factor in the development of renal failure in DM cases, clinicians seek to tally the excessive amounts of reactive species of oxygen and nitrogen, as well as their metabolites, through laboratory tests of biological fluids. Both of the said species decompose quickly, so their detection is complicated, which adds to the importance of methods designed for identification of the products of oxidative damage, such as lipids, proteins, and nucleic acids [15].

The known markers of OS are malonic dialdehyde, thiobarbituric acid, and glycation end products, as well as 4-hydroxynonenal and 8-deoxyguanosine. Gaging the levels of endogenous intoxication in T1DM patients at various stages of albuminuria can help identify early biomarkers of primary kidney

damage [24, 32]. The levels of conjugated dienes, ketodienes, and trienes, as well as medium-molecular peptides, can be increased as early as at the A1 stage of CKD 1–3.

In recent years, researchers have grown more interested in studying OS and its role in the pathogenesis of various diseases, including CKD. In this work, we observed pronounced changes in the concentration of POM products in T1DM patients without CKD. This is consistent with the data reported by other authors, who also note that OS may be a significant factor contributing to the progression of diabetic nephropathy [33]. In T1DM patients with stages 1–3 CKD, we registered growth of the total blood plasma POM products concentration, which was detected in both spontaneous and metal-induced tests, in line with the reports emphasizing the role of OS in boosting the progression of CKD [34]. The most significant increase in the concentration of POM products was identified in T1DM patients with stage 3 CKD, which may indicate more pronounced disorders in the antioxidant system and a higher level of OS in this group. Other researchers received similar results [35]. In addition, it was found that patients at later stages of CKD exhibit significantly elevated levels of OS markers compared with patients at early stages of the disease, which underscores the need to monitor OS as a potential prognostic marker enabling assessment of the severity of the disease and the risk of CKD progression. Given that OS can add to the damage of cells and tissues, its monitoring can be an important tool in clinical practice that allows timely identification of patients at risk [35, 36].

We have also found that the reserve and adaptive potential of blood plasma was significantly reduced in the stage 1 CKD subgroup. This fact confirms that even at the early stages of the disease, plasma's functional state changes, which may indicate the need for more careful monitoring and early intervention seeking to prevent the progression of the disease. In addition, the analysis of plasma TAC level in patients at various stages of CKD showed a significant decrease thereof:

in the stage 1 CKD subgroup, it dropped by 19%, in the stage 2 CKD subgroup — by 39%, and in the stage 3 CKD subgroup — by 51%. These data emphasize the importance of assessing the antioxidant status of CKD patients, since a decreasing TAC may signal growth of the OS level and overall health deterioration. It is important to remember that early diagnosing and adequate treatment can significantly affect the quality of life of such patients and the respective prognoses. According to our data, T1DM patients without CKD have a significant direct correlation with the overall level of antioxidants. This may mean that in these cases, antioxidants play an important role in protecting cells from OS, which is common against the background of DM. There are studies that stress the critical importance of maintaining high levels of antioxidants in the matter of prevention of DM-related complications [33]. The strong inversed connection with the total amount of blood plasma POM products, especially late-stage, is another described phenomenon. This may indicate that an increase in the level of oxidative products is associated with a deterioration of the antioxidant status. According to some data, OS can hamper antioxidant activity [37], which is consistent with our observations. We have also registered different correlation patterns in T1DM patients at different stages of CKD. In T1DM and stage 1 CKD cases, the correlation with late-stage POM products was inversed, that with reserve adaptive potential and antioxidant status — direct. This may point to the persisting possibility of adaptation of the antioxidant system at the early stages of CKD. In T1DM and stage 2 CKD cases, the correlation with antioxidant status was direct, that with late-stage POM products — inversed. This may mean that as the disease progresses, the antioxidant system begins to weaken. In T1DM and stage 3 CKD cases, the correlation with both early- and late-stage POM products was inversed. The strong inversed correlation with the amount of early- and late-stage POM products may indicate a significant deterioration in the OS and antioxidant response at this stage. It was previously shown that the progression of CKD is associated with a growing OS and diminishing antioxidant activity [38], which is consistent

with our data on the correlation between the stages of CKD and the levels of oxidative products. Other authors also confirm that patients with DM and CKD have a significantly lower antioxidant status, which is associated with a deteriorating kidney function and a growing level of oxidative markers [39].

A comprehensive study of these indicators in T1DM patients with early stages 1–3 CKD, as well as correlation analysis, allow considering them as promising biomarkers of OS in the context of progressive diabetic nephropathy [40, 41].

## CONCLUSIONS

This study has shown that T1DM patients with early CKD have growing blood plasma levels of primary and secondary LPP products (in heptane and isopropanol lipid extract), as well as early- and late-stage neutral and basic POM products in spontaneous and metal-induced modes, and the plasma TAC decreases. In T1DM cases with concomitant early-stage CKD, the severity of OS progresses, maximizing at stage 3. Dropping GFR, an integral indicator of kidney function, in T1DM patients with early-stage CKD is accompanied by a growing amount of products of LPP (secondary products in isopropanol extract of lipids, early- and late-stage neutral and basic POM products in spontaneous and metal-induced modes) and POM. In parallel, we observed a decreasing blood plasma TAC. The resulting data suggest that blood plasma POM products and TAC can be easily measured and informative indicators of progression of CKD at initial stages in T1DM patients. Studying the respective interaction may help design new anti-inflammatory strategies that can slow the progression of CKD. The development of algorithms for predicting the risk of CKD based on early OS markers will be an important step towards successful prevention. The results of this study expand the knowledge about the impact of OS on CKD in T1DM cases. They also refine the current understanding of the role of OS in the pathogenesis of CKD in T1DM patients and support further research, modernization of diagnostic and prognostic criteria, and improvement of preventive and therapeutic measures for such patients.

## References

1. Saharnyj diabet 2 tipa u vzroslyh: klinicheskie rekomendacii. Rubrikator klinicheskikh rekomendacij. 2022 [data dostupa: 2025 janvar' 26]. Dostupna po ssylke: [https://cr.minzdrav.gov.ru/schema/290\\_2](https://cr.minzdrav.gov.ru/schema/290_2).
2. Dedov II, Shestakova MV, Vikulova OK, Zheleznyakova AV, Isakov MA, Sazonova DV, i dr. Saharnyj diabet v Rossijskoj Federacii: dinamika jepidemiologicheskix pokazatelej po dannym Federal'nogo registra saharного diabeta za period 2010–2022 gg. Saharnyj diabet. 2023; 26 (2): 104–23. DOI:10.14341/DM13035. Russian.
3. Radia M.M.K. From pre-diabetes to diabetes: Diagnosis, treatments and translational research. *Medicina* (Kaunas). 2019; 55 (9): 546. DOI:10.3390/medicina55090546.
4. Kidney Disease: Improving Global Outcomes (KDIGO) Diabetes Work Group. KDIGO 2022 Clinical Practice Guideline for Diabetes Management in Chronic Kidney Disease. *Kidney Int.* 2022; 102 (5S): S1–S127. DOI: 10.1016/j.kint.2022.06.008.
5. Vikulova OK, Elfirmova AR, Zheleznyakova AV, Isakov MA, Shamhalova MSh, Shestakova MV, i dr. Kal'kuljator riska razvitiya hronicheskoy bolezni pochek: novye vozmozhnosti prognozirovaniya patologii u pacientov s saharным diabedom. *Consilium Medicum.* 2022; 24 (4): 224–33. DOI:10.26442/20751753.2022.4.201684. Russian.
6. Dedov II, Shestakova MV, Vikulova OK, Zheleznyakova AV, Isakov MA. Jepidemiologicheskije karakteristiki saharного diabeta v Rossijskoj Federacii: kliniko-statisticheskij analiz po dannym registra saharного diabeta na 01.01.2021. *Saharnyj diabet.* 2021; 24 (3): 204–2. DOI: 10.14341/DM12759. Russian
7. Perkins BA, Bebu I, de Boer IH, Molitch M, Tamborlane W, Lorenzi G, et al. Risk Factors for Kidney Disease in Type 1 Diabetes. *Diabetes Care.* 2019; 42 (5): 883–90. Available from: <https://doi.org/10.2337/dc18-2062>.
8. Patidar K, Deng JH, Mitchell CS, Ford Versypt AN. Cross-Domain Text Mining of Pathophysiological Processes Associated with Diabetic Kidney Disease. *Int J Mol Sci.* 2024; 25 (8): 4503. DOI: 10.3390/ijms25084503.
9. Shutov AM. Hronicheskaja bolezni' pochek. Obshhherossijskaja obshhhestvennaja organizacija «Rossijskoe nauchnoe medicinskoe obshhestvo terapevtov» [Jelektronnyj resurs]. 2022 [data dostupa: 2025 janvar' 26]. Dostupno po ssylke: [https://www.rnmot.ru/public/uploads/RNMOT/clinical/2022/Shutov\\_MR%20HBP%20dlja%20terapevtov.pdf](https://www.rnmot.ru/public/uploads/RNMOT/clinical/2022/Shutov_MR%20HBP%20dlja%20terapevtov.pdf). Russian.
10. Tsuchida-Nishiwaki M, Uchida HA, Takeuchi H, Nishiwaki N, Maeshima Y, Saito C, et al. Association of blood pressure and renal outcome in patients with chronic kidney disease; a post hoc analysis of FROM-J study. *Sci Rep.* 2021; 11 (1): 14990. DOI: 10.1038/s41598-021-94467-z.
11. Varkevisser RDM, Mul D, Aanstoet HJ, Wolffenbuttel BHR, van der Klauw MM. Differences in lipid and blood pressure measurements between individuals with type 1 diabetes and the general population: a cross-sectional study. *BMJ Open.* 2023; 13 (10): 073690. DOI: 10.1136/bmjopen-2023-073690.

12. Eckardt KU, Delgado C, Heerspink HJL, Pecoits-Filho R, Ricardo AC., Stengel B, et al. Trends and perspectives for improving quality of chronic kidney disease care: conclusions from a Kidney Disease: Improving Global Outcomes (KDIGO) Controversies Conference. *Kidney Int.* 2023; 104 (5): 888–903 DOI: 10.1016/j.kint.2023.05.013.
13. Siligato R, Gembillo G, Cernaro V, Torre F, Salvo A, Granese R, et al. Maternal and Fetal Outcomes of Pregnancy in Nephrotic Syndrome Due to Primary Glomerulonephritis. *Front Med (Lausanne).* 2020; 7: 563094. DOI: 10.3389/fmed.2020.563094.
14. Vyas DA, Eisenstein LG, Jones DS. Hidden in Plain Sight — Reconsidering the Use of Race Correction in Clinical Algorithms. *N Engl J Med.* 2020; 383 (9): 874–82. DOI: 10.1056/NEJMms2004740.
15. Jha R, Lopez-Trevino S, Kankanamalage HR, Jha JC. Diabetes and Renal Complications: An Overview on Pathophysiology, Biomarkers and Therapeutic Interventions. *Biomedicines.* 2024; 12 (5): 1098. DOI: 10.3390/biomedicines12051098.
16. Saharnyj diabet 1 tipa u vzroslyh: klinicheskie rekomendacii. Rubrikator klinicheskikh rekomendacij. 2022 [data dostupa: 2025 janvar' 26]. Dostupno po ssylke: [https://cr.minzdrav.gov.ru/schema/286\\_2](https://cr.minzdrav.gov.ru/schema/286_2). Russian.
17. Hronicheskaja bolezn' pochek (HBP): klinicheskie rekomendacii. Rubrikator klinicheskikh rekomendacij. 2021 [data dostupa: 2025 janvar' 26]. Dostupno po ssylke: [https://cr.minzdrav.gov.ru/schema/469\\_2](https://cr.minzdrav.gov.ru/schema/469_2). Russian.
18. Wallander M, Axelsson KF, Nilsson AG, Lundh D, Lorentzon M. Type 2 Diabetes and Risk of Hip Fractures and Non-Skeletal Fall Injuries in the Elderly: A Study From the Fractures and Fall Injuries in the Elderly Cohort (FRAILCO). *J Bone Miner Res.* 2017; 32 (3): 449–60. Available from: <https://doi.org/10.1002/jbmr.3002>.
19. Fomina MA, Wallander M, Axelsson KF, Nilsson AG, Lundh D, Lorentzon M. Type 2 Diabetes and Risk of Hip Fractures and Non-Skeletal Fall Injuries in the Elderly: A Study From the Fractures and Fall Injuries in the Elderly Cohort (FRAILCO). *J Bone Miner Res.* 2017; 32 (3): 449–60. DOI: 10.1002/jbmr.3002.
20. Tonnejck L, Muskiet MH, Smits MM, van Bommel EJ, Heerspink HJ, van Raalte DH, Joles JA. Glomerular Hyperfiltration in Diabetes: Mechanisms, Clinical Significance, and Treatment. *J Am Soc Nephrol.* 2017; 28 (4): 1023–39. DOI: 10.1681/ASN.2016060666.
21. Kanbay M, Copur S, Guldan M, Ozbek L, Hatipoglu A, Covic A, Mallamaci F, Zoccali C. Proximal tubule hypertrophy and hyperfunction: a novel pathophysiological feature in disease states. *Clin Kidney J.* 2024; 17 (7): 195. DOI: 10.1093/cjk/sfae195.
22. Jin L, Wang X, Liu Y, Xiang Q, Huang R. High levels of blood glycemic indicators are associated with chronic kidney disease prevalence in non-diabetic adults: Cross-sectional data from the national health and nutrition examination survey 2005–2016. *J Clin Transl Endocrinol.* 2024; 36: 100347. DOI: 10.1016/j.jcte.2024.100347.
23. Kanbay M, Copur S, Bakir CN, Covic A, Ortiz A, Tuttle KR. Glomerular hyperfiltration as a therapeutic target for CKD. *Nephrol Dial Transplant.* 2024; 39 (8): 1228–38. DOI: 10.1093/ndt/gfae027.
24. Jung CY, Yoo TH. Pathophysiologic Mechanisms and Potential Biomarkers in Diabetic Kidney Disease. *Diabetes Metab J.* 2022; 46 (2): 181–97. DOI: 10.4093/dmj.2021.0329.
25. Hassan HA, Ahmed HS, Hassan DF. Free radicals and oxidative stress: Mechanisms and therapeutic targets: Review article. *Hum Antibodies.* 2024; 3. DOI: 10.3233/HAB-240011.
26. Wang N, Zhang C. Oxidative Stress: A Culprit in the Progression of Diabetic Kidney Disease. *Antioxidants (Basel).* 2024; 13 (4): 455. DOI: 10.3390/antiox13040455.
27. Król-Kulikowska M, Banasik M, Kepinska M. The Effect of Selected Nitric Oxide Synthase Polymorphisms on the Risk of Developing Diabetic Nephropathy. *Antioxidants (Basel).* 2024; 13(7): 838. DOI:10.3390/antiox13070838.
28. Wang H, Ba Y, Xing Q, Du JL. Diabetes mellitus and the risk of fractures at specific sites: a meta-analysis. *BMJ Open.* 2019; 9 (1): 024067. DOI: 10.1136/bmjopen-2018-024067.
29. Zhao DM, Zhong R, Wang XT, Yan ZH. Mitochondrial dysfunction in diabetic nephropathy: insights and therapeutic avenues from traditional Chinese medicine. *Front Endocrinol (Lausanne).* 2024; 15: 1429420. DOI: 10.3389/fendo.2024.1429420.
30. Mazziari A, Porcellati F, Timio F, Reboli G. Molecular Targets of Novel Therapeutics for Diabetic Kidney Disease: A New Era of Nephroprotection. *Int J Mol Sci.* 2024; 25 (7): 3969. DOI: 10.3390/ijms25073969.
31. Lin W, Shen P, Song Y, Huang Y, Tu S. Reactive Oxygen Species in Autoimmune Cells: Function, Differentiation, and Metabolism. *Front Immunol.* 2021; 12: 635021. Available from: <https://doi.org/10.3389/fimmu.2021.635021>.
32. Vodošek Hojs N, Bevc S, Ekart R, Hojs R. Oxidative Stress Markers in Chronic Kidney Disease with Emphasis on Diabetic Nephropathy. *Antioxidants (Basel).* 2020; 9 (10): 925. Available from: <https://doi.org/10.3390/antiox9100925>.
33. Zhang P, Li T, Wu X, Nice EC, Huang C, Zhang Y. Oxidative stress and diabetes: antioxidative strategies. *Front Med.* 2020; 14 (5): 583–600. DOI: 10.1007/s11684-019-0729-1.
34. Daenen K, Andries A, Mekahli D, et al. Okislitel'nyj stress pri hronicheskoy boleznii pochek. *Pediatr Nephrol.* 2019; 34: 975–91. Available from: <https://doi.org/10.1007/s00467-018-4005-4>.
35. Smith A, et al. Molecular mechanisms of oxidative stress in pathologies. *Journal of Molecular Biology.* 2022; 20 (3).
36. Johnson B, et al. Therapeutic approaches targeting antioxidant imbalance. *Medical Research Reviews.* 2023; 25 (1).
37. Cejlikman V.E. O vlijanii okislitel'nogo stressa na organizm cheloveka. *Mezhdunarodnyj nauchnyj zhurnal.* 2022; 3 (117). Dostupno po ssylke: <https://research-journal.org/archive/3-117-2022-march/vliyanie-okislitel'nogo-stressa-na-organizm-cheloveka> (data obrashhenija: 16.02.2025). DOI: 10.23670/IRJ.2022.117.3.037.
38. Lju Dzh, Chen S, Bisvas S, Nagrani N, Chu Ju, Chakrabarti S, i dr. Okislitel'nyj stress, vyzvannyj gljukozoj, i uskorennoe starenie jendotelial'nyh kletok oposredovany istoshheniem mitohondrial'nyh SIRTs. *Physiol. Rep.* 2020; 8: e14331. DOI: 10.14814/phy2.143312020.
39. Wang C, et al. Reactive oxygen species and their role in cellular signaling. *Nature Reviews Molecular Cell Biology.* 2021; 18 (5).
40. Walle M, Whittier DE, Frost M, Müller R, Collins CJ. Meta-analysis of Diabetes Mellitus-Associated Differences in Bone Structure Assessed by High-Resolution Peripheral Quantitative Computed Tomography. *Curr Osteoporos Rep.* 2022; 20 (6): 398–409. DOI: 10.1007/s11914-022-00755-6.
41. Darenskaya M, Kolesnikov S, Semenova N, Kolesnikova L. Diabetic Nephropathy: Significance of Determining Oxidative Stress and Opportunities for Antioxidant Therapies. *Int J Mol Sci.* 2023; 24 (15): 12378. DOI: 10.3390/ijms241512378.

## Литература

1. Сахарный диабет 2 типа у взрослых: клинические рекомендации. Рубрикатор клинических рекомендаций. 2022 [дата доступа: 2025 январь 26]. Доступна по ссылке: [https://cr.minzdrav.gov.ru/schema/290\\_2](https://cr.minzdrav.gov.ru/schema/290_2).
2. Дедов И. И., Шестакова М. В., Викулова О. К., Железнякова А. В., Исаков М. А., Сазонова Д. В., и др. Сахарный диабет в Российской Федерации: динамика эпидемиологических показателей по данным Федерального регистра сахарного диабета за период 2010–2022 гг. *Сахарный диабет.* 2023; 26 (2): 104–23. DOI:10.14341/DM13035.
3. Radia M.M.K. From pre-diabetes to diabetes: Diagnosis, treatments and translational research. *Medicina (Kaunas).* 2019; 55 (9): 546. DOI:10.3390/medicina55090546.
4. Kidney Disease: Improving Global Outcomes (KDIGO) Diabetes Work Group. KDIGO 2022 Clinical Practice Guideline for Diabetes Management in Chronic Kidney Disease. *Kidney Int.* 2022; 102 (5S): S1–S127. DOI: 10.1016/j.kint.2022.06.008.
5. Викулова О. К., Елфимова А. Р., Железнякова А. В., Исаков М. А., Шамхалова М. Ш., Шестакова М. В., и др. Калькулятор риска развития хронической болезни почек: новые возможности прогнозирования патологии у пациентов с сахарным диабетом. *Consilium Medicum.* 2022; 24 (4): 224–33. DOI: 10.26442/20751753.2022.4.201684.
6. Дедов И. И., Шестакова М. В., Викулова О. К., Железнякова А. В.,



- Исаков М. А. Эпидемиологические характеристики сахарного диабета в Российской Федерации: клиничко-статистический анализ по данным регистра сахарного диабета на 01.01.2021. Сахарный диабет. 2021; 24 (3): 204–2. DOI: 10.14341/DM12759.
7. Perkins BA, Bebu I, de Boer IH, Molitch M, Tamborlane W, Lorenzi G, et al. Risk Factors for Kidney Disease in Type 1 Diabetes. *Diabetes Care*. 2019; 42 (5): 883–90. Available from: <https://doi.org/10.2337/dc18-2062>.
  8. Patidar K, Deng JH, Mitchell CS, Ford Versypt AN. Cross-Domain Text Mining of Pathophysiological Processes Associated with Diabetic Kidney Disease. *Int J Mol Sci*. 2024; 25 (8): 4503. DOI: 10.3390/ijms25084503.
  9. Шутов А. М. Хроническая болезнь почек. Общероссийская общественная организация «Российское научное медицинское общество терапевтов» [Электронный ресурс]. 2022 [дата доступа: 2025 январь 26]. Доступно по ссылке: [https://www.rnmot.ru/public/uploads/RNMOT/clinical/2022/Шутов\\_МР%20ХБП%20для%20терапевтов.pdf](https://www.rnmot.ru/public/uploads/RNMOT/clinical/2022/Шутов_МР%20ХБП%20для%20терапевтов.pdf).
  10. Tsuchida-Nishiwaki M, Uchida HA, Takeuchi H, Nishiwaki N, Maeshima Y, Saito C, et al. Association of blood pressure and renal outcome in patients with chronic kidney disease; a post hoc analysis of FROM-J study. *Sci Rep*. 2021; 11 (1): 14990. DOI: 10.1038/s41598-021-94467-z.
  11. Varkevisser RDM, Mul D, Aanstoot HJ, Wolffenbuttel BHR, van der Klauw MM. Differences in lipid and blood pressure measurements between individuals with type 1 diabetes and the general population: a cross-sectional study. *BMJ Open*. 2023; 13 (10): 073690. DOI: 10.1136/bmjopen-2023-073690.
  12. Eckardt KU, Delgado C, Heerspink HJL, Pecoits-Filho R, Ricardo AC, Stengel B, et al. Trends and perspectives for improving quality of chronic kidney disease care: conclusions from a Kidney Disease: Improving Global Outcomes (KDIGO) Controversies Conference. *Kidney Int*. 2023; 104 (5): 888–903 DOI: 10.1016/j.kint.2023.05.013.
  13. Siligato R, Gembillo G, Cernaro V, Torre F, Salvo A, Granese R, et al. Maternal and Fetal Outcomes of Pregnancy in Nephrotic Syndrome Due to Primary Glomerulonephritis. *Front Med (Lausanne)*. 2020; 7: 563094. DOI: 10.3389/fmed.2020.563094.
  14. Vyas DA, Eisenstein LG, Jones DS. Hidden in Plain Sight — Reconsidering the Use of Race Correction in Clinical Algorithms. *N Engl J Med*. 2020; 383 (9): 874–82. DOI: 10.1056/NEJMms2004740.
  15. Jha R, Lopez-Trevino S, Kankanamalage HR, Jha JC. Diabetes and Renal Complications: An Overview on Pathophysiology, Biomarkers and Therapeutic Interventions. *Biomedicines*. 2024; 12 (5): 1098. DOI: 10.3390/biomedicines12051098.
  16. Сахарный диабет 1 типа у взрослых: клинические рекомендации. Рубрикатор клинических рекомендаций. 2022 [дата доступа: 2025 январь 26]. Доступно по ссылке: [https://cr.minzdrav.gov.ru/schema/286\\_2](https://cr.minzdrav.gov.ru/schema/286_2).
  17. Хроническая болезнь почек (ХБП): клинические рекомендации. Рубрикатор клинических рекомендаций. 2021 [дата доступа: 2025 январь 26]. Доступно по ссылке: [https://cr.minzdrav.gov.ru/schema/469\\_2](https://cr.minzdrav.gov.ru/schema/469_2).
  18. Wallander M, Axelsson KF, Nilsson AG, Lundh D, Lorentzon M. Type 2 Diabetes and Risk of Hip Fractures and Non-Skeletal Fall Injuries in the Elderly: A Study From the Fractures and Fall Injuries in the Elderly Cohort (FRAILCO). *J Bone Miner Res*. 2017; 32 (3): 449–60. Available from: <https://doi.org/10.1002/jbmr.3002>.
  19. Fomina MA, Wallander M, Axelsson KF, Nilsson AG, Lundh D, Lorentzon M. Type 2 Diabetes and Risk of Hip Fractures and Non-Skeletal Fall Injuries in the Elderly: A Study From the Fractures and Fall Injuries in the Elderly Cohort (FRAILCO). *J Bone Miner Res*. 2017; 32 (3): 449–60. DOI: 10.1002/jbmr.3002.
  20. Tonneijck L, Muskiet MH, Smits MM, van Bommel EJ, Heerspink HJ, van Raalte DH, Joles JA. Glomerular Hyperfiltration in Diabetes: Mechanisms, Clinical Significance, and Treatment. *J Am Soc Nephrol*. 2017; 28 (4): 1023–39. DOI: 10.1681/ASN.2016060666.
  21. Kanbay M, Copur S, Guldani M, Ozbek L, Hatipoglu A, Covic A, Mallamaci F, Zoccali C. Proximal tubule hypertrophy and hyperfunction: a novel pathophysiological feature in disease states. *Clin Kidney J*. 2024; 17 (7): 195. DOI: 10.1093/ckj/sfae195.
  22. Jin L, Wang X, Liu Y, Xiang Q, Huang R. High levels of blood glycemic indicators are associated with chronic kidney disease prevalence in non-diabetic adults: Cross-sectional data from the national health and nutrition examination survey 2005–2016. *J Clin Transl Endocrinol*. 2024; 36: 100347. DOI: 10.1016/j.jcte.2024.100347.
  23. Kanbay M, Copur S, Bakir CN, Covic A, Ortiz A, Tuttle KR. Glomerular hyperfiltration as a therapeutic target for CKD. *Nephrol Dial Transplant*. 2024; 39 (8): 1228–38. DOI: 10.1093/ndt/gfae027.
  24. Jung CY, Yoo TH. Pathophysiological Mechanisms and Potential Biomarkers in Diabetic Kidney Disease. *Diabetes Metab J*. 2022; 46 (2): 181–97. DOI: 10.4093/dmj.2021.0329.
  25. Hassan HA, Ahmed HS, Hassan DF. Free radicals and oxidative stress: Mechanisms and therapeutic targets: Review article. *Hum Antibodies*. 2024; 3. DOI: 10.3233/HAB-240011.
  26. Wang N, Zhang C. Oxidative Stress: A Culprit in the Progression of Diabetic Kidney Disease. *Antioxidants (Basel)*. 2024; 13 (4): 455. DOI: 10.3390/antiox13040455.
  27. Król-Kulikowska M, Banasik M, Kepinska M. The Effect of Selected Nitric Oxide Synthase Polymorphisms on the Risk of Developing Diabetic Nephropathy. *Antioxidants (Basel)*. 2024; 13(7): 838. DOI:10.3390/antiox13070838.
  28. Wang H, Ba Y, Xing Q, Du JL. Diabetes mellitus and the risk of fractures at specific sites: a meta-analysis. *BMJ Open*. 2019; 9 (1): 024067. DOI: 10.1136/bmjopen-2018-024067.
  29. Zhao DM, Zhong R, Wang XT, Yan ZH. Mitochondrial dysfunction in diabetic nephropathy: insights and therapeutic avenues from traditional Chinese medicine. *Front Endocrinol (Lausanne)*. 2024; 15: 1429420. DOI: 10.3389/fendo.2024.1429420.
  30. Mazzieri A, Porcellati F, Timio F, Reboli G. Molecular Targets of Novel Therapeutics for Diabetic Kidney Disease: A New Era of Nephroprotection. *Int J Mol Sci*. 2024; 25 (7): 3969. DOI: 10.3390/ijms25073969.
  31. Lin W, Shen P, Song Y, Huang Y, Tu S. Reactive Oxygen Species in Autoimmune Cells: Function, Differentiation, and Metabolism. *Front Immunol*. 2021; 12: 635021. Available from: <https://doi.org/10.3389/fimmu.2021.635021>.
  32. Vodošek Hojs N, Bevc S, Ekart R, Hojs R. Oxidative Stress Markers in Chronic Kidney Disease with Emphasis on Diabetic Nephropathy. *Antioxidants (Basel)*. 2020; 9 (10): 925. Available from: <https://doi.org/10.3390/antiox9100925>.
  33. Zhang P, Li T, Wu X, Nice EC, Huang C, Zhang Y. Oxidative stress and diabetes: antioxidative strategies. *Front Med*. 2020; 14 (5): 583–600. DOI: 10.1007/s11684-019-0729-1.
  34. Daenen K, Andries A, Mekahli D, et al. Окислительный стресс при хронической болезни почек. *Pediatr Nephrol*. 2019; 34: 975–91. Available from: <https://doi.org/10.1007/s00467-018-4005-4>.
  35. Smith A, et al. Molecular mechanisms of oxidative stress in pathologies. *Journal of Molecular Biology*. 2022; 20 (3).
  36. Johnson B, et al. Therapeutic approaches targeting antioxidant imbalance. *Medical Research Reviews*. 2023; 25 (1).
  37. Цейликман В. Е. О влиянии окислительного стресса на организм человека. *Международный научный журнал*. 2022; 3 (117). Доступно по ссылке: <https://research-journal.org/archive/3-117-2022-march/vliyanie-okislitel'nogo-stressa-na-organizm-cheloveka> (дата обращения: 16.02.2025). DOI: 10.23670/IRJ.2022.117.3.037.
  38. Лю Дж., Чен С., Бисвас С., Награни Н., Чу Ю., Чакрабартти С., и др. Окислительный стресс, вызванный глюкозой, и ускоренное старение эндотелиальных клеток опосредованы истощением митохондриальных SIRT6. *Physiol Rep*. 2020; 8: e14331. DOI: 10.14814/phy2.143312020.
  39. Wang C, et al. Reactive oxygen species and their role in cellular signaling. *Nature Reviews Molecular Cell Biology*. 2021; 18 (5).
  40. Walle M, Whittier DE, Frost M, Müller R, Collins CJ. Meta-analysis of Diabetes Mellitus-Associated Differences in Bone Structure Assessed by High-Resolution Peripheral Quantitative Computed Tomography. *Curr Osteoporos Rep*. 2022; 20 (6): 398–409. DOI: 10.1007/s11914-022-00755-6.
  41. Darenskaya M, Kolesnikov S, Semenova N, Kolesnikova L. Diabetic Nephropathy: Significance of Determining Oxidative Stress and Opportunities for Antioxidant Therapies. *Int J Mol Sci*. 2023; 24 (15): 12378. DOI: 10.3390/ijms241512378.

## FEATURE OF BIOELECTRICAL IMPEDANCE ANALYSIS AND ELECTROMYOGRAPHY DATA IN CHILDREN WITH CEREBRAL PALSY

Vlasenko SV, Lyovin GV<sup>✉</sup>, Osmanov EA

Scientific Research Institute of Children's Balneology, Physiotherapy and Medical Rehabilitation, Yevpatoria, Russia

Assessment of muscle functional state in children with cerebral palsy (CP) is an important aspect of developing personalized rehabilitation programs. The combined use of bioelectrical impedance analysis (BIA) and electromyography (EMG) makes it possible to optimize the diagnosis methods and improve therapy efficacy. The study aimed to compare groups of patients with CP ( $n = 91$ ) and healthy children ( $n = 94$ ) using BIA and EM. Based on the BIA data the patient were divided into four categories: A — increased body fat percentage (BFP), reduced skeletal muscle mass (SMM); B — decreased BFP, increased SMM; C — increase in both indicators; D — decrease in both indicators. The analysis considered gender and average age of each group. Patients with CP (M: BFP  $p = 0.0001$ , SMM  $p = 0.0015$ ; F: BFP  $p = 0.0003$ , SMM  $p = 0.0009$ ), regardless of gender, showed similar distribution: the majority belonged to categories C (M — 50%; F — 46.9%) and D (M — 32.5%; F — 28.1%). The group of healthy people (M: BFP  $p = 0.0005$ , SMM  $p = 0.0004$ ; F:  $p = 0.0013$ ,  $p = 0.0008$ ) showed the opposite trend: the majority of patients belonged to categories A (34%) and B (34%). In the group of females, the majority of patients belonged to group B (40.4%), group C ranked second based on the number of patients (27.6%), which was considerably lower, than in the group of children with CP. The phase angle values were also traced: there were significant differences ( $p < 0.05$ ) with superiority of categories A and B, regardless of the group and gender. The EMG data also showed superiority of categories A and B when considering turn amplitudes. A conclusion was drawn about the skeletal muscular function differences in the specified categories of patients.

**Keywords:** children, ICP, muscle activity, bioimpedance, rehabilitation, electromyography

**Author contribution:** Vlasenko SV — study concept, developing methods, experimental data analysis and systematization, interpretation of the results; Lyovin GV — data acquisition, systematization, and accumulation, statistical processing, manuscript writing and formatting; Osmanov EA — comparative analysis of data, synthesis of the results, drawing conclusions, manuscript editing, dealing with graphics.

**Compliance with ethical standards:** the study was approved by the Ethics Committee of the scientific Research Institute of Children's Balneology, Physiotherapy and Medical Rehabilitation (protocol No. 21 dated 14 December 2022). All the patients submitted the informed consent to participation in the study.

✉ **Correspondence should be addressed:** Gleb V. Lyovin  
Mayakovsky, 6, Yevpatoria, 297412, Russia; levingv2002@gmail.com

**Received:** 19.12.2024 **Accepted:** 18.02.2025 **Published online:** 27.02.2025

**DOI:** 10.24075/brsmu.2025.012

**Copyright:** © 2025 by the authors. **Licensee:** Pirogov University. This article is an open access article distributed under the terms and conditions of the Creative Commons Attribution (CC BY) license (<https://creativecommons.org/licenses/by/4.0/>).

## ОСОБЕННОСТИ ДАННЫХ БИОИМПЕДАНСОМЕТРИИ И ЭЛЕКТРОМИОГРАФИИ У ДЕТЕЙ С ДЕТСКИМ ЦЕРЕБРАЛЬНЫМ ПАРАЛИЧОМ

С. В. Власенко, Г. В. Лёвин<sup>✉</sup>, Э. А. Османов

Научно-исследовательский институт детской курортологии, физиотерапии и медицинской реабилитации, Евпатория, Россия

Оценка функционального состояния мышц у детей с детским церебральным параличом (ДЦП) является важным аспектом для разработки персонализированных реабилитационных программ. Совместное использование биоимпедансометрии (БИМ) и электромиографии (ЭМГ) позволяет оптимизировать методы диагностики и повысить эффективность терапии. Целью работы было провести сравнение группы пациентов с ДЦП ( $n = 91$ ) и здоровых детей ( $n = 94$ ) с помощью БИМ и ЭМГ. Согласно данным БИМ, пациенты были разделены по четырем категориям: А — увеличение доли жировой массы (ДЖМ), уменьшение скелетно-мышечной массы (СММ); В — уменьшение ДЖМ, увеличение СММ; С — увеличение обоих показателей; D — уменьшение обоих показателей. При анализе учитывали половой признак и средний возраст для каждой из групп. Пациенты с ДЦП (M: ДЖМ  $p = 0.0001$ , СММ  $p = 0.0015$ ; Ж: ДЖМ  $p = 0.0003$ , СММ  $p = 0.0009$ ) независимо от пола продемонстрировали схожее распределение — большая часть заняла категории С (M — 50%; Ж — 46,9%) и D (M — 32,5%; Ж — 28,1%). Группа здоровых детей (M: ДЖМ  $p = 0.0005$ , СММ  $p = 0.0004$ ; Ж:  $p = 0.0013$ ,  $p = 0.0008$ ) показала диаметрально противоположную тенденцию — количественное преимущество пациентов мужского пола оказалось у категорий А (34%) и В (34%). В группе женского пола большая часть пациентов оказалась в В (40,4%), на втором месте по количеству пациентов — в С (27,6%), что гораздо ниже, чем в группе детей с ДЦП. Отслеживали также значения фазового угла — достоверная разница ( $p < 0,05$ ) с преимуществом в категориях А и В, независимо от группы и пола. Данные электромиографии также обозначили преимущество категорий А и В при рассмотрении амплитуды турнов. Сделан вывод о наличии функциональных различий скелетной мускулатуры у обозначенных категорий пациентов.

**Ключевые слова:** дети, ДЦП, мышечная деятельность, биоимпедансометрия, реабилитация, электромиография

**Вклад авторов:** С. В. Власенко — концепция исследования, разработка методологии, анализ и систематизация экспериментальных данных, интерпретация результатов; Г. В. Лёвин — сбор, систематизация и аккумулирование данных, статистическая обработка, написание и оформление рукописи; Э. А. Османов — сравнительный анализ данных, обобщение результатов, формулировка выводов, редактирование рукописи, работа с графическим материалом.

**Соблюдение этических стандартов:** исследование одобрено этическим комитетом ГБУЗ РК «НИИ ДКФ и МР» (протокол № 21 от 14 декабря 2022 г.). Все пациенты подписали добровольное информированное согласие на участие.

✉ **Для корреспонденции:** Gleb Валерьевич Лёвин  
ул. Маяковского, д. 6, г. Евпатория, 297412, Россия; levingv2002@gmail.com

**Статья получена:** 19.12.2024 **Статья принята к печати:** 18.02.2025 **Опубликована онлайн:** 27.02.2025

**DOI:** 10.24075/vrgmu.2025.012

**Авторские права:** © 2025 принадлежат авторам. **Лицензиат:** РНИМУ им. Н. И. Пирогова. Статья размещена в открытом доступе и распространяется на условиях лицензии Creative Commons Attribution (CC BY) (<https://creativecommons.org/licenses/by/4.0/>).

Cerebral palsy (CP) is one of the leading causes of childhood disability. According to the epidemiological research data, its prevalence is 1.5–4 cases per 1000 newborns [1–2]. CP is characterized by persistent motor impairment caused by non-progressive central nervous system lesions occurring in perinatal period. Such impairment considerably limits daily activity and reduces the patients' quality of life, which emphasizes the need to develop effective approaches to diagnosis and rehabilitation [3–4].

Metabolic disorders associated with alteration of body composition represent one of the key problems of patients with CP. Such children often show loss of muscle weight against the background of increasing adipose tissue, which negatively affects overall metabolic status and hampers rehabilitation [5–6]. In this regard, developing the methods allowing one to accurately estimate body composition and identify early signs of metabolic disorder is relevant.

In recent years, bioelectrical impedance analysis (BIA) is widely used to assess body composition. This noninvasive method enables quantification of the body fat and muscle mass percentage, along with the hydration level, which is especially important for patients with CP [7–9]. The advantage of BIA is its high accuracy, together with the possibility of multiple use posing no risk for the patient, which enables the dynamic monitoring of changes in body composition during rehabilitation [10–11]. Introduction of BIA into clinical practice contributes to early identification of the groups at risk and the development of personalized approaches to treatment [12–13].

However, the existing methods to assess metabolic status in children with CP often do not consider specifics of their condition [14–16]. Introduction of BIA represents an innovative approach capable of increasing the diagnosis accuracy and contributing to the development of targeted rehabilitation strategies.

Thus, the relevance of the issue of CP, the importance of BIA for the diagnosis of metabolic disorders and the innovative approach to detection of such disorders emphasize the need for further research in this field.

The study aimed to assess the capabilities of BIA in terms of detecting metabolic disorders in children with CP. The hypothesis is that the use of BIA will make it possible to not only quantify changes in body composition, but also reveal the features of metabolic processes, which can contribute to optimization of treatment and rehabilitation measures.

## METHODS

A total of 94 patients with CP were included in the study (with spastic monoparesis, spastic diplegia, spastic tetraparesis, and other CP types). The control group was represented by healthy children ( $n = 94$ ).

Inclusion criteria: age 6–16 years, average age 10.6 ( $\pm 1.19$ ); no cognitive disorder. All the participants diagnosed with CP were assigned levels I–III according to the Gross Motor Function Classification System (GMFCS), which indicated mild-to-moderate motor disorders and the ability to stand and move without assistance.

Exclusion criteria: patient's refusal of participation in the study; concomitant central nervous system disorder; general contraindications for rehabilitation procedures; GMFCS level IV indicating severe motor disorder and inability to stand or walk without assistance.

Patients were divided into two groups: 1) children with CP; 2) healthy children. The children's gender was taken into account when dividing.

All participants were assessed by multifrequency bioimpedance analysis (BIA) involving the use of tetrapolar electrodes, and flexor and extensor muscles of the forearm were examined by interference electromyography (iEM) using the Neuro-MVP hardware and software complex (Neurosoft, Ivanovo, Russia). The method represents a popular tool to assess functional state of muscles, which allows one to use the method in rehabilitation medicine for more personalized approach to prescription of procedures and assessment of the quality of ongoing treatment [17–18]. BIA is a noninvasive body composition assessment method based on measuring tissue electrical resistance [19–20]. The method becomes more and more topical for medical rehabilitation, especially for children with CP, since it allows one to obtain information on the distribution of fat and muscle mass, as well as on the overall health status [21–22]. The relevance of the method is emphasized by the fact that it is used as an auxiliary tool for planning rehabilitation programs considering the patient's nutritional status, assessing the effectiveness of the procedures prescribed based on BIA indicators, adjusting covert nutritional problems [23–24]. All the above finally enables maximum personalization of rehabilitation approaches, thereby improving the patient's quality of life and outcome. In this study, electromyography was used to objectify the BIA data: it is possible to indirectly judge about the BIA data interpretation correctness by tracing changes in the skeletal muscle functional activity.

Based on the BIA results the patients were assigned to the following subgroups, and membership was preserved based on the fact of diagnosis.

- 1.A – Increased BFP and decreased SMM ( $\downarrow$ )
- 1.B – Decreased BFP and increased SMM ( $\downarrow$ )
- 1.C – Increased BFP and SMM ( $\uparrow$ )
- 1.D – Decreased BFP and SMM ( $\downarrow$ )

Appropriate features were considered in healthy children, among whom there were groups 2.A., 2.B., 2.C., 2.D. with the above specifics.

The decrease and increase in BIA indicators were determined based on median values for the groups: median for group 1 (M) BFP — 10.36; SMM — 14.27; for group 1 (F) BFP — 7.58; SMM — 15.98; group 2 (M) BFP — 20.17; SMM — 22.98; group 2 (F) BFP — 26.95; SMM — 16.59. The phase angle values of each group served as a criterion for estimation of the muscle tissue functional viability [25–27]. BMI was estimated in each group. The resulting percentile values were reconciled with the WHO standard error grids for appropriate age and gender categories [28–30]. BMI deviation was considered significant with z-score  $> 1.1$  and z-score  $< -1.1$ .

Statistical processing was conducted using the STATISTICA 10.0 software package (StatSoft Inc., USA).

Quantitative indicators — mean, standard deviation.

Distribution testing — Shapiro–Wilk test, Levene's test for assessment of dispersion homogeneity.

Significance was assessed using factorial analysis of variance, F-distribution estimate; Bonferroni adjustment was used for pairwise comparison.

## RESULTS

The analysis of BIA data of male patients with CP (age differences in the comparison group,  $p < 0.0001$ ) (Table 1) revealed predominance of the groups showing both increase and decrease in the studied parameters (A — 8.1%; B — 9.40%; C — 50%; D — 32.5%) (Fig. 2), and the phase angle values ( $\mu = 7.215$ ) of groups A (+0.51; +7%) and B (+1.095; 15.17%) were higher than that of groups C (–1.06; –14.62%)

**Table 1.** Bioimpedance measurements for male patients with cerebral palsy

Indicator	CP				
	M (n = 62)				
	↑↓ (n = 5) Average age — 9	↓↑ (n = 6) Average age — 11.6	↓↓ (n = 31) Average age — 8.4	↑↑ (n = 20) Average age — 11.8	p-value
BFP	17.51 (±1.58)	9.55 (±0.77)	4.6 (±1.83)	17.79 (±2.85)	0.0001
SMM	11.87 (±0.37)	15.94 (±0.99)	8.37 (±2.31)	22.92 (±4.94)	0.0015
PA	7.72 (±0.05)	8.31 (±0.12)	6.16 (±0.09)	6.67 (±0.11)	0.012
BMI	22	17.95	15.73	23.8	
Z-score (BMI)	0.86	-0.29	-0.93	1.38	

**Note:** CP — cerebral palsy; BMI — body mass index; BFP — body fat percentage; SMM — skeletal muscle mass; PA — phase angle.

and D (-0.55; -7.55%), which could indicate skeletal muscle failure and body's overall untrained state in the latter groups, regardless of higher SMM ( $\mu = 14.76$ ) in group D (+8.145; +55.23%).

Significant BMI deviation based on z-score was reported for the category of patients with both BFP and SMM increase; other groups remain commonly distributed, which reflects low analytic function of BMI when used to assess the patients' nutritional status.

In the group of females (age differences in the comparison groups,  $p < 0.001$ ) (Table 2), a general trend towards distribution of the majority of patients across groups C and D (A — 18.75%; B — 6.25%; C — 46.9%; D — 28.1%) can be traced and determined in patients with CP, with predominance of better phase angle estimates ( $\mu = 7.89$ ) in groups A (+0.5; +6.1%) and B (+1.14; 14.5%). BMI assessment also showed a trend towards significant deviation in group D, while other groups were within the ranges corresponding to reference percentile values.

BIA indicators of the group of male patients without CP (differences in the groups,  $p < 0.001$ ) (Table 3) make it possible to reveal an opposite distribution pattern: the number of patients in groups A and B predominates (A — 34%; B — 34%; C — 19.2%; D — 12.8%), which represents indirect evidence of the relationship between better tissue quality and non-homogeneous distribution, since such feature is specific for healthy children. Furthermore, better phase angle measurement results ( $\mu = 6.215$ ) also persist in groups A (+0.47; +7.48%) and B (+0.71; +11.34%). BMI assessment does not allow one to speak about significant differences between groups, since all the values remain within the reference percentiles.

Assessment of BIA parameters in the group of healthy female patients (differences in the comparison groups,  $p < 0.001$ ) (Table 4) demonstrates a modest advantage of groups B and C

(A — 19.2%; B — 40.4%; C — 27.6%; D — 12.8%) with persistent trend towards better phase angle values ( $\mu = 6.57$ ) in the first two groups (A = +0.25; +3.8%; B = +0.52; +7.91%) and, according to percentile tables, towards significant BMI deviation in group D only.

The interference electromyography (iEM) method allows us to note that the turn amplitude (Atur) is symmetrically larger in groups A and B of both genders (Table 5). This makes it possible to directly judge about the functional characteristics of the upper limb muscles and indirectly judge about the state of other muscle groups. Despite higher muscle mass values in group D, the Atur values here are lower, than in the first two groups. This can be indicative of the fact that the muscle mass increase is not always correlated to functional activity of muscles, which emphasizes the importance of comprehensive approach to assessment of the skeletal muscle state. Moreover, the SMM quantity is similar in groups A and C, and the skeletal muscle activity is higher in the group with mixed alterations. This can indicate differences in neuromuscular function and adaptation between these two groups.

Taking into account the iEM and BIA data obtained, it can be concluded that there are some functional differences in the skeletal muscle tissue in groups A and B.

## DISCUSSION

The study has revealed significant differences in body composition and the skeletal muscle functional state between patients with CP and healthy children. The findings are consisted with the data of other studies, in which specific body composition alterations were also reported for children with CP, such as decreased muscle mass and increased body fat percentage [8, 10, 12]. However, our results complement the existing knowledge showing that these alterations are heterogeneous.

**Table 2.** Bioimpedance measurements for female patients with cerebral palsy

Indicator	CP				
	F (n = 32)				
	↑↓ (n = 6) 1 Average age — 11	↓↑ (n = 2) 12 Average age — 12	↓↓ (n = 15) 8 Average age — 8.4	↑↑ (n = 9) Average age — 11.55	p-value
BFP	11.51 (±1.47)	3.4 (±0.77)	4.52 (±1.47)	13.03 (±2.47)	0.0003
SMM	13.52 (±0.44)	24.8 (±3.05)	8.89 (±2.71)	19.76 (±3.56)	0.0009
PA	8.40 (±0.28)	9.03 (±1.01)	7.36 (±0.98)	6.80 (±0.35)	0.023
BMI	18.15	15.2	15.06	19.27	
Z-score (BMI)	0.63	-0.97	-1.05	1.23	

**Note:** CP — cerebral palsy; BMI — body mass index; BFP — body fat percentage; SMM — skeletal muscle mass; PA — phase angle.



**Table 3.** Bioimpedance measurements for male patients without cerebral palsy

Indicator	Patients without CP				
	M (n = 47)				
	↑↓ (n = 16) Average age — 11.2	↓↑ (n = 16) Average age — 11.4	↓↓ (n = 9) Average age — 10	↑↑ (n = 6) Average age — 9.4	p-value
BFP	27.04 (±2.44)	15.69 (±1.39)	16.14 (±1.29)	22.13 (±0.90)	0.0005
SMM	17.61 (±1.81)	28.38 (±2.18)	19.25 (±2.07)	26.05 (±0.57)	0.0004
PA	6.68 (±0.64)	6.92 (±0.47)	5.45 (±0.83)	5.81 (±0.21)	0.021
BMI	18.46	19.54	17.27	18.1	
Z-score (BMI)	-0.05	0.75	-0.94	-0.32	

**Note:** CP — cerebral palsy; BMI — body mass index; BFP — body fat percentage; SMM — skeletal muscle mass; PA — phase angle.

Phase angle reduction reported for groups C and D of males with CP is correlated to the iEM data showing low Atur in these groups, despite the increased SMM. This confirms the hypothesis about the structural and functional dissociation of muscles in CP reported in the studies [11]. In girls with CP, the phase angle values were higher, which could be due to hormonal features and adaptive capacity of metabolism.

In healthy children, the distribution across groups (A — 34%, B — 34% in males; B — 40.4% in females) and high Atur values confirm the relationship between multidirectional BFP/SMM alterations and better quality of muscles. This is in line with the concept of physiological heterogeneity of normal body composition [26, 29].

In female patients with CP, a similar trend towards distribution across groups C and D was observed, which confirmed the common nature of metabolic disorders in children with CP, regardless of their gender. However, girls had higher phase angle values, than boys, which could be due to

differences in the endocrine profile and the features of fat and muscle mass distribution.

The differences in body composition and functional state of muscles found in patients with CP can be explained by several mechanisms. First, limited physical activity and decreased motor functions in children with CP lead to muscle mass reduction and increased body fat percentage [14]. Second, neuromuscular disorders typical for CP can cause reduction of muscle functional activity, even when muscle mass is preserved or increased, which is confirmed by the iEM data [24]. Third, the differences in endocrine profile and metabolic processes between boys and girls can affect fat and muscle mass distribution, as well as functional characteristics of muscles [12].

**Study limitations.** The lack of data on the participants' hormonal status is a limitation of the study. To refine the results obtained it is necessary to conduct further research involving a larger number of participants and considering additional factors, such as physical activity level, hormonal status, and nutritional specifics.

**Table 4.** Bioimpedance measurements for female patients without cerebral palsy

Indicator	Patients without CP				
	F (n = 47)				
	↑↓ (n = 9) Average age — 10.6	↓↑ (n = 19) Average age — 10.8	↓↓ (n = 13) Average age — 11.5	↑↑ (n = 6) Average age — 10.2	p-value
BFP	37.05 (±4.61)	23.01 (±1.31)	16.76 (±4.56)	32.17 (±3.17)	0.0013
SMM	13.30 (±0.30)	18.39 (±0.59)	13.87 (±1.29)	18.60 (±0.61)	0.0008
PA	6.82 (±0.20)	7.09 (±0.69)	6.02 (±1.05)	6.36 (±0.88)	0.019
BMI	20.73	18.4	16.1	20.55	
Z-score (BMI)	0.83	-0.38	0.73	-1.57	

**Note:** CP — cerebral palsy; BMI — body mass index; BFP — body fat percentage; SMM — skeletal muscle mass; PA — phase angle.

**Table 5.** Indicators of interference EM of the groups compared

CP (gender)	Groups	Tested muscles (Turns amplitude (mkV))			
		<i>m. flexor carpi ulnaris</i>		<i>m. extensor digitorum</i>	
		Right	Left	Right	Left
		Males	A	223.05 (±12.20)	242.44 (±6.84)
B	270.75 (±22.04)		255.20 (±5.21)	313.74 (±11.27)	301.36 (±13.58)
C	172.59 (±14.50)		166.07 (±11.98)	212.15 (±10.17)	204.33 (±10.03)
D	200.65 (±8.98)		198.84 (±6.39)	221.24 (±6.03)	218.48 (±12.98)
Females	A	180.38 (±14.80)	188.96 (±9.20)	201.98 (±9.10)	203.55 (±6.52)
	B	233.26 (±9.45)	240.02 (±8.32)	247.05 (±9.10)	250.24 (±8.07)
	C	139.65 (±5.23)	142.33 (±6.39)	155.03 (±6.71)	159.90 (±11.63)
	D	128.48 (±7.68)	137.94 (±8.25)	134.35 (±8.99)	148.10 (±10.29)

## CONCLUSIONS

The study has revealed significant differences in the structural and functional muscle tissue characteristics of children with CP. This is confirmed by the BIA data showing that the groups that are heterogeneous based on the muscle and adipose tissue composition predominate in healthy patients, while homogeneous groups predominate in children with CP. The phase angle specifics reported for members of the studied groups suggest qualitative differences in muscle state between groups A/B and C/D, which is confirmed by the lack of positive correlation between the SMM quantity and the maximum

phase angle values. The iEM data reported for groups A and B demonstrate higher amplitude activity. This makes it possible to confirm the importance of body's physiological heterogeneity and disproves the linear "volume – power" relationship. The findings emphasize the need to include the muscle structural and metabolic status estimates in the rehabilitation algorithms for CP in order to improve their effectiveness. The study of molecular mechanisms underlying the reported imbalance between bioelectric parameters (phase angle, iEM) and muscle tissue metabolism is a promising area. This will enable the development of targeted methods to adjust muscle dysfunction associated with CP.

## References

- McIntyre S, Goldsmith S, Webb A, Ehlinger V, Hollung SJ, McConnell, et al. Global CP Prevalence Group. Global prevalence of cerebral palsy: A systematic analysis. *Developmental medicine and child neurology*. 2022; 64 (12): 1494–506. Available from: <https://doi.org/10.1111/dmcn.15346>.
- Novak I, Morgan C, Fahey M, Finch-Edmondson M, Galea C, Hines, et al. State of the Evidence Traffic Lights 2019: Systematic Review of Interventions for Preventing and Treating Children with Cerebral Palsy. *Current neurology and neuroscience reports*. 2020; 20 (2): 3. Available from: <https://doi.org/10.1007/s11910-020-1022-z>.
- Patel DR, Neelakantan M, Pandher K, Merrick J. Cerebral palsy in children: a clinical overview. *Translational pediatrics*. 2020; 9 (Suppl 1): S125–S135. Available from: <https://doi.org/10.21037/tp.2020.01.01>.
- Panda S, Singh A, Kato H, Kokhanov A. Cerebral Palsy: A Current Perspective. *NeoReviews*. 2024; 25 (6): e350–e360. Available from: <https://doi.org/10.1542/neo.25-6-e350>.
- Jesus AO, Stevenson RD. Optimizing Nutrition and Bone Health in Children with Cerebral Palsy. *Physical medicine and rehabilitation clinics of North America*. 2020; 31 (1): 25–37. Available from: <https://doi.org/10.1016/j.pmr.2019.08.001>.
- Metshein M, Tuulik VR, Tuulik V, Kumm M, Min M, Annus P. Electrical Bioimpedance Analysis for Evaluating the Effect of Pelotherapy on the Human Skin: Methodology and Experiments. *Sensors (Basel, Switzerland)*. 2023; 23 (9): 4251. Available from: <https://doi.org/10.3390/s23094251>.
- Arruda RCBF, Tassitano RM, da Silva Brito AL, de Sousa Martins OS, Cabral PC, de Castro Antunes MM. Physical activity, sedentary time and nutritional status in Brazilian children with cerebral palsy. *Jornal de pediatria*. 2022; 98 (3): 303–9. Available from: <https://doi.org/10.1016/j.jpmed.2021.07.005>.
- Costa A, Martin A, Arreola V, Riera SA, Pizarro A, Carol, et al. Assessment of Swallowing Disorders, Nutritional and Hydration Status, and Oral Hygiene in Students with Severe Neurological Disabilities Including Cerebral Palsy. *Nutrients*. 2021; 13 (7): 2413. Available from: <https://doi.org/10.3390/nu13072413>.
- Savikangas T, Valadão P, Haapala EA, Finni T. Effects of multicomponent exercise intervention on cardiometabolic risk factors in children and young adults with cerebral palsy: a multiple-baseline trial. *BMC sports science, medicine & rehabilitation*. 2024; 16 (1): 219. Available from: <https://doi.org/10.1186/s13102-024-01006-0>.
- Więch P, Ćwirlej-Sozańska A, Wiśniowska-Szurlej A, Kilian J, Lenart-Domka E, Bejer A, et al. The Relationship Between Body Composition and Muscle Tone in Children with Cerebral Palsy: A Case-Control Study. *Nutrients*. 2020; 12 (3): 864. Available from: <https://doi.org/10.3390/nu12030864>.
- Talma H, Chinapaw MJ, Bakker B, HiraSing RA, Terwee CB, Altenburg TM. Bioelectrical impedance analysis to estimate body composition in children and adolescents: a systematic review and evidence appraisal of validity, responsiveness, reliability and measurement error. *Obesity reviews: an official journal of the International Association for the Study of Obesity*. 2013; 14 (11): 895–905. Available from: <https://doi.org/10.1111/obr.12061>.
- Snik DAC, de Roos NM. Criterion validity of assessment methods to estimate body composition in children with cerebral palsy: A systematic review. *Annals of physical and rehabilitation medicine*. 2021; 64 (3): 101271. Available from: <https://doi.org/10.1016/j.rehab.2019.05.003>.
- Jiang F, Tang S, Eom JJ, Song KH, Kim H, Chung S, et al. Accuracy of Estimated Bioimpedance Parameters with Octapolar Segmental Bioimpedance Analysis. *Sensors (Basel, Switzerland)*. 2022; 22 (7): 2681. Available from: <https://doi.org/10.3390/s22072681>.
- Szkoda L, Szopa A, Kwiecień-Czerwień I, Siwiec A, Domagalska-Szopa M. Body Composition in Outpatient Children with Cerebral Palsy: A Case-Control Study. *International journal of general medicine*. 2023; 16: 281–91. Available from: <https://doi.org/10.2147/IJGM.S393484>.
- Jahan I, Sultana R, Muhit M, Akbar D, Karim T, Al Imam MH, et al. Nutrition Interventions for Children with Cerebral Palsy in Low- and Middle-Income Countries: A Scoping Review. *Nutrients*. 2022; 14 (6): 1211. Available from: <https://doi.org/10.3390/nu14061211>.
- Sørensen SJ, Brække G, Kok K, Sørensen JL, Born AP, Mølgaard C, et al. Nutritional screening of children and adolescents with cerebral palsy: a scoping review. *Developmental medicine and child neurology*. 2021; 63 (12): 1374–81. Available from: <https://doi.org/10.1111/dmcn.14981>.
- Friedman JM, van Essen P, van Karnebeek CDM. Cerebral palsy and related neuromotor disorders: Overview of genetic and genomic studies. *Molecular genetics and metabolism*. 2022; 137 (4): 399–419. Available from: <https://doi.org/10.1016/j.ymgme.2021.11.001>.
- Alcan V, Zinnuroğlu M. Current developments in surface electromyography. *Turkish journal of medical sciences*. 2023; 53 (5): 1019–31. Available from: <https://doi.org/10.55730/1300-0144.5667>.
- Murakami Y, Honaga K, Kono H, Haruyama K, Yamaguchi T, Tani M, et al. New Artificial Intelligence-Integrated Electromyography-Driven Robot Hand for Upper Extremity Rehabilitation of Patients With Stroke: A Randomized, Controlled Trial. *Neurorehabilitation and neural repair*. 2023; 37 (5): 298–306. Available from: <https://doi.org/10.1177/15459683231166939>.
- Yamaguchi S, Inami T, Ishida H, Nagata N, Murayama M, Morito A, et al. Bioimpedance analysis for identifying new indicators of exercise-induced muscle damage. *Scientific reports*. 2024; 14 (1): 15299. Available from: <https://doi.org/10.1038/s41598-024-66089-8>.
- Ward LC, Brantlov S. Bioimpedance basics and phase angle fundamentals. *Reviews in endocrine & metabolic disorders*. 2023; 24 (3): 381–91. Available from: <https://doi.org/10.1007/s11154-022-09780-3>.
- Uemura K, Doi T, Tsutsumimoto K, Nakakubo S, Kim MJ, Kurita S, et al. Predictivity of bioimpedance phase angle for incident disability in older adults. *Journal of cachexia, sarcopenia and muscle*. 2020; 11 (1): 46–54. Available from: <https://doi.org/10.1002/jcsm.12492>.
- Mehra A, Starkoff BE, Nickerson BS. The evolution of bioimpedance analysis: From traditional methods to wearable technology. *Nutrition*. 2024; 129: 112601. Available from: <https://doi.org/10.1016/j.nut.2024.112601>.
- Sung WJ, Kim WJ, Hwang Y, Kim JS, Lim SH, Hong BY. Body composition of school-aged children with disabilities. *Pediatrics international: official journal of the Japan Pediatric Society*. 2020; 62 (8): 962–9. Available from: <https://doi.org/10.1111/ped.14248>.

25. Du J, Yu H, Shi P, Fang F. High Precision Portable Bioimpedance Spectrometer for Enhanced Clinical Diagnostics. 2024; 794–9. Available from: <https://doi.org/10.1109/icma61710.2024.10633039>.
26. Akamatsu Y, Kusakabe T, Arai H, Yamamoto Y, Nakao K, Ikeue K, et al. Phase angle from bioelectrical impedance analysis is a useful indicator of muscle quality. *Journal of cachexia, sarcopenia and muscle*. 2022; 13 (1): 180–9. Available from: <https://doi.org/10.1002/jcsm.12860>.
27. DiVincenzo O, Marra M, Di Gregorio A, Pasanisi F, Scalfi L. Bioelectrical impedance analysis (BIA) -derived phase angle in sarcopenia: A systematic review. *Clinical nutrition*. 2021; 40 (5): 3052–61. Available from: <https://doi.org/10.1016/j.clnu.2020.10.048>.
28. Wu H, Ding P, Wu J, Yang P, Tian Y, Zhao Q. Phase angle derived from bioelectrical impedance analysis as a marker for predicting sarcopenia. *Frontiers in nutrition*. 2022; 9: 1060224. Available from: <https://doi.org/10.3389/fnut.2022.1060224>.
29. Jaleel A, Chilumula M, Chukkala Satya SG, Singnale P, Telikicherla UR, Pandurangi R. The Assessment of Nutritional Status of Adolescents Aged 15-18 Years Using BMI Cutoffs and BMI Z Scores: A Secondary Analysis of National Family Health Survey-5 (2019-21) Data. *Cureus*. 2024; 16 (5): e59800. Available from: <https://doi.org/10.7759/cureus.59800>.
30. Calcaterra V, Pelizzo G, Cena H. BMI Is a Poor Predictor of Nutritional Status in Disabled Children. What Is the Most Recommended Method for Body Composition Assessment in This Pediatric Population, *Frontiers in pediatrics*. 2019; 7, 226. Available from: <https://doi.org/10.3389/fped.2019.00226>.

## Литература

1. McIntyre S, Goldsmith S, Webb A, Ehlinger V, Hollung SJ, McConnell, et al. Global CP Prevalence Group. Global prevalence of cerebral palsy: A systematic analysis. *Developmental medicine and child neurology*. 2022; 64 (12): 1494–506. Available from: <https://doi.org/10.1111/dmcn.15346>.
2. Novak I, Morgan C, Fahey M, Finch-Edmondson M, Galea C, Hines, et al. State of the Evidence Traffic Lights 2019: Systematic Review of Interventions for Preventing and Treating Children with Cerebral Palsy. *Current neurology and neuroscience reports*. 2020; 20 (2): 3. Available from: <https://doi.org/10.1007/s11910-020-1022-z>.
3. Patel DR, Neelakantan M, Pandher K, Merrick J. Cerebral palsy in children: a clinical overview. *Translational pediatrics*. 2020; 9 (Suppl 1): S125–S135. Available from: <https://doi.org/10.21037/tp.2020.01.01>.
4. Panda S, Singh A, Kato H, Kokhanov A. Cerebral Palsy: A Current Perspective. *NeoReviews*. 2024; 25 (6): e350–e360. Available from: <https://doi.org/10.1542/neo.25-6-e350>.
5. Jesus AO, Stevenson RD. Optimizing Nutrition and Bone Health in Children with Cerebral Palsy. *Physical medicine and rehabilitation clinics of North America*. 2020; 31 (1): 25–37. Available from: <https://doi.org/10.1016/j.pmr.2019.08.001>.
6. Metshin M, Tuulik VR, Tuulik V, Kumm M, Min M, Annus P. Electrical Bioimpedance Analysis for Evaluating the Effect of Pelotherapy on the Human Skin: Methodology and Experiments. *Sensors (Basel, Switzerland)*. 2023; 23 (9): 4251. Available from: <https://doi.org/10.3390/s23094251>.
7. Arruda RCBF, Tassitano RM, da Silva Brito AL, de Sousa Martins OS, Cabral PC, de Castro Antunes MM. Physical activity, sedentary time and nutritional status in Brazilian children with cerebral palsy. *Jornal de pediatria*. 2022; 98 (3): 303–9. Available from: <https://doi.org/10.1016/j.jpmed.2021.07.005>.
8. Costa A, Martin A, Arreola V, Riera SA, Pizarro A, Carol, et al. Assessment of Swallowing Disorders, Nutritional and Hydration Status, and Oral Hygiene in Students with Severe Neurological Disabilities Including Cerebral Palsy. *Nutrients*. 2021; 13 (7): 2413. Available from: <https://doi.org/10.3390/nu13072413>.
9. Savikangas T, Valadao P, Haapala EA, Finni T. Effects of multicomponent exercise intervention on cardiometabolic risk factors in children and young adults with cerebral palsy: a multiple-baseline trial. *BMC sports science, medicine & rehabilitation*. 2024; 16 (1): 219. Available from: <https://doi.org/10.1186/s13102-024-01006-0>.
10. Więch P, Ćwirlej-Sozańska A, Wiśniowska-Szurlej A, Kilian J, Lenart-Domka E, Bejer A, et al. The Relationship Between Body Composition and Muscle Tone in Children with Cerebral Palsy: A Case-Control Study. *Nutrients*. 2020; 12 (3): 864. Available from: <https://doi.org/10.3390/nu12030864>.
11. Talma H, Chinapaw MJ, Bakker B, HiraSing RA, Terwee CB, Altenburg TM. Bioelectrical impedance analysis to estimate body composition in children and adolescents: a systematic review and evidence appraisal of validity, responsiveness, reliability and measurement error. *Obesity reviews: an official journal of the International Association for the Study of Obesity*. 2013; 14 (11): 895–905. Available from: <https://doi.org/10.1111/obr.12061>.
12. Snik DAC, de Roos NM. Criterion validity of assessment methods to estimate body composition in children with cerebral palsy: A systematic review. *Annals of physical and rehabilitation medicine*. 2021; 64 (3): 101271. Available from: <https://doi.org/10.1016/j.rehab.2019.05.003>.
13. Jiang F, Tang S, Eom JJ, Song KH, Kim H, Chung S, et al. Accuracy of Estimated Bioimpedance Parameters with Octapolar Segmental Bioimpedance Analysis. *Sensors (Basel, Switzerland)*. 2022; 22 (7): 2681. Available from: <https://doi.org/10.3390/s22072681>.
14. Szkoda L, Szopa A, Kwiecień-Czerwieńiec I, Siwiec A, Domagalska-Szopa M. Body Composition in Outpatient Children with Cerebral Palsy: A Case-Control Study. *International journal of general medicine*. 2023; 16: 281–91. Available from: <https://doi.org/10.2147/IJGM.S393484>.
15. Jahan I, Sultana R, Muhi M, Akbar D, Karim T, Al Imam MH, et al. Nutrition Interventions for Children with Cerebral Palsy in Low- and Middle-Income Countries: A Scoping Review. *Nutrients*. 2022; 14 (6): 1211. Available from: <https://doi.org/10.3390/nu14061211>.
16. Sørensen SJ, Brekke G, Kok K, Sørensen JL, Born AP, Mølgaard C, et al. Nutritional screening of children and adolescents with cerebral palsy: a scoping review. *Developmental medicine and child neurology*. 2021; 63 (12): 1374–81. Available from: <https://doi.org/10.1111/dmcn.14981>.
17. Friedman JM, van Essen P, van Karnebeek CDM. Cerebral palsy and related neuromotor disorders: Overview of genetic and genomic studies. *Molecular genetics and metabolism*. 2022; 137 (4): 399–419. Available from: <https://doi.org/10.1016/j.ymgme.2021.11.001>.
18. Alcan V, Zinnuroglu M. Current developments in surface electromyography. *Turkish journal of medical sciences*. 2023; 53 (5): 1019–31. Available from: <https://doi.org/10.55730/1300-0144.5667>.
19. Murakami Y, Honaga K, Kono H, Haruyama K, Yamaguchi T, Tani M, et al. New Artificial Intelligence-Integrated Electromyography-Driven Robot Hand for Upper Extremity Rehabilitation of Patients With Stroke: A Randomized, Controlled Trial. *Neurorehabilitation and neural repair*. 2023; 37 (5): 298–306. Available from: <https://doi.org/10.1177/15459683231166939>.
20. Yamaguchi S, Inami T, Ishida H, Nagata N, Murayama M, Morito A, et al. Bioimpedance analysis for identifying new indicators of exercise-induced muscle damage. *Scientific reports*. 2024; 14 (1): 15299. Available from: <https://doi.org/10.1038/s41598-024-66089-8>.
21. Ward LC, Brantlov S. Bioimpedance basics and phase angle fundamentals. *Reviews in endocrine & metabolic disorders*. 2023; 24 (3): 381–91. Available from: <https://doi.org/10.1007/s11154-022-09780-3>.
22. Uemura K, Doi T, Tsutsumimoto K, Nakakubo S, Kim MJ, Kurita S, et al. Predictivity of bioimpedance phase angle for incident disability in older adults. *Journal of cachexia, sarcopenia and muscle*. 2020; 11 (1): 46–54. Available from: <https://doi.org/10.1002/jcsm.12492>.
23. Mehra A, Starkoff BE, Nickerson BS. The evolution of bioimpedance analysis: From traditional methods to wearable technology. *Nutrition*. 2024; 129: 112601. Available from: <https://doi.org/10.1016/j.nut.2024.112601>.
24. Sung WJ, Kim WJ, Hwang Y, Kim JS, Lim SH, Hong BY. Body composition of school-aged children with disabilities. *Pediatrics international: official journal of the Japan Pediatric Society*. 2020; 62 (8): 962–9. Available from: <https://doi.org/10.1111/ped.14248>.
25. Du J, Yu H, Shi P, Fang F. High Precision Portable Bioimpedance Spectrometer for Enhanced Clinical Diagnostics. 2024; 794–9.

- Available from: <https://doi.org/10.1109/icma61710.2024.10633039>.
26. Akamatsu Y, Kusakabe T, Arai H, Yamamoto Y, Nakao K, Ikeue K, et al. Phase angle from bioelectrical impedance analysis is a useful indicator of muscle quality. *Journal of cachexia, sarcopenia and muscle*. 2022; 13 (1): 180–9. Available from: <https://doi.org/10.1002/jcsm.12860>.
27. Di Vincenzo O, Marra M, Di Gregorio A, Pasanisi F, Scafi L. Bioelectrical impedance analysis (BIA) -derived phase angle in sarcopenia: A systematic review. *Clinical nutrition*. 2021; 40 (5): 3052–61. Available from: <https://doi.org/10.1016/j.clnu.2020.10.048>.
28. Wu H, Ding P, Wu J, Yang P, Tian Y, Zhao Q. Phase angle derived from bioelectrical impedance analysis as a marker for predicting sarcopenia. *Frontiers in nutrition*. 2022; 9: 1060224. Available from: <https://doi.org/10.3389/fnut.2022.1060224>.
29. Jaleel A, Chilumula M, Chukkala Satya SG, Singnale P, Telikicherla UR, Pandurangi R. The Assessment of Nutritional Status of Adolescents Aged 15-18 Years Using BMI Cutoffs and BMI Z Scores: A Secondary Analysis of National Family Health Survey-5 (2019-21) Data. *Cureus*. 2024; 16 (5): e59800. Available from: <https://doi.org/10.7759/cureus.59800>.
30. Calcaterra V, Pelizzo G, Cena H. BMI Is a Poor Predictor of Nutritional Status in Disabled Children. What Is the Most Recommended Method for Body Composition Assessment in This Pediatric Population, *Frontiers in pediatrics*. 2019; 7, 226. Available from: <https://doi.org/10.3389/fped.2019.00226>.



## THE EFFECT OF STERILIZATION METHODS ON THE CYTOTOXICITY OF CERAMIC MEDICAL IMPLANTS

Bilyalov AR <sup>✉</sup>, Piatnitskaia SV, Rafikova GA, Akbashev VN, Bikmeyev AT, Akhatov ISh, Shangina OR, Chugunov SS, Tikhonov AA

Bashkir State Medical University of the Ministry of Health of the Russian Federation, Ufa, Russia

The choice of the sterilization method for ceramic implants is critically important, as it can affect the chemical and physico-mechanical properties of the material and its biocompatibility. Higher cytotoxicity, which is a possible side effect of sterilization, hinders osseointegration. This study aimed to determine the cytotoxicity of porous ceramic samples after sterilization using the most common methods. Samples of hydroxyapatite (HA), tricalcium phosphate (TCP), and aluminum oxide (AO) were prepared by stereolithography, and bone allograft samples were made using the DLP method. The annealing lasted for 4 hours, with a peak temperature of 800 °C and the temperature increment of 3 °C per minute; the sintering temperature was up to 1200 °C. We used the following sterilization methods: autoclaving at 1 atmosphere, 120 °C, for 45 minutes; radiation sterilization, 25 seconds with an absorbed dose of 25 kGy; plasma peroxide sterilization, 42 minutes; dry heat sterilization at 180 °C, for 60 minutes. Cytotoxicity was determined with the help of an MTT assay (24-hour exposure in a CO<sub>2</sub> incubator). The results of the study: for HA, high porosity means growth of values in transition from autoclaving (0.1115) to plasma peroxide sterilization (0.2023). Medium and low porosity show similar results, with peaks in dry-heat sterilization (0.4954 and 0.4505). As for AO, it exhibited high viability when subjected to this method. The TCP samples have shown stable results, but their low-porosity variation had the values growing after autoclaving (0.078 to 0.182, dry-heat sterilization). The study forms the basis for optimizing the ceramic implants manufacturing technology and sterilization methods to ensure their high biocompatibility.

**Keywords:** medical ceramics, 3D printing, additive technologies, sterilization, implants, cell viability, ceramics

**Funding:** the work was supported by the Russian Science Foundation under grant No. 23-15-20042.

**Author contribution:** Bilyalov AR — study conceptualization, data analysis, article editing; Piatnitskaia SV — cytotoxicity evaluation (MTT test), analysis of the results; Rafikova GA — preparation of digital models and sample production, analysis of mechanical and biological properties of materials; Akbashev VN — sterilization experiments, analysis of the effect of sterilization methods on materials; Bikmeyev AT — mathematical modeling of material parameters, interpretation of the data obtained; Akhatov ISh — coordination of work, general guidance, article editing; Shangina OR — analysis of the samples' porosity and density, statistical data processing; Chugunov SS — samples heat treatment and sintering, description of materials and methods; Tikhonov AA — assessment of microstructural changes using SEM, writing the section "Electron microscopy."

✉ **Correspondence should be addressed:** Azat R. Bilyalov  
Lenina, 3, ap. 119, 450008, Ufa, Republic of Bashkortostan, Russia; azat.bilyalov@gmail.com

**Received:** 14.12.2024 **Accepted:** 18.02.2025 **Published online:** 27.02.2025

**DOI:** 10.24075/brsmu.2025.009

**Copyright:** © 2025 by the authors. **Licensee:** Pirogov University. This article is an open access article distributed under the terms and conditions of the Creative Commons Attribution (CC BY) license (<https://creativecommons.org/licenses/by/4.0/>).

## ВЛИЯНИЕ МЕТОДОВ СТЕРИЛИЗАЦИИ НА ЦИТОТОКСИЧНОСТЬ КЕРАМИЧЕСКИХ МЕДИЦИНСКИХ ИМПЛАНТОВ

А. Р. Билялов <sup>✉</sup>, С. В. Пятницкая, Г. А. Рафикова, В. Н. Акбашев, А. Т. Бикмеев, И. Ш. Ахатов, О. Р. Шангина, С. С. Чугунов, А. А. Тихонов

Башкирский государственный медицинский университет Министерства здравоохранения Российской Федерации, Уфа, Россия

Выбор метода стерилизации керамических имплантов играет ключевую роль, поскольку может оказывать влияние на химические и физико-механические свойства материала и его биосовместимость. Возможное повышение цитотоксичности после стерилизации негативно влияет на остеоинтеграцию. Целью исследования было определить цитотоксичность керамических образцов с пористой структурой после проведения наиболее распространенных методов стерилизации. Методом стереолитографии были подготовлены образцы из гидроксиапатита, трикальцийфосфата и оксида алюминия. Образцы из костного аллогraftа были изготовлены методом DLP. Отжиг проводили при 800 °C и скорости нагрева 3 °C в минуту 4 ч, а спекание при температуре до 1200 °C. Использовали следующие методы стерилизации: автоклавирование при 1 атм, 120 °C, 45 мин; радиационная стерилизация, 25 с с поглощенной дозой 25 кГр; плазменно-перекисная стерилизация, 42 мин; стерилизация сухим жаром при 180 °C 60 мин. Цитотоксичность определяли МТТ-тестом с экспозицией в CO<sub>2</sub> инкубаторе 24 ч. Результаты исследования: для ГА высокая пористость увеличивает значения при переходе от автоклавирования (0,1115) к плазменно-перекисной стерилизации (0,2023). Средняя и низкая пористость показывают аналогичное поведение, с пиками при сухожаровой стерилизации (0,4954 и 0,4505). Для ОА характерна высокая жизнеспособность при сухожаровой стерилизации. Результаты для ТКФ стабильны, но при низкой пористости заметен рост после автоклавирования (0,078 до 0,182 при стерилизации сухим жаром). Исследование формирует основу для оптимизации технологии изготовления и методов стерилизации керамических имплантов для обеспечения их высокой биосовместимости.

**Ключевые слова:** медицинская керамика, 3D-печать, аддитивные технологии, стерилизация, импланты, жизнеспособность клеток, керамика

**Финансирование:** работа выполнена при поддержке Российского научного фонда по гранту № 23-15-20042.

**Вклад авторов:** А. Р. Билялов — концепция исследования, анализ данных, редактирование статьи; С. В. Пятницкая — проведение экспериментальных исследований по оценке цитотоксичности (МТТ-тест), анализ результатов; Г. А. Рафикова — подготовка цифровых моделей и изготовление образцов, анализ механических и биологических свойств материалов; В. Н. Акбашев — проведение экспериментов по стерилизации, анализ влияния методов стерилизации на материалы; А. Т. Бикмеев — математическое моделирование параметров материалов, интерпретация полученных данных; И. Ш. Ахатов — координация работы, общее руководство, редактирование статьи; О. Р. Шангина — анализ пористости и плотности образцов, статистическая обработка данных; С. С. Чугунов — проведение термической обработки и спекания образцов, описание материалов и методов; А. А. Тихонов — оценка микроструктурных изменений с использованием СЭМ, написание раздела «Электронная микроскопия».

✉ **Для корреспонденции:** Azat Rinatovich Bilyalov  
ул. Ленина, д. 3, к. 119, 450008, Республика Башкортостан, г. Уфа, Россия; azat.bilyalov@gmail.com

**Статья получена:** 14.12.2024 **Статья принята к печати:** 18.02.2025 **Опубликована онлайн:** 27.02.2025

**DOI:** 10.24075/vrgmu.2025.009

**Авторские права:** © 2025 принадлежат авторам. **Лицензиат:** РНИМУ им. Н. И. Пирогова. Статья размещена в открытом доступе и распространяется на условиях лицензии Creative Commons Attribution (CC BY) (<https://creativecommons.org/licenses/by/4.0/>).

Porosity and density of ceramic materials are key parameters that determine their mechanical and biological properties. These characteristics play a crucial role in the design of materials for medical implants.

Porosity, as an indicator of the number of voids in a material, significantly affects its ability to interact with surrounding tissues [1]. High porosity improves biological compatibility, creating conditions for the invasion of osteogenic cells and the formation of blood vessels in the implant structure [2]. This process, known as osseointegration, is critically important for implant survival. In addition, high porosity promotes free circulation of biological fluids, which restores metabolism in surrounding tissues and accelerates the process of bone regeneration [3].

However, high porosity has disadvantages. It reduces the mechanical strength of implants, which is especially critical when they are constantly under high cyclic loads, as is the case for supporting surfaces of joints or the spine. At the same time, low porosity can hinder osseointegration, limiting the development of bone tissue and slowing down the healing process [4].

Density affects mechanical properties of a material, including strength, elastic modulus, impact viscosity, wear resistance, yield strength, and fatigue. High density materials usually have high strength, as the distances between atoms in them are shorter, which translates into stronger interatomic bonds. Consequently, such materials are more resistant to mechanical stress. At the same time, the solidity of high-strength non-biological materials disallows penetration of cells into the structures made of them, which can negatively affect biological compatibility of implants, hindering osseointegration. To have control over mechanical properties of the implants, in some cases, they are designed as composite products from well-known materials in use [5]. Employing of composites and composite coatings, which are a mixture of the source metal and a bioresorbable material, yield a porous structure that is gradually populated by body cells and simultaneously provide a structural matrix for bone tissue growth [6].

Materials based on hydroxyapatite (HA), tricalcium phosphate (TCP), and preserved bone allograft possess a unique combination of mechanical and biological properties, which makes them indispensable in restorative and regenerative medicine. Their porosity is essential for osteogenesis: it creates an optimal environment for the formation of new bone tissue and integration of the implant with the bone structure. The surfaces of ceramic implants made of HA and TCP have pronounced osteoconductive properties and create optimal conditions for adhesion and proliferation of osteogenic cells. Unlike bone allo- and xenimplants, ceramics possesses no biological factors that induce osteogenesis, but its microporous structure promotes the formation of bone tissue through passive osteoconduction. As for osteoinduction, it is enabled by the gradual release of calcium and phosphate ions into the environment, which stimulates osteoblast proliferation and mesenchymal stem cell differentiation. In addition, mechanical properties of porous ceramic implants play an important role in bone regeneration: they render structural support for new bone formation and vascularization. The optimal size of pores (100–300  $\mu\text{m}$ ) ensures favorable conditions for osteogenic cell adhesion and vascularization [7, 8]. In particular, such pores improve the interaction of the material with bone tissue, which promotes formation of new bone [9].

The osteoinductive properties of materials reflect their ability to stimulate the formation of new bone tissue. Bioceramics based on HA and TCP is highly biocompatible and offers good osteoconductivity. Implants made of such bioceramics have

a structure that promotes the growth of bone tissue on their surface. However, ceramics, as a rule, are not outstandingly osteoinductive, like some other materials; it is more of a framework for bone tissue, a mechanical support. Allogeneic implants obtained from donors of the same species often have pronounced osteoinductive and osteoconductive properties. They can be both mineralized and demineralized, and it is the latter type that is more osteoinductive. Xenimplants of animal origin may offer good osteoconductivity, but their osteoinductivity is limited. Due to differences in cellular components and proteins, xenimplants may not always interact effectively with human bone tissue, which limits their osteoinductive potential compared to alloimplants. They can be used to replace bone tissue in certain situations, but their new bone growth stimulation potential is more modest [10].

The choice of the method of sterilization is especially important from the viewpoint of the safety and effectiveness of medical devices and implants. There are many sterilization methods available to medical professionals, and each of them has a different effect on implantable biomaterials. Physical methods rely on thermal treatment, filtration, and radiation. Chemical methods involve use of chemical agents to kill microorganisms (sterilization with gas or liquid) [11, 12]. Combined methods, like hydrogen peroxide gas plasma sterilization and generation of active oxygen species under ultraviolet, show high efficiency [13, 14].

Previous studies have shown that sterilization alters physico-chemical properties of implants made of porous bioceramic materials, but they did not compare the biological effects produced by different methods of sterilization on the said materials [11, 15].

This study aims to determine the cytotoxicity of porous ceramic samples sterilized using common methods, with the goal of applying the findings to further improve the materials and manufacturing technology for ceramic implants.

## METHODS

### Sample preparation

#### *Preparation of the digital model*

At the first stage, we designed the geometry of the samples in the Kompas-3D software (ASCON Group *Proyektirovaniya*, Russia): cylinders 2 mm high and 4 mm in diameter. The size of the samples was adapted to the standard trays used for MTT (methyl thiazolyl tetrazolium) assay, which ensured full conformity of their shapes to the regulatory requirements. The shrinkage during heat treatment and binder annealing was about 20%, which is typical for ceramic materials undergoing high-temperature sintering. Figure 1 shows a cylindrical 3D model of a ceramic sample (diameter 4 mm, height 2 mm), built with the 20% shrinkage factored in.

#### *Printing samples of hydroxyapatite, tricalcium phosphate, and aluminum oxide*

Before starting the 3D printing, we conducted a preliminary polymerization test, thus establishing parameters such as the wavelength of the laser radiation and the thickness of the layer of the photopolymerized paste. The test yielded optimal values of these parameters, which were used for printing. The technology employed to make samples of hydroxyapatite, tricalcium phosphate, and aluminum oxide was laser stereolithography. We used a Ceramaker 900 printer (3D Ceram Sinto, France),

and photopolymerized ceramic paste with a 355 nm laser, which ensured high accuracy and uniformity of the structure of the samples (Figure 2).

#### Cleaning of samples

After the printing, the samples were cleaned mechanically in a Cerakleaner system (3D Ceram Sinto, France). Figure 3 shows printed samples cleaned of unpolymerized paste residues. The cleaning was necessary to prepare the samples for heat treatment.

Next, the samples were put into a high-temperature furnace Kittec CLL15 (KITTEC GmbH, Germany) for annealing at 800 °C. The heating rate was 3 °C per minute; the total time of exposure equaled 4 hours. These parameter values ensured uniform heating of the sample, which reduced the likelihood of cracking and completely removed moisture as well as the polymer binder.

At the final stage, the samples were heat-treated and sintered in an L15/14/C450 laboratory furnace (Nabertherm GmbH; Germany). The temperature conditions of sintering were selected individually for each type of ceramic material in order to prevent undesirable structural changes. For AO, we opted for higher temperatures, since this material retains its structure even under intense heat. For TCP and HA, the sintering temperatures were lower, since high heat can alter their structure: TCP is subjects to phase transformations, and HA can be partially transformed into TCP. Taking these specifics into account, we selected optimal temperature conditions to avoid undesirable changes and produced three types of ceramic samples with different porosities: high, medium, and low [16]. Figure 4 shows the final samples after heat treatment under different sintering conditions.

#### Printing of samples from bone allograft suspension

To perform 3D printing with the DLP (Digital Light Processing) technology, we prepared a suspension from bone allograft powder grounded to a fraction of 0-5 microns. The samples were polymerized from the suspension in an Elegoo Mars 4 3D printer (ELEGOO, China); the layer thickness was 25 µm (Fig. 5).

3D printing yielded "green body" samples; the next stage was to subject them to two-stage heat treatment. The first stage, in which the samples were heated to a temperature of 700 °C at a rate of 3 °C per hour, produced weakly consolidated, highly porous (up to 42.3%) samples (Fig. 6). The second stage involved sintering at 1300 °C for 1 hour with the heating rate of 120 °C per hour, and yielded relatively durable and dense samples.

#### Determination of porosity and density

In our study, the porosity and density of each sample were determined using data on mass, volume, and theoretical density of the respective material.

The mass of each sample was measured with the help of analytical scales (accuracy 0.001 g).

The volume was calculated from the samples' geometric parameters (cylindrical shape) using the following expression:

$$V = \pi \times r^2 \times h,$$

where  $V$  is the volume of the sample,  $r$  is the radius of the cylinder base, and  $h$  is the height of the sample.

The density (sample) of each sample was determined in accordance with:

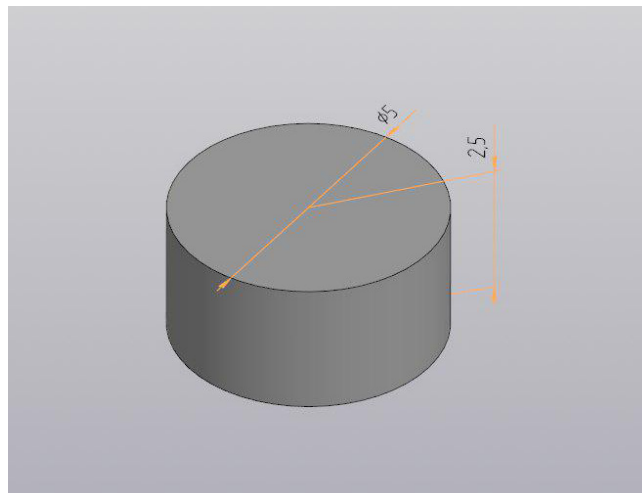


Fig. 1. Cylindrical 3D model of ceramic samples, 20% shrinkage factored in

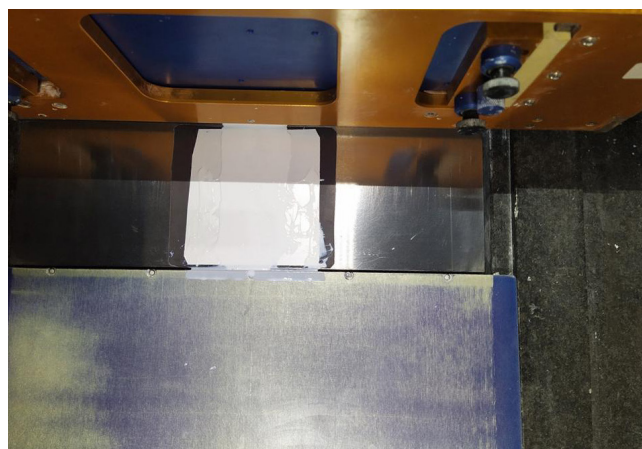


Fig. 2. Printing samples of hydroxyapatite on a Ceramaker 900 3D printer

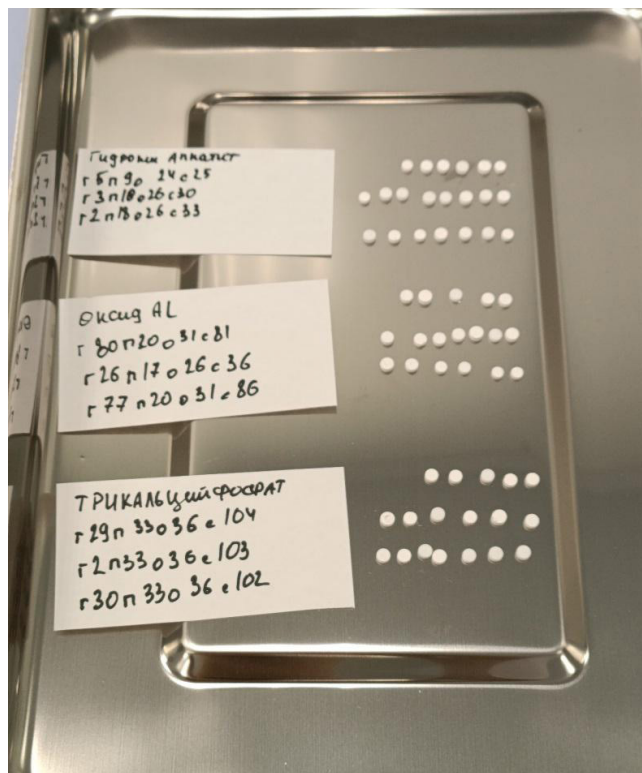


Fig. 3. 3D printed ceramic samples after mechanical cleaning



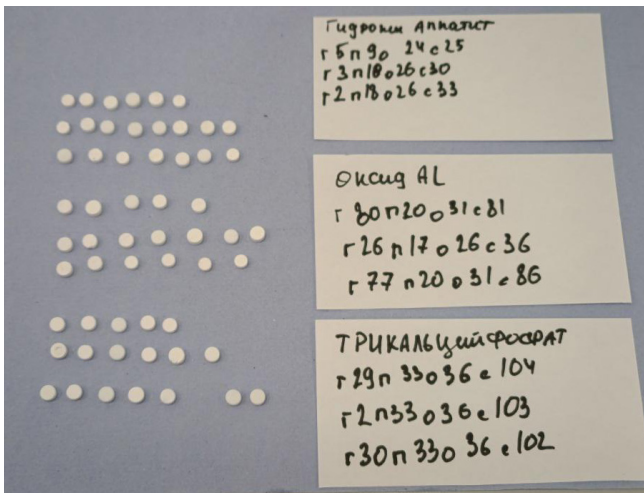


Fig. 4. Ceramic samples from HA and TCP after annealing and sintering

$$\rho_{\text{sample}} = \frac{m_{\text{sample}}}{V_{\text{sample}}}$$

where  $m_{\text{sample}}$  is the mass of the sample,  $V_{\text{sample}}$  is the volume of the sample.

Porosity ( $P$ ) was determined by the following expression:

$$\text{Porosity (\%)} = \left(1 - \frac{\rho_{\text{sample}}}{\rho_{\text{theoretical}}}\right) \times 100,$$

where  $\rho_{\text{theoretical}}$  is the theoretical density of the material without pores.

Having measured the mass, volume, density, and porosity of the samples, we found that the selected parameters produce significant variations depending on the type of ceramic material and the sintering mode (see Table). These variations stem from the peculiarities of phase transitions during heat treatment, which affect the degree of compaction of the material and the formation of pores.

### Electron microscopy

Scanning electron microscopy (SEM) was used to evaluate the microstructure, average particle size, and degree of sintering under various temperatures. Before scanning, the samples were precisely fractured to obtain sections showing internal structure and allowing to thoroughly analyze microstructural changes after sintering. The microscope used for the



Fig. 5. Printing of ceramic samples from a bone allograft in an Elegoo Mars 4 3D printer

purpose was a Quattro S environmental scanning electron microscope (Thermo Fisher Scientific, the Netherlands); the level of magnification was  $\times 10,000$ . We paid special attention to determining the average size of the particles and the degree of their compaction during sintering (Figure 7).

### Cytotoxicity assessment method

To assess cytotoxicity, we used the MTT test, which determines the total metabolic activity of living cells by the ability of mitochondrial succinate dehydrogenase to reduce MTT (3-(4,5-dimethylthiazol-2-yl)-2,5-diphenyl-tetrazolium bromide), which has a yellow color, to dark purple formazane, the crystals of which dissolve in dimethylsulfoxide (DMSO).

For the MTT test, we diluted the cells to a concentration of 50,000 cells/ml, and plated 200  $\mu\text{l}$  per well in a 96-well plate, with or without prepared implants. The plate was then placed in a  $\text{CO}_2$  incubator for 24 hours. During the plating, the suspension was mixed by repeated pipetting (3 times).

According to regulatory documents, a negative control sample is a piece of material that, when tested under the respective standard, does not exhibit cytotoxicity. A positive control sample is a piece of material that, when tested under the said standard, exhibits cytotoxicity, and the results of such a test are reproducible.

For negative control, we used cells without the studied samples of materials, cultivated on polypropylene. The positive control was a DMSO solution at a final concentration of 10% in the well.



Fig. 6. Ceramic samples from bone allograft after annealing and sintering



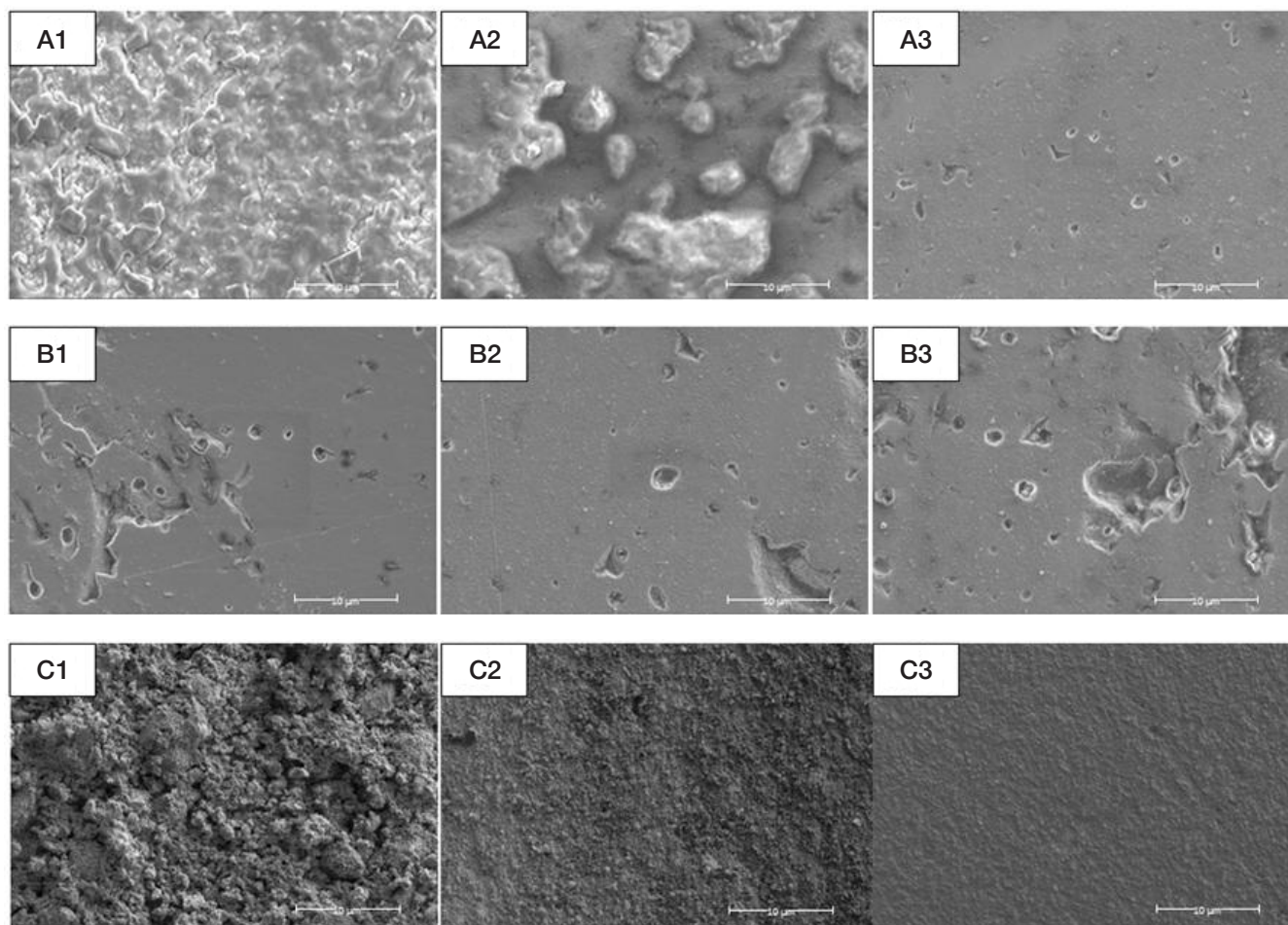


**Fig. 7.** The microstructure of the additive material made from hydroxyapatite (A1–3), tricalcium phosphate (B1–3), aluminum oxide (C1–3)

There were five samples of each material. To control the reagent, we allocated three wells of the plate, filled them with a complete culture medium, but not the cells.

#### MTT test protocol

The MTT test was conducted after 24 hours of cultivation. At the end of the cultivation, the serum-containing medium was replaced with a serum-free culture medium, and each well received 20 µl of MTT solution with a concentration of 5 mg/ml in saline solution, which made the ultimate concentration 0.5 mg/ml. After 3.5 hours, we observed intense formation of formazane crystals through a microscope. Then, the medium was carefully removed from all the wells, without affecting the bottom with cells and samples.

DMSO was added in a volume of 100 µl, half of the volume of the medium in each well during cultivation. After 60 minutes, 100 µl of the purple solution were transferred to a new 96-well plate in the same order, and analyzed in a Tecan Spark 10M plate reader (Tecan, USA) at 530 nm, with a reference wavelength of 620 nm.

To assess viability, we normalized the results by subtracting the average value as a reagent control measure. The relative viability was assessed using the following expression:

$$Vb = \frac{D_{530} - D_{620}}{\bar{D}_{530} - \bar{D}_{620}} \times 100,$$

where  $Vb$  is the relative viability,  $D_{530}$  is the optical density of the sample at 530 nm,  $D_{620}$  is the optical density of the sample at 620 nm,  $\bar{D}_{530}$  is the average optical density at 530 nm for negative control,  $\bar{D}_{620}$  is the average optical density at 620 nm for negative control.

#### Sterilization methods

Steam sterilization under pressure (autoclaving) was conducted in a NUT-2540EKA autoclave sterilizer (Tuttnauer, Israel) at 1 atm., 120 °C, for 45 minutes.

For radiation sterilization, we used a complex built on the LU-7-2 linear resonance accelerator (Russian Federal Nuclear Center — Russian National Experimental Physics Research Institute, Russia), following the medical devices radiation sterilization protocol "Alloplant Surgical Allografts TR-119-RS-2007". The beam was positioned perpendicular to the conveyor, the frequency was 5 Hz. The movement speed was 6 mm/s, the time of exposure — 25 seconds, and the absorbed dose — 25 kGy. The absorbed dose was measured using SO PD(F)-5/50 detectors (All-Russian Scientific Research Institute for Physical-Engineering and Radiotechnical Metrology, Russia).

Plasma peroxide sterilization was conducted in a STERRAD® 100S system (Advanced sterilization products, USA); the time of exposure was 42 minutes.

For dry heat sterilization, we used a Binder FD53 drying oven (Binder GmbH, Germany), parameters of the process were 180 °C and 60 minutes.

#### RESULTS

The results of the MTT test demonstrate that cell survival directly depends on the sterilization method, degree of porosity, and type of material.

The results presented in the table indicate that cell viability is the highest after dry heat sterilization. Medium and low porosity,

Table. MTT test results for the studied materials with different porosities

Positive control $0.025 \pm 0.019$						
Negative control $0.608 \pm 0.004$						
Negative control (alloplant) $0.881 \pm 0.008$						
Sample parameters			Optical density of samples for different sterilization methods			
Sample material	Porosity level	Porosity value (%)	Autoclaving	Fast electron flow	Plasma peroxide sterilization	Dry heat
Hydroxyapatite	High	35.11	$0.167 \pm 0.049$	$0.096 \pm 0.043$	$0.122 \pm 0.024$	$0.567 \pm 0.70$
	Moderate	26.91	$0.256 \pm 0.046$	$0.440 \pm 0.074$	$0.372 \pm 0.050$	$0.541 \pm 0.051$
	Low	18.33	$0.261 \pm 0.054$	$0.427 \pm 0.060$	$0.337 \pm 0.046$	$0.531 \pm 0.047$
Aluminum oxide	High	56.02	$0.064 \pm 0.012$	$0.103 \pm 0.003$	$0.104 \pm 0.002$	$0.333 \pm 0.042$
	Moderate	22.13	$0.058 \pm 0.003$	$0.097 \pm 0.005$	$0.103 \pm 0.005$	$0.372 \pm 0.052$
	Low	10.27	$0.105 \pm 0.011$	$0.338 \pm 0.021$	$0.337 \pm 0.046$	$0.433 \pm 0.056$
Tricalcium phosphate	High	20.34	$0.059 \pm 0.013$	$0.098 \pm 0.006$	$0.103 \pm 0.000$	$0.511 \pm 0.001$
	Moderate	15.57	$0.070 \pm 0.007$	$0.073 \pm 0.008$	$0.103 \pm 0.000$	$0.519 \pm 0.002$
	Low	10.69	$0.072 \pm 0.006$	$0.130 \pm 0.040$	$0.205 \pm 0.002$	$0.516 \pm 0.010$
Alloplant p0468			$0.457 \pm 0.042$	$0.616 \pm 0.059$	$0.412 \pm 0.054$	$0.542 \pm 0.052$
Alloplant p0476			$0.435 \pm 0.038$	$0.494 \pm 0.053$	$0.485 \pm 0.048$	$0.638 \pm 0.045$
Relative survival rate (%)						
Hydroxyapatite	High	35.11	27.67	15.97	20.26	93.82
	Moderate	26.91	42.38	72.85	61.64	89.58
	Low	18.33	43.14	70.64	55.79	87.95
Aluminum oxide	High	56.02	10.54	17.05	17.23	55.18
	Moderate	22.13	9.66	16.11	17.1	61.62
	Low	10.27	17.38	56.01	55.71	73.29
Tricalcium phosphate	High	20.34	9.77	16.27	17	84.66
	Moderate	15.57	11.59	12.14	17.08	85.84
	Low	10.69	11.92	21.5	33.89	85.48
Alloplant p0468			51.87	69.92	46.77	61.52
Alloplant p0476			49.38	56.07	55.05	72.42

as a rule, provides optimal conditions for cell viability, combining sufficient area for cell adhesion and mechanical strength.

The analysis of the subgroups indicates that for hydroxyapatite implants, high porosity increases values in the context of a switch from autoclaving (0.1115) to combined plasma peroxide sterilization (0.2023) (Fig. 8). Medium and low porosity show similar results, with peaks in dry-heat sterilization (0.4954 and 0.4505, respectively). As for aluminum oxide, the values are moderate for all porosities, but they were pushed up by dry heat sterilization. The test results for tricalcium phosphate are relatively stable, but in low porosity, the values were growing noticeably after autoclaving (0.078 to 0.182).

## DISCUSSION

To date, there is no consensus on which of the methods of sterilization of new materials is the safest in terms of the effect on cell viability in the context of cytotoxicity [17].

Steam sterilization under pressure (autoclaving) is one of the most common methods that ensures complete decontamination of medical devices in a short time, but implant materials can be sensitive to temperature and pressure. This method is applicable to metals and bio-glass, but it is highly probable that applying it to other materials will alter their physico-chemical characteristics, resulting in a loss of operational properties [18].

In our study, autoclaving had a negative effect on ceramic samples, which resulted in lower cell viability as shown by the MTT test, especially for materials with low and high porosity. The possible reason is modification of the surface of the

samples under the influence of temperature and pressure, which complicates cell adhesion.

Sterilization by dry heat was the method that ensured highest cell viability. One of the possible explanations is that this treatment eliminates moisture absorbed into the hygroscopic structure of porous ceramics from the air. However, this assumption is based on the general mechanisms of thermal effects on implants, and requires further confirmation using materials science methods, such as X-ray phase analysis and gas chromatography. In addition, we should not discard the possible alteration of physical characteristics of the samples' surface after dry heat sterilization, which could affect cell adhesion.

Thus, the dry heat method is promising for the sterilization of ceramic implants, but additional studies are needed to definitively assess its effect on the material's microstructure and mechanical properties. Such studies would confirm or deny the effect of sterilization by dry heat on the characteristics of the materials. The effect of ionizing radiation, a high-energy electron beam, can trigger formation of nano- and submicropores, crystallization of amorphous calcium phosphate, recrystallization of crystalline hydroxyapatite, phase transformations (possibly the formation of tricalcium phosphate with a monoclinic lattice and an amorphous phase). In addition, high-energy electron irradiation can modify the sample surface by coating it with thin nanoscale particles of CaO,  $\alpha$ -Ca<sub>3</sub>(PO<sub>4</sub>)<sub>2</sub>, and hydroxyapatite. Despite its effectiveness, this method may be not applicable in cases where it is necessary to preserve the exact structure of the material [19].

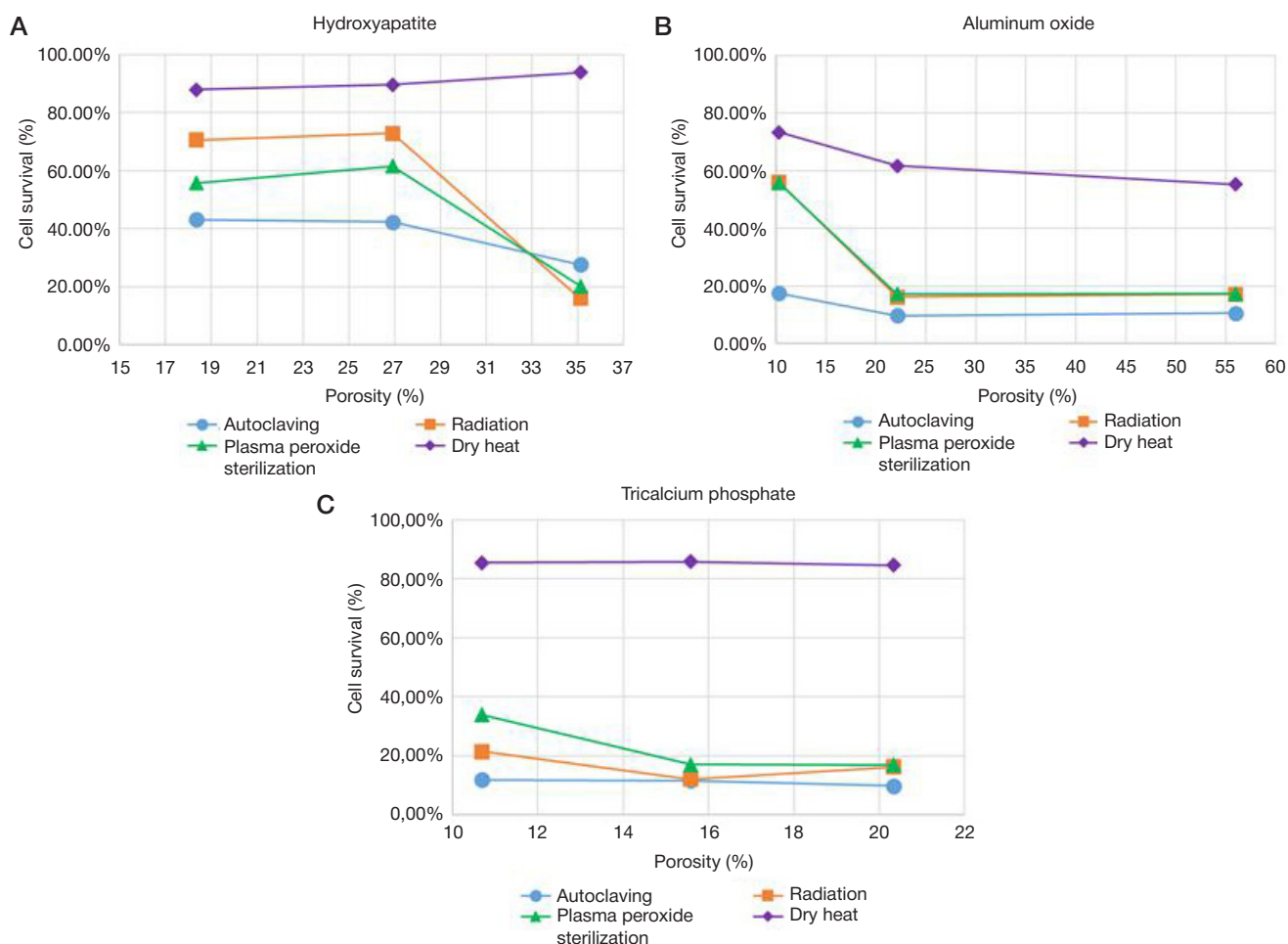


Fig. 8. The dependence of cell survival in the studied samples on the degree of porosity when subjected to various sterilization methods

## CONCLUSIONS

The results of the study showed that the viability of cells depends both on the method of sterilization and on the degree of porosity of the material. Sterilization by dry heat yielded better cell viability figures; autoclaving and irradiation by fast electrons had a more pronounced negative effect. Analysis of the effect of porosity has shown that the dependence of cell viability on this parameter is not linear. In some cases, materials with low porosity demonstrated higher relative cell survival, which may be due to the peculiarities of cell adhesion and interaction with the biomaterial. At the same time, medium porosity ensured an optimal combination of mechanical strength and cellular viability. Thus, the choice of the sterilization method

and the degree of porosity of the material should be based on a comprehensive analysis of biological and mechanical characteristics, and factor in the specific clinical tasks. Further studies, including the analysis of microstructural changes, will allow a deeper understanding of the mechanisms underlying the effect of sterilization on the properties of ceramic implants. The degree of porosity and the choice of sterilization method are important in creating porous ceramic implants made using additive technologies. 3D printing allows creating personalized medical products with controllable physical, chemical and biological properties, which combine high mechanical strength and biocompatibility. The results of this study form the basis for further research and development of medical ceramic materials with improved properties.

## References

- Naik V, Jain A, Rao R, Naik B. Comparative evaluation of clinical performance of ceramic and resin inlays, onlays, and overlays: A systematic review and meta analysis. *J Conserv Dent.* 2022; 25 (4): 347.
- Abbasi N, Hamlet S, Love RM, Nguyen NT. Porous scaffolds for bone regeneration. *J Sci Adv Mater Devices.* 2020; 5 (1): 1–9.
- Sagdoldina Z, Kot M, Baizhan D, Buitkenov D, Sulyubayeva L. Influence of Detonation Spraying Parameters on the Microstructure and Mechanical Properties of Hydroxyapatite Coatings. *Materials.* 2024; 17 (21): 5390.
- Bilyalov AR, Minasov BSh, Yakupov RR, Akbashev VN, Rafikova GA, Bikmееv AT, i dr. Ispol'zovanie keramicheskoy 3D-pechati dlja zadach tkanevoj inzhenerii: obzor. *Politравma.* 2023; 1: 89–109. Russian.
- Văruț RM, Rotaru LT, Truicu FN, Singer CE, Iulian-Nicolae I, Popescu AIS, et al. Comparative Analysis of Osteointegration in Hydroxyapatite and Hydroxyapatite-Titanium Implants: An In Vivo Rabbit Model Study. *J Funct Biomater.* 2024; 15 (7): 181. DOI: 10.3390/jfb15070181. PMID: 39057303; PMCID: PMC11278386.
- Villardell AM, et al. Cold spray as an emerging technology for biocompatible and antibacterial coatings: state of art. *J Mater Sci.* 2015; 50: 4441–62.
- de Carvalho ABG, Rahimnejad M, Oliveira RLMS, Sikder P, Saavedra GSFA, Bhaduri SB, et al. Personalized bioceramic grafts for craniomaxillofacial bone regeneration. *Int J Oral Sci.* 2024; 16

- (1): 62. DOI: 10.1038/s41368-024-00327-7. PMID: 39482290; PMCID: PMC11528123.
8. Zhao C, Liu W, Zhu M, Wu C, Zhu Y. Bioceramic-based scaffolds with antibacterial function for bone tissue engineering: A review. *Bioact Mater.* 2022; 18: 383–98. DOI: 10.1016/j.bioactmat.2022.02.010. PMID: 35415311; PMCID: PMC8965760.
  9. Nikolova MP, Chavali MS. Recent advances in biomaterials for 3D scaffolds: A review. *Bioact Mater.* 2019; 4: 271–92.
  10. Albrektsson T, Johansson C. Osteoinduction, osteoconduction and osseointegration. *Eur Spine J.* 2001; 10 (Suppl 2): S96–S101. Available from: <https://doi.org/10.1007/s005860100282>.
  11. Li X, Guo B, Xiao Y, Yuan T, Fan Y, Zhang X. Influences of the steam sterilization on the properties of calcium phosphate porous bioceramics. *J Mater Sci Mater Med.* 2016; 27 (1): 5.
  12. Mohapatra S. Sterilization and Disinfection. *Essentials of Neuroanesthesia.* 2017: 929–44. DOI: 10.1016/B978-0-12-805299-0.00059-2. Epub 2017 Mar 31. PMCID: PMC7158362.
  13. Adler S, Scherrer M, Daschner FD. Costs of low-temperature plasma sterilization compared with other sterilization methods. *Journal of Hospital Infection.* 1998; 40 (2): 125–34. Available from: [https://doi.org/10.1016/S0195-6701\(98\)90091-3](https://doi.org/10.1016/S0195-6701(98)90091-3).
  14. Philip N, Saoudi B, Crevier MC, Moisan M, Barbeau J, Pelletier J. The respective roles of UV photons and oxygen atoms in plasma sterilization at reduced gas pressure: The case of N<sub>2</sub>-O<sub>2</sub> mixtures. *IEEE Transactions on Plasma Science.* 2002; 30 (4 l): 1429–36. <https://doi.org/10.1109/TPS.2002.804203>.
  15. Guo T, Oztug NAK, Han P, Ivanovski S, Gulati K. Influence of sterilization on the performance of anodized nanoporous titanium implants. *Mater Sci Eng C.* 2021; 130: 112429.
  16. Bogdanova EA, Skachkov VM, Skachkova OV, Sabirzyanov NA. Effect of High Temperatures on the Microstructure and Properties of Fluorine-Containing Hydroxyapatite-Based Materials. *Inorganic Materials.* 2020; 56 (2): 172–7. DOI: 10.1134/S002016852002003X. EDN EMVJPV.
  17. Kinnari TJ, Esteban J, Zamora N, Fernandez R, López-Santos C, Yubero F, et al. Effect of surface roughness and sterilization on bacterial adherence to ultra-high molecular weight polyethylene. *Clin Microbiol Infect.* 2010; 16 (7): 1036–41.
  18. Costa L, Luda MP, Trossarelli L, Brach Del Prever EM, Crova M, Gallinaro P. Oxidation in orthopaedic UHMWPE sterilized by gamma-radiation and ethylene oxide. *Biomaterials.* 1998; 19 (7–9): 659–68.
  19. Kostyuchenko AV, Kochlar GS, Ievlev VM. Electron Irradiation Effect in Surface Modification of Hydroxyapatite Ceramics. *Inorganic Materials.* 2019; 55 (12): 1285–9. DOI: 10.1134/S0020168519120070.

## Литература

1. Naik V, Jain A, Rao R, Naik B. Comparative evaluation of clinical performance of ceramic and resin inlays, onlays, and overlays: A systematic review and meta analysis. *J Conserv Dent.* 2022; 25 (4): 347.
2. Abbasi N, Hamlet S, Love RM, Nguyen NT. Porous scaffolds for bone regeneration. *J Sci Adv Mater Devices.* 2020; 5 (1): 1–9.
3. Sagdoldina Z, Kot M, Baizhan D, Buitkenov D, Suluybayeva L. Influence of Detonation Spraying Parameters on the Microstructure and Mechanical Properties of Hydroxyapatite Coatings. *Materials.* 2024; 17 (21): 5390.
4. Билялов А. Р., Минасов Б. Ш., Якупов Р. Р., Акбашев В. Н., Рафикова Г. А., Бикмеев А. Т., и др. Использование керамической 3D-печати для задач тканевой инженерии: обзор. *Политравма.* 2023; 1: 89–109.
5. Văruț RM, Rotaru LT, Truicu FN, Singer CE, Iulian-Nicolae I, Popescu AIS, et al. Comparative Analysis of Osteointegration in Hydroxyapatite and Hydroxyapatite-Titanium Implants: An In Vivo Rabbit Model Study. *J Funct Biomater.* 2024; 15 (7): 181. DOI: 10.3390/jfb15070181. PMID: 39057303; PMCID: PMC11278386.
6. Vilardeell AM, et al. Cold spray as an emerging technology for biocompatible and antibacterial coatings: state of art. *J Mater Sci.* 2015; 50: 4441–62.
7. de Carvalho ABG, Rahimnejad M, Oliveira RLMS, Sikder P, Saavedra GSFA, Bhaduri SB, et al. Personalized bioceramic grafts for craniomaxillofacial bone regeneration. *Int J Oral Sci.* 2024; 16 (1): 62. DOI: 10.1038/s41368-024-00327-7. PMID: 39482290; PMCID: PMC11528123.
8. Zhao C, Liu W, Zhu M, Wu C, Zhu Y. Bioceramic-based scaffolds with antibacterial function for bone tissue engineering: A review. *Bioact Mater.* 2022; 18: 383–98. DOI: 10.1016/j.bioactmat.2022.02.010. PMID: 35415311; PMCID: PMC8965760.
9. Nikolova MP, Chavali MS. Recent advances in biomaterials for 3D scaffolds: A review. *Bioact Mater.* 2019; 4: 271–92.
10. Albrektsson T, Johansson C. Osteoinduction, osteoconduction and osseointegration. *Eur Spine J.* 2001; 10 (Suppl 2): S96–S101. Available from: <https://doi.org/10.1007/s005860100282>.
11. Li X, Guo B, Xiao Y, Yuan T, Fan Y, Zhang X. Influences of the steam sterilization on the properties of calcium phosphate porous bioceramics. *J Mater Sci Mater Med.* 2016; 27 (1): 5.
12. Mohapatra S. Sterilization and Disinfection. *Essentials of Neuroanesthesia.* 2017: 929–44. DOI: 10.1016/B978-0-12-805299-0.00059-2. Epub 2017 Mar 31. PMCID: PMC7158362.
13. Adler S, Scherrer M, Daschner FD. Costs of low-temperature plasma sterilization compared with other sterilization methods. *Journal of Hospital Infection.* 1998; 40 (2): 125–34. Available from: [https://doi.org/10.1016/S0195-6701\(98\)90091-3](https://doi.org/10.1016/S0195-6701(98)90091-3).
14. Philip N, Saoudi B, Crevier MC, Moisan M, Barbeau J, Pelletier J. The respective roles of UV photons and oxygen atoms in plasma sterilization at reduced gas pressure: The case of N<sub>2</sub>-O<sub>2</sub> mixtures. *IEEE Transactions on Plasma Science.* 2002; 30 (4 l): 1429–36. <https://doi.org/10.1109/TPS.2002.804203>.
15. Guo T, Oztug NAK, Han P, Ivanovski S, Gulati K. Influence of sterilization on the performance of anodized nanoporous titanium implants. *Mater Sci Eng C.* 2021; 130: 112429.
16. Богданова Е. А., Скачков В. М., Скачкова О. В., Сабирзянов Н. А. Влияние высоких температур на микроструктуру и свойства фторсодержащих материалов на основе гидроксиапатита. *Неорганические материалы.* 2020; 56 (2): 181–6.
17. Kinnari TJ, Esteban J, Zamora N, Fernandez R, López-Santos C, Yubero F, et al. Effect of surface roughness and sterilization on bacterial adherence to ultra-high molecular weight polyethylene. *Clin Microbiol Infect.* 2010; 16 (7): 1036–41.
18. Costa L, Luda MP, Trossarelli L, Brach Del Prever EM, Crova M, Gallinaro P. Oxidation in orthopaedic UHMWPE sterilized by gamma-radiation and ethylene oxide. *Biomaterials.* 1998; 19 (7–9): 659–68.
19. Костюченко А. В., Кочлар Г. С., Иевлев В. М. Эффект электронного облучения в модификации поверхности керамики на основе гидроксиапатита. *Неорганические материалы.* 2019; 55 (12): 1363–7. DOI 10.1134/S0020168519120078.



## COGNITIVE CORRELATES OF DECEPTION RECOGNITION IN THE ELDERLY AND SENIORS

Petrash EA<sup>1</sup>✉, Lisichkina AA<sup>1</sup>, Karpenko AS<sup>2</sup>, Nikishina VB<sup>1</sup>, Polonets AI<sup>1</sup><sup>1</sup> Pirogov Russian National Research Medical University, Moscow, Russia<sup>2</sup> Moscow State Institute of International Relations (University) of the Ministry of Foreign Affairs of the Russian Federation, Moscow, Russia

The relevance of the proposed study is due to the need to find solutions in reducing the vulnerability of elderly and seniors to deception and fraudulent actions. The purpose of the study is to assess the cognitive correlates of deception recognition in the elderly and seniors. The sample size was 87 elderly and senile subjects (60–89 years old) — 38 men and 49 women. Research methods: MoCA (Montreal Cognitive Assessment); Sally–Anne test; Pragmatic intervention short stories Winner's Task; experimental method Read the Mind in the eye (RMET); Dembo–Rubinstein self-esteem scale; trust self-esteem scale. Based on the findings of the study, the cognitive correlates of deception recognition in the elderly and seniors were identified. It is reliably found that with age, as ageing progresses regardless of education level, there is a decline in cognitive level, which, in general, is natural in the process of normative ageing. These changes lead to a decrease in the level of understanding of the mental model, which in turn makes it more difficult to recognise emotions and increase trust. The empirical study supported the hypothesis that there is a correlation between cognitive level and the ability to recognise deception. The lower the general cognitive level, the worse the deception is recognised and the more trusting a person becomes.

**Keywords:** elderly age, senior age, mental model, deception recognition, cognitive level**Compliance with ethical standards:** the study was approved by the Ethical Committee of the N.I. Pirogov RNIMU (protocol No. 239 of 15 April 2024); all participants signed voluntary informed consent for the study.✉ **Correspondence should be addressed:** Ekaterina A. Petrash  
Ostrovityanova, 1, Moscow, 117997, Russia; petrash@mail.ru**Received:** 13.02.2025 **Accepted:** 26.02.2025 **Published online:** 28.02.2025**DOI:** 10.24075/brsmu.2025.010**Copyright:** © 2025 by the authors. **Licensee:** Pirogov University. This article is an open access article distributed under the terms and conditions of the Creative Commons Attribution (CC BY) license (<https://creativecommons.org/licenses/by/4.0/>).

## КОГНИТИВНЫЕ КОРРЕЛЯТЫ РАСПОЗНАВАНИЯ ОБМАНА В ПОЖИЛОМ И СТАРЧЕСКОМ ВОЗРАСТЕ

Е. А. Петраш<sup>1</sup>✉, А. А. Лисичкина<sup>1</sup>, А. С. Карпенко<sup>2</sup>, В. Б. Никишина<sup>1</sup>, А. И. Полонец<sup>1</sup><sup>1</sup> Российский национальный исследовательский медицинский университет имени Н. И. Пирогова, Москва, Россия<sup>2</sup> Московский государственный институт международных отношений (университет) Министерства иностранных дел Российской Федерации, Москва, Россия

Актуальность предлагаемого исследования обусловлена необходимостью поиска путей снижения уязвимости лиц пожилого и старческого возраста к обману и мошенническим действиям. Целью исследования было оценить когнитивные корреляты распознавания обмана в пожилом и старческом возрасте. Объем выборки составил 87 испытуемых пожилого и старческого возраста (60–89 лет) — 38 мужчин и 49 женщин. Использовали методику MoCA (Montreal Cognitive Assessment); тест Салли–Энн; Pragmatic intervention short stories Winner's Task; экспериментальную методику Read the Mind in the eye (RMET); шкалу самооценки Дембо–Рубинштейн; шкалу самооценки доверия. На основании полученных результатов исследования выявлены когнитивные корреляты распознавания обмана в пожилом и старческом возрасте. Достоверно установлено, что с возрастом, по мере старения вне зависимости от уровня образования происходит снижение когнитивного уровня, что, в целом, является закономерным в процессе нормативного старения. Эти изменения приводят к снижению уровня понимания модели психического, что, в свою очередь, затрудняет распознавание эмоций и повышает уровень доверия. Эмпирическое исследование подтвердило гипотезу о наличии корреляции между когнитивным уровнем и способностью распознавать обман. Чем ниже общий когнитивный уровень, тем хуже распознается обман и тем более доверчивым становится человек.

**Ключевые слова:** пожилой возраст, старческий возраст, модель психического, распознавание обмана, когнитивный уровень**Соблюдение этических стандартов:** исследование одобрено этическим комитетом РНИМУ им. Н. И. Пирогова (протокол № 239 от 15 апреля 2024 г.); все участники подписали добровольное информированное согласие на обследование.✉ **Для корреспонденции:** Екатерина Анатольевна Петраш  
ул. Островитянова, д. 1, г. Москва, 117997, Россия; petrash@mail.ru**Статья получена:** 13.02.2025 **Статья принята к печати:** 26.02.2025 **Опубликована онлайн:** 28.02.2025**DOI:** 10.24075/vrgmu.2025.010**Авторские права:** © 2025 принадлежат авторам. **Лицензиат:** РНИМУ им. Н. И. Пирогова. Статья размещена в открытом доступе и распространяется на условиях лицензии Creative Commons Attribution (CC BY) (<https://creativecommons.org/licenses/by/4.0/>).

According to statistics from the Unified Center of Legal Defense, between 2014 and 2024, the number of people deceived by phone frauds increased by 72%, with more than 79% of victims being elderly people. According to the FBI Elder Fraud Report for 2023, the total amount of money lost as a result of financial crimes against the elderly was approximately \$3.4 billion. This age group is characterized by cognitive changes with a tendency to a decrease in cognitive abilities, which increases the risk of being deceived.

The formation of functional systems, as well as their differentiation during the ontogenetic development of elderly people, occurred under conditions of lesser technological

influence, rather than in the context of total digitalization. Accordingly, in today's realities in the conditions of intensive digitalization and technological changes, deception in most cases is carried out through means of technical mediation (phone calls, instant messengers), which, in turn, along with the naturally occurring decrease in neuroplasticity of the brain as normative aging occurs, complicates their resistance to fraud.

Conducting a theoretical and methodological analysis of the scientific elaboration of the issues under consideration, a bibliometric analysis of publication activity was carried out (according to the scientific database "The Lens"). It is worth noting that in the foreign literature in the chronological range

of the last 14 years (2010–2025), searching for scientific publications by keywords — scholarly search "lie detection" an increase in research interest is recorded. This is evidenced by a steady increase in publication activity in the specified period. The total number of publications in the specified period from 01.01.2010 to 14.01.2025 is 1830 scientific papers. At least 100 works are published annually, therefore a steady interest in the chosen topic can be noted, however, since 2017 there has been an increase in publication activity by 30% (from 102 works in 2017 to 143 in 2025). Then, specifying our request in accordance with the age category of the carrier, namely elderly and old people. By request — scholarly search — elderly, field of study — lie detection, only 4 publications were found, which is less than 3% of the total share of publications on the specified topic. Based on the conducted analysis of the studies, two research vectors are formed — the vector of research on the recognition of deception and the vector of research on the process of deceptive actions.

Analyzing the deception recognition methods used in existing studies, two main directions are clearly visible: the subjective assessment of the verifier and the objective assessment of deception using specialized auxiliary tools. Subjective assessment of the verifier is based on parameters that are considered to be signs of a lie based on observation — facial expression, gestures, postures, change in voice, frequency of eye contact and other telltale signs; or based on linguo semantic analysis — change in intonation, speech rate, change in voice timbre and the appearance of a tremor in the voice). Objective assessment methods of deception include hardware methods (EEG, PET, MRI, non-verbal behavior scanning method and psychophysiological changes using a polygraph). Objective methods allow us to record changes in the brain activity of the cerebral cortex, as well as the structures of the limbic system.

A content analysis of scientific publications indicates that the most active researcher in the field of detection is Aldert Vrij. The author has published more than 300 papers on the subject matter, 108 for the period from 2010 to 2025. The author's most focused attention is on the topic of the relationship between verbal and non-verbal behavior and deception, and he also addresses issues of speech content and deception. A. Vrij identified 17 non-verbal parameters of lies, dividing them into vocal and non-vocal non-verbal behavior [1–10].

Also, in the works of one of the leading experts in the field of lie detection by recording facial micro expressions is Paul Ekman. The author uses the concepts of lies and deception as synonyms: "I define a lie or a deception as an act that is intended to foster in another person a belief or understanding that the deceiver considers false. It is done intentionally, without prior notification of the intent to deceive, and without having been explicitly asked to do so by the target" [6–10]. At the same time, for the identification of deception, tools related to verbal (semantic meaning of the word, characteristics of the tempo and prosody of speech, grammatical structure of statements) and non-verbal (micro expressions, facial expressions, gestures, posture, visual contact) manifestations of the participant in communication are used. Some of the listed parameters are also used by A. Vrij.

In Russian science, understanding deception is a less studied and relatively new area of research. One of the authors studying a similar topic is the Soviet and Russian scientist, a specialist in the field of psychology of understanding, V.V. Znakov [11], thanks to whose works it is possible to differentiate the terms lie, untruth and deception. On the one hand, any judgment supplied with distorted facts should be

considered false, regardless of the speaker's intention to lie or the lack of it. On the other hand, when classifying a lie within the framework of psychology, in order to classify a judgment as false, it is enough for one of the participants in communication to believe that he is lying. That is, the determining factor is precisely the intention to distort the facts. The main similarity between deception and lies is the conscious, purposeful intention of the participant in communication to distort the truth. But still, these semantically similar concepts have a key aspect that will allow us to draw a line in their differentiation. Deception is a half-truth communicated to a partner with the expectation that he will draw erroneous conclusions from it that do not correspond to the intentions of the deceiver [11]. In this case, the concept of "half-truth" implies a partial communication of true facts and details with the conscious concealment of others necessary for a complete understanding. Thus, deception aims to direct the movement of the participant's thoughts "along the path of actualizing frequently encountered familiar situations" [11]. The deceived person, against his will, becomes an accomplice to the deceptive act, because he becomes a victim of biased knowledge.

Recognizing deception is a complex process that involves several aspects at once — cognitive, emotional, social. To understand deception, a necessary condition is the ability to understand and interpret one's own mental state and the mental state of another. "Representations of mental states allow us to predict and explain human behavior, i.e. the conceptual system underlying such representations has explanatory power..." [12].

Mental models (in foreign literature the definition Theory of mind is used), representing a metacognitive ability, provide a person with the opportunity to form an idea of the intentions, desires, sincerity of another person in the context of a changing social context in order to make an appropriate decision.

One of the most crucial elements of the theory of mind is the understanding that one's own mental state differs significantly from another's state, it is not identical to another's state. Since mental states are not directly observable, the assumption that other people have them becomes a tool that helps make predictions and interpret the behavior of others.

The theory of mind begins its development in early childhood and undergoes certain changes throughout life, moving along a U-shaped trajectory. The phenomenon of understanding deception, which is subject to change, shows that as people approach elderly and old age, they make more mistakes in understanding the hidden intentions of others and become less sensitive to signals that warn of the unsafety of the current situation.

According to studies on the influence of age on the functioning of the mental model, changes can be observed as early as 60 years of age [13], while other authors indicate that changes begin at the age of 50 [14]. Although time frames may vary, most studies contain similar conclusions, according to which elderly and senior people make more errors in interpreting false beliefs than young adults.

The present study aims to shift the focus from the liar's influence and its characteristics to the methods and features of processing verified information, as well as the cognitive characteristics of the verifier.

The theoretical and methodological foundations were based on the provisions of the theory of the mental model (theory of mind) developed by G. Woodruff and D. Premack [15], further developed by E.A. Sergienko [12,16,17]; the provisions of the emotional theory of P. Ekman [6–10]; the provisions of the theory of A. Vrij on the model of truthfulness assessment [1–5].

David Premack and Guy Woodruff were the first to propose the concept of a theory of mind and emphasized that understanding the mental states of others has a significant impact on everyday life and affects the quality of life. Later studies conducted with patients with mental disorders and local brain lesions [15] showed that the theory of mind should be divided into two structural components. The cognitive or "cold" component includes cognitive processing of thoughts, beliefs, and intentions of other people, and understanding of non-literal statements. Within the cognitive component, first- and second-order representations are distinguished. First-order representations are representations of an individual's own thoughts that arise through the formation of one's own point of view ("I think she thinks that..."). Thus, we have the ability to understand that others have their own consciousness and perception, which differs from ours. Second-order representations are more complex constructions of deep ideas about oneself and involve the simultaneous acceptance of two points of view ("he thinks she thinks that..."). In this case, first-order representations develop first in ontogenesis.

The emotional "hot" component of the mental model includes understanding of feelings, emotions, and affective states of other people. It is necessary to differentiate between the similar at first glance concepts of empathy and the emotional component. Empathy implies the ability to feel and experience emotions, feelings of another person, without necessarily understanding the reason that caused them. While the emotional component assumes the ability to accept the point of view of another ("to step into his shoes.") with a true understanding of his mental state without the need to feel his emotions, feelings.

Moreover, the behavior of other people is not completely predictable, and therefore the success of interaction with the social environment correlates with the ability to decipher the mental states and intentions of others. The presence of changes in the components of the mental model (theory of mind) leads to a decrease in susceptibility and assessment of those signals that would warn of possible negative, dangerous actions on the part of other people. This is what allows us to classify older people as a more vulnerable category of the population, which exposes them to the risk of becoming victims of social exploitation, fraud and deception. This, in turn, leads to an increased level of stress, empathic distress, and, consequently, to difficulties in establishing friendly and family relationships [18].

As E.A. Sergienko points out in his works, age-related changes in social contacts and their emotional accompaniment, occurring with age, lead to the manifestation of selective motivation in relation to various forms of social activity. The main manifestation of this is the voluntary structuring of one's social space: protecting oneself from negative and traumatic experiences while focusing primarily on trusting relationships. However, even with such socio-emotional selectivity, in old age, when interacting with other people, a person needs to understand the intentions and their truthfulness, beliefs, and emotions of other people. And such an ability to understand the mental world of the Other is not limited to either intellectual or cognitive abilities [12].

The theory of mind, which is a cognitive mechanism that ensures successful interaction with another person, allows one to understand not only emotions, but also to perceive multilayered structures (the so-called first-, second-, and third-order representations). The theory of mind is a natural human ability, but its full development requires many years of experience in social interaction. Different people can develop

more or less effective models of mind [15]. Examples of the emotion category are expressed using facial movements that vary to some extent around a typical set (prototype). The "skeleton" of each emotion prototype can also be variable, but within certain limits [6–8]. According to A. Vrij's truthfulness assessment model, those who tell the truth provide more details that can be verified and receive a higher coefficient of such details (verifiable details/total number of details) than liars. Moreover, these details are manifested precisely in behavior [4–5].

As a result of conceptual modeling, a model of cognitive markers in the process of deception recognition was formed, including the stages of implicit recognition (the stage of the first impression and putting forward two alternative hypotheses about truth/falsity; the stage of obtaining information through special signal systems that confirm or refute hypotheses; the stage of assessing information and drawing conclusions about the degree of sincerity/insincerity of the interlocutor) and explicit recognition (the stage of emotional response in the form of conscious experiences; the stage of using certain information/abilities/skills in detecting lies). At the same time, in implicit recognition, cognitive markers are implemented in the recognition of emotions and the formation of a mental model; in explicit recognition, cognitive markers are realized in the level of self-esteem and behavioral strategies (Fig. 1).

The aim of the study was to investigate cognitive markers of deception recognition in old and senile age.

## METHODS

The study involved 87 elderly and senior subjects (60–89 years old) — 38 men and 49 women. Inclusion criteria for the study: elderly and senior ages; absence of cognitive impairments, implying loss of orientation in place, time and one's own personality (MoCA range from 17 to 30 points). Exclusion criteria were the presence of diagnosed mental and behavioral disorders; history of acute circulatory disorders; severe impairments of motor functions, as well as impairments of gnostic functions. The subjects were divided into study groups based on age: the first study group consisted of 42 elderly people, which corresponds to 60–75 years (according to WHO). The second study group consisted of 45 people aged 75–89 years, which corresponds to senior age.

The study was conducted at the Russian Gerontological Scientific and Clinical Center under the conditions of written voluntary informed consent.

The study was conducted using the following methods: the MoCA (Montreal Cognitive Assessment) technique for assessing neurocognitive status [19]; the Sally-Ann Test for assessing the integrity of the mental model [18, 20]; the Pragmatic intervention short stories Winner's Task, which allows assessing a person's ability to understand false statements and differentiate them from humorous statements (which also allows assessing the integrity of the mental model) (6 stories out of 10 were used: stories No. 1, No. 2, No. 3, No. 6, No. 7, No. 8) [21]; the experimental Read the Mind in the eye (RMET) technique, which allows assessing the ability to non-verbally recognize the internal states of other people [18, 22]; the Dembo-Rubinstein self-esteem scale (based on indicators of health, ability, beauty, intelligence, authority, confidence, character); a trust scale that allows you to subjectively assess your own level of trust (how trusting am I in relation to other people).

Among the research methods, a clinical interview with audio recording was also conducted, including three main questions:

- Can you remember a situation when someone tried to deceive you and how you behaved at that moment?

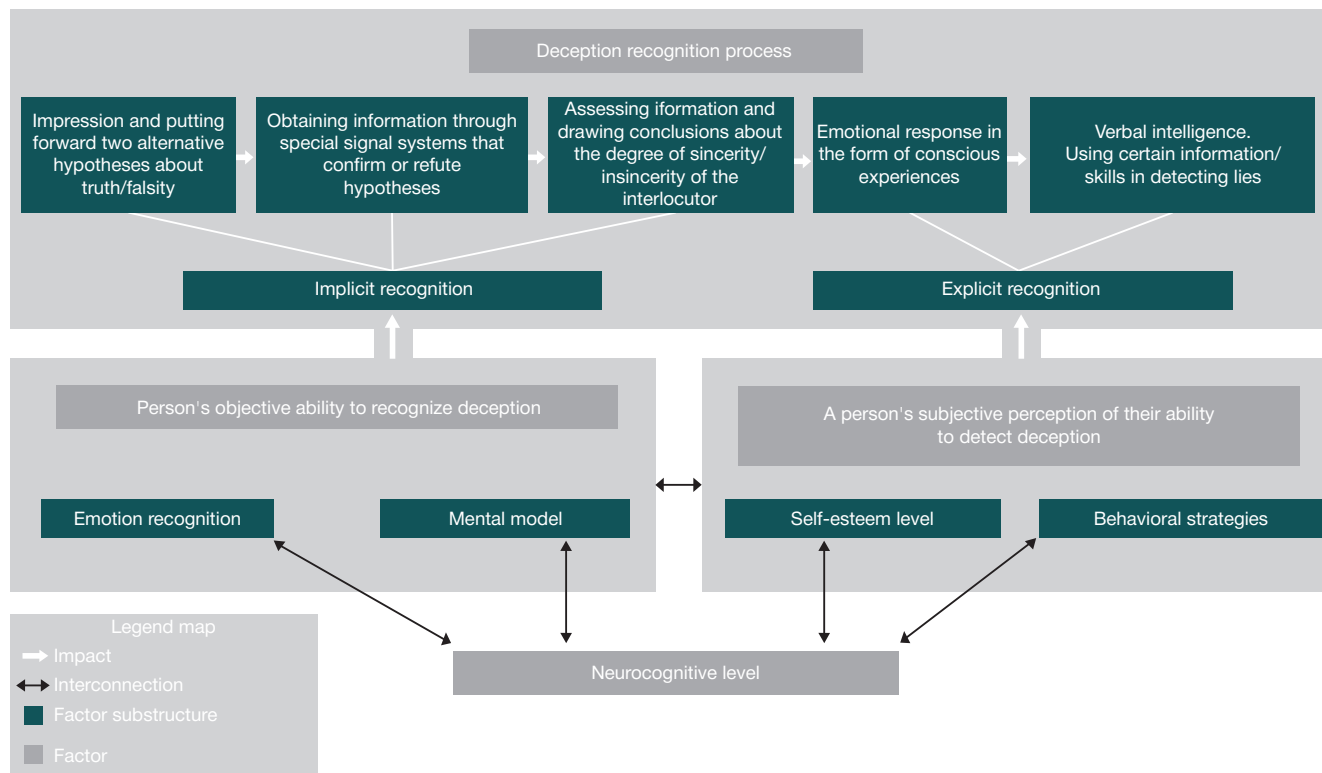


Fig. 1. Schematic diagram of the conceptual model of cognitive markers of deception recognition in elderly and senior age

• By what signs would you determine that your interlocutor is lying?

• How many friends and close relatives do you have and how often do you communicate with them?

The primary processing of the research results was represented by quantitative data processing and included the compilation of a final diagnostic card with coding of nominative data, compilation of a general data table with calculation of the mean value, mean deviation, minimum and maximum value, and median.

Secondary processing was carried out using mathematical processing methods: correlation analysis within each group (Fisher criterion), Mann–Whitney criterion and Wald–Wolfowitz criterion to identify differences between groups. Spearman's r-rank correlation criterion was used to assess the relationships of the parameters under study.

## RESULTS

The study revealed significant differences in the assessment of the neurocognitive level ( $p = 0.027$ ), emotion recognition ( $p = 0.034$ ) and the integrity of the mental model ( $p = 0.022$ ) in elderly and senior age (Fig. 2).

More pronounced mild cognitive decline at a senior age compared to the elderly leads to a lower level of understanding of the theory of mind, which in turn leads to difficulty understanding the emotions and intentions of others in the process of interaction.

Carrying out a comparative analysis of first- and second-order representations, which characterize the level of understanding of the mental model, as a general trend, one should note isolated difficulties in representing one's own thoughts (first-order representations), as well as the deficiency of second-order representations both in elderly and senior age. As a result of assessing the significance of differences between the groups of elderly and senior subjects in terms of correct

answers when assessing the level of understanding of the mental model, statistically significant differences were revealed both in first-order representations ( $p = 0.022$ ) and in second-order representations ( $p = 0.024$ ). It is necessary to note that at senior age isolated errors in first-order representations and a deficit in second-order representations are more significant in comparison with elderly age. Both elderly and senior people experience significant difficulties in accepting two points of view simultaneously, which characterizes second-order representations ("he thinks that she thinks that..."). Isolated errors in first-order representations, which characterize the representation of one's own thoughts and are manifested through the formation of one's own point of view ("I think that she thinks..."), generally indicate the preservation of this level of representation.

Analyzing the self-assessment scales, it was also established that both elderly and seniors at the level of self-assessment record a decrease in their intelligence and abilities indicators with an increase in trustfulness (Fig. 2). Moreover, the specified intelligence and abilities indicators at senior age are significantly lower than in elderly age ( $p = 0.021$  and  $p = 0.024$ , respectively), and the indicators on the trust scale are significantly higher —  $p = 0.034$ .

Next, each research group was divided into two by the level of education in order to assess the significance of differences in the level of expression of cognitive correlates of deception recognition in elderly and senior age. The comparison was carried out within the boundaries of each of the time frames under consideration — separately in elderly and senior age — in groups with higher and secondary specialized education. It was reliably established that in both elderly and senior individuals with higher education, the integrity of the mental model and the cognitive level are significantly higher in comparison with individuals of a senior age. At the same time, the level of trust in these groups is significantly lower than in groups with secondary specialized education (Fig. 3).



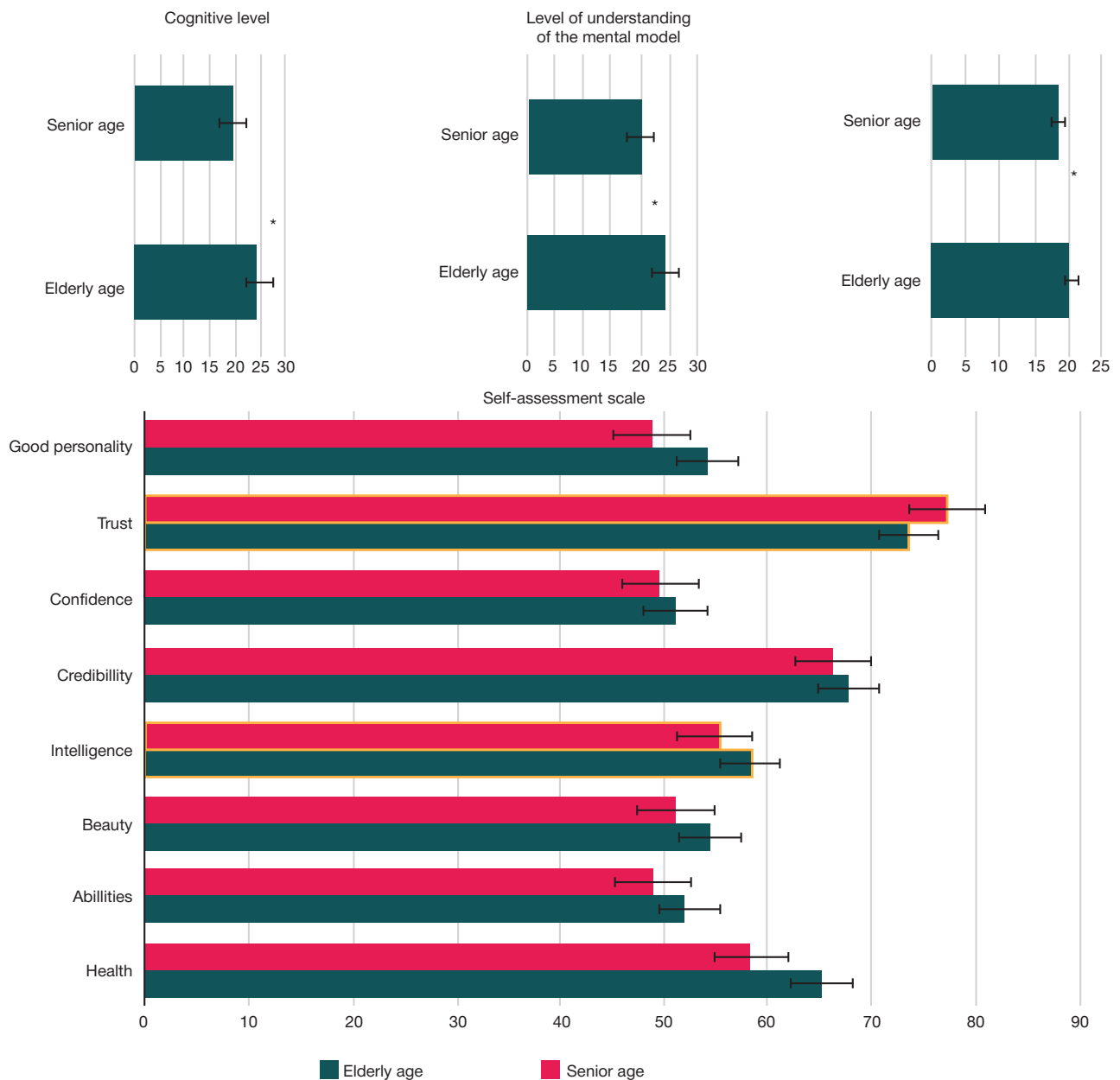


Fig. 2. Indicators of average trends of the studied indicators by groups of subjects in elderly and senior age

To establish the relationships between the studied indicators characterizing explicit and implicit recognition of deception, a correlation analysis procedure was carried out for the studied age groups (Table 1–2).

As a result, in the group of elderly subjects, directly proportional statistically significant correlations were found between the indicators of the cognitive level with the level of understanding of the mental model ( $r = 0.64$ ) and recognition of emotions ( $r = 0.49$ ) with inversely proportional statistically significant correlations with the trust scale ( $r = -0.27$ ). Also, statistically significant correlations were found between the indicator of the level of understanding of the mental model with recognition of emotions ( $r = 0.45$ ) and the trust scale ( $r = -0.31$ ). Analyzing the obtained system of correlations, we can state that the cognitive level acts as the leading correlate in the recognition of deception in elderly age.

Similar results were obtained in the group of people of senior age. Directly proportional statistically significant correlations between the indicators of the cognitive level with the level of understanding of the mental model ( $r = 0.57$ ) and emotion

recognition ( $r = 0.51$ ) with inversely proportional statistically significant relationships with the trust scale ( $r = -0.32$ ). The trust scale is also characterized by a statistically significant inversely proportional correlation with the level of understanding of the mental model ( $r = -0.48$ ). In turn, the level of understanding of the mental model is characterized by a statistically significant directly proportional correlation with emotion recognition ( $r = 0.44$ ) (Table 2).

However, statistically significant inversely proportional correlations between age and cognitive level ( $r = -0.37$ ) and level of understanding of the mental model ( $r = -0.32$ ) were also found in the group of senior people. Such relationships were not found in the group of elderly people.

Based on the data of the clinical interview with audio recording, the following conclusions can be made, which are mostly subjective assessments. Almost all participants responded to the question about their level of gullibility by saying, 'Yes, I am very trusting!' According to the trust scale values distribution, it can be seen that most of the subjects either gave half/slightly more than half, or almost the maximum

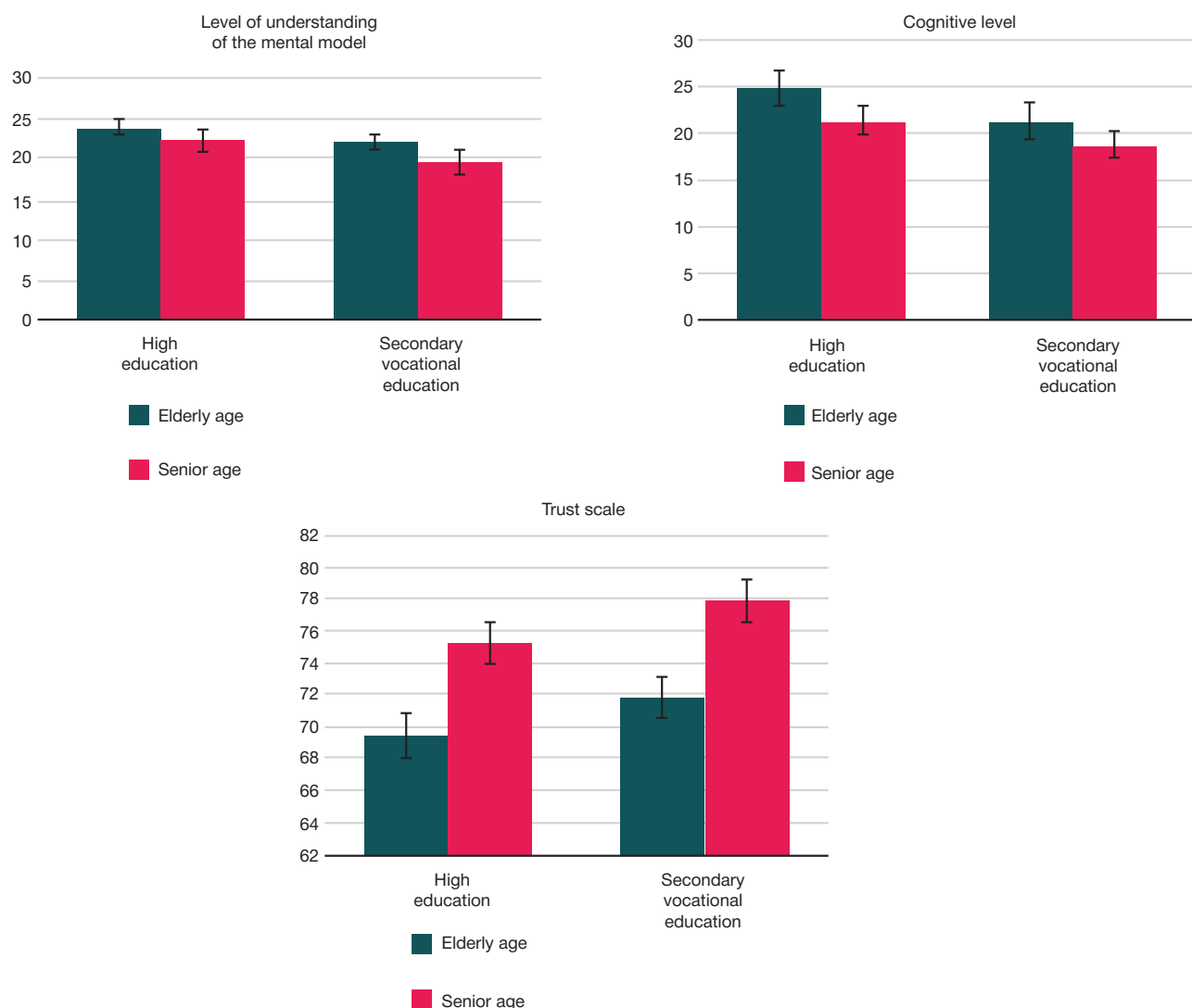


Fig. 3. Indicators of average trends in the level of understanding of the mental model, cognitive level and level of trust in elderly and senior age, considering the level of education

value. This confirms the fact that most subjects consider themselves gullible. When asked about the rationality of such high trust, the subjects give extremely idealistic answers. Many believe that the people around them, for the most part, do not have evil intent upon them and the chance of running into a liar is extremely small. If this does happen, then "God will forgive." This belief is a form of compensatory mechanism that helps to justify the decrease in the ability to recognize one's worldview.

Among the subjects, regardless of age group, 30% do not make any attempts to recognize lies. Therefore, it is not difficult to deceive this group. Noting a high level of trust, 46% cannot remember being deceived at least once. When asked how they were able to determine that they are gullible if they have not been lied to, patients find it difficult to answer. This fact also speaks in favor of the emergence of a special compensation mechanism due to a decrease in criticism. An explicit strategy for recognizing deception prevails in 48% of the subjects. At the same time, each from this group notes the importance of eye movements during deception. This understanding of the signs of a lie is very formulaic, but even such simple knowledge can be useful.

Most subjects, when recalling a situation of deception, first of all talk about phone fraud. At the same time, elderly people are quite resistant to this particular type of scam. These were often heard about the fact that one should not say the word

"yes" in a conversation, disclose personal data and the need to verify any incoming information. Nevertheless, several patients talked about situations of successful deception by phone. When asked about the reason for the success of the fraud, the victims noted the fast pace of speech, the abundance of information and its substantive aspect, which concerned the health of the victim or close circle. Based on the obtained data, it is possible to conclude about the relative success of counteracting phone fraud but also note the serious vulnerability in this regard in case of exposure to a topic that is emotionally significant for the recipient.

As an additional observation, it should also be noted that only a few subjects actually read the voluntary informed consent. The rest signed the document without reading it in full and without any questions. This allows us to conclude that the job status of the interlocutor has a high influence on behavior. The patients were reassured by the fact that the papers for signature were given to them by a person who introduced himself as an employee of the clinic. This may indicate the effectiveness of deceptive actions in relation to the elderly using "authority" (for instance, introducing himself as an employee of law enforcement or health care). 75% of the subjects do not feel lonely. Most patients have hobbies and an extensive social circle. Although many claim that at this age they have fewer friends and relatives, and it is increasingly

**Table 1.** Results of the correlation analysis of the studied parameters in the group of elderly subjects (Spearman's r-rank correlation coefficient,  $p < 0.05$ )

Parameters	Age	Cognitive level	Level of understanding of the mental model	Emotion recognition	Trust scale
Age	1				
Cognitive level	-0.23	1			
Level of understanding of the mental model	-0.21	0.64*	1		
Emotion recognition	-0.09	0.49*	0.45*	1	
Trust scale	0.09	-0.27*	-0.31*	-0.15	1

**Note:** \* — statistically significant correlation.

difficult to make new acquaintances, they do not experience a lack of communication. Some of the interviewees noted the effectiveness of the "Moscow Longevity" program as a way to maintain stable interpersonal communication.

## DISCUSSION

Based on the results obtained, cognitive correlates of deception recognition in elderly and senior age were identified. It has been reliably established that with age, as people get older, regardless of the level of education, there is a decrease in the cognitive level, which, in general, is natural in the process of normative aging. These changes lead to a decline in the comprehension of the theory of mind, which in turn complicates emotion recognition and increases trust levels.

The results obtained correspond to the data of earlier studies. Sergienko E.A. (2020) with co-authors points out that after 60 years, elderly people arbitrarily structure their social space and focus on trusting relationships, thereby trying to minimize negative experiences [12, 16–17]. However, even with such socio-emotional selectivity, it is impossible to completely exclude interaction with other people, in which there is a need to understand the intentions, truthfulness, beliefs, emotions of other people. Such understanding is provided precisely due to the theory of mind, which is understood as a cognitive mechanism that ensures successful interaction with another person. Violation of the integrity of the mental model, caused by cognitive changes, just leads to an increase in the vulnerability of elderly and senior people to deception.

However, unlike the results of the study presented in the works of A.I. Milekhin (2019), which points to the phenomenon of denial of sociocognitive changes or specific cognitive

anosognosia [23]; the majority of subjects who took part in our study, both in elderly (76%) and in senior age (82%), subjectively noted that they had become more trusting. At the same time, our results are consistent with the results of A.I. Milekhin in terms of the deficit of second-order representations in determining the mental model with the relative preservation of first-order representations.

## CONCLUSIONS

An empirical study confirmed the hypothesis of a correlation between cognitive level and the ability to recognize deception. The lower the overall cognitive level, the worse the ability to recognize deception and the more trusting a person becomes.

During the clinical interview with audio recording, the most common compensatory strategies were identified: idealism, "biased optimism", "halo effect", positive bias. In addition, patients demonstrated vulnerability to sensory overload due to short-term memory impairment, observed in 46% of subjects.

Thus, based on the obtained results from empirical study, it has been reliably established that the cognitive correlates of implicit deception recognition in elderly and senior age are emotion recognition and the level of understanding of the mental model. The correlates of explicit deception recognition in elderly and senior age are self-assessment of the level of one's own credulity and behavioral strategies. The success of deception recognition is lower with increasing age. With age, there is a decrease in the level of the mental model, which is manifested in the difficulty of simultaneously understanding two points of view (second-order representations), which, in turn, leads to an increase in the level of trust.

**Table 2.** Results of the correlation analysis of the studied parameters in the group of senior subjects (Spearman's r-rank correlation coefficient,  $p < 0.05$ )

Parameters	Age	Cognitive level	Level of understanding of the mental model	Emotion recognition	Trust scale
Age	1				
Cognitive level	-0.37*	1			
Level of understanding of the mental model	-0.32*	0.57*	1		
Emotion recognition	-0.09	0.51*	0.44*	1	
Trust scale	0,09	-0,32*	-0,48*	-0,15	1

**Note:** \* — statistically significant correlation.

## References

- Vrij A. Detecting lies and deceit: Pitfalls and opportunities. Chichester, UK: Wiley, 2008; 503 p.
- Vrij A. Eliciting cues to deception and truth: What matters are the questions asked. *J of Applied Research in Memory and Cognition*. 2012; 1 (2): 110–7.
- Vrij A, Fisher R, Mann S, Leal S. A cognitive load approach to lie detection. *Journal of Investigative Psychology and Offender Profiling*. 2008; 5 (1–2).
- Vrij A. Detekcija obmana i lzhi. SPb.: Prajm-evroznaк. 2005, 320 s. Russian.
- Vrij A. Vyjavlenie priznakov lzhi i pravdy: vazhny zadavaemye voprosy. *Zhurnal prikladnyh issledovanij v oblasti pamjati i poznanija*. 2012; 110–7. Russian.
- Jekman, Pol. Psihologija lzhi. SPb.: Piter, 1999, 270 s. Russian.
- Jekman, Pol., Frizen U. Uznaj lzheca po vyrazheniju. SPb.: Piter, 2010; 272 s. Russian.
- Jekman, Pol. Psihologija jemocij. SPb.: Piter, 2010; 336 s. Russian.
- Ekman P, Friesen WV, Scherer KR. Body movement and voice pitch in deceptive interaction. *Semiotica*. 1976; 16 (1): 23–27. Available from: <https://doi.org/10.1515/semi.1976.16.1.23>.
- Ekman P. Deception, lying, and demeanor. *N. Y.*, 1997; p. 93–105.
- Znakov V. V. Psihologija vozmoznogo: Novoe napravlenie issledovanij ponimania. M.: Izd-vo «Institut psihologii RAN», 2022; 365 s. Russian.
- ergienko E. A., Ulanova A. Ju., Lebedeva E. I. Model' psihicheskogo: Struktura i dinamika. M.: Izd-vo «Institut psihologii RAN», 2020; 503 s. Russian.
- Egorov D. M. Psihologicheskaja specifika zakonornostej raspoznavanija lzhi. *Vestnik Tomskogo gosudarstvennogo universiteta*. 2015; 393: 191–5. Russian.
- Zhbankova O. V. Primenenie ajtrekinga v praktike professional'nogo otbora kadrov. *Jeksperimental'naja psihologija*. 2018; 156–165. Russian.
- Premack D, Woodruff G. Does the chimpanzee have a theory of mind? *Behavioral and Brain Sciences*. 1978; 1 (4): 515–26. Available from: <https://doi.org/10.1017/s0140525x00076512>.
- Sergienko E. A. Model' psihicheskogo (Theory of mind) kak mental'nyj mehanizm stanovlenija sub#ektnosti. *Sub#ekt, lichnost' i psihologija chelovecheskogo bytija*. 2005; 113–45. Russian.
- Sergienko E. A. Model' psihicheskogo i social'noe poznanie. *Psihologicheskie issledovanija*. 2015; 8 (42): 6. Available from: <http://psystudy.ru/index.php/eng/2015v8n42e/1174-sergienko42e.html>. Russian.
- Baron-Cohen S, Wheelwright S, Hill J, Raste Y, Plumb I. The Reading the Mind in the Eyes Test Revised Version: A Study with Normal Adults, and Adults with Asperger Syndrome or High-functioning Autism. *Journal of Child Psychiatry and Psychiatry*. 2001; 42
- Nasreddine ZS, Phillips NA, Bédirian V, Charbonneau S, Whitehead V, Collin I, et al. The Montreal Cognitive Assessment, MoCA: a brief screening tool for mild cognitive impairment. *Journal of the American Geriatrics Society*. 2005; 53 (4): 695–9.
- Baron-Cohen S, Leslie AM, Frith U. Does the autistic child have a "theory of mind"? *Cognition*. 1985; 21: 37–46.
- Winner E, Leekam S, Brownell H, Happé F, Blum A, Pincus D. Distinguishing lies from jokes: theory of mind deficits and discourse interpretation in right hemisphere brain-damaged patients. *Brain and Language*. 1998; 62 (1): 89–106.
- Leslie AM, Frith U. Autistic children's understanding of seeing, knowing and believing (англ.) *British Journal of Developmental Psychology*. 1988; 6 (4): 315–24. DOI: 10.1111/j.2044-835X.1988.tb01104.x.
- eljohin A. I. Specifika ponimania obmana v pozhilom i starcheskom vozraste. *Psihologija i pravo*. 2019; 9 (4): 187–210. DOI: 10.17759/psylaw.2019090414. Russian.

## Литература

- Vrij A. Detecting lies and deceit: Pitfalls and opportunities. Chichester, UK: Wiley, 2008; 503 p.
- Vrij A. Eliciting cues to deception and truth: What matters are the questions asked. *J of Applied Research in Memory and Cognition*. 2012; 1 (2): 110–7.
- Vrij A, Fisher R, Mann S, Leal S. A cognitive load approach to lie detection. *Journal of Investigative Psychology and Offender Profiling*. 2008; 5 (1–2).
- Фрай О. Детекция обмана и лжи. СПб.: Прайм-еврознак. 2005, 320 с.
- Фрай О. Выявление признаков лжи и правды: важны задаваемые вопросы. *Журнал прикладных исследований в области памяти и познания*. 2012; 110–7.
- Экман, Пол. Психология лжи. СПб.: Питер, 1999, 270 с.
- Экман, Пол., Фризен У. Узнай лжеца по выражению. СПб.: Питер, 2010; 272 с.
- Экман, Пол. Психология эмоций. СПб.: Питер, 2010; 336 с.
- Ekman P, Friesen WV, Scherer KR. Body movement and voice pitch in deceptive interaction. *Semiotica*. 1976; 16 (1): 23–27. Available from: <https://doi.org/10.1515/semi.1976.16.1.23>.
- Ekman P. Deception, lying, and demeanor. *N. Y.*, 1997; p. 93–105.
- Знаков В. В. Психология возможного: Новое направление исследований понимания. М.: Изд-во «Институт психологии РАН», 2022; 365 с.
- Сергиенко Е. А., Уланова А. Ю., Лебедева Е. И. Модель психического: Структура и динамика. М.: Изд-во «Институт психологии РАН», 2020; 503 с.
- Егоров Д. М. Психологическая специфика закономерностей распознавания лжи. *Вестник Томского государственного университета*. 2015; 393: 191–5.
- ЖБанкова О. В. Применение айтрекинга в практике профессионального отбора кадров. *Экспериментальная психология*. 2018; 156–165.
- Premack D, Woodruff G. Does the chimpanzee have a theory of mind? *Behavioral and Brain Sciences*. 1978; 1 (4): 515–26. Available from: <https://doi.org/10.1017/s0140525x00076512>.
- Сергиенко Е. А. Модель психического (Theory of mind) как ментальный механизм становления субъектности. *Субъект, личность и психология человеческого бытия*. 2005; 113–45.
- Сергиенко Е. А. Модель психического и социальное познание. *Психологические исследования*. 2015; 8 (42): 6. Available from: <http://psystudy.ru/index.php/eng/2015v8n42e/1174-sergienko42e.html>.
- Baron-Cohen S, Wheelwright S, Hill J, Raste Y, Plumb I. The Reading the Mind in the Eyes Test Revised Version: A Study with Normal Adults, and Adults with Asperger Syndrome or High-functioning Autism. *Journal of Child Psychiatry and Psychiatry*. 2001; 42
- Nasreddine ZS, Phillips NA, Bédirian V, Charbonneau S, Whitehead V, Collin I, et al. The Montreal Cognitive Assessment, MoCA: a brief screening tool for mild cognitive impairment. *Journal of the American Geriatrics Society*. 2005; 53 (4): 695–9.
- Baron-Cohen S, Leslie AM, Frith U. Does the autistic child have a "theory of mind"? *Cognition*. 1985; 21: 37–46.
- Winner E, Leekam S, Brownell H, Happé F, Blum A, Pincus D. Distinguishing lies from jokes: theory of mind deficits and discourse interpretation in right hemisphere brain-damaged patients. *Brain and Language*. 1998; 62 (1): 89–106.
- Leslie AM, Frith U. Autistic children's understanding of seeing, knowing and believing (англ.) *British Journal of Developmental Psychology*. 1988; 6 (4): 315–24. DOI: 10.1111/j.2044-835X.1988.tb01104.x.
- Мелёхин А. И. Специфика понимания обмана в пожилом и старческом возрасте. *Психология и право*. 2019; 9 (4): 187–210. DOI: 10.17759/psylaw.2019090414.



In issue 6 (November–December 2024) of the Bulletin of RSMU a few errors were made:

### IMPACT OF TUMOR ON THE CELL CYCLE AND DIFFERENTIATION OF HEMATOPOIETIC STEM CELLS

Aktanova AA, Bykova MV, Skachkov IP, Denisova VV, Pashkina EA

✉ **Correspondence should be addressed:** Alina A. Aktanova  
Yadrintsevskaya, 14, Novosibirsk, 630099, Russia; aktanova\_al@mail.ru

**Received:** 02.12.2024 **Accepted:** 16.12.2024

**DOI:** 10.24075/brsmu.2024.065

The following corrections should be applied:

	Published text:	Correction:
p. 27, item "Funding"	Funding: the study was supported by the Russian Science Foundation, project No. 23–25–10099.	Funding: the study was supported by the Russian Science Foundation in cooperation with the Government of the Novosibirsk Region, project No. 23–25–10099.
с. 27, пункт «Финансирование»	Финансирование: исследование выполнено при финансовой поддержке Российского Научного Фонда, проект № 23–25–10099.	Финансирование: исследование выполнено при финансовой поддержке Российского Научного Фонда совместно с Правительством Новосибирской области, проект № 23–25–10099.